Development of microemulsion delivery systems for bioactive compounds

Quan Yuan

2020

Development of microemulsion delivery systems for bioactive compounds

A thesis presented in partial fulfilment of the requirements

for the degree of

Doctor of Philosophy in Food Technology

at Massey University, Auckland, New Zealand

Quan Yuan

2020

ABSTRACT

Many bioactive compounds for health benefits are not readily stable against degradation and their solubility is also very low. As a result, a delivery system is required to encapsulate and protect bioactive compounds for their food applications. Emulsion is one of the delivery systems which has been studied by many researchers. But emulsion tends to destabilize during storage and its opaque optical properties makes it difficult for its use and incorporation into clear foods or beverages without affecting their original appearance. Therefore, microemulsion, which is known to be transparent, has been investigated to some extent to encapsulate and deliver bioactive compounds as a potential delivery system.

The objective of this research was to fabricate oil-in-water (O/W) microemulsions which might be utilised as the delivery system for bioactive compounds. This thesis is mainly composed of two sections. The first section was to produce microemulsions via emulsion dilution method and water titration method as well as to study the characteristics of these microemulsions. Beta-carotene was a type of bioactive compound used in the second section to study the effect of beta-carotene on the formation and properties of microemulsion which was fabricated using the same methods described above.

At first, emulsion dilution method was employed to fabricate microemulsions with different types and concentrations of oils, such as peanut oil, fractionated coconut oil, isopropyl myristate (IPM), lemon oil and Capmul 708G, and also with different surfactants (Tween 20, 40, 60 and 80). It was found that peanut oil and fractionated coconut oil could not be utilised to form microemulsions by this method, whereas IPM and lemon oil had the ability to fabricate microemulsions. When 1% Tween 80 was introduced as the surfactant and dilution medium, microemulsion could be formed when the concentration of IPM was less than 0.1% and that of lemon oil was less than

0.2%. Among the different types of Tween surfactants, Tween 80 was the most efficient when its solution containing Tween micelles was used as a dilution medium compared to the other Tween surfactants because more lemon oil could be incorporated into the Tween 80 micelles with an increase in Tween 80 concentration.

In the following study, a water titration method was employed to create ternary or pseudo phase diagrams which indicated the ability to fabricate microemulsions of a mixture system. Various types of oils (Captex 100, Capmul PG-8, Capmul PG-12, Capmul PG-2L, lemon oil, Capmul MCM C8, Capmul 708G and Captex 355) and surfactants (Tween 80, Tween 20, Span 80 and Kolliphor EL) were used in this study. Absolute ethanol and propylene glycol (PG) were also incorporated as cosurfactant and cosolvent, respectively. It is concluded that all these oils and surfactants could be utilised by the water titration method to produce microemulsions, however, their ability to form microemulsions were different. Capmul 708G, which is a monoglyceride, was the most efficient in terms of producing microemulsions compared to diglyceride and triglyceride. Tween 20 and Kolliphor had the similar emulsifying properties compared to Tween 80 whereas Span 80 was not efficient. Both absolute ethanol and PG could assist the formation of microemulsions when they were introduced into the mixture system of oil, surfactant and water.

In the following study, microemulsions containing 0.1% and 0.4% lemon oil and an emulsion containing 1.5% lemon oil (larger oil droplets), which were fabricated by the emulsion dilution method, were chosen to incorporate beta-carotene as a lipophilic model bioactive compound into lemon oil in order to study its impact on the formation and properties of the resulting microemulsion and emulsion systems. The encapsulation of beta-carotene into 0.1% and 0.4% lemon oil caused a significant increase in the particle size of the O/W microemulsions, but the particle size was still within the size range of microemulsion. As a result, the beta-carotene-loaded microemulsions containing 0.1 and 0.4% lemon oil were visually clear in appearance.

However, the incorporation of beta-carotene did not increase and alter the particle size of the emulsion containing 1.5% lemon oil. The microemulsion sample containing 0.1% lemon oil and the emulsion containing 1.5% lemon oil were stored at 25 °C without exposed to oxygen and light for one month. While, the microemulsion containing 0.4% lemon oil was selected and placed at three different temperatures (4, 25 and 37 °C) for 1 month: at 4 and 37 °C without exposure to both oxygen and light and at 25 °C, four different environmental conditions (i.e. with oxygen/light, with oxygen and without light, without oxygen and with light, without oxygen/light). The results showed that the rate of beta-carotene degradation was lower in all these three samples when compared to the beta-carotene present in a hexane solution without encapsulation. Higher temperature accelerated the degradation rate of beta-carotene. As a consequence, the 0.4% lemon oil microemulsion at 4 °C exhibited the slowest degradation rate of beta-carotene.

Next, the microemulsions fabricated by the water titration method were selected to encapsulate beta-carotene to study the encapsulation capacity of these microemulsion systems as well as their ability to protect beta-carotene against oxidative degradation during storage. Capmul 708G, Tween 80, Milli-Q water and PG mixture system were chosen to fabricate microemulsions and two formulations (L910 and L990) were prepared to incorporate beta-carotene. L910 was comprised of 81% Capmul 708G, 9% Tween 80, 5% water and 5% PG, whereas L990 contained 9% Capmul 708G, 1% Tween 80, 45% water and 45% PG. It was able to see clearly from this experiment that the L910 system could incorporate more beta-carotene than L990. Both L910 and L990 could reduce the degradation rate of beta-carotene when loaded into them compared to their presence in hexane solutions without encapsulation. Similar to the previous experiment as described above, when the beta-carotene incorporated microemulsions were placed at 4 °C and away from oxygen and light, beta-carotene had the highest retention rate after storage for 1 month. Furthermore, beta-carotene degradation rate in L910 was slower than that in L990, indicating L910 was more

effective than L990 in terms of incorporating and protecting beta-carotene.

It is shown clearly from the present study that microemulsions could be formed via the water titration and emulsion dilution methods. The type and concentration of oil phase and surfactant had a significant influence on the determination of whether a mixture system could form a microemulsion as well as the properties of the formed microemulsion. The microemulsions produced by these two different methods could be utilised to encapsulate beta-carotene as the incorporation of beta-carotene did not have a significant influence on the properties of the original microemulsions. Moreover, microemulsions provided the stability and protection to beta-carotene against oxidative degradation that could be caused by oxygen, light and temperature during storage, which might be possible to be applied to some liquid foods and beverages.

ACKNOWLEDGEMENTS

I am honoured to be able to study in Massey University (School of Food and Advanced Technology) for the past six years (including Graduate Diploma in Food Technology).

First of all, I would like to deliver my greatest appreciation to my supervisors, Dr. Sung Je Lee and Professor Marie Wong for their guidance and support throughout my PhD study. It has been a great honour to have Dr. Lee as my chief supervisor. I have learned a lot from him during these years. His way of thinking, academic writing skills, enthusiasm about academic research and suggestions have enlightened me on my PhD research. Sincere thanks go out to my co-supervisor, A/P Wong for her constructive feedbacks and suggestions during each meeting and in writing of journal articles as well as this thesis. Moreover, I am thankful for her guidance and supervision while I am using HPLC to analyse some samples.

I would like to express my deepest gratitude to all the laboratory managers, Ms. Helen Matthews (who has left Massey Uni.), Ms. Rachel Liu and Mr. Kenneth Teh (who has left Massey Uni.) for their kind help. They have given me trainings about how to use laboratory equipment and have helped me to order consumptions, which ensure the smooth completion of my PhD project. In addition, many thanks go out to Ms. Niki Minards who is working in Manawatu Microscopy and Imaging Centre for preparing and analysing samples for TEM imaging.

Encouragement and support from my friends, Yanyu Yang and Renee Fu really help me a lot during PhD study. I am thankful for knowing them here in New Zealand and they are a big fortune to me apart from knowledge.

Finally, I would like to thank my grandmother, my parents and my partner for their love and support.

TABLE OF CONTENTS

LIST OF FIGURES

LIST OF TABLES

LIST OF ABBREVIATIONS

ALA	α-linolenic acid
ANOVA	Analysis of variance
AUC	Area under curve
CPP	Critical packing parameter
DHA	Docosahexaenoic acid
DLS	Dynamic Light Scattering
DSC	Differential Scanning Calorimetry
EM	Electron Microscopy
EMDG	Ethoxylated mono-di-glyceride
EPA	Eicosapentaenoic acid
HLB	Hydrophilic-lipophilic balance
HPLC	High Performance Liquid Chromatography
IPM	Isopropyl myristate
IPP	Isopropyl palmitate
LCT	Long chain triglycerides
MCT	Medium chain triglycerides
N/A	Not Applicable
NaCl	Sodium chloride
nm	nanometer
NMR	Nuclear Magnetic Resonance
O/W	Oil-in-water
PDI	Polydispersity index
PEO	Polyethoxylated
PG	Propylene glycol
PIT	Phase inversion temperature
POE	Polyoxyethylene oleyl ether
PSD	Particle size distribution

RSD	Relative standard deviation
SANS	Small-angle neutron scattering
SAXS	Small-angle X-ray scattering
S.D.	Standard deviation
SEM	Scanning Electron Microscopy
TEM	Transmission Electron Microscopy
TPD	Ternary phase diagram
VCO	Virgin coconut oil
W/O	Water-in-oil

Chapter 1 Introduction

1.1 Background information

Nanotechnology has been a rapidly growing research area in various food sectors as an emerging technology. According to the research papers and review articles, the term nanotechnology is defined as the manipulation, fabrication, and application of materials that have at least one dimension (length, width or height) smaller than 100 nm for their desired structural and functional characteristics (Huang et al., 2010, Tarafdar and Raliya, 2012, Yu and Huang, 2013, Nakajima et al., 2015). The potentials of nanotechnology have been explored in various food areas, including the improvement of food preservation and packaging (Mihindukulasuriya and Lim, 2014, Yu et al., 2016, Dar et al., 2019), the development of new functional foods and beverages (Chen and Wagner, 2004, Rao and McClements, 2013) and the improvement of nutrient delivery (e.g., bioavailability, controlled release and intake) (Bilia et al., 2014, Cho et al., 2014, Acevedo-Fani et al., 2015). The important application of nanotechnology is also linked to encapsulation that enables the design and development of novel delivery systems for bioactive compounds with improved water solubility, stability, functionality, and bioavailability which ultimately lead to the development of new functional foods and beverages. The types of nanocarriers or nanoencapsulation that have been developed include nanoemulsions, nanoparticles, solid lipid nanoparticles, nanoliposomes, nanofibers, nanotubes and microemulsions (Weiss et al., 2007, Momin et al., 2013, Onwulata, 2013, Singh, 2016).

Emulsions can be prepared via high energy or low energy emulsification methods. High energy emulsification methods require a high energy input and high shear forces using mechanical devices, such as high pressure homogenizers, microfluidizers, high shear mixers and ultrasonic devices. However, the formation of nanometre-scaled droplets smaller than 100 nm by high energy emulsification methods is not readily feasible due to a significant amount of energy being lost through dissipation as heat.

On the contrary, low energy emulsification methods use internal chemical energy stored in ternary systems (oil-water-surfactant) to form microemulsions (< 50 nm) by using intrinsic physicochemical properties of surfactant molecules and environmental conditions. Thus, the low energy emulsification methods do not require a high mechanical shear force in producing emulsions. Low energy emulsification methods however have some limitations, because only a certain type of surfactants and oils can be used. High concentration of synthetic surfactants is required to produce microemulsions which limit their application in food industry, thus low energy methods are mainly used and studied in the field of pharmaceuticals for delivery of drugs. Nevertheless, low energy emulsification methods are increasingly investigated for their use in food applications as the techniques are efficient in producing microemulsion with droplets smaller than 50 nm with transparent optical properties.

In recent years, it has also been shown that microemulsions can be produced by using another approach, which can be referred to as “emulsion dilution method”, involving a two-step process: i) preparation of emulsions by high energy method and ii) dissolution of oil droplets into aqueous surfactant micelle solutions (Rao and McClements, 2012a). This technique also needs to be investigated more extensively because of its high potential for food application in developing functional food beverages. Therefore, it is necessary to find out the oils and surfactants which can be utilised by this method to fabricate microemulsions.

Water titration method has been employed by most researchers to form microemulsions via constructing ternary or pseudo ternary phase diagrams (Patel et al., 2012, Lidich et al., 2016, Tang et al., 2019). Briefly speaking, water or buffer solution was added dropwise into the mixture of oil (s), surfactant (s) and/or cosurfactant. Different types of oils and surfactants as well as cosurfactant and cosolvent were chosen to construct ternary or pseudo ternary phase diagrams in the present study to find out the most suitable mixture systems to produce microemulsions.

Microemulsions are reported to be good delivery systems for bioactive compounds (Amar et al., 2004, Ariviani et al., 2015, Chen and Zhong, 2015, Cheng et al., 2017, Calligaris et al., 2019). In this research, beta-carotene was chosen to study the encapsulation capacity and protection ability of microemulsions fabricated by the aforementioned methods for bioactive compounds.

The objectives of the present research were:

To study the effects of types and concentrations of oils and surfactants on the formation and properties of microemulsions using emulsion dilution method.

To investigate the effects of types and concentrations of oils and surfactants on the formation and properties of microemulsions using water titration method.

To determine the effect of incorporation of cosurfactant and cosolvent on the formation and properties of microemulsions using the water titration method.

To explore the encapsulation of beta-carotene on the properties of empty microemulsions fabricated by emulsion dilution method and water titration method.

To explore the stability of beta-carotene encapsulated in the microemulsions with different concentrations of oil phase fabricated by emulsion dilution method under different environmental conditions.

To study the stability of beta-carotene incorporated in W/O and O/W microemulsions produced by water titration method under different environmental conditions.

1.2 Overview of thesis

This thesis describes the fabrication of microemulsions via emulsion dilution method and water titration method which can be utilised to encapsulate and protect beta-carotene. This thesis is comprised of eight chapters which are listed as follows:

Chapter 1 lists the background information for conducting the present study and the objectives of this study.

Chapter 2 is the literature review of this study which describes the methods to fabricate microemulsions, formulation of microemulsions, properties and characterization of microemulsions as well as lists the type of bioactive compounds that have been encapsulated in the microemulsions in literature.

Chapter 3 shows the main methods and materials utilised in this study.

In Chapter 4, the emulsion dilution method was employed to fabricate microemulsions with different types of oils and surfactants to study their ability to produce microemulsions.

In Chapter 5, the water titration method was employed to fabricate microemulsions with different types of oils and surfactants. Cosurfactants and cosolvents were also introduced in this chapter. Ternary or pseudo ternary phase diagrams were introduced to study the ability of different mixture systems of oil, surfactant, water with/without cosurfactant and/or cosolvent to produce microemulsions.

Chapter 6 characterizes the encapsulation of beta-carotene into microemulsions and emulsions fabricated via emulsion dilution method. The beta-carotene loaded samples were stored at different conditions to determine the degradation rate of beta-carotene.

In Chapter 7, beta-carotene was incorporated into microemulsions (W/O and O/W) produced by water titration method which were stored at different environmental conditions to determine the protection abilities of these microemulsions on beta-carotene.

Chapter 8 highlights the overall conclusions of the present research work and recommends some ideas for future study.

Chapter 2 Literature Review

2.1 Introduction

In food industry, functional foods, which are aimed at using food to enhance health, have been more focused on recently due to the demand of modern health-conscious consumers, who are interested in foods that are health-enhancing and disease-preventing. A simple way to produce functional foods is to incorporate bioactive compounds (such as carotenoids, phytosterols, omega-3 fatty acids, polyphenols and fat-soluble vitamins) into food products. However, these bioactive compounds are insoluble in water and sensitive to food preparation conditions, including temperature change and exposure to light and oxygen (McClements et al., 2007). In this respect, the introduction of delivery system, in which bioactive compounds are incorporated and thus protected, is essential. Microemulsion is one of the delivery systems that were normally employed in the literature.

A microemulsion is a thermodynamically stable, homogenous, optically isotropic, low viscous and transparent solution which contains the mixture of water, oil, surfactants and possibly cosurfactants or cosolvents (Flanagan and Singh, 2006, Chauhan et al., 2019). A microemulsion can be fabricated via low energy emulsification method, including water titration method, oil titration method and cosurfactant titration method as well as emulsion dilution method which is a combination of high and low energy emulsification method. While employing the water titration method, a ternary of pseudo ternary phase diagram is generally constructed to illustrate the formulation of water, oil, surfactant and/or cosurfactant/cosolvent that can form microemulsions. Different types of oils and surfactants were introduced by researches to produce microemulsions (Fanun et al., 2001, Boonme et al., 2006, Anoopinder et al., 2016, Hu et al., 2019), but only a few of them were food-grade ingredients.

In addition, though a number of studies have incorporated lipophilic bioactive compounds into microemulsions, few of them have determined the effect of microemulsions on the stability of bioactive compounds incorporated in them. In this review, preparation methods, formulation and properties and characterization of microemulsions are described. Some basic knowledge of lipophilic bioactive compounds as well as bioactive compounds loaded microemulsions is also provided.

2.2 Emulsion

Emulsion is a type of dispersion system with two or more immiscible liquids, normally oil and water, in which one liquid phase is dispersed as droplets into another phase (McClements, 2005). The droplets suspended in emulsion are named as dispersed phase, while the phase containing dispersed droplets is referred to as continuous phase. An emulsion system containing oil droplets dispersed in aqueous phase is referred to as an oil-in-water (O/W) emulsion, while the reverse system with water droplets dispersed in oil phase is called a water-in-oil (W/O) emulsion. Emulsion, the particle size of which is normally very large, is also known as conventional emulsion or macroemulsion (McClements and Rao, 2011). It is thermodynamically unstable because the interface between oil and water phase has larger positive free energy (McClements, 2011) and it tends to have phase separation over time (McClements and Rao, 2011). In addition, emulsion is opaque or turbid because the droplet size of emulsion is similar to the wavelength of light, thereby the emulsion scatters light strongly (McClements and Rao, 2011).

2.3 Nanoemulsion

Nanoemulsion, which is also termed as mini-emulsion (McClements and Rao, 2011, Saberi et al., 2014) and ultrafine emulsion (Fernandez et al., 2004, Yang et al., 2012),

can be considered as conventional emulsion with very small droplets. It tends to be optically transparent or translucent, since its particle size is much smaller than the wavelength of light (Fernandez et al., 2004, Solans et al., 2005). However, there is not a consensus on the exact range of nanoemulsion particle size, which, in the literature, ranges from 10 nm to 100 nm up to 500 nm (Fernandez et al., 2004, Solans et al., 2005, Lee and McClements, 2010, Sole et al., 2010, Anton and Vandamme, 2011, McClements and Rao, 2011). In addition, nanoemulsion system is not thermodynamically stable and has the tendency to breakdown after some time. Nevertheless, nanoemulsion is able to remain stable for a long time, because small particle size ensures its stability to flocculation, coalescences and gravitational separation (Tadros et al., 2004, Wooster et al., 2008). Accordingly, nanoemulsion is a kinetically stable system (Fernandez et al., 2004, Sole et al., 2010), which maintains its stability to dilution or temperature change (Anton and Vandamme, 2011). Like conventional emulsion, the droplets suspended in nanoemulsion are named as dispersed phase, while the phase containing dispersed droplets is referred to as continuous phase. Nanoemulsion can be classified into oil-in-water (O/W) nanoemulsion, which contains oil droplets dispersed in aqueous phase and water-in-oil (W/O) nanoemulsion, in which water droplets dispersed in oil phase.

2.4 Microemulsion

A microemulsion is a thermodynamically stable, homogenous (heterogeneous at molecular level), optically isotropic, low viscous and transparent solution which contains the mixture of water, oil (or hydrocarbons), surfactants and possibly cosurfactants or cosolvents (Paul and Moulik, 1997, Flanagan and Singh, 2006, Chauhan et al., 2019). Like nanoemulsions, the size range of microemulsion particle diameters defined is not the same in different journal articles, from 4 nm to 50 nm up to 200 nm (Flanagan and Singh, 2006, McClements and Rao, 2011, Rao and McClements, 2011, McClements, 2012). The author believed that the diameter of microemulsion was

smaller than 50 nm. The comparison of emulsion, nanoemulsion and microemulsion are illustrated in Table 2.1.

Table 2.1 Comparison of emulsion, nanoemulsion and microemulsion

System	Droplet diameter	Thermodynamic stability	Appearance
Emulsion	> 100 nm	Unstable	Opaque
Nanoemulsion	< 100 nm	Unstable	Translucent or transparent
Microemulsion	< 50 nm	Stable	Transparent

Some researchers stated that microemulsions can also be termed as swollen micelles (Paul and Moulik, 1997, Malcolmson et al., 1998, McClements and Rao, 2011). However, Flanagan and Singh (2006) insisted a swollen micelle which is a system that contains a low volume fraction of oil or water is different from a microemulsion, which is referred to as a system with sufficient dispersed phase incorporated into the micelle formed by the surfactant. A considerable number of surfactants that help form microemulsions have ultralow interfacial tension, hence the free energy of the microemulsion system is much lower than that of the phase-separated components. As a result, microemulsions are able to be fabricated spontaneously, without the supplying of any energy. However, in practice, a certain amount of external energy (i.e., stirring and heating), is necessary when making microemulsions, due to the existence of kinetic energy barriers between phase-separated components and the microemulsion, or slow transport of components (McClements and Rao, 2011, McClements, 2012).

Microemulsions can be divided into single phase and multiphase microemulsions in terms of phase conditions (Flanagan and Singh, 2006). In a single phase microemulsion, if the oil concentration is very high, this microemulsion belongs to the W/O microemulsion category. Whereas at very high water concentrations, the microemulsion is an O/W microemulsion. Besides, other structures, such as lamellar liquid crystalline,

micelle, reverse micelle and bicontinuous structures, may exist inside the single-phase system. All these systems can exist either alone or together with other systems when different concentrations of water, oil and surfactants are mixed to fabricate microemulsions. The existence of multiphase microemulsions is because the surfactant concentration is not enough. Multiphase microemulsions have three different appearances, an O/W microemulsion in combination with an extra oil phase on the top, a W/O microemulsion in combination with an extra water phase on the bottom and a bicontinuous microemulsion with extra oil layer on the top and extra water on the bottom (Flanagan and Singh, 2006). According to Winsor (1948), these three multiphase microemulsions can be referred to as Winsor I, II and III systems. In addition, the single phase microemulsion is named as Winsor IV system, which is the primary interest of researchers in the area of food (Flanagan and Singh, 2006). Schematic graphs of Winsor I, II, III and IV systems are shown in Figure 2.1.

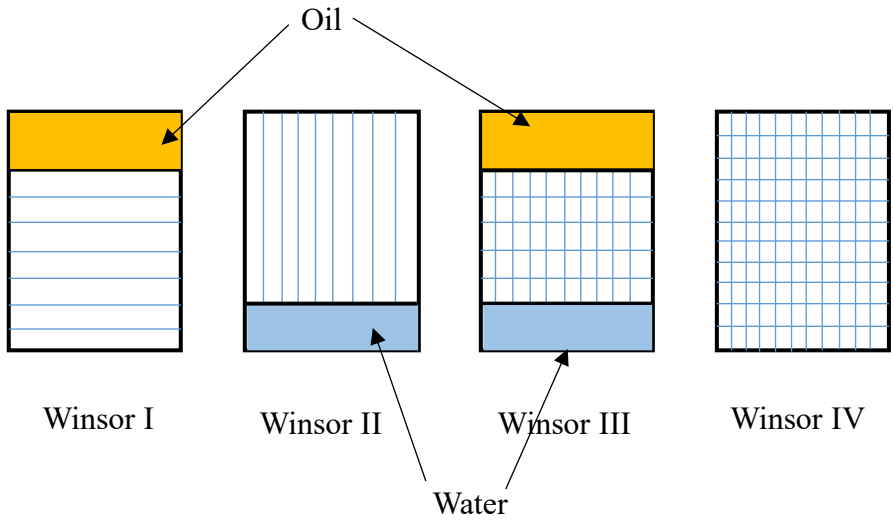

Figure 2.1 Schematic graphs of Winsor I, II, III and IV systems.
Adapted from Winsor (1948)

2.4.1 Methods for preparing microemulsion

As has already been described, external energy is usually needed in the formation of microemulsions although a microemulsion is an equilibrium system. In theory, high

energy can be employed to make microemulsions. However, a high energy method is not efficient, and the mixture of water, oil and surfactant may have a high viscosity which can limit the homogenization process (Flanagan and Singh, 2006). Therefore, the high energy approach is seldom used to fabricate microemulsions. Low energy emulsification method, which only requires very low energy input, has been employed to fabricate microemulsions (Fanun, 2010, Araujo et al., 2018, Yadav et al., 2018, Guo et al., 2019a). However, only certain types of surfactants and oils can be used to fabricate microemulsion by the low energy emulsification method (Flanagan and Singh, 2006, Chauhan et al., 2019)

2.4.1.1 Phase inversion temperature (PIT) method

PIT method depends on change in the spontaneous curvature of surfactant with changing temperature (Talegaonkar et al., 2008). Only surfactant which is sensitive to temperature change can be utilized in this method, i.e. polyethoxylated (PEO) non-ionic surfactants (Flanagan and Singh, 2006). The change in temperature results in the change in the hydration of the poly (oxyethylene) chains, thereby the curvature of surfactants change (Solans and Sole, 2012). At low temperature, the head group of the surfactant is highly hydrated; therefore, it is more soluble in water, so it favours the formation of O/W microemulsion. But according to Anton and co-workers, not every polyethoxylated (PEO) non-ionic surfactant could be employed in the PIT method. The PEO headgroup of some PEO non-ionic surfactants are either too big or small, and the oil chain of some PEO non-ionic surfactants are either too long or too short, which makes them not very sensitive to temperature change, in other words, they cannot result in the phase inversion with the change in temperature (Anton et al., 2007). In a PIT method, with the increase in temperature, head group dehydrates progressively, causing the reduction in the solubility of surfactant in water. At the phase inversion temperature, spontaneous curvature of the surfactant molecule is zero and droplets have an ultralow interfacial tension (Flanagan and Singh, 2006). Therefore, emulsion with very small droplet size is

formed. A stable O/W microemulsion is fabricated after the emulsion is rapidly cooled to a low temperature (Talegaonkar et al., 2008). PIT could be determined by measuring viscosity changes during cooling (Souza et al., 2009, Chen et al., 2015) and turbidity changes after heating (Chen et al., 2015).

Valoppi et al. (2017) utilized the PIT method to prepare O/W microemulsions with lemon oil, peanut oil, Tween 80 and NaCl solution. The aqueous phase was prepared by mixing 10, 15, 20 and 30% Tween 80 with 0.8M NaCl solution. Then, the aqueous phase was added into the oil phase under magnetic stirring at 600 rpm for 10 minutes at ambient temperature to fabricate the coarse emulsion. After that, the coarse emulsion was transferred into a vial, sealed and heated at 90 °C, which was 15 °C higher than its PIT, for 30 minutes. In the end, the sample was placed in an ice-water bath while it was hand shaken until a transparent homogenous solution was obtained (Valoppi et al., 2017).

2.4.1.2 Emulsion dilution method

The emulsion dilution method (a combination of high energy and low energy emulsification methods) was also employed by some researchers to make microemulsions (Weiss and McClements, 2000, Rao and McClements, 2012a, Ziani et al., 2012a, b, Salimi et al., 2014). The high energy emulsification approach was utilized to make a small molecular surfactant stabilized O/W emulsion, which was then diluted into a surfactant micelle solution. Schematic diagrams of emulsion dilution method are shown in Figure 2.2. The principle of this method was the movement (or solubilization) of oil molecules from initial emulsion droplets into surfactant micelles. It is well known that the initial O/W emulsion is thermodynamically unstable. While, the surfactant micelle solution is thermodynamically stable due to the decrease in free energy caused by the hydrophobic effect (rearrangement of surfactant molecules, forcing part of the surfactant to be removed from water). However, the monolayer formed by surfactants may not be in the optimum curvature, which is able to be obtained after the transport of

oil molecules into surfactant micelles until they become saturated (Ziani et al., 2012b, a). As a result, the surfactant micelle whose effective diameter is 9.9 nm when swells, while the initial emulsion droplets shrink, resulting in the change in the particle size of the mixture system to the microemulsion range (Rao and McClements, 2012a).

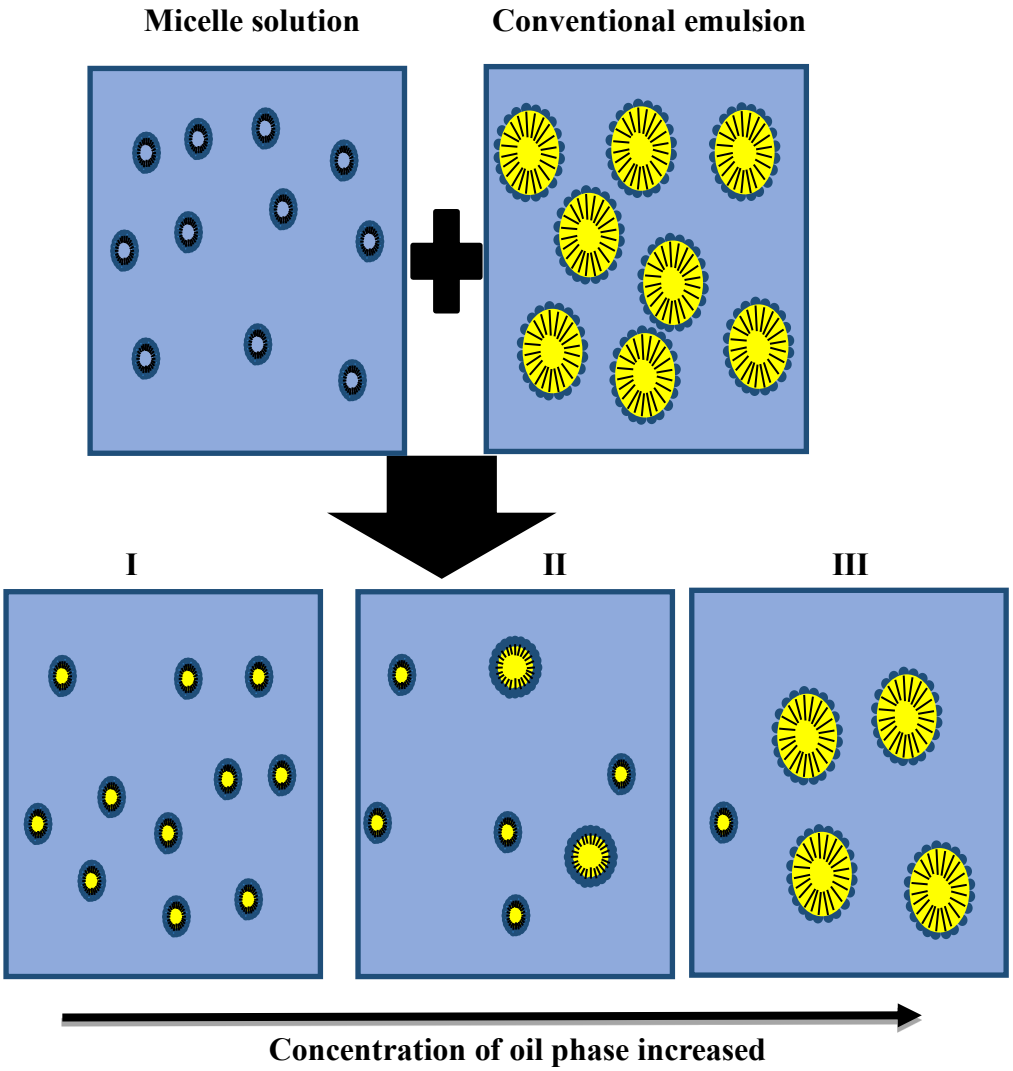

Figure 2.2 Schematic graphs of emulsion dilution method. I. All the oil phase is solubilised in micelles, forming microemulsions. Micelles are saturated at this point. II. Mixture of microemulsion and emulsion droplets. III. Mainly emulsion droplets.

Rao and McClements (2012a) utilized lemon oils (1×, 3×, 5×, 10×) and Tween 80 to form O/W microemulsions to study the effect of oil phase composition on the formation and stability of the microemulsions. A 1% Tween 80 micelle solution was used to dilute

the preformed 1% Tween 80 stabilized lemon O/W emulsion, the turbidity of the emulsion decreased dramatically until reaching zero, which meant that oil droplet size also reduced. In addition, the turbidity of the emulsion increased with an increase in lemon oil concentration; as well the appearance of the emulsion changed from transparent to opaque. On the other hand, at very low oil concentration, particle diameter was very small, at around 12 nm, while after the surfactant micelles are saturated with the oil, the emulsion system becomes a mixture of swollen micelles and non-dissolved oil droplets, causing the increase in particle diameter and particle size distribution (PSD). Though swollen micelles still exist, they scatter light much less than larger particles, such that any light scattering by swollen micelles cannot be recognized by the DLS instrument.

Similarly, Rao and McClements (2012c) utilized sucrose monopalmitate (SMP) and Tween 80 to fabricate microemulsions, they stated that SMP had higher solubilization capacity (the maximum amount of oil that can be solubilized in a given amount of micelle solution) than Tween 80 if the concentration used was the same. This was because SMP has a smaller hydrophilic headgroup than Tween 80, resulting in a higher packing capacity and lower optimum curvature of SMP. In addition, the combination of SMP and Tween 80 resulted in a much higher solubilization capacity, which was the addition of solubilization capacities of SMP and Tween 80. On the other hand, they adjusted the pH of the aqueous solution to 3.5, which is close to the pH of acidic beverages, to study the stability of the final emulsions in acidic conditions. As a result, emulsions stabilized by SMP had poor stability against acidic conditions, but a combination of SMP and Tween 80, increased the acid stability of the emulsions.

2.4.1.3 Water titration method

Most researchers utilized the water titration method (dilution of surfactant and oil mixtures with water at constant temperature) to fabricate microemulsions (Fanun et al.,

2001, Boonme et al., 2006, Xu et al., 2010, Zhang and Zhong, 2010, Yi et al., 2012, Basheer et al., 2013, Qu et al., 2014, Sevcikova et al., 2014, Chouhan and Saini, 2016, Syed and Peh, 2018). In the water titration method, the mixture of oil and surfactant, at a ratio of 1:9, 2:8, 3:7, 4:6, 5:5, 6:4, 7:3, 8:2 and 9:1, was titrated by water at a set increment (normally 10%). A ternary phase diagram (TPD) can be accordingly created with each ingredient taking up one apex of the phase diagram. If the mixture system contains more than three components, a pseudo ternary phase diagram is used, with one corner of the diagram is a fixed ratio of two components. Nine dilution lines (Figure 2.3) exist on the ternary and pseudo ternary phase diagram, according to the ratio of oil to surfactant.

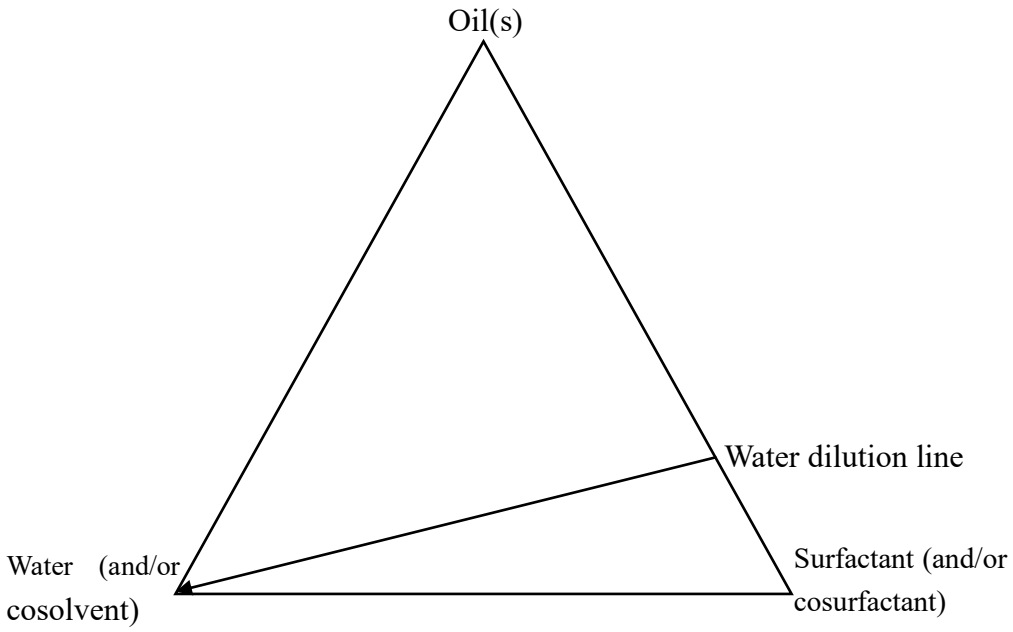

Figure 2.3 Schematic diagram of ternary or pseudo ternary phase diagram. Arrow means the direction of adding water to the mixture of oil(s) and surfactant (and/or cosurfactant).

In the literature, authors employed different ways to name the dilution line. Some used dilution line x : y where x : y meant the ratio of oil phase to surfactant(s) (with or without cosurfactant) (Zargar-Shoshtari et al., 2010). Some described dilution line as Nx which x meant the percentage of surfactant(s) (with or without cosurfactant) in the mixture of

oil and surfactant(s) (with or without cosurfactant) (Fanun, 2008). In this case, x was 10, 20, 30, 40, 50, 60, 70, 80 and 90. While, Dxy was employed by some other authors and x : y represented the ratio of surfactant(s) (with or without cosurfactant) to oil phase (Garti et al., 2006, Feng et al., 2009b). Along each dilution line, water is added dropwise into the mixture of oil and surfactant under continuous stirring, thereby water droplets are formed. If water content is higher than the critical amount, the coalescence rate of water droplets is higher than that of oil droplets, so phase inversion occurs. At phase inversion point, interfacial tension is minimum, resulting in the formation of small droplets (Fernandez et al., 2004). The mechanism of water titration method is shown in Figure 2.4.

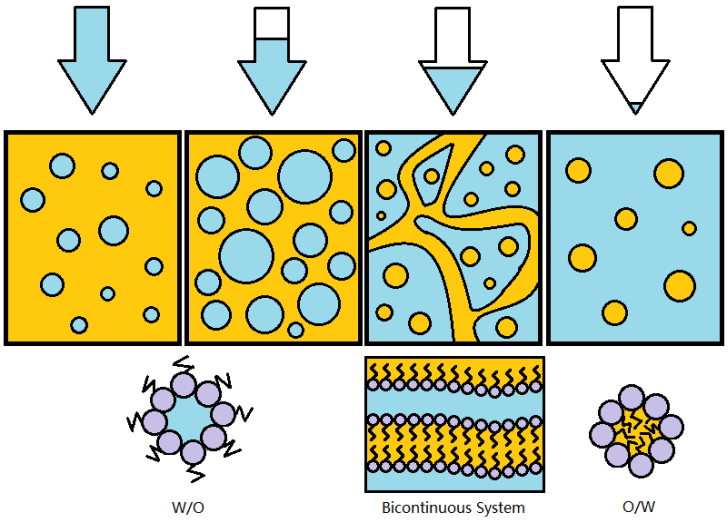

Figure 2.4 Mechanism of water titration method
Adapted from: McClements and Rao (2011)

2.4.1.4 Oil titration method

A few researchers tried to fabricate microemulsions by oil titration method (titration of surfactant and water mixtures with oil) (Garti et al., 2001, Flanagan et al., 2006, Rukmini et al., 2012). Hamed et al. (2012) successfully fabricated clove bud essential oil (CEO)- and eugenol-in-water microemulsions via the oil titration method. They at first prepared 5% Tween 20 micelle solution and then titrated the Tween 20 solution with CEO and

eugenol separately. The mixtures were then vortexed for 2 minutes before stored at 27 ± 2 °C for 24 hours. The experimental data showed that only 1.1% (v/w) CEO and 0.9% (v/w) eugenol could be incorporated in the 5% Tween 20 solution to fabricated the O/W microemulsions (Hamed et al., 2012). However, in another study, oil titration method was employed to form the W/O microemulsions by Rukmini and co-researchers. Specifically speaking, the mixture of Span 80, Span 20 and Tween 20 was mixed with water before they were titrated by dehydrated virgin coconut oil dropwise (Rukmini et al., 2012).

2.4.1.5 Other methods

It was also reported that oil phase (soybean oil and curcumin), surfactants (soybean lecithin and Tween 80) and deionized water when mixed together under constant stirring could fabricate microemulsions (Lin et al., 2012). On the other hand, cosurfactant titration method was utilized by Swaroopa et al. (2014) to fabricate microemulsions by IPM or oleic acid, Tween 80 or Cremophor RH 40, ethanol and water. In detail, water and surfactant were added to the oil phase to form an macroemulsion via stirring. After that, cosurfactant was added to the macroemulsion dropwise until a transparent solution (microemulsion) was fabricated. Hu and co-workers used both cosurfactant titration method and water titration method to prepare microemulsions with cyclohexane as the oil phase, isopropanol as the cosurfactant, water as well as different kinds of surfactants, including MOA-9 and Cremophor EL-10. They reported that the range of O/W microemulsions and W/O microemulsions in the pseudo ternary phase diagrams constructed by both methods were not significantly different from each other (Hu et al., 2019)

2.4.2 Formulations of microemulsion

Microemulsion system is comprised of aqueous phase, lipid phase and surfactant, while in some systems, the addition of cosurfactants and/or cosolvents is necessary.

Formulations of microemulsions in some researches are indicated in Table 2.8.

2.4.2.1 Lipid phase

Types and concentrations of lipid phase have a large effect on the formation and stability of microemulsions. According to Flanagan and Singh (2006), the formation of microemulsion with LCT, which have large molecular weight, is more difficult than making microemulsion with hydrocarbon mineral oils, since the long chain fatty acids in the LCT molecules are too large to penetrate into the interfacial films. As a result, most researchers who intended to study microemulsions normally used hydrocarbon mineral oils to replace triglycerides (Weiss et al., 1997, Weiss and McClements, 2000, Boonme et al., 2006, Basheer et al., 2013). In addition, MCT (Fanun et al., 2001, Roohinejad et al., 2015, Ho et al., 2019), essence oil (Ziani et al., 2012a, b, Yadav et al., 2018), monoglyceride (Thakkar et al., 2014) and diglyceride (Chen et al., 2013) were utilized in some researches. There were also some studies using LCT to fabricate microemulsions (Flanagan et al., 2006, Roohinejad et al., 2015, Subongkot and Ngawhirunpat, 2017).

Malcolmson et al. (1998) utilized the polyoxyethylene surfactants, C18:1E10 (polyoxyethylene-10-oleyl ether) and C12E10 (polyoxyethylene-10-lauryl ether) to make microemulsions via PIT method. Different types and concentrations of oils (three alkanes, three 1-alkenes, isopropyl myristate and two triglycerides) were used to investigate the effect of oil phase on microemulsion formation. If the surfactant used was C18:1E10, heptane has the shortest chain length, hence it was able to penetrate the interfacial film to the largest extent, resulting in the highest oil incorporation concentration (8% heptane incorporated in 20-22% surfactant). The lowest concentration of C18:1E10 to fabricate a microemulsion was 6%. While, if the chain length of hydrocarbon oil increased to 16 (hexadecane), the maximum oil concentration incorporated in the surfactant micelle solution was 5% and the lowest concentration of

C18:1E10 needed to form a microemulsion was 8%. Similarly, when using 1-alkenes, the incorporation of 1-heptene into the surfactant micelle was the highest, at about 8%, compared with 5% and 6% for 1- hexadecane and 1-octadecene. Besides, the formation area in the ternary phase diagram was similar for all these six hydrocarbon oils. If surfactant was isopropyl myristate, maximum oil incorporation concentration was 7% at 20% C18:1E10 and the minimum concentration of surfactant was 10%. As for triglyceride oils, soybean oil, which is LCT, had a higher maximum oil incorporation concentration than Miglyol 812, which is MCT, while the area in ternary phase diagram to form microemulsion with these two oils were similar. On the other hand, if using C12E10 as the surfactant, a microemulsion was formed only in a small area in ternary phase diagram when soybean oil was the lipid phase. In addition, since the chain length of hexadecane, 1-hexadecene, octadecane and 1-octadecene were 16 and 18, which were much higher than 12 in hydrophobic part of the surfactant, maximum oil incorporation concentration of these oils was very small. While if chain length reduced to 14 for isopropyl myristate, which is closer to chain length of the surfactant, maximum oil incorporation concentration was much higher and a much larger region in the ternary phase diagram could form microemulsion. With the further decrease of chain length to 7 (heptane and 1-heptene), the region where microemulsions could form was even larger.

Similarly, Warisnoicharoen et al. (2000) utilized three different types of triglycerides (tributyrin, soybean oil and Miglyol 812) and two different single-chain oils (ethyl ester of fatty acid oil) to fabricate microemulsion, stating that if the surfactant used was C12E10, oil with the smallest molecular volume had the highest maximum oil solubilization concentration. Nevertheless, if C18:1E10 was the surfactant, oil with the largest molecular volume tended to be solubilized to the greatest extent. The reason for this phenomenon may be because when using C12E10 as the surfactant, lower molecular volume oil can be incorporated into the surfactant micelles, which are nearly spherical, as a cosurfactant, while larger molecular volume oil cannot be readily incorporated since

soybean oil and Miglyol 812 have already existed in a spherical form. On the other hand, if the surfactant used was C18:1E10, oil with a very short chain may not be able to act as a cosurfactant, while it tended to locate towards the center of micelles.

Essential oils could also be employed to fabricate microemulsions (Xu et al., 2010, Edris and Malone, 2012, Chen et al., 2014, Cheng et al., 2017). According to Edris and Malone (2012), the major compounds of the essential oils could determine the solubilization of the oil into the microemulsion, but other small compounds had an effect as well. They found clove bud oil could formed the largest amount of microemulsions, which followed by thyme oil and oregano oil when they introduced these three phenolic-bearing essential oils to create ternary phase diagrams with Tween 20 or Tween 80 and water. The main compounds of clove bud oil, thyme oil and oregano oil were eugenol (85.29%), linalool (44.4%) and carvacrol (58.57%), respectively. Clove bud oil could form the largest amount of microemulsion was because unsaturated short-chain hydrophobic tail of eugenol could help to increase the mobility of the interfacial film. For thyme oil mixture system, linalool had a structure like surfactant, but its concentration was smaller than eugenol, then it formed fewer amount of microemulsions. However, carvacrol, which has a similar structure to eugenol, had a poor solubilization in microemulsion systems. Besides, pure carvacrol formed fewer amount of microemulsions compared to oregano oil (Edris and Malone, 2012).

2.4.2.2 Aqueous phase

In most studies, aqueous phase contained only water (Yang et al., 2017b, Nazari et al., 2019, Tang et al., 2019) or phosphate buffer solution (Roohinejad et al., 2015, Anoopinder et al., 2016, Ho et al., 2019). While, a few studies introduced cosolvent, including propylene glycol (PG) (Garti et al., 2001, Cheng et al., 2017), glycerol (Garti et al., 2001), into the aqueous phase. Polizelli and co-workers introduced sodium chloride (NaCl) into mixture systems which contained soybean oil, sodium bis-2-

ethylhexyl sulphosuccinate (AOT), L-α-phosphatidylcholine (PC) and water where the ratio of AOT to PC was 1:1. It was found that microemulsion area in the TPD of the mixture system without NaCl was 2.1%, while it increased to 6.6, 7.0, 8.2, 11.5 and 11.3% if 2%, 5%, 8%, 11% and 15% NaCl were previously dissolved in the aqueous phase (Polizelli et al., 2008).

2.4.2.3 Surfactant

Chemically, surfactants consist of both hydrophobic and hydrophilic groups which exhibit amphiphilic property (Whitehurst, 2004). Protein, polysaccharide emulsifiers and small molecular surfactants are generally utilized in the food industry. Emulsion stabilized with protein and polysaccharide emulsifiers, which are natural ingredients, is much safer than that stabilized with small molecular surfactants, which are synthetic. Protein and polysaccharide emulsifiers cannot be utilized to fabricate microemulsion alone, since only small molecular surfactants are able to generate ultralow interfacial tension at a particular monolayer curvature (McClements, 2012). Non-ionic surfactants have been normally utilized in researches because they have relatively low toxicity and irritation potential (Flanagan and Singh, 2006). The commonly used non-ionic surfactants are POE (polyoxyethylene oleyl ether, CmEn), polyoxyethylene ethers (e.g., Brji 30) and polyoxyethylene sorbitan esters (Tweens), labrasol (PEG-8 caprylic/capric glycerides) and sucrose esters. The effect of surfactant on the formation of microemulsion relies on the physicochemical structures of the surfactant. Apart from non-ionic surfactants, anionic (Szymula, 2004), cationic (Johnson and Shah, 1985) and zwitterionic (Patel et al., 2006, Chatzidaki et al., 2015) surfactants are also used to produce microemulsions.

HLB and CPP (Critical Packing Parameter) values can be introduced to choose a suitable surfactant. HLB is a value that indicates the affinity of surfactant for oil and water phase (Hasenhuettl and Hartel, 2008, McClements and Rao, 2011). The HLB value is

associated with the proportion of hydrophilic against hydrophobic parts in surfactants. The emulsifiers with low HLB value are usually used in the formation of W/O emulsions, while higher HLB value emulsifiers are used in the preparation of O/W emulsions (Liang, 2001).

On the other hand, CPP is short for critical packing parameter of the surfactant micelle. Equation 2.1 is used to calculate CPP:

$$\text{CPP} = \frac{v}{a \times l} \qquad [2.1]$$

On this equation, v is volume of the hydrophobic surfactant tail, a means the optimal area of the headgroup, and l represents chain length of hydrophobic tail. If surfactant molecules are associated with each other, they tend to form monolayers which have optimum curvature. At optimum curvature, the monolayer has the lowest free energy, any change in the optimum curvature, besides, needs the application of external energy. If CPP equals to 1, monolayers with zero curvature are favoured; if CPP is more than 1, optimum curvature tends to be concave, forming W/O emulsions; while if CPP is less than 1, optimum curvature tends to be convex, forming O/W emulsions (Flanagan and Singh, 2006, McClements and Rao, 2011). The change in temperature or composition may result in the alteration in CPP of the surfactant. If ionic surfactant is used to form the microemulsion, the addition of salts causes a reduction in hydrophilic headgroup area of the surfactant, thereby increasing the CPP value (Lawrence and Rees, 2012).

Fanun (2009) indicated the ability to fabrication monophasic microemulsions of oil, water and surfactant system was influenced by the chain length of the surfactant. They utilized different types of sugar esters to create ternary phase diagrams with peppermint oil and water, finding with the increase in the chain length of the surfactant, the formation of monophasic microemulsions reduced. Edris and co-worker had the same finding while they utilized Tween 20 and Tween 80 to fabricated microemulsions with three different types of essential oils (clove bud oil, thyme oil and oregano oil) and water.

They illustrated that mixture system with Tween 80 formulated fewer amount of microemulsions compared to that with Tween 20 regardless of the type of oil used. Besides, Tween 20 had a better ability to prevent the formation of liquid crystals compared to Tween 80. The reason for these phenomena was due to the shorter tail of Tween 20 which could interact more efficiently with the oils (Edris and Malone, 2012).

According to Lawrence and Rees (2012), double chain surfactants alone, such as didodcecyl ammonium bromide (DDAB) and AOT, which have small headgroups compared to their hydrophobic tails, are able to fabricate microemulsions. However, single chain surfactants alone are not able to fabricate microemulsions since they cannot decrease the interfacial tension sufficiently. The addition of cosurfactant is required for single chain surfactants. Some detailed information about cosurfactants will be discussed later in the following part. In addition, a second surfactant is added into the mixture system can be used to facilitate the formation of microemulsion. According to Patel et al. (2006), in a mixture system of a combination of Tween 80 and lecithin (ratio was 2:1 or 3:1), propylene glycol and ethyl oleate had a decreased liquid crystalline phase compared to that without Tween 80. And the microemulsion region for the mixture system with Tween 80 and lecithin was larger than that for the mixture system containing only lecithin.

2.4.2.4 Cosurfactant and cosolvent

In order to make microemulsions, high concentrations of surfactant are needed, which may cause the issue of bio-incompatibility (Alany et al., 2000). Most single chain surfactants are not able to reduce the interfacial tension small enough to fabricate a microemulsion (Lee, 2011). Cosurfactants were introduced by some researchers (Feng et al., 2009b, Zhang et al., 2009) to help in making microemulsions with decreasing concentration of surfactant. Cosurfactant, which is short or medium chain alcohol, amines or acids (Flanagan and Singh, 2006, Vaidya and Ganguli, 2019), is also an

amphiphilic substance, which can reduce interfacial tension (Gradzielski, 1998), but it cannot stabilize emulsions alone due to its small head group (McClements, 2005). Cosurfactant is miscible with the surfactant. Adding cosurfactant into the surfactant can further reduce the interfacial tension. Important functions of cosurfactant are that it is able to increase the fluidity of the interface and increase the mobility of hydrocarbon tail of the surfactant, making it possible for oil to penetrate between the surfactant tails. In addition, since it partitions between oil and water phases, it can affect the solubility properties of these phases. If ionic surfactant is used to prepare a microemulsion, the cosurfactant has the ability to reduce interactive repulsions between the charged headgroups of the surfactant (Lawrence and Rees, 2012). A cosolvent is a highly polar molecule which is not particularly surface active, but it can change the physicochemical properties of the surfactant (McClements and Rao, 2011) and change the properties of the aqueous phase, for example, viscosity and solubility (Komaiko and McClements, 2016). Normally used cosolvents was polyols, such as propylene glycol and glycerol. The term “cosurfactant” and “cosolvent” were sometimes mixed up in the literature. Xiao et al. (2013) and Salimi et al. (2014) referred to glycerol and PG as a cosurfactant, respectively.

When using POE surfactants to fabricate microemulsions, a cosurfactant was not necessary, as a microemulsion was formed by heating the surfactant/oil/water mixture system to 80 ℃ prior to cooling to room temperature (Flanagan et al., 2006). However, if lecithin was used as the surfactant, the addition of cosurfactant was necessary (Trotta et al., 1996, Flanagan et al., 2006). Lecithin is too lipophilic, as it has two long hydrocarbon chains it cannot form a zero mean curvature surfactant layer spontaneously, which is the basis to prepare bi-continuous microemulsions (Shinoda et al., 1991). Besides, an oil and water mixture system with lecithin as the only surfactant tends to form lamellar liquid crystals (Bergenstahl and Fontell, 1983). Cosurfactants can be used to increase the hydrophilicity of U-type microemulsions (appearance of the

microemulsion had no change with the increase in water concentration along one dilution line in the TPD), it can be partially incorporated in the polar parts of the surfactant layers to change the spontaneous curvature of the surfactant layers from being slightly curved towards water to be more planar or curved towards oil, and to decrease the stability of the lamellar liquid crystals, thus facilitating the formation of a microemulsion (Shinoda et al., 1991). However, if the microemulsion which contains cosurfactant is diluted, the cosurfactant may move from the interface to the continuous phase, resulting in the breakdown of the microemulsion. In addition, the use of some cosurfactants may cause toxicity and irritation, thus they cannot be used in the food industry (Flanagan and Singh, 2006). According to Patel et al. (2006), a cosolvent can be utilized to fabricate a microemulsion without the addition of cosurfactants. It is known that water, oil and lecithin mixture systems are not able to form microemulsions. Patel et al. (2006) employed propylene glycol (PG) as the cosolvent to replace 80% and 90% water and showed that these two formulations could form microemulsions, while most regions in the phase diagram could only form a liquid crystalline phase. However, if using PG as the aqueous phase, the region in the phase diagram that could form microemulsion was much larger.

Zhang and co-workers employed different types of short chain organic acids, such as propionic acid, acetic acid, butyric acid, hexanoic acid, sorbic acid, citric acid, lactic acid, as the cosurfactants with glycerol monolaurate, Tween 80 and water mixture system. Phase diagrams were created by titrating the oil-surfactant phase with the aqueous phase. They stated that without the addition of cosurfactants, microemulsions could not be fabricated. When propionic acid was introduced into the mixture system, microemulsions were formed and the increase in propionic acid concentration resulted in the formation of more microemulsions. Moreover, the increase in chain length of the short chain organic acids caused the formation of fewer microemulsions in the phase diagram (Zhang et al., 2009). Similar results have been found by Al-Malah et al. (2011),

who illustrated the addition of acetic acid (a weak electrolyte) to Tween 80-diethyl oxalate-water mixture system could fabricate more microemulsions in the pseudo ternary phase diagram than with propanoic acid. A strong electrolyte, such as NaCl and $CaCl_2$ did not have a significant effect on the formation of microemulsions (Al-Malah et al., 2011).

Xu et al. (2010) prepared a neem O/W microemulsion successfully with a combination of Tween-80 and sodium dodecyl benzene sulfonate (SDBS) acting as the surfactant. Three different alcohols, amyl alcohol, hexyl alcohol and heptyl alcohol were also used as the cosurfactants. Mixture systems with all these cosurfactants were able to form microemulsions. In addition, it was concluded from the pseudo ternary phase diagram they obtained that the region of microemulsions prepared with hexyl alcohol was a larger area than that of microemulsions prepared with amyl alcohol and heptyl alcohol. Moreover, Tween 80 and five different alcohols were utilized to prepare an isopropyl palmitate-in-water microemulsion by Basheer et al. (2013), who found that formulations with all these alcohols could fabricate microemulsions, and 1-butanol was the most suitable cosurfactant, followed by 1-pentanol and 1-propanol. While, 1-ethanol and 1-methanol were the least suitable cosurfactants, and the region for microemulsion formation was the same for them all. However, different findings were reported by Sevcikova et al. (2014) who showed the use of pentanol resulted in the largest microemulsion area of the mixtures of 1-monoacylglycerol of C10:0, Tween 80 and cosurfactant, while propanol acting as the cosurfactant lead to the smallest microemulsion areas compared to when butanol, ethanol and pentanol were used as the cosurfactants.

Table 2.2 Compositions of microemulsions in the literature

Lipid phase (encapsulated compound)	Surfactant	Cosurfactant/cosolvent	Reference
Isopropyl palmitate	Tween 20, 40, 60, 80	Methanol, 1-ethanol, 1-propanol, 1-butanol, pentanol	Basheer et al. (2013)
Isopropyl palmitate	Brij 97	1-Butanol	Boonme et al. (2006)
Soybean oil	EMD[a], POE, phospholipid	1-Propanol	Flanagan et al. (2006)
Isopropyl myristate	Soybean lecithin, Lysolecithin	Ethanol, 1-propanol, 1-butanol	Trotta et al. (1996)
Neem oil	Tween 80, SDBS[b]	Amyl alcohol, hexyl alcohol, heptyl alcohol	Xu et al. (2010)
Lemon oil	Sucrose monopalmitate ester, Tween 80	N/A	Rao and McClements (2012c)
n-Tetradecane,	Tween 20,40,60,80; polyoxyethylene-10-isooctylphenyl ether (Triton X-100)	N/A	Weiss and McClements (2000)
Glycerol monolaurate	Tween 80	Propionic acid	Zhang et al. (2008b)
Glycerol monolaurate	Tween 80	Propionic acid, acetic acid, butyric acid, hexanoic acid, sorbic acid, citric acid, lactic acid	Zhang et al. (2009)
Beta-carotene	SDS	Pentanol	Szymula (2004)
n-octane	C12E5	N/A	Burauer et al. (2003)
Diacylglycerol Oil	Mixtures of decaglycerol monolaurate, hexaglycerol trioleate, Tween 80, Span 80, sucrose ester and sodium caseinate	Sorbitol	Chen et al. (2013)
Peppermint oil	Tween 80	Ethanol, n-propanol, n-butanol	Chen et al. (2014)
Sweet fennel oil	Mixture of Tween 20 and Span 80	N/A	Barradas et al. (2015)
Cinnamon oil	Tween 80	Ethanol	Wang et al. (2014)
Spearmint oil, orange oil, Capmul MCM EP[c]	Mixture of Tween 20 and labrasol, Tween 20, mixture of Tween 20 and Tween 60	PG	Cheng et al. (2017)
1-monoacylglycerol of C10:0, C11:0, C12:0 and C14:0	Tween 80	Ethanol, propanol, butanol, pentanol	Sevcikova et al. (2014)

Cassia oil	Tween 80	Ethanol	Xu et al. (2012)
Soybean oil (curcumin)	Soybean lecithin, Tween 80	N/A	Lin et al. (2012)
Limonene	Tween 60	Butanol	Zhang and Zhong (2010)
Adlay seed oil, mixture of adlay seed oil and Labrafil M 1944 CS (triterpene)	Cremophor RH40	PEG[d] 400	Qu et al. (2014)
Olive oil	Mixture of Tween 80 and Span 20	PG	Salimi et al. (2014)
Peppermint oil (beta-carotene)	Mixture of Tween 20 and sunflower lecithin	N/A	Chen and Zhong (2015)
Soybean oil (ascorbic acid, folic acid, ferrous sulfate, sodium acetate, NaCl)	Mixture of AOT and phosphatidylcholine, mono-olein, mixture of mono-olein and AOT	N/A	Polizelli et al. (2008)
Ethyl ester fish oil, triglyceride fish oil (CoQ10)	Tween 80	PG	Deutch-Kolevzon et al. (2011)
Ethyl butyrate, ethyl caprylate, ethyl oleate, n-octane (vitamin E)	Cremophor EL-35	PG, ethanol	Feng et al. (2009b)
Mixture of dodecane and pentanol	Octaethylene glycol monododecyl ether (C12E8)	N/A	Ezrahi et al. (1997)
Capryol 90 (phyllanthin)	Cremophor RH 40	Transcutol P	Hanh et al. (2015)
Diethyl oxalate	Tween 80	Isopropyl glycol	Al-Malah et al. (2011)
Peppermint oil (CoQ10)	Mixture of Tween 20 and sunflower lecithin	N/A	Chen et al. (2015)
Ethyl butyrate (artocarpanone, ascorbic acid)	Tween 80	PEG[d] 400	Dong et al. (2016)
Limonene	Sodium oleate	Citronellol, ethanol	Klossek et al. (2014)
R (+)-Limonene, MCT	Tween 60, 80, Brij 96V, triglyceride monooleate, L1695	Ethanol, PG, glycerol	Garti et al. (2001)
Jojoba oil (lycopene)	Brij 96V	Hexanol	Garti et al. (2004)
R (+)-Limonene	Tween 80	Mixture of ethanol and glycerol	Amar et al. (2004)
Lauryl alcohol (ketoconazole)	Labrasol	Ethanol	Patel et al. (2011)
IPM	Mixture of Tween 80 and lecithin	N/A	Moreno et al. (2003)
Monolaurin	Tween 20	Pentanol, dodecanol	Fu et al. (2009)

Monolaurin	Tween 20, Tween 80, mixture of Tween 20 and Tween 80	Mixture of Pentanol and dodecanol	Fu et al. (2008)
Peppermint oil	Sugar caprate, sugar laurate, sugar stearate, EMDG[a], Tween 80	N/A	Fanun (2009)
Jojoba oil	Brij 96V, Tween 20, 60, 80,	Ethanol, butanol, pentanol, hexanol, heptanol, octanol	Shevachman et al. (2004)
Labrafil M 1944 CS (carbamazepine)	Accenon CC	Transcutol P	Patel et al. (2012)
Capryol 90 (curcumin)	Cremophor RH40	Transcutol P	Hu et al. (2012)
Capmul PG-8[e], Capmul PG-12[f], Captex 200P[g], Capmul PG-2L[h]	Cremophor EL	N/A	Prajapati et al. (2011)
Virgin coconut oil	Mixture of Span 80, Span 20 and Tween 20	N/A	Rukmini et al. (2012)
a-Linolenic acid	Mixture of Span 80 and Cremophor EL	N/A	Liu and Wang (2010)
Oleic acid	Tween 20	Ethanol	Deng et al. (2015)
D-limonene	Isotridecanol ethoxylate-6	Isopropanol	Yang et al. (2014)
Oleic acid (garlic oil)	Cremophor RH40	Ethanol, n-butanol	Zheng et al. (2013a)
Sunflower oil, high oleic sunflower oil	Tween 80	Ethanol	Fasolin et al. (2012)
Labrafac lipophile WL 1349, soybean oil, Labrafil M1944 CS (myricetin)	Mixture of Tween 80 and Cremophor RH40	Transcutol HP	Guo et al. (2016)
Clove bud oil, thyme oil, oregano oil	Tween 80, Tween 20	PG, ethanol	Edris and Malone (2012)
IPM	Egg lecithin, soya lecithin	Ethanol	Ruth et al. (1995)
IPM, lemon oil, isoamyl acetate	Tween 20	Glycerin	Aboudzadeh et al. (2018)
Capmul PG-8[e]	Cremophor EL	Transcutol P	Chouhan and Saini (2016)
Orange oil (ramipril)	Tween 80	PG	Yadav et al. (2018)
Ethyl oleate (resveratrol)	Labrasol	Polyglyceryl-6-isostearate	Juškaitė et al. (2015)
Capmul MCM	Tween 80	PEG[d] 400	Thakkar et al. (2014)
IPM (Cefaclor monohydrate)	3:1 Mixture of Span 80 and Tween 80	PG	Ozturk and Guven (2019)

IPM (resveratrol)	Cremophor RH40	PEG[d] 400	Tang et al. (2019)

[a]EMD or EMDG: ethoxylated mono- or diglycerides
[b]SDBS: sodium dodecyl benzene sulfonate
[c]Capmul MCM EP: C8/C10 mono-/diglyceride
[d]PEG: polyethylene glycol
[e]Capmul PG-8, [f]Capmul PG-12, [g]Captex 200P and [h]Capmul PG-2L: PG monocaprylate, PG monolaurate, PG dicaprylocaprate and PG dilaurate, respectively.

2.4.3 Characterization of microemulsion

If the microemulsion is fabricated by the emulsion dilution method, then it must be an O/W microemulsion. In the literature, only particle size, PSD and turbidity were measured to characterize the microemulsions prepared by this method (Rao and McClements, 2012c, Ziani et al., 2012b).

On the other hand, as mentioned earlier, ternary phase diagrams or pseudo ternary phase diagrams were introduced to study whether water-oil-surfactant (and cosurfactant/cosolvent) mixture systems with different formulations lead to the formation of a clear isotropic one phase microemulsion or other structures (coarse colloidal dispersions, some liquid crystalline phases and gels) (Zargar-Shoshtari et al., 2010). Characterization of microemulsions is carried out to determine phase behaviour of microemulsions with different formulations. This method is comprised of two levels, a macroscopic level and a microscopic level. At the macroscopic level, visual inspection, viscosity and electrical conductivity measurements are introduced (Flanagan and Singh, 2006, Zargar-Shoshtari et al., 2010). On the other hand, microstructure of the microemulsion is determined in the microscopic level (Flanagan and Singh, 2006). Visual inspection is the simplest technique and is used to distinguish microemulsions from coarse colloidal dispersions, liquid crystals and gels (Zargar-Shoshtari et al., 2010).

2.4.3.1 Optical property

The appearance of an emulsion is dependent on the way it interacts with electromagnetic radiation in the visible region of light spectrum (Chantrapornchai et al., 1998).

Microemulsion is a transparent solution. Visual inspection was generally employed by researchers to construct the TPD in the water titration method (Xiao et al., 2013, Qu et al., 2014, Guo et al., 2019a). However, apart from visual inspection, turbidity was also measured by a UV/visible spectrophotometer in some literature (Rao and McClements, 2011, Rao and McClements, 2012c). In a study conducted by Rao and McClements (2012c), 10% lemon oil emulsion was added into 1% SMP solution and the turbidity of the emulsion decreased steeply in the first 200 seconds, then decreased slightly from 200 to 600 seconds, and remained constantly afterwards. The reduction in turbidity meant that lemon oil droplets scattered less light, which was due to the decrease in lemon oil concentration and/or the reduction in particle size (Rao and McClements, 2012c).

2.4.3.2 Electrical conductivity

Electrical conductivity is employed to determine whether a microemulsion is oil-continuous or water-continuous (Flanagan and Singh, 2006). It is an indication of the percolation threshold or PIT. Published literature included conductivity measurement to characterize the mixture system, to be as an indicator for phase inversion (Shevachman et al., 2004, Fanun, 2010, Zargar-Shoshtari et al., 2010, Deutch-Kolevzon et al., 2011, Cheng et al., 2017). One or more dilution lines were chosen to determine the change in conductivity with the addition of water. Some researchers directly measured the conductivity of the mixture system (Shevachman et al., 2004, Klossek et al., 2014, Cheng et al., 2017), while some researchers added a small amount of NaCl into the non-ionic system to better detect conductivity changes (Fanun, 2010, Deutch-Kolevzon et al., 2011). They claimed the addition of an electrolyte with small quantity to the system did not have any influence on the area of microemulsion region.

Boonme et al. (2006) constructed a water/IPP (Isopropyl palmitate)/Brij 97+1-bunanol (2:1) pseudo ternary phase diagram using the water dilution approach and utilized a Riac CM/100 conductivity meter fitted with an YSI 3418 electrode to determine electrical

conductivity. The results showed that when water concentration was less than 10%, conductivity of the mixture system was very low, which illustrated that water mobility was restricted (Fanun, 2007), thus the system was oil continuous. The conductivity significantly increased if the water content increased from 10% to 30%, at which point the conductivity increased sharply. The sharp change in conductivity at 30% water content may be due to the transition of an oil continuous microemulsion (W/O) to a water continuous microemulsion (O/W).

Similar trends of conductivity change have been reported by Zargar-Shoshtari et al. (2010), who measured conductivity of IPM, Cremophor EL, Imwitor and water mixture systems as well as Myritol 318, Tween 85, Transcutol P, Imwitor and water mixture systems as a function of water content. In the Cremophor EL system, along the dilution line 7:3, the viscosity was very low initially and slowly increased until 10% water concentration. The viscosity steeply increased up to 40% water content, which was slightly increased until reaching a plateau. Zargar-Shoshtari et al. (2010) illustrated the maximum viscosity change existed when water concentration was about 23%. This critical point (maximum viscosity change) is also known as the percolation threshold (φ_c) point, at which W/O microemulsion transition to bi-continuous or O/W microemulsions. φ_c is calculated from the electrical conductivity ($d\sigma$) relative to change in water content ($d\varphi$) and this value changes in different mixture systems. Along the dilution line 5:5, φ_c was 31%, while it was 21% and 25% along the dilution line 6:4 and 8:2 respectively for a Tween 85 mixture system. The increase in φ_c with the increasing surfactant concentration may be due to the increase in hydration of ethylene oxide groups caused by the greater interaction of water molecules with surfactant head groups (Zargar-Shoshtari et al., 2010).

However, a mixture system of vitamin E/ethyl butyrate/ Cremophor EL-35/ethanol/water along the dilution line D82 (Wvitamin E/ethyl butyrate : WCremophor

EL-35/ethanol = 2:8), conductivity increased quickly when water concentration increased from 0% to 28%, which kept constant when water concentration was between 28% and 40% and decreased substantially when water concentration was more than 40%. Thus, at less than 28% water content, the system was a W/O microemulsion and at greater than 40% water content, the system was an O/W microemulsion. Bi-continuous microemulsion existed when the water content was between 28% and 40% (Feng et al., 2009b).

2.4.3.3 Viscosity

Distinct mixture structures have different viscosities. A microemulsion is a Newtonian liquid with low viscosity while a lamellar liquid crystal is a non-Newtonian structure with relatively high viscosity. In addition, O/W microemulsions have a lower viscosity than W/O microemulsion, since in W/O microemulsion this oil is the continuous phase, which can have a higher viscosity than water (Zargar-Shoshtari et al., 2010). Similar to conductivity, viscosity could also be an indicator of phase transition (Shevachman et al., 2004, Feng et al., 2009b, Deutch-Kolevzon et al., 2011).

A rotational viscometer was used to measure the viscosity of a water/sucrose laurate (L1695)/ ethoxylated mono-di-glyceride (EMDG)/(IPM + ethanol) mixture system as a function of water content by Fanun (2007). The weight ratio of (L1695 + EMDG) and (IPM + ethanol) was 4:6 and weight ratio of (L1695/EMDG) and (IPM/ethanol) was 5:5. The author demonstrated that viscosity change depended on the alteration in structure of the mixture system. At a water content below 20%, the viscosity of the mixture system increased, and spherical droplets changed to non-spherical larger droplets. By increasing the water content from 20% to 60%, the system viscosity decreased due to the movement of surfactants to the water-oil interface in a bi-continuous structure. When the water content was increased above 60% there was a slight increase in viscosity due to a change from a bi-continuous microemulsion to O/W microemulsion, this was followed by a

sharp decrease in viscosity with further water addition as there was a decrease in the inter-droplet interactions.

Besides, Zargar-Shoshtari et al. (2010) constructed a pseudo ternary phase diagram for IPM/Cremophor EL/Imwitor/water mixture system and studied dynamic viscosity change as a function of water content alteration. Along the dilution line 7:3, viscosity of the system increased from 18 mPa/s to 34 mPa/s as water content increased to 20%, which was followed by a gradual reduction in viscosity with the further increase in water content. They also stated that the highest viscosity existed in water content 20% was due to the presence of two different colloidal structures. That is to say, when water concentration was 20%, W/O microemulsion altered to bicontinuous microemulsion or O/W microemulsion. Similarly, when the ratio of vitamin E and ethyl butyrate to Cremophoer EL-35 and ethanol was 2:8 in the microemulsions, viscosity increased gradually when water content was between 10% and 30% and increased dramatically when water content was about 30%. The maximum viscosity existed when water content was 40% and it reduced substantially after that (Feng et al., 2009b).

2.4.3.4 Microstructure

Though the preparation of microemulsions is simple, characterization of their microstructure is quite complicated. Many methods are required to fully characterize the structure of a microemulsion (Flanagan and Singh, 2006). The already discussed electrical conductivity and viscosity are two of the attributes which can be used to identify microemulsion structures (Podlogar et al., 2004, Boonme et al., 2006, Zargar-Shoshtari et al., 2010). In addition, nuclear magnetic resonance (NMR), small-angle neutron scattering (SANS), small-angle X-ray scattering (SAXS), electron microscopy (EM), differential scanning calorimetry (DSC) and polarized light microscopy were employed in literature to characterize the microstructure of microemulsions (Moulik and Paul, 1998, Mittal and Kumar, 1999, Glatter et al., 2001, Shukla et al., 2002, de Campo

et al., 2004, Podlogar et al., 2004, Boonme et al., 2006, Fanun, 2007, 2008).

NMR NMR technique is applied to determine phase structures, micellar size and shape, counterion binding, hydration, solubilization and etc (Moulik and Paul, 1998, Mittal and Kumar, 1999). NMR-active nuclei, 1H and 13C are usually measured in the researches, which can be found in most surfactant molecule. NMR method measures self-diffusion coefficient (D) of each component in the mixture system. By simply obtaining self-diffusion coefficients of oil and water, it is able to elucidate whether a microemulsion is O/W, W/O or bicontinuous microemulsion (Mittal and Kumar, 1999):

W/O microemulsion: Dwater << Doil and Doil is close to D0oil (D0 means self-diffusion coefficient of pure solvent);

O/W microemulsion: Doil << Dwater and Dwater is close to D0water;

Bicontinuous microemulsion: Doil and Dwater both high.

Mittal and Kumar (1999) also calculated the relative diffusion coefficient, D/D_0, of water and oil. If the value of D/D_0 for water and oil is of the same order of magnitude, it is possible that the microemulsion is bi-continuous. On the contrary, an O/W or W/O microemulsion exists if D/D_0 values of water and oil have a difference of one order of magnitude or more.

A microemulsion prepared with water, mixed surfactants (EMDG+L1695 1:1 w/w) and R (+)-limonene has been studied along the dilution line N60 by pulsed gradient spin echo nuclear magnetic resonance (PGSE-NMR) by Fanun (2008). According to the criteria described above, when water percentage was less 20% and more than 70%, the system was a W/O microemulsion and O/W microemulsion, whilst the system had a bi-continuous structure with water percentage between 20% and 70%. Moreover, at 0.10 water volume fraction, diffusion coefficients for L1695 and EMDG were very low. The

diffusion coefficient value for L1695 increased with increasing water volume fraction up to 0.90, while at this point, the diffusion coefficient value for EMDG stayed the same as that in 0.10 water volume fraction. This phenomenon indicated that EMDG was in the centre of the hexagonal arrangement which was bordered by L1695.

Krauel et al. (2005) prepared microemulsions by mixing ethyl oleate, mixed surfactants (sorbitan monolaurate and Tween 80), butanol and water. Three samples (SOR 4:6 with 10% water, SOR 6:4 with 30% water and SOR 9:1 with 10% water) were measured using the self-diffusion NMR method. The self-diffusion coefficients of water, oil and surfactant in each sample were measured and these values were compared with self-diffusion coefficients measured for neat components. In a sample with the composition s/o 4:6 and 10% water, oil had the highest diffusion coefficient and water and surfactant had slower diffusion coefficients, it was considered to be a W/O microemulsion. For a sample (SOR 6:4, 30% water), diffusion coefficients for oil and water were similar and the surfactant had a slower diffusion coefficient, it was considered to be a continuous microemulsion. While in the last sample, water diffused faster than oil and both water and oil had a higher diffusion coefficient than surfactant, so the sample was determined to be a solution, not an O/W microemulsion, in which oil and surfactant diffused at the same speed.

SANS and SAXS Light scattering, SANS and SAXS are three different categories of scattering techniques. In scattering approaches, an incident radiation beam is applied to the sample and the receptor is used to record the intensity and angle of the beam which is scattered by the sample in order to measure the size, shape or structure of the sample (Acharya and Hartley, 2012). SANS and SAXS, the combination of which is named as small angle scattering, are important methods to study size, shape and internal structures of microemulsions. In small angle scattering, incident beam of X-ray or neutron is scattered by the sample at a small angle of 0.1 to 10 º close

to the original beam (Singh, 2017). Moreover, the two types of scattering radiation (neutron and X-ray) are sensitive to different physical properties of the sample. SANS uses neutron, which has a wavelength of approximately 0.5 nm, to interact with the atomic nuclei of the sample. While, SAXS uses X-ray, which has a wavelength of 0.1-0.2 nm, to interact with the electron shells of the sample (Schroffenegger and Reimhult, 2019). The scattering length densities of the particles and the solvent determine the scattering intensity (Fanun, 2008). As for SANS, the scattering length must be obtained experimentally, since it is a complicated function of the atomic number. While in the SAXS approach, scattering length density is proportional to the electron density, which is a linear function of the number of electrons (Glatter et al., 2001).

Teubner and Strey model was normally introduced by researchers to analyze scattering data (Regev et al., 1996, Ezrahi et al., 1997, Kohling et al., 2002, Fanun, 2008). It fits with bicontinuous structure (Fanun, 2010) and gives two variables, namely repeat distance (also called periodicity) and correlation length to describe the microstructure (Acharya and Hartley, 2012). On the other hand, Feriberger and co-workers introduced Generalized Indirect Fourier Transformation (GIFT) model, in which scattering intensity is determined by the form factor P(q) and structure factor S(q). They also indicated that GIFT model could be applied in globular microemulsions as well as bicontinuous microemulsions (Freiberger et al., 2007). However, Podlogar et al. (2004) pointed out the GIFT model could not fit to the sharp peak which was developed at low q (scattering vector) values.

Shukla et al. (2002) used SANS method to measure the particle size of O/W microemulsions, which were composed of mixed surfactants, different types of pharmaceutical oils and a PG/H2O. The results showed that very small particle size, around 10 nm, was observed for the microemulsions. Besides, SANS technique was employed by de Campo et al. (2004) to investigate the microstructure of dense

microemulsions, which contained Tween 80, R (+)-limonene, ethanol glycerol and water and the effect of each component on the microemulsion. They stated that Tween 80 micelles were slightly elongated in water, with a maximal diameter of 13 nm, and its head group region was hydrated. The addition of R (+)-limonene swelled micelles, making them a little more globular. In addition, ethanol could be redistributed into the interface and helped reducing the aggregation number of Tween 80 molecules in the micelles, resulting in the shrink of micelles. However, they pointed SANS could not detect bicontinuous structures, which should be measured by self-diffusion NMR.

Podlogar et al. (2004) introduced SAXS technique with GIFT model to study the microstructure of water/Tween 40/Imvitor 308/IPM system. They indicated that scattering was very weak when the mixture had no water, and it substantially increased with the addition of water. And, at 25% water percentage, the maximum scattering intensity reached, which was reduced afterwards with the increase in water content. They illustrated with the addition of water, W/O droplets converted from rod-like micelles, cross-section and maximal dimensions of which were 5 and 14 nm, to more spherical droplets. On the other hand, Fanun (2008) used Teubner and Strey equation to obtain the values of periodicity and correlation length of the mixture system of EMDG/L1695/R (+)-limonene/ water along the dilution line N60. They found that the scattering curve had a single intensity maximum $q \neq 0$, which was followed by a high-angle tail. Besides, with the increase in water content, the position of the maximum moved to a lower angle. Periodicity and correlation length increased with the increase in water content in the beginning, but the growth rate of correlation length was smaller than that of periodicity. Correlation length reached its maximum when water concentration was about 30%, and d increased over the whole range of water dilution (Fanun, 2008).

Electron Microscopy (EM) EM involves transmission electron

microscopy (TEM) and scanning electron microscopy (SEM). TEM is a useful method to study the microstructure of microemulsions, since it is able to produce images directly at high resolution (Mittal and Kumar, 1999). Cryo-TEM technique and freeze-fracture TEM (FFTEM) technique (Vinson et al., 1991) were employed by researchers to determine the microstructure of microemulsions. FFTEM, which includes cryofixation, cryofracture, fractured surface replication with a thin carbon film and replicate cleaning, is a type of cryo-TEM (Gulik-Krzywicki, 1997). In cryofixation step, the sample must be frozen rapid enough to avoid phase separation, crystallization and etc. (Gulik-Krzywicki, 1997). FFTEM method is also named as FE-EM (freeze etching electron microscopy) method (Feng et al., 2009b). But in cryo-TEM the sample was frozen directly, without any replica, before directly imaged (Belkoura et al., 2004). Regev et al. (1996) studied the structure of system containing a 1:1:2 oil/alcohol/surfactant weight ratio along the water dilution line using cryo-TEM method. They found that the system exhibited spherical swollen micelles at high water content. If water percentage declined to 60%, the local ordering of the closely packed spherical swollen micelles occurred. When water content was 40% and 50%, various striated structures of distinct length, thickness and order took the place of spherical structures. The structure of sample containing 30% and 20% water was similar to that containing 50% and 40% water. In addition, a ternary system of triglyceride/monoglyceride/water was established by Gulikkrzywicki and Larsson (1984) and FFTEM was employed to measure the system microstructure, which illustrated that microemulsion showed oriented stacks of small smooth lamellae and liquid crystalline exhibited extended, regularly stacked, smooth fractured lamellae.

SEM is not normally used to determine the microstructure of microemulsions due to the invasive sample preparation (Acharya and Hartley, 2012). However, FESEM Cryo-field emission scanning electron microscopy (cryo-FESEM) was introduced by Boonme and co-workers to study the structure of microemulsion samples. Unlike conventional SEM

which heats a tungsten wire filament or a Lanthanum Hexaboride (LaB6) filament to generate and release electrons, FESEM employs a field emission cathode with a very sharp tungsten wire tip (diameter < 100 nm) at one end (Joy, 2019). In the FESEM approach, an electron beam after the cathode is placed in a negative potential and the electrical field at the tip reaches approximately 10 volts/nm, rather than applying heat to the cathode (Joy, 2019). In FESEM approach, electron beam emission happens after the cathode is placed in a negative potential and the electrical field at the tip reached about 10 volts/nm, rather than applying heat to the cathode (Joy, 2019). when It was shown by Boone and co-workers that no globular structures were found by cryo-FESEM when water content was less than 15%, above which microemulsion with globular structures could be detected. But they also illustrated that cryo-FESEM could not determine whether the globular microemulsion was W/O or O/W (Boonme et al., 2006). Though the sample preparation process in cryo-FESEM is only comprised of freezing and fracturing, the formation of ice crystals while transferring samples can sometimes happen (Acharya and Hartley, 2012). Thus, extra attention should be paid to differentiate the ice droplets and microemulsion particles. Boonme et al. (2006) explained ice droplets exist on the surface of the mixture system instead of embedding into the system, which helps to distinguish microemulsion droplets from ice contamination.

DSC DSC method is based on the fact that the structure or composition of a material alters when it is heated or cooled. This change is always accompanied by the exchange of heat. DSC is a method to measure the heat flow into or out of a material when it undergoes a controlled temperature change (Alexander et al., 2019). Boonme et al. (2006) Mapped DSC curves of pure water, pure IPP and mixture system of IPP/water/Brij 97:1-butanol (2:1) with different concentrations of water. They illustrated that there was a large exotherm at -18 ^{o}C and an endotherm at 0 ^{o}C of pure water. When water content was less than 30%, no exotherm was detected of the DSC curves of the mixture system. But when water content was more than 30%,

exotherm was detected and it moved towards -18 ° C with the increase in water concentration. Besides, pure IPP had a exotherm at 8° C and an endotherm at 12 °C. In terms of the mixture system, exotherm and endotherm peaks of IPP could be detected when water content was 0% to 25%, and became smaller with the increase in water concentration, due to the dilution of IPP. When water concentration was between 30% and 35%, IPP peaks disappeared. Thus, it could be concluded that when water content was between 30% and 35%, water transferred from the internal phase into the external phase, namely, W/O microemulsion altered into O/W microemulsion (Boonme et al., 2006).

Polarized light microscopy Polarized light microscopy is a simple way to distinguish liquid crystal from microemulsion. According to Basheer et al. (2013), the phenomenon of birefringence appears when observing anisotropic liquid crystal under polarized light microscope, in which some parts of the sample are dark and others are light. Conversely, it appears dark if the sample is microemulsion due to its isotropic property.

Other characterization methods Apart from the aforementioned methods, there are some other methods which can be employed to study the structure of microemulsions, such as electron paramagnetic resonance (EPR) spectroscopy (Kalaitzaki et al., 2015), Fourier transform infrared spectroscopy (FT-IR) (Hao et al., 1997, Zargar-Shoshtari et al., 2010) and etc. EPR spectroscopy uses an adequate spin probe to study the interfacial properties of the surfactant monolayer. Kalaitzaki and co-workers analyzed EPR data to obtain the values of order parameters and rotational correlation times, finding these two values increased with the increase in water content in one dilution line, which indicated that rigidity of the surfactant monolayer increased (Kalaitzaki et al., 2015).

Zargar-Shoshtari et al. (2010) determined using FT-IR spectroscopy the percentages of free water (water molecules interact with each other), bound water (water molecules interact with surfactant head group) and trapped water (non-hydrogen-bonded monomers trapped between surfactant tails) of the cremophor EL/water/IPM/Imwitor along the dilution line 7:3, finding that bounded water was relatively higher compared to the other two in the initial. With the increase in water content, surfactant head groups started to become saturated, resulting in the interaction of water molecules, so free water concentration increased while bound water concentration reduced. In the meantime, the percentage of trapped water, 10% of the total water content, did not change within the whole dilution range.

2.4.3.5 Particle size and PSD

Dynamic light scattering (DLS) and static light scattering (SLS) techniques are generally employed to measure the particle size and PSD of an emulsion. The principle of DLS technique is to measure the intensity fluctuations which occurs when light is scattered by particles that move randomly due to Brownian movement. The DLS technique measures the intensity of the scattered light which is detected at a fixed angle or several scattered angles. The scattered light intensity is then translated, via its correlation function, into the diffusion coefficient of particles (D) which is used to calculate the radius of particles (r) using the Stokes–Einstein equation (Equation 2.2).

$$\mathrm{r} = \frac{kT}{6\pi\eta\mathrm{D}} \qquad [2.2]$$

where k is the Boltzmann constant, T the temperature in kelvin and η the viscosity of the aqueous phase (cP). DLS can measure particles with diameter between 3 nm and 5 μm (McClements, 2007). When a laser beam passes through an emulsion, droplets in emulsion scatter this laser beam.

Instruments that base on SLS technique have a Mie theory mathematical model, which can predict the scattering pattern of an emulsion that relies on particle size and PSD of

the emulsion. Particles of diameter range from 100 nm to 1000 μm are able to be measured by SLS technique (McClements, 2007). Therefore, dynamic light scattering was generally employed to determine the particle size and PSD of microemulsions (Zargar-Shoshtari et al., 2010, Deutch-Kolevzon et al., 2011, Zheng et al., 2013a). PSD of microemulsions normally only have one peak, which is not the case of nanoemulsions and macroemulsions, the PSD of which can have one peak or sometimes multiple peaks can be narrow or broad (McClements, 2012).

Before the measurement of particle size and PSD, a microemulsion is diluted to avoid any particle interaction (Shevachman et al., 2004), but the microemulsion may breakdown with water dilution (McClements, 2012). According to Kalaitzaki et al. (2015), particle size determination of the concentrated microemulsion in the oil-rich region was not possible because it contained a high concentration of surfactant. So, it is well documented that so-called U-type microemulsions were chosen to determine their particle size and PSD (Shevachman et al., 2004, Kalaitzaki et al., 2015). With the addition of water, a W/O microemulsion changes into an O/W microemulsion gradually and continuously without any phase separation, then these isotropic regions will form U-type microemulsions, which are also named as water dilutable microemulsions (Amar et al., 2004).

According to Kalaitzaki et al. (2015), who measured the particle size of R-(+)-limonene/Tween 20/ethanol/PG/water system along the dilution line 7:3 via the DLS method, the particle diameter reduced from 15 to 8.2 nm with an increase in water concentration from 70% to 90%. This was because when water concentration was lower, the attractive interactions between the dispersed oil droplets caused droplet aggregation (Kalaitzaki et al., 2015).

Characterization of all the above properties provides useful information of phase

behaviour of the mixture systems with different formulations of water, oil, surfactants with or without cosurfactants, thereby a ternary phase diagram or pseudo ternary phase diagram can be completely.

2.4.3.6 Stability

A microemulsion is a thermodynamically stable system under a certain condition, meaning it tend to keep kinetically stable forever if the initial condition does not change (McClements, 2012). However, if any of this condition was changed, for example, the temperature was increased, the microemulsion might become unstable (McClements, 2012). Remaining stable is quite necessary in order that the microemulsion is to be applied to food products. Some researchers employed a centrifuge to evaluate the stability of a microemulsion (Juškaitė et al., 2015, Shaaban et al., 2015, Yang et al., 2017b). Juškaitė et al. (2015) also used heating-cooling and freeze-thaw cycles to determine whether a microemulsion was thermodynamically stable. Specifically speaking, the tested microemulsions were stored at 4, 20, 32 and 45 ºC for more than 2 days in the heating-cooling cycle, and at -21, 4 and 25 ºC in the freeze-thaw cycle. The microemulsion was considered to be stable if a microemulsion was still transparent without any phase separation (Juškaitė et al., 2015). On the other hand, Guo et al. (2016) diluted the microemulsion for 100 and 200 times to study its stability via visual inspection.

Valoppi and co-workers fabricate lemon oil microemulsion with Tween 80, NaCl solution, lemon oil and peanut oil by PIT method. They diluted the microemulsion with acidic solution with different pH values (2.1, 3.0 and 4.6), stored them at 20 ºC and measured their absorbance values. The results showed the microemulsion was stable after diluted by acidic solution since no phase separation happened and the turbidity value kept low during storage (Valoppi et al., 2017).

2.5 Microemulsion as a delivery system for lipophilic bioactive compounds

Bioactive compounds are “nutritional” substances which naturally exist in small quantities in foods and are produced in vivo or by food-processing operation (Kitts, 1994). There are a variety of bioactive compounds available, which are different in the physicochemical and physiological properties due to their distinct molecular properties (McClements et al., 2007). Due to their health-promoting properties, bioactive compounds have attracted considerable interest in a number of fields, such as food, pharmaceuticals, cosmetics. However, bioactive compounds used as functional ingredients in foods are limited due to their poor solubility, chemical instability, and undesirable sensory attributes (e.g. astringent, bitter, off-odours), leading to poor oral bioavailability as well as reduced consumer acceptance (Kitts, 1994). In this review, lipophilic bioactive compounds are mainly focused on.

Since bioactive compounds are sensitive to oxygen, temperature, light and other food components, it is essential to design a delivery system to carry them. Besides, lipophilic bioactive compounds are highly insoluble in water at ambient temperatures, which limits their incorporation into food matrix (Rao et al., 2013). A suitable food delivery system should have the following functions. First, it should be conveniently incorporated into foods or beverages, and it should be compatible with foods or beverages, which means that the delivery system must not influence appearance, flavour, texture and shelf-life of them. Second, the bioactive compounds should be physically and chemically stable during production, storage, transport and consumption. Third, it should be able to control the release of the bioactive compounds at an expected rate in the suitable place within the human body after consumption. Finally, it should be made with food grade ingredients using simple and low cost processing method (McClements et al., 2007).

Microemulsion has been utilized by some researches as carriers to deliver bioactive compounds (Spernath et al., 2002, Salimi et al., 2014, Roohinejad et al., 2015, Calligaris et al., 2017, Cheng et al., 2017, Guo et al., 2019a). W/O microemulsions can deliver hydrophilic bioactive compounds, while O/W microemulsions deliver lipophilic bioactive compounds. Microemulsions have long been utilized in the pharmaceutical area to incorporate drugs and much literature have reported that microemulsion could enhance the oral bioavailablity of drugs (Cui et al., 2009, Kim et al., 2017, Yang et al., 2017a). Only as few researchers employed *in vivo* approaches to study the bioavailability of bioactive compound loaded microemulsions (Xiao et al., 2013, Salimi et al., 2014).

2.5.1 Carotenoids

Carotenoids are natural pigments, which contribute to the yellow to red colours of many foods and vegetables (McClements et al., 2007, Ribeiro, 2009). They are synthesized by microorganisms and plants and more than 600 types of carotenoids are found in nature (Ribeiro, 2009). The main structure of carotenoids is a 40-carbon polyene chain, which may be terminated by ring structure or completed by oxygen-containing functional groups (Namitha and Negi, 2010). Carotenoids are divided into two groups: xanthophylls which contain oxygen (such as lutein and zeaxanthin) and carotenes which do not have oxygen atoms (such as lycopene and beta-carotene) (McClements et al., 2007). Since carotenoids have unsaturated chemical structures (i.e. eight isoprenoid units containing conjugated double bonds), they are sensitive to oxidative degradation against heat, light and oxygen (Ribeiro, 2009).

Carotenoids have several health benefits. Provitamin A activity is the most well-studied function of carotenoids and carotenoids with β-ionone end groups have provitamin A activity (Namitha and Negi, 2010). After digestion, carotenoids are converted to vitamin A, which is very important for a good vision. Besides, deficiency of vitamin A is a major

cause of premature death in developing countries (Maiani et al., 2009). Carotenoids also have antioxidant activity, which can protect cells and tissues from being oxidised by radical species, such as free radicals, hydrogen peroxide and singlet oxygen (Maiani et al., 2009, Namitha and Negi, 2010). Their antioxidant function mainly depends on the conjugated double bonds in the polyene backbone of carotenoids, which makes it possible for carotenoid molecules to absorb excited energy from other molecules (Namitha and Negi, 2010).

Beta-carotene is the most widespread carotenoid, which contributes to the orange-yellow colour of many fruits and vegetables, for example, carrot, mango, pumpkin and acerola (Ribeiro, 2009). It is the major and most active precursor of vitamin A and it may decrease the risk of some cancers and heart disease (Naves and Moreno, 1998). Beta-carotene can function as a redox reagent, an immunological regulator. In vivo, it generally function as an antioxidant and singlet oxygen quencher (Burri, 1997). Lycopene is a natural red pigment, which is mainly found in tomatoes (Ribeiro, 2009). It has an acyclic open-chain structure with 13 double bonds, 11 of which are conjugated coplanar double bonds (Shi and Le Maguer, 2000), which enables it has the highest antioxidant function of all the carotenoids (Sajilata et al., 2008). It does not have any provitamin A activity since it does not have a β-ionone ring structure (Shi and Le Maguer, 2000). According to Rao and Agarwal (2000), it can inhibit the proliferation of cells and has anticarcinogenic and antiatherogenic activities. Some researchers stated that lycopene may have the ability to decrease the risk of prostate cancer (Basu and Imrhan, 2007, Schwarz et al., 2008) and cardiovascular disease (Arab and Steck, 2000). Lutein and zeaxanthin are stereo isomers (Boon et al., 2010), which are found in green leafy vegetables, fruits and marigold flower (Ribeiro, 2009). They, which are usually termed as macular pigments (Stringham and Hammond, 2005), both contribute to the prevention of age-related macular degeneration and cataract (Sajilata et al., 2008).

Roohinejad et al. (2015) successfully prepared beta-carotene-encapsulated O/W microemulsions with medium chain monoglyceride Capmul MCM C8 and Tween 80 with particle size range from 12 nm to 100 nm by the water titration method. They employed an in vitro cell culture model (human epithelial colorectal adenocarcinoma, Caco-2) to study the cytotoxicity of microemulsions containing 30% oil phase, 20% Tween 80 and 50% phosphate buffer solution, stating that the viability of Caco-2 cells against beta-carotene microemulsions at concentrations of 0.03125% (v/v) was higher than 90%. However, when concentration of the microemulsion was increased to more than 0.0625% (v/v), the cell viability decreased to be less than 80% for both blank and beta-carotene-loaded microemulsions.

In another study, beta-carotene microemulsions (< 10 nm) were fabricated via the PIT approach using peppermint oil as the carrier oil, combination of sunflower lecithin and Tween 20 as the surfactants and these microemulsions were stable during storage for 65 days at 21 ºC (Chen and Zhong, 2015). The microemulsions provided protection to beta-carotene against degradation during ambient storage and under UV radiation as well as thermal treatment compared to the control (beta-carotene dissolved in ethyl acetate).

Garti and co-workers successfully incorporated lycopene into jojoba oil microemulsions by the water titration method with Brij 96V as the surfactant and hexanol as the cosurfactant, trying to determine lycopene solubilization along the dilution line 7:3. They stated that in W/O and O/W microemulsion with 10% and 90% water, respectively, the maximal solubilization efficiency (solubilization capacity value adjusted for the oil content) was almost 20 times larger than the solubility of lycopene in jojoba oil (Garti et al., 2004).

In a study conducted by Guo et al. (2019b), microemulsions containing R-(+)-limonene, Tween 80, Transcutol HP (the ratio of Tween 80 to Transcutol HP was 2:1) and water

was employed to encapsulate lycopene. The authors showed that lycopene content remained in the microemulsions were significantly higher than that dissolved in olive oil after storage for eight weeks at 4 and 25 ºC. Besides, when stored at 4 ºC, the microemulsion could better protect lycopene from degradation than that stored at 25 ºC. The relative oral availability of lycopene in rats of lycopene-loaded microemulsion enhanced 2.1 times compared to the control solution (lycopene in olive oil) (Guo et al., 2019b).

Amar et al. (2004) incorporated free lutein and lutein ester into Tween 80/R-(+)-limonene/ethanol/glycerol/water mixture system along the dilution line 6:4. They reported the solubilization capacity of both free lutein and lutein ester was much higher in the reverse micelles and the W/O microemulsions than in the O/W microemulsions, but it was the highest in the bicontinuous microemulsion.

2.5.2 Phytosterol

Phytosterols are a group of plant sterols which exist in the unsaponifiable part of plant oils. They are steroid alcohols (Spernath et al., 2003). Their structures are similar to human cholesterol and the most common phytosterols in diets are stigmasterol, β-sitosterol and campesterol (Kris-Etherton et al., 2002). According to European Food Safety (2009), the consumption of phytosterols may be associated with the decrease of LDL cholesterol, the high level of which is one recognized risk factor for coronary heart disease. It is also stated that intake of 2 to 2.4 g phytosterols/day from appropriate foods results in a 9% reduction in LDL cholesterol. However, incorporation of phytosterols into food is not easy since they have high melting point, making them crystallized easily during storage. Therefore, phytosterols are esterified into polyunsaturated fatty acids during food processing, which will be digested by lipase to free phytosterols after consumption by human beings (McClements et al., 2007).

Spernath et al. (2003) encapsulated phytosterols into the mixture system of Tween 60, water, R-(+)-limonene, ethanol and PG along the dilution line 6:4, finding the solubility of phytosterols in the mixture system was 12 times more than it in the R-(+)-limonene. They also stated that the phytosterols had a large influence on the spontaneous curvature of the micelles.

2.5.3 Omega-3 fatty acids

Omega-3 fatty acids, which are also named as ω-3 or n-3 fatty acids, are a family of polyunsaturated fatty acids (PUFAs) that have double bond on carbon 3 from the methyl end (the methyl carbon is carbon one) (Calder, 2013). Among all omega-3 fatty acids, α-linolenic acid (ALA, 18:3), eicosapentaenoic acid (EPA, 20:5) and docosahexaenoic acid (DHA, 22:6) are the most common ones and EPA and DHA are the most bioactive of these three ω -3 fatty acids (McClements et al., 2007). ALA occupies 50% fatty acids in green leafy tissues of plants, but green leaves are not major dietary source of ALA due to their insufficient fat content. Some seed oils and nuts are the main dietary source of ALA. EPA and DHA are mainly obtained from seafood (e.g. fish) (Calder, 2013) and algea oil (Lane et al., 2014, Chen et al., 2016). Omega-3 fatty acids are associated with gene expression, intracellular signal transduction and eicosanoid metabolism. They are able to decrease the risk of cardiovascular disease, inflammatory bowel diseases, rheumatoid arthritis and hypertension (Simopoulos, 1991, Belluzzi, 2002, Calder, 2004, Grynberg, 2005, Calder, 2008a, b). DHA is essential for the development and function of the brain and retina, and vital for pregnant and lactating women and their infants (Horrocks and Yeo, 1999, Karthik and Anandharamakrishnan, 2016).

Human body is not able to synthesize ALA, nor can it elongate and desaturate ALA into EPA and/or DHA after intaking ALA. So, humans must directly obtain desirable amount of ALA, EPA and DHA from the food (Narayan et al., 2006). Nevertheless, omega-3 fatty acids are highly sensitive to oxidation due to their high polyunsaturation and tend

to be degraded during storage, producing unpleasant off-flavours (Gulotta et al., 2014). Besides, it is difficult to encapsulate omega-3 fatty acids into foods or beverages due to their low water solubility, poor oxidative stability and complex bioavailability (Walker et al., 2015).

Chen et al. (2017) successfully encapsulated ALA into the microemulsion which was comprised of isoamyl acetate, castor oil ethoxylates 35 (EL-35), ethanol and water. The authors reported that the solubility of ALA in microemulsion was much higher than that in pure oil phase. Also, about 74% ALA was still in the microemulsion after storage for 10 days at 20 ºC. However, if ALA was dissolved in oil solution, 50% ALA was lost after 10 days at the same storage condition. This result showed that the microemulsion could protect ALA from being oxidized.

Liu and Wang (2010) fabricated cosurfactant free ALA incorporated O/W microemulsions emulsified with mixed surfactants of Span 80 and Cremophor EL-35. And they also indicated when ALA concentration was low, the ALA molecules were solubilized in the oil core of the droplets, and when ALA concentration increased, the ALA molecules were solubilized in the hydrophilic shells of the microemulsions.

2.5.4 Polyphenols

Polyphenols are plant-derived functional components (Onwulata, 2013) and they have one or more hydroxyl groups attached to a benzene ring (Ou et al., 2019). Based on their structures, they can be categorized into flavonoids, phenolic acid derivatives, stilbenes, lignans and phenolic monoterpenes, of which flavonoids are the most common ones (Qu et al., 2018). They contribute to the colour of the flowers, fruits and vegetables (Qu et al., 2018).

Resveratrol (trans-3,5,49-trihydroxystilbene) is one type of stilbenes, which have two

aromatic rings linked by a two-carbon bridge with a double band (Qu et al., 2018), and is found in grapes, berries, red wines and peanuts (Alarcon de la Lastra and Villegas, 2005). It is generally named as “red wine medicine” (Vang, 2013). It contributes to anti-inflammatory (Radko et al., 2016), anti-aging (Alarcon de la Lastra and Villegas, 2005), antioxidant (Delmas et al., 2011), antimicrobial (Filip et al., 2003), anti-obesity (Szkudelska and Szkudelski, 2010, Springer and Moco, 2019) and anticarcinogenic (Walle et al., 2004, Patel et al., 2010) functionalities.

Curcumin (diferuloylmethane), is a polyphenolic compound extracted from the rhizome of natural product turmeric (Curcuma Longa) which is a plant in the ginger family (Li et al., 2016, Pinheiro et al., 2016). It is chemically named 1,7-bis(4-hydroxy-3-methoxyphenyl)-1,6-heptadiene-3,5-dione, and it has strong yellow colour (Huang et al., 2010). It was documented to have anti-inflammatory (Chan et al., 1998, Wang et al., 2008), antitumor (Khar et al., 1999), antioxidant (Bayrak et al., 2008, Dolai et al., 2011) and anticarcinogenic (Chan et al., 1998, Shim et al., 2004, Zhou et al., 2014) activities.

Catechin is flavonoid polyphenolic compound, which is naturally found in green tea leaves and fruits (Higdon and Frei, 2003). It is also rich in red wine (Lin et al., 2018). The major catechins are epigallocatechin gallate (EGCG), epigallocatechin (EGC), epicatechin (EC) and epicatechin gallate (ECG) (Bhushani et al., 2016). Catechins were reported to have antioxidant (Bhushani et al., 2016), anticarcinogenic (Higdon and Frei, 2003), anti-inflammatory (Bilia et al., 2014) properties.

Resveratrol encapsulated microemulsions were fabricated by Juškaitė et al. (2017) via the oil titration approach using 5% ethyl oleate as the oil phase, 9.5% PEG-8 caprylic/capric glycerides as the surfactant, 47.5% polyglyceryl-6-isostearate as the cosurfactant and 38% aqueous phase, stating that the incorporation of resveratrol into the microemulsion could improve its stability after exposed to UVB irradiation. After

subjected to UV-light for four hours, the concentration of resveratrol remaining in the microemulsion was about 70.9%, compared to 16.3% in ethanolic solution.

Lin and co-workers fabricated curcumin encapsulated food-grade microemulsions using soybean oil, lecithin, Tween 80 and water via the water titration method, illustrating the encapsulated microemulsions were stable without any aggregation within the storage for 6 months. The encapsulation efficiency of the curcumin was more than 95%. They also investigated the impact of two different types of microemulsions with the droplet diameter of 30 nm and 80 nm on the viability of the human liver hepatocellular carcinoma cell line (HepG2) and the human embryonic kidney cells (HEK293). The results showed that both microemulsions did not have any significant reduction on the growth of HEK293 cells, with more than 80% of viability when the concentration of curcumin was 15 μ M, but they both resulted in the significant death of HepG2 cells even when the concentration of curcumin was quite low, i.e., 5 μ M for formula A and 2 μ M for formula B. When the concentration of curcumin was 15 μ M, formula A enabled HepG2 cells had the lowest viability, at about 5% (Lin et al., 2014).

In a study conducted by Bergonzi et al. (2014), a microemulsion containing 3.3%vitamin E, 53.8% Tween 20, 6.6% ethanol and 36.3% water was employed to encapsulate curcumin. The maximum solubility of curcumin was 14.57 mg/ml in this microemulsion, which was approximately 10,000 times higher than it in water solution. The loaded microemulsion could be diluted by buffer solution and it was stable (particle size and curcumin concentration kept unchanged) for at least two months when it was stored at 4 ºC and away from light.

According to Anoopinder et al. (2016), catechin-incorporated microemulsion was fabricated by Capmul MCM, Tween 80, Labrasol, phosphate buffer (PH 7.4) solution as well as catechin. The experiment results showed that the microemulsion provided

protection against catechin degradation while exposed to UV source.

2.5.5 Oil-soluble Vitamins

Vitamins, which are essential for human growth and development, are categorized into two types according to their solubility, i.e., water-soluble vitamins (vitamin B and C) and oil-soluble vitamins (vitamin A, D, E and K) (Velikov and Pelan, 2008).

Vitamin A includes retinoid and its four derivatives (retinal, retinoic acid, retinyl palmitate and retinyl acetate) as well as carotenoids which were discussed in Section 2.5.1 (Jesse and Gregory, 2017). Retinoids are normally stored in animal tissues (Combs, 2012). Enough intake of vitamin A helps human beings to maintain normal reproductive performance as well as visual function (Combs, 2012).

Vitamin E is comprised of eight different types, i.e., α-, β-, γ-, and δ-tocopherol and α-, β-, γ-, and δ- tocotrienol (Sylvester et al., 2011), of which α-tocopherol is most biologically active. Tocopherols and tocotrienols have the similar structure, with a long aliphatic chain attached to a chromanol ring at the 2-position. The difference between them is that tocotrienol have an unsaturated side chain with three double bonds (Hu et al., 2011), while tocopherols have a saturated side chain (Sylvester et al., 2011). Vitamin E has the function of antioxidation (Hu et al., 2011) and anti-inflammation (Sozen et al., 2019).

Vitamin D, which is also named as “sunshine vitamin” (Badiu and Luque, 2010), contains two different forms, vitamin D_2 (ergocalciferol) and vitamin D_3 (cholecalciferol) (Guttoff et al., 2015). Vitamin D_3 can be found in some vegetables and fungal substances, but vitamin D_2 is only produced by the skin after exposed to the sun (Maruotti and Cantatore, 2013). The lack in vitamin D is related to bone disease, osteoporosis and fracture, muscle weakness and etc. (Badiu and Luque, 2010, Guttoff

et al., 2015).

ATRA (all-trans retinoic acid)-loaded microemulsion was fabricated by Subongkot and Ngawhirunpat (2017) using 45% oleth-5, 45% Transcutol P, 5% fish oil and 5% distilled water. 18 mg/ml ARTA could be incorporated into the microemulsion and about 64.7% ARTA was still remained in the microemulsion after stored 25 ºC for 6 months. Study of *in vitro* intestinal absorption was also conducted using Franz diffusion cells and microemulsion cytotoxicity test was determined by a lactate dehydrogenase cytotoxicity detection kit. The experimental data showed that the microemulsion could enhance the intestinal absorption of ATRA and the cytotoxicity of ATRA-loaded microemulsion was not significantly different from that of fish oil (Subongkot and Ngawhirunpat, 2017).

Food-grade vitamin E microemulsions, which had good stability against temperature, salinity and acidity, were fabricated by Feng et al. (2009b) via the water titration method using ethyl butyrate, Cremophor EL-35, ethanol and water. The release rate of vitamin E was studied via a dialysis bag and a pure vitamin E ethanol solution was used as a reference, finding the release rate of the incorporated vitamin E was lower than that of pure vitamin E ethanol solution within the first 10 h. But the release rate of the microemulsion reached 92.6% in 48 h, which was higher than that of the pure vitamin E ethanol solution, which indicated an ideal release efficiency of the microemulsion. The researchers also investigated the cytotoxicity assay of vitamin E in microemulsion with cancer cells H446, illustrating the cell toxicity of the microemulsion was actually lower than the solo components (Cremophor EL-35 and ethyl butyrate) (Feng et al., 2009b).

According to Ho and co-workers, an O/W microemulsion which was composed of Captex 355, Capryol 90, Solutol HS15 and buffer solution (pH 7) could encapsulate vitamin D_3. In this microemulsion, the weight of vitamin D_3, Captex 355, Capryol 90

and Solutol HS15 was 0.14, 225, 45 and 180mg, respectively. After stored at 25 ºC and 60% relative humidity for two years in a light-protectable glass vial, 93% vitamin D was still remained in the microemulsion (Ho et al., 2019).

2.6 Literature review conclusions

Some researchers have successfully incorporated bioactive compounds into microemulsions as the delivery systems to prevent the degradation of sensitive bioactive compounds during fabrication, transportation and storage. This review article has presented preparation methods, formulations, properties and characterization approaches of microemulsions. In addition, some bioactive compounds as well as their applications in microemulsions have been overviewed briefly. A few studies evidenced that bioactive compounds could be incorporated into microemulsions without influencing the properties of both bioactive components and delivery systems. However, further researches still need to be performed to incorporate more types of bioactive compounds to microemulsions, which are made from food-grade ingredients, using low energy emulsification methods.

Chapter 3 Materials and Methods

This chapter provides information on general materials and methods used in the research presented in this thesis.

3.1 Materials

3.1.1 Surfactants

Six different types of non-ionic small molecule surfactants were utilised throughout the project, including Tween 20 (polyoxyethylene sorbitan monolaurate), Tween 40 (polyoxyethylene sorbitan monopalmitate), Tween 60 (polyoxyethylene sorbitan monostearate), Tween 80 (polyoxyethylene sorbitan monooleate), Kolliphor EL (macrogolglycerol ricinoleate 35) and Span 80 (sorbitan monooleate). Tween 20, Tween 40, Tween 60, Tween 80 and Span 80 were purchased from Sigma-Aldrich Co. (St Louis, MO, USA). Kolliphor EL was provided by BASF Co. (Ludwigshafen, Germany). The physical appearance, HLB value and structure of each surfactant are shown in Table 3.1 and Figure 3.1.

Table 3.1 Appearance and HLB value of six different types of small molecule surfactants used in the study

Name	Appearance (at 25 °C)	HLB value
Tween 20	Yellow to yellow-green, viscous liquid	16.7
Tween 40	Liquid-gel	15.6
Tween 60	Liquid-gel	14.9
Tween 80	Golden-yellow, viscous liquid	15.0
Kolliphor EL	White to yellowish, oily liquid	12-14
Span 80	Yellow, viscous liquid	4.3

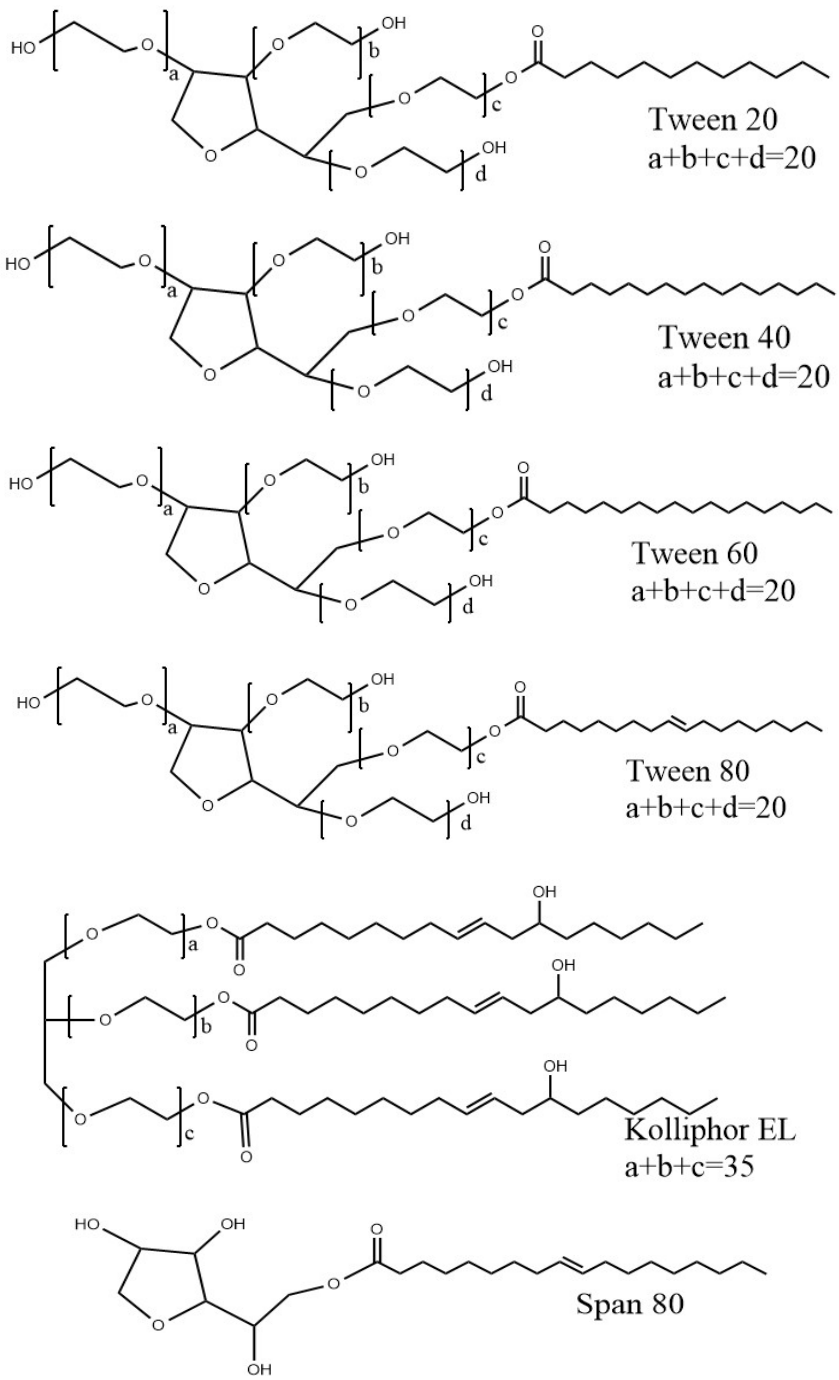

Figure 3.1 Chemical structures of six different types of small molecule surfactants.

3.1.2 Oils

Eleven different oils were used as oil phase in this study to fabricate emulsions by water titration method and emulsion dilution method. Fractionated coconut oil was obtained from by Bakels Edible Oil (NZ) Ltd. Lemon oil (cold-pressed, food grade, single fold) and isopropyl palmitate (IPM) (98%) were purchased from Sigma-Aldrich

Co. (St Louis, MO, USA). Peanut oil (Pams, Auckland, New Zealand) was purchased from a local supermarket. Capmul MCM C8 (glyceryl mono/dicaprylate), Capmul 708G (glyceryl monocaprylate), Capmul PG-2L (propylene glycol dilaurate), Capmul PG-12 (propylene glycol mono-laurate), Capmul PG-8 (propylene glycol mono-caprylate), Captex 100 (propylene glycol dicaprate ester) and Captex 355 (caprylic/ capric triglyceride) were kindly donated by Abitec Corporation (Janesville, WI, USA). Lemon oil and fractionated coconut oil were stored at 4 °C, while the other oils were stored at ambient temperature. Table 3.2 shows some properties of each oil.

3.1.3 Propylene glycol and absolute ethanol

Propylene glycol and absolute ethanol were purchased from Sigma-Aldrich Co. (St Louis, MO, USA). Absolute ethanol and propylene glycol were used as cosurfactant and cosolvent, respectively, in fabricating emulsions via the water titration method.

3.1.4 Water

Milli-Q quality water (water purified by treatment with Milli-Q apparatus, Millipore Corporation, MA, USA) was used for the preparation of all solutions. In this study, the concentrations of components in solutions were prepared and expressed on a weight by weight basis (% w/w) unless stated otherwise.

Table 3.2 Chemical composition, refractive index and viscosity of oils used

Product name	Chemical Name	Composition	Refractive index	Viscosity (mPa•s)
Lemon oil	N/A	A mixture of mainly monoterpenes (limonene and β-pinene)	1.4731	2.0
Fractionated coconut oil	N/A	A mixture of 57.6% caprylic acid and 42.4% capric acid	1.4489	28.9
Peanut oil	N/A	A mixture of many fatty acids	1.4635	77.6
IPM	N/A	Ester of isopropyl alcohol and myristic acid	1.4368	6.1
Capmul MCM C8	Glyceryl mono-dicaprylate	Ester of glycerol and fatty acids (including 97.3% caprylic acid. There are 58.2% monoester and 34.7% diester	1.4522	95.1
Capmul 708G	Glyceryl monocaprylate	A monoester (88.3%) of glycerol and caprylic acid	1.4479	100
Capmul PG-2L	Propylene glycol dilaurate	22% monoester and 77% diester of PG and 99.6% lauric acid	1.4439	21.7
Capmul PG-12	Propylene glycol monolaurate	More than 90% PG monoester of mainly lauric acid	1.4388	27.3
Capmul PG-8	Propylene glycol monocaprylate	97.6% monoester and 2.1% diester of PG and 100% caprylic acid	1.4327	15.0
Captex 100	Propylene glycol dicaprate ester	PG diesters of the mixture of 99.3% capric aid and 0.7% caprylic acid	1.4371	14.7
Captex 355	Triglycerides caprylic/ capric acid	An MCT composed of 57.2% caprylic acid, 42.1% capric acid and 0.7% lauric acid	1.4469	30

3.2 Methods

3.2.1 Emulsion dilution method

3.2.1.1 Preparation of primary emulsion

An O/W primary emulsion, which is also named as stock emulsion, was prepared by a two-step homogenisation process. In the first step, 10% oil phase was mixed with 1% surfactant solution (1% surfactant mixed with 99% Milli-Q water) using an Ultra-Turrax (VirTis Company, NY, USA) at 11,000 rpm for 1 minute to form a coarse emulsion. In the second step, the coarse emulsion was homogenized using a two-stage high pressure valve homogenizer (APV 2000, SPX Corporation, NC, USA) at 500/50 bars by passing it through four times to produce a fine emulsion. Figure 3.2 shows the Ultra-Turrax and two-stage high pressure homogenizer used in this study.

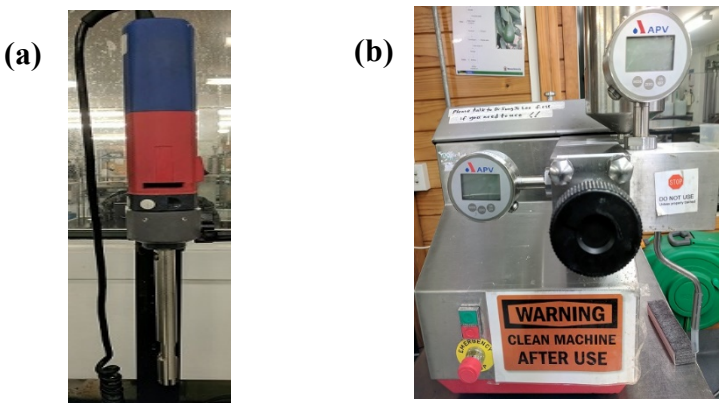

Figure 3.2 (a) Ultra-Turrax and (b) two-stage high pressure homogenizer.

3.2.1.2 Preparation of secondary emulsion

Different amounts of primary emulsion were added into 1% surfactant solution and mixed thoroughly with a vortex mixer (VELP Scientifica, MB, Italy) to obtain a series of secondary emulsions with different concentrations of oil (0.1-2%). The secondary emulsions prepared were stored overnight at ambient temperature (25 ± 0.5 °C) and then analysed by measuring particle size, PSD and turbidity in order to determine the concentrations of oil from which microemulsions were fabricated.

Emulsion dilution method was utilised in Chapter 4 and Chapter 6 to prepare the secondary emulsions. A schematic diagram that illustrates the preparation of primary and secondary emulsions is also shown in Figure 3.3.

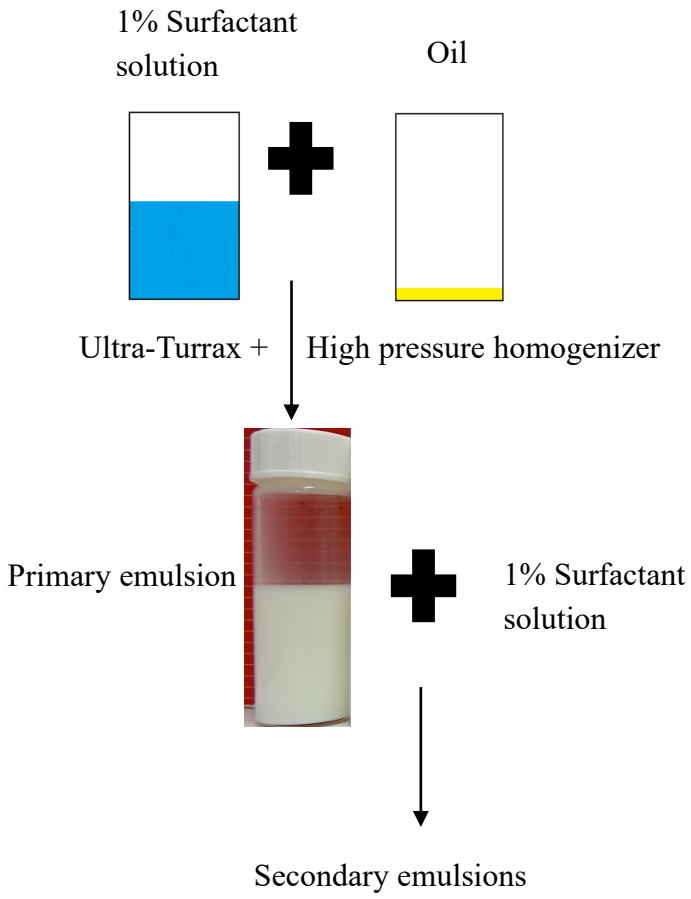

Figure 3.3 Schematic diagram of emulsion dilution method.

3.2.2 Water titration method

A ternary phase diagram (TPD), also known as Gibbs triangle, was constructed using water titration method to define the compositional range of three components (water, oil and surfactant) that enables to form microemulsion. Firstly, oil and surfactant were mixed at the weight ratios of 1:9, 2:8, 3:7, 4:6, 5:5, 6:4, 7:3, 8:2 and 9:1. Secondly, these mixtures were then diluted dropwise with Milli-Q water in 10% w/w increments, under moderate agitation using a vortex mixer. Each sample was further allowed to

equilibrate at ambient temperature (25 ± 0.5 °C) for at least 24 hours before evaluation. Five different kinds of phases were visually observed: (i) a transparent liquid; (ii) a viscous gel; (iii) a turbid liquid, (iv) a phase-separated mixture and (v) a liquid crystal.When a sample did not have the tendency to flow after tilting to an angle of 90°, it was identified as gel (Syed and Peh, 2014). An Olympus CH-30 light microscope with the analyzer (U-ANT) and the polarizer (U-POT) was employed to identify the presence of liquid crystal. Under polarised light, liquid crystal showed birefringence since it was anisotropic. The transparent liquid was defined as microemulsion if its appearance did not change after it was stored at 25 °C for one month and was centrifuged at 3500 rpm for 30 minutes. The formulations which led to a transparent liquid were prepared freshly again to determine the type of microemulsion (O/W, bicontinuous or W/O). SigmaPlot software (version 12.5, Systat Software Inc., Chicago, IL, USA) was employed to create a Gibbs triangle to define the phase boundaries. The total monophasic region, denoted as A_T, was introduced to determine the solubilisation capacities of microemulsions (Garti et al., 1995). Figure 3.4 illustrates a TPD in which the dilution line W91, W82, W73, W64, W55, W46, W37, W28 and W19 represent the ratios of oil to surfactant at 1:9, 2:8, 3:7, 4:6, 5:5, 6:4, 7:3, 8:2 and 9:1, respectively. On each line, the concentration of water is increased from 0 to 100% (right side to left side on the figure). Code L110, L120, L130……L980, L990 were employed to describe each dot in the TPD, in which the last two number means water concentration and the first number, which is also the second figure of the dilution line code, indicates the proportion of oil in the mixture of oil and surfactant. For example, L110 means a sample with 10% water, 9% oil and 81% surfactant. The relationship between these codes and sample composition is listed in Appendix (Table 1). The water titration method was used as the approach to produce emulsions in Chapter 5 and Chapter 7.

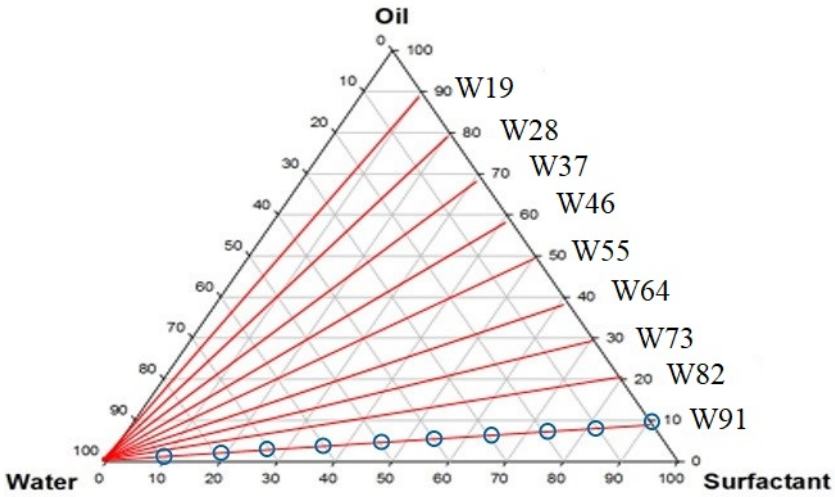

Figure 3.3 Schematic graph of a TPD comprising of three components (water, oil and surfactant) at different ratios.

3.2.3 Particle size and size distribution

A Zetasizer Nano ZS (Malvern Instruments Ltd., Worcestershire, UK) (Figure 3.5a) which uses a dynamic light scattering (DLS) technique was utilised to determine the particle size and particle size distribution (PSD) of oil droplets in emulsions at 25 ± 0.5°C without any further dilution. DLS technique detects the Brownian motion of particles in a solution to determine the size of these particles. The refractive index of Milli-Q water was 1.33, and that of oils determined by Abbe 5 refractometer (Bellingham + Stanley Ltd., Kent, UK) (Figure 3.5b) is shown in Table 3.2. Particle size was reported as Z-average mean. Polydispersity index (PDI) was also recorded. PDI describes the degree of broadness of particle size distribution. For the emulsion dilution method, the particle size and PSD of both primary and secondary emulsions were measured immediately after the preparation and also after storage for 1 day. For the emulsion samples prepared by the water titration method, their particle size was analysed after 24 hours that the emulsions were equilibrated.

(a) 

(b) 

Figure 3.4 Photos of (a) Malvern Zetasizer Nano ZS and (b) refractometer.

3.3 Statistical analysis

The preparation of emulsions was replicated at least two times. All emulsion samples were analysed in at least duplicate. The results were reported as average and standard deviation (S.D.). All experimental data obtained were analysed statistically using a statistical software Minitab 17.3.1 (Minitab, Inc, USA). Statistical significance was determined by analysis of variance (ANOVA) with Tukey test. P value of < 0.05 was considered as statistically significant.

Chapter 4 Formation of microemulsions by emulsion dilution method: Effects of oil and surfactant type and concentration

4.1 Abstract

Emulsion dilution method normally involves a two-step process consisting of the formation of a stock emulsion by high energy emulsification method and the dilution of the stock emulsion with a surfactant solution. In this study, emulsion dilution method was used to produce O/W microemulsions containing oil droplets of mean diameter size smaller than 50 nm. The effects of different types of oils (triglycerides and non-triglycerides) and surfactants (Tween 20, 40, 60 and 80) and their concentration on the fabrication of microemulsion were investigated. Triglyceride oils, such as peanut oil and coconut oil, could not be used to form microemulsions by emulsion dilution method while non-triglyceride oils, such as IPM and lemon oil, were able to be utilised to form microemulsions. Capmul 708G could not be used to prepare microemulsion since its primary emulsion had a phase separation quickly. However, IPM could only fabricate microemulsion (< 50 nm) when its concentration was less than 0.1% when Tween 80 was used as surfactant and its concentration was 1%. In case of lemon oil, the oil concentration that could be incorporated in microemulsions after dilution was increased to 0.2%. Among small molecule surfactants (Tween 20, 40, 60 and 80), Tween 80 was found to be the most efficient as a dilution medium in making microemulsions. In addition, the amount of lemon oil that could be solubilised within small molecule micelles increased with increasing Tween 80 (dilution medium) concentration. This study provides important information about the effects of type and concentration of surfactant and oil on the formation and characteristics of microemulsions fabricated via emulsion dilution method.

4.2 Introduction

There has been an increasing interest in the food industry, in recent years, in designing a delivery system encapsulating bioactive compounds that can be incorporated into transparent food or beverages (Velikov and Pelan, 2008, Sagalowicz and Leser, 2010). In this respect, microemulsion is one of the colloidal dispersions that have attracted a considerable degree of attention. Microemulsion is a thermodynamically stable system, meaning it can be formed spontaneously without the supply of external energy (Paul and Moulik, 1997, Flanagan and Singh, 2006). Nevertheless, practically, a certain external energy, such as stirring and heating, is necessary when making microemulsions, due to the existence of kinetic energy barriers between phase-separated components and microemulsion or slow mass transport (McClements, 2012). Microemulsion tends to be transparent since its particle size is smaller than 50 nm in diameter. A microemulsion contains oil phase, aqueous phase and surfactant but it normally requires a large amount of surfactant (Lawrence and Warisnoicharoen, 2006, Komaiko and McClements, 2016) and can only be fabricated using small molecule surfactants (McClements, 2012). In order to fabricate a microemulsion, a cosurfactant or cosolvent is generally required (Chauhan et al., 2019).

Tween families are small molecule surfactants which are commonly used to fabricate microemulsions (Ziani et al., 2012b, Chai et al., 2014, Deng et al., 2016, Ma et al., 2016). Tween is the commercial brand name of polysorbate, which is comprised of a series of polyoxyethylene-type non-ionic surfactants, including Tween 20, Tween 40, Tween 60 and Tween 80. The series of Tweens vary only in alkyl chain length. Tween 20, 40, 60 and 80 consist of 12, 16, 18 and 18 carbons, respectively, in the alkyl chain. In addition, the alkyl chain of Tween 80 is unsaturated unlike that of Tween 20, 40 and 60 (Graca et al., 2007). HLB (hydrophilic-lipophilic balance) values of Tween 20, 40, 60 and 80 are 16.7, 15.6, 14.9 and 15.0, respectively (Griffin, 1946), therefore, they tend to form O/W emulsions.

Emulsion dilution method, which is a combination of high energy and low energy emulsification methods, is employed by some researches to make microemulsions (Rao and McClements, 2012c, Ziani et al., 2012a, b). The principle of this method is the transport (or solubilisation) of oil molecules from initial emulsion droplets into surfactant micelles. It involves the dilution of an O/W conventional emulsion, which is made by high energy emulsification method, via a surfactant micelle solution. The O/W emulsion, as it is well known, is thermodynamically unstable, but the surfactant micelle solution is thermodynamically stable due to the decrease in free energy caused by hydrophobic effect (rearrangement of surfactant molecules forcing non-polar part of the surfactant to be removed from water) (Ziani et al., 2012b). However, the micelle monolayers formed by surfactants are not in their optimum curvature, which is the driving force of oil molecules solubilised into surfactant micelles until they become saturated (Weiss et al., 1997). Accordingly, surfactant micelle swells, whereas the initial emulsion droplets shrink, resulting in the change in the particle size of the mixture system to the size range of microemulsion (<50 nm) (Rao and McClements, 2012a).

The objective of this study was to investigate the effects of types and concentrations of oils and surfactants on the formation of microemulsion by emulsion dilution method. Results obtained from this study provide useful information to fabricate decent colloidal delivery systems which can be utilised in transparent foods or beverages.

4.3 Materials and Methods

4.3.1 Materials

In this chapter, Tween 20, 40, 60 and 80 were utilised as the surfactants. Fractionated coconut oil, peanut oil, lemon oil, IPM and Capmul 708G were used as the oil phase.

4.3.2 Analysis of primary and secondary emulsions

Emulsions were prepared via the emulsion dilution method as previously described in Section 3.1.5 of Chapter 3.

4.3.2.1 Particle size and size distribution

Particle size and PSD of both primary and secondary emulsions were measured after the preparation and after storage for 1 day at ambient temperature (25 °C). The methods used were introduced in Chapter 3 (Section 3.1.7).

4.3.2.2 Turbidity and appearance

Turbidity of primary and secondary emulsions was determined by measuring absorbance using a UV-visible spectrophotometer (UV-1700, Shimadzu Corp., Japan) (Figure 4.1) at 600 nm. 1% surfactant solution was utilized as a reference. In addition, each emulsion was observed and monitored visually for its appearance and photos were taken. Turbidity and visual appearance were determined after the preparation of emulsions and after storage for 1 day at ambient temperature (25 °C).

Figure 4.1 Photo of UV-visible spectrophotometer

Turbidity is the measurement of cloudiness or opacity of a solution in which the particles suspended result in the scattering of light which passes through it. The higher

the turbidity, the less amount of light passes through the solution, leading to lower transmittance (Wang et al., 2010). Absorbance, in addition, is linearly related to turbidity as shown in Equation 4.1.

$$T_b = 2.303*A/L \quad [4.1]$$

where T_b, A and L represent turbidity, absorbance and cell's optical path length, respectively (Damodaran, 2007). As a consequence, both transmittance and absorbance can be utilised to represent the degree of turbidity.

Absorbance value of primary emulsion was 4 (the highest absorbance could be measured by spectrophotometer) before and after storage. Absorbance of a solution can be determined by Lambert-Beer's Law (Equation 4.2).

$$A = \varepsilon*C*L \quad [4.2]$$

where, A, ε, C and L mean absorbance, molar extinction coefficient, sample concentration and cell's optical path length, respectively (Rohatgi-Mukherjee, 1986). In this case, absorbance was proportional to sample concentration.

4.3.3 Effect of some variables

4.3.3.1 Effect of oil type

Five different types of oil (coconut oil, peanut oil, lemon oil, IPM and Capmul 708G) were used as oil phase in preparing primary emulsions. All these primary emulsions were diluted into 1% Tween 80 solution to make a series of secondary emulsions. All samples were stored at ambient temperature and their particle size, PSD and turbidity were determined immediately after preparation and after storage for 1 day.

4.3.3.2 Effect of surfactant type

Four different types of surfactants (Tween 20, 40, 60 and 80) were mixed with Milli-Q water to make 1% surfactant solutions. They were then used to fabricate 10% lemon O/W primary emulsions. After that, all these primary emulsions were diluted into 1%

surfactant solution (Tween 20, 40, 60 and 80) to make a series of secondary emulsions. All samples were stored at ambient temperature and their particle size, PSD and turbidity were determined immediately after preparation and after storage for 1 day.

4.3.3.3 Effect of surfactant micelle solution concentration

The primary emulsion was prepared by homogenizing 10% lemon oil, 1% Tween 80 and 89% Milli-Q water. Aliquots of primary emulsions were then titrated into different concentrations of Tween 80 micelle solutions (0.5, 1 and 2%) to obtain secondary emulsions. In addition, the primary emulsion was diluted into Milli-Q water to make a series of control samples. All samples were stored at ambient temperature and their particle size, PSD and turbidity were determined immediately after preparation and after storage for 1 day.

4.4 Results and Discussion

4.4.1 Formation of microemulsions

A primary emulsion was fabricated by mixing 10% lemon oil and 1% Tween 80 solution via high energy homogenisation method. The primary emulsion was then diluted into 1% Tween 80 micellar solution to obtain a series of secondary emulsions with different oil concentrations (0.1% - 2.0% lemon oil). The mean particle size, PSD, turbidity and appearance of primary and secondary emulsions were measured after preparation and also after storage at 25^{o}C for one day.

The initial mean particle size of primary (stock) emulsion containing 10% lemon oil was 226 nm in diameter and after storage for 1 day it did not significantly change (228 nm). Figure 4.2 illustrates that the particle size distribution (PSD) of primary emulsion analysed immediately after preparation and after storage at ambient temperature for 1 day. It can be seen that the PSD of stock emulsion was multimodal. The emulsion had

two populations of particles with their size being <150 nm and >500 nm in diameter. However, after storage for 1 day, most lemon oil particles had a diameter greater than 1000 nm. This phenomenon was due to the fact that lemon oil has relatively high water solubility, which favours the occurrence of Ostwald ripening, a process which involves the diffuse of oil molecules from small droplets to large droplets (Wooster et al., 2008). As a result, the emulsion after storage had a population of relatively large droplets and a broad particle size distribution.

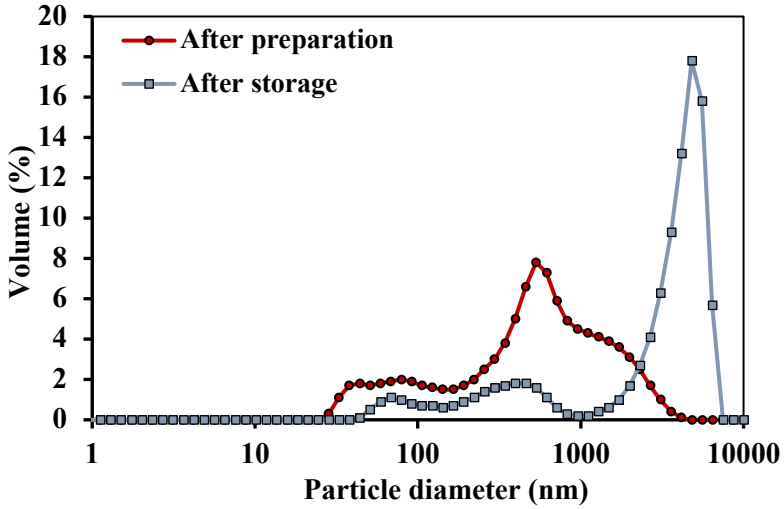

Figure 4.2 Particle size distribution of stock (primary) emulsion after preparation and after storage at ambient temperature for 1 day.

As shown in Figure 4.3a, the dilution of this primary emulsion resulted in a significant decrease in its particle size, especially when its oil concentration diluted was below 0.5%. The particle size decrease was more significant with increasing dilution rate, i.e. decreasing oil concentration in the secondary emulsions. The particle size of secondary emulsions after preparation was also decreased when stored for 1 day at all oil concentrations (Figure 4.3a). After storage, the particle size of secondary emulsions containing 0.1, 0.2 and 0.3% lemon oil was 14, 31 and 72 nm, respectively, and their PSD was monomodal (Figure 4.5). This led to a decrease in the absorbance value for the secondary emulsions after storage at lemon oil concentration from 0.1% to 2% (Figure 4.3b).

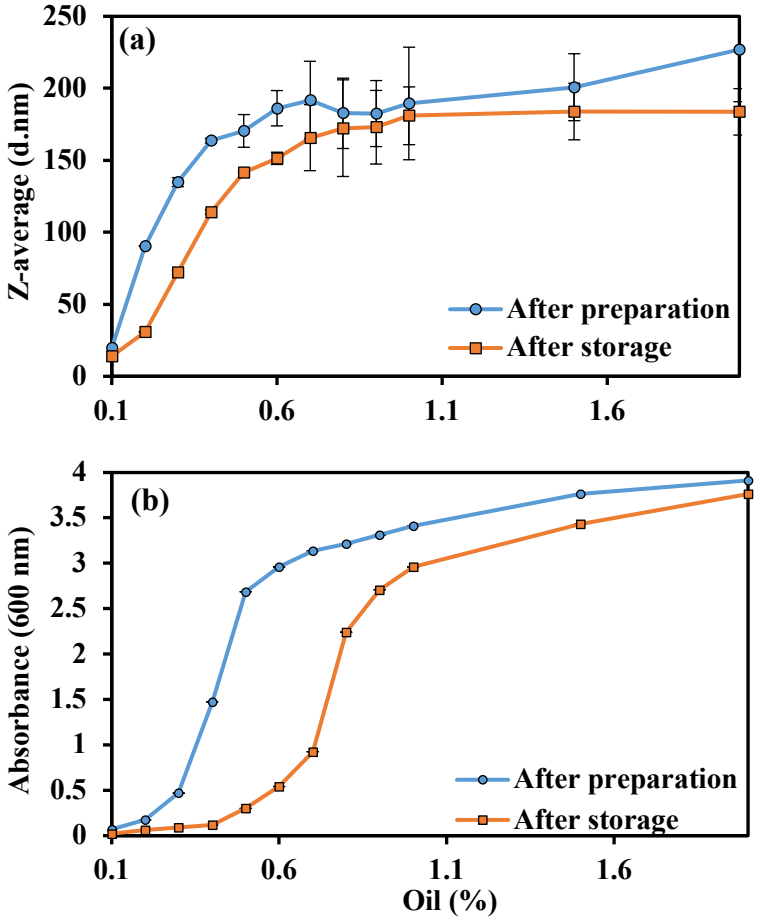

Figure 4.3 Particle size and absorbance of 0.1%-2.0% secondary emulsions after preparation and after storage for 1 day. (a) Particle size (b) Absorbance. Data are presented as the mean and standard deviation of two independent measurements with duplicate (n=4) and error bars mean standard deviation.

With the increase in lemon oil from 0.1% to 2%, absorbance value increased as well (Figure 4.3b). This complies with Equation 4.2, which implies that absorbance is proportional to sample concentration. According to Wang et al. (2010), additionally, turbidity depends on the shape, size and concentration of particles in the solution. Moreover, the visual observation of appearance showed that the appearance of the secondary emulsions varied from clear to translucent and to opaque with increasing lemon oil concentration (Figure 4.4).

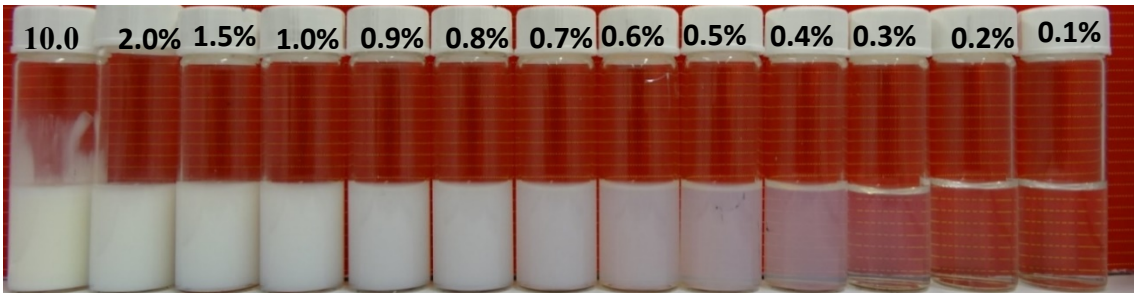

Figure 4.4 Appearance of secondary emulsions (0.1-2.0% lemon oil) made from the dilution of 1% Tween 80-stabilised 10% lemon oil primary emulsion by different 1% Tween 80 solutions after storage at ambient temperature for 1 day. Numbers mean lemon oil concentration.

In summary, when lemon oil concentration was 0.1% and 0.2%, secondary emulsions had small droplet size (< 40 nm), low absorbance and unimodal PSD, meaning that the lemon oil droplets from primary emulsions were completely solubilised into Tween 80 micelles, which had a particle size of 9.2 nm (determined in the preliminary experiment). As such, these secondary emulsions were microemulsions. The maximum amount of oil that could be incorporated into micelles to make a microemulsion is defined as Cmax. Thus, in this case, Cmax was 0.2% based on the assumption of a microemulsion defined as smaller than 50 nm in diameter. When lemon oil concentration was 0.3%, obtained from PSD data, a group of particles with diameter of more than 50 nm formed apart from a group of particles with diameter of less than 25 nm. After that, with the increase in lemon oil concentration especially from 0.5%, the particle size and absorbance value increased, and the resulting emulsion appearance became turbid as shown in Figures 4.4 and 4.5, meaning not all lemon oil droplets could be incorporated into Tween 80 micelles. In other words, all Tween 80 micelles are completely saturated so that any additional lemon oil droplets do not result in the change of the system. In these emulsions, swollen micelles are believed to exist together with lemon oil droplets. Therefore, 0.3% lemon oil concentration could be considered as a transition point between microemulsion and conventional emulsion.

The finding of this study was in consistence with the findings from Rao and McClements (2012a), who also used 10% lemon oil (1-fold) and 1% Tween 80 to fabricate a primary emulsion which was then diluted by 1% Tween 80 solution to fabricate secondary emulsions. They found that when lemon oil concentration was less than 0.2%, microemulsions were obtained and the particle sizes of these microemulsions were smaller than 30 nm. Ziani et al. (2012b) had the similar observations as well.

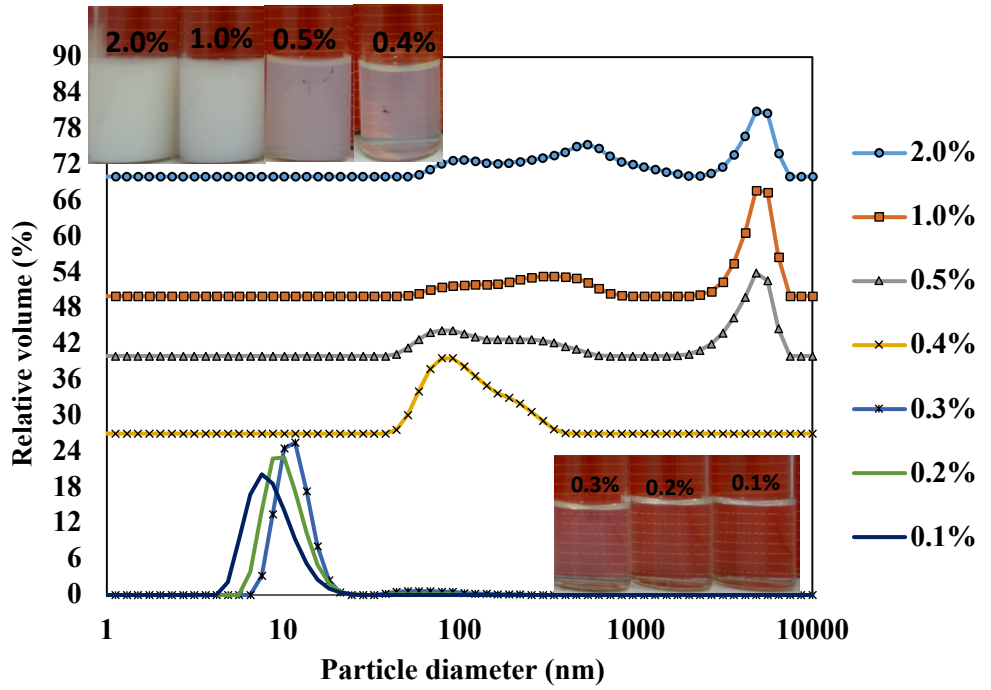

Figure 4.5 Particle size distribution of secondary emulsions with different concentrations of lemon oil. The data has been offset on the y-axis to distinguish different curves.

4.4.2 Influence of oil type on droplet solubilisation

Apart from lemon oil, fractionated coconut oil, IPM, peanut oil and Capmul 708G were also used to prepare emulsions by emulsion dilution method. 1% Tween 80 solution was utilised to prepare the primary emulsion containing 10% oil. Peanut oil is comprised mainly of long chain fatty acids, around 80% of which are unsaturated

fatty acids (Jones, 1990). Fractionated coconut oil is also called liquid coconut oil, which is obtained after removing all the long chain fatty acids of virgin coconut oil (Lim, 2012). Thus, it is a medium chain triglyceride, which contains caprylic acid (C8:0) and capric acid (C10:0). The lemon oil utilised is obtained from lemon peel via cold pressing and it is an essential oil which is mainly composed of limonene, β-pinene and γ-terpinene (Misharina et al., 2010) unlike the coconut oil and peanut oil are chemically triglycerides. Besides, IPM is the ester of isopropyl alcohol and myristic acid, which is also referred to as isopropyl tetradecanoic acid (Klaffenbach and Kronenfeld, 1997) and has a structural formula $C_{17}H_{34}O_2$. Capmul 708G is comprised of 88.3% of glyceryl monoesters, so that it can be considered as a medium chain monoglyceride.

Based on the data shown in Table 4.1, the particle size of primary emulsion made by lemon oil was not significantly different from the other primary emulsions prepared using different oils, despite of the fact that lemon oil was low in viscosity. This is because that if oil phase is viscous like triglyceride oils, it is difficult for the oil phase to be disrupted by homogenisation (Pandolfe, 1981, Galooyak and Dabir, 2015). On the other hand, the PDI of lemon oil primary emulsion was 0.44 ± 0.04, which indicates that this emulsion had a very broad PSD compared to the other primary emulsions. Besides, this emulsion had a multimodal PSD curve (Figure 4.6). In terms of IPM, fractionated coconut oil and peanut oil, the primary emulsions prepared by them had a relatively larger particle size (Table 4.1), but a narrower PSD (Figure 4.6). The only difference was that coconut oil and peanut oil emulsions had unimodal distribution, while IPM emulsion had a bimodal distribution with one population between 10 nm and 100 nm, and the other one between 100 nm and 1000 nm. Primary emulsion prepared using Capmul 708G had phase separation immediately after preparation (Figure 4.7), thus it was not possible to determine its particle size and to fabricate secondary emulsions, indicating that Capmul 708G is not suitable to use

in making microemulsions by emulsion dilution method.

Table 4.1 Z-average particle size and PDI (polydispersity index) of primary emulsions (10% oil and 1% Tween 80). Data are presented as the mean and standard deviation of two independent measurements with duplicate (n=4).

Oil type	Z-average (d.nm)	PDI
Lemon oil	226 ± 20	0.44 ± 0.04
Coconut oil	245 ± 2	0.26 ± 0.01
IPM	240 ± 6	0.30 ± 0.02
Peanut oil	264 ± 2	0.27 ± 0.01

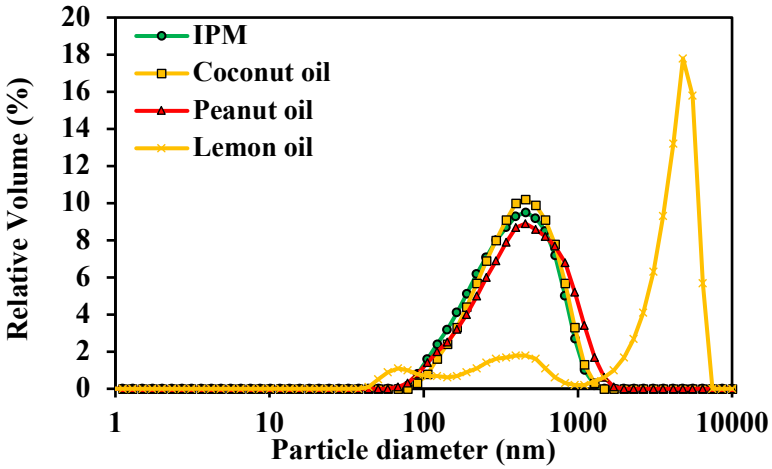

Figure 4.6 Particle size distribution of primary (stock) emulsions prepared with different types of oils and 1% Tween 80 solution after storage at ambient temperature for 1 day.

Figure 4.7 Phase separation of primary emulsion prepared using10% Capmul 708G oil and 1% Tween 80.

Primary emulsion was then diluted by 1% Tween 80 solution to form secondary emulsions containing different concentrations of oil phase (0.1% to 2.0%) to determine the effect of oil type on the formation of microemulsion. According to Figure 4.8a, the particle size of secondary emulsions containing peanut oil and coconut oil was not significantly changed with the increase of oil concentration from 0.1% to 2.0%. It remained constant at around 200 nm and 230 nm for the emulsions containing coconut oil and peanut oil, respectively. Moreover, their particle size distributions were not changed with an increase in oil phase concentration (data not shown). This suggests that peanut oil and coconut oil could not form microemulsions as they cannot be incorporated into Tween 80 micelles, which is attributable to their triglyceride structure, relatively large molecular weight, low water solubility and high viscosity. These results were confirmed by absorbance measurement (Figure 4.8b) and visual observation. Regardless of oil phase concentration, all secondary emulsions containing coconut oil and peanut oil were opaque. As a result, absorbance value was measured to be increased dramatically when the primary emulsion droplets of coconut oil or peanut oil were added into the system. The absorbance value of peanut oil secondary emulsions was steeper than that of coconut oil secondary emulsions. This could be due to the larger droplet size of peanut oil emulsions as shown in Table 4.1.

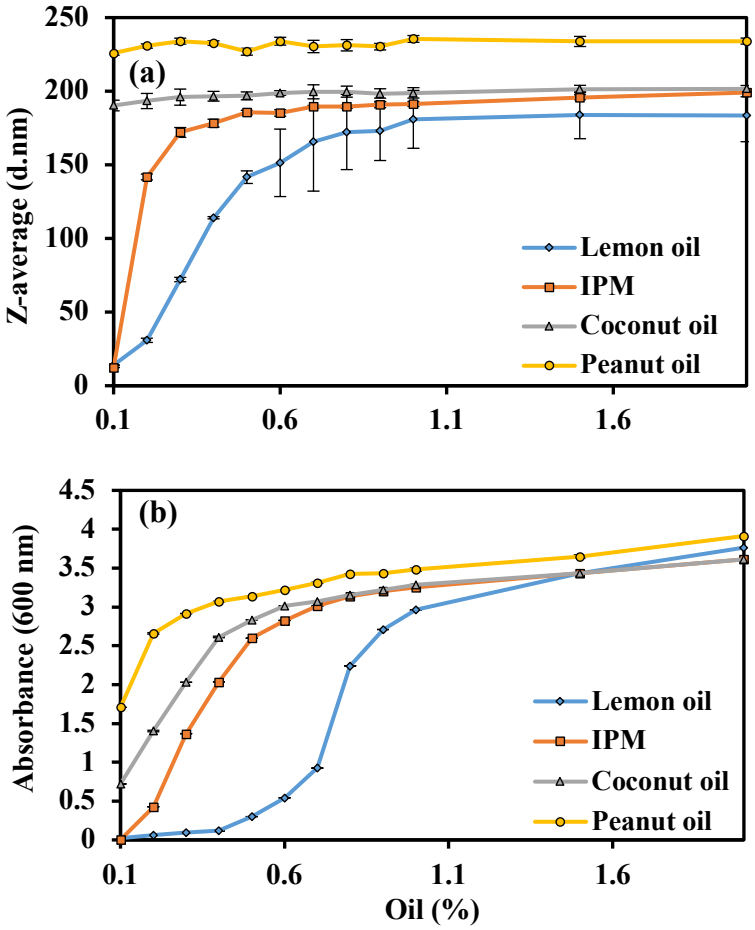

Figure 4.8 Particle size and absorbance of 0.1%-2.0% secondary emulsions prepared with four different types of oil after storage at ambient temperature for 1 day. (a) Particle size (b) Absorbance. Data are presented as the mean and standard deviation of two independent measurements with duplicate (n=4) and error bars mean standard deviation.

Contrarily, IPM and lemon oil were able to form microemulsion. The maximum concentration of lemon oil that could be incorporated into 1% Tween 80 solution, as stated in the above, to fabricate microemulsion was 0.2%; whereas for IPM, this value was 0.1%. When IPM concentration was 0.1%, the particle size of secondary emulsion was 12 nm and the solution was clear (data not shown). However, the secondary emulsions became turbid if IPM concentration was equal to and higher than 0.2% and its Z-average size was 142 nm in diameter. The reason why more lemon oil could be accommodated by Tween 80 micelles may be due to the fact that the molecular weight of lemon oil was smaller than that of IPM and the water solubility of lemon oil was

higher than that of IPM.

The results were consistent with some experimental data from Ziani et al. (2012a) who tried to investigate the effect of oil phase on oil droplet solubilisation using 10% vitamin E, vitamin D and lemon oil (4-fold) together with 1% Tween 80. They stated that relatively large molecular size of vitamin E or vitamin D acetate made them unable to be incorporated within the hydrophobic interior of Tween 80 micelles. Moreover, lemon oil has relatively low viscosity, which means it is easier to diffuse and transport between particles than oils with high viscosity (Ziani et al., 2012a).

4.4.3 Influence of surfactant concentration on droplet solubilization

Tween 80 solutions at different concentrations (0, 0.5, 1 and 2%) were employed to dilute an O/W primary emulsion containing 10% lemon oil emulsified in 1% Tween 80 solution to fabricate a series of secondary emulsions to determine the influence of surfactant concentration on droplet solubilisation. Figure 4.9 shows the particle size change in secondary emulsions when different concentrations of Tween 80 micelle solutions were used as dilution medium. It can be seen that when 1% Tween 80-stabilised 10% lemon oil primary emulsion was diluted by Milli-Q water (0% Tween 80), the particle size of the resulting secondary emulsions was relatively constant, ranging from 188 nm to 240 nm but no significantly different, which was close to the particle size of the original primary emulsion. As a result, the secondary emulsions were all opaque regardless of their lemon oil concentration from 0.1% to 2.0%. In other words, the dilution of primary emulsion with Milli-Q water did not facilitate the fabrication of microemulsions, regardless of the final oil concentration of secondary emulsions. This phenomenon could be due to the lack or relatively low concentration of surfactant micelles, thus resulting in the low solubility or diffusion of lemon oil (Rao and McClements, 2012a). Rao and co-workers also demonstrated that the water solubility of limonene which is the main component of lemon oil was 0.0005% (Rao

and McClements, 2012a). On the contrary, using Tween 80 solution as a dilution medium resulted in the formation of microemulsions. In particular, when the dilution medium used was 0.5, 1 and 2% of Tween 80, Cmax was shown to increase as 0.1, 0.2 and 0.3%, respectively, with increasing surfactant concentration. The visual appearance of samples shown in Figure 4.10 was in agreement with the results of the particle size determination shown in Figure 4.9. When the primary emulsion was diluted by 0.5, 1 and 2% Tween 80 solutions, the secondary emulsion was transparent when the lemon oil concentration was smaller than 0.1, 0.2 and 0.3%, respectively. As a consequence, it can be concluded that with increasing surfactant micelle concentration, the maximum amount of lemon oil that could be diffused out from the primary emulsion and then solubilised and incorporated into surfactant micelles increased, which can be attributed to the increasing amount of surfactant micelles available to accommodate more oil (Rao and McClements, 2012c).

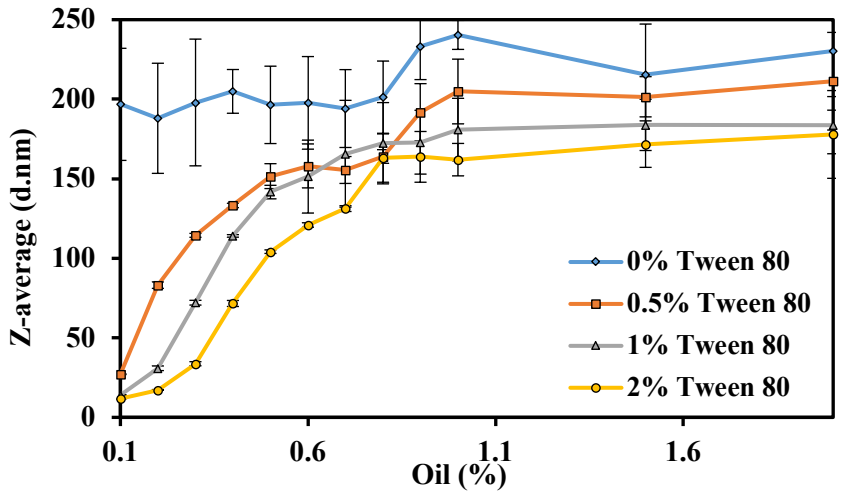

Figure 4.9 Particle size of secondary emulsions (0.1 - 2.0% oil) made from the dilution of 1% Tween 80-stabilised 10% lemon oil primary emulsion into Tween 80 micelle solutions at different surfactant concentrations (0, 0.5, 1 and 2%) after storage at ambient temperature for 1 day. Data are presented as the mean and standard deviation of two independent measurements with duplicate (n=4) and error bars mean standard deviation.

Another experiment carried out in this study was that the concentration of Tween 80

used to prepare stock emulsion was increased from 1% to 2%. Particle size of primary emulsion after preparation was 246 ± 6 nm, which was even higher than that prepared with 10% lemon oil and 1% Tween 80. After that, different concentrations (0.5, 1 and 2%) were employed to dilute the prepared stock emulsion to study the influence of surfactant concentration which was used to prepare primary emulsion on droplet solubilisation. Similar to the results when 1% Tween 80 was employed to make primary emulsion, the increase in the concentration of Tween 80 micelle solution used to dilute primary emulsion resulted in the increase in Cmax value. As drawn from the data shown in Figures 4.11 and 4.12, it can be concluded that the Cmax value for stock emulsion diluted by 0.5, 1 and 2% Tween 80 was 0.1, 0.3 and 0.5%, respectively.

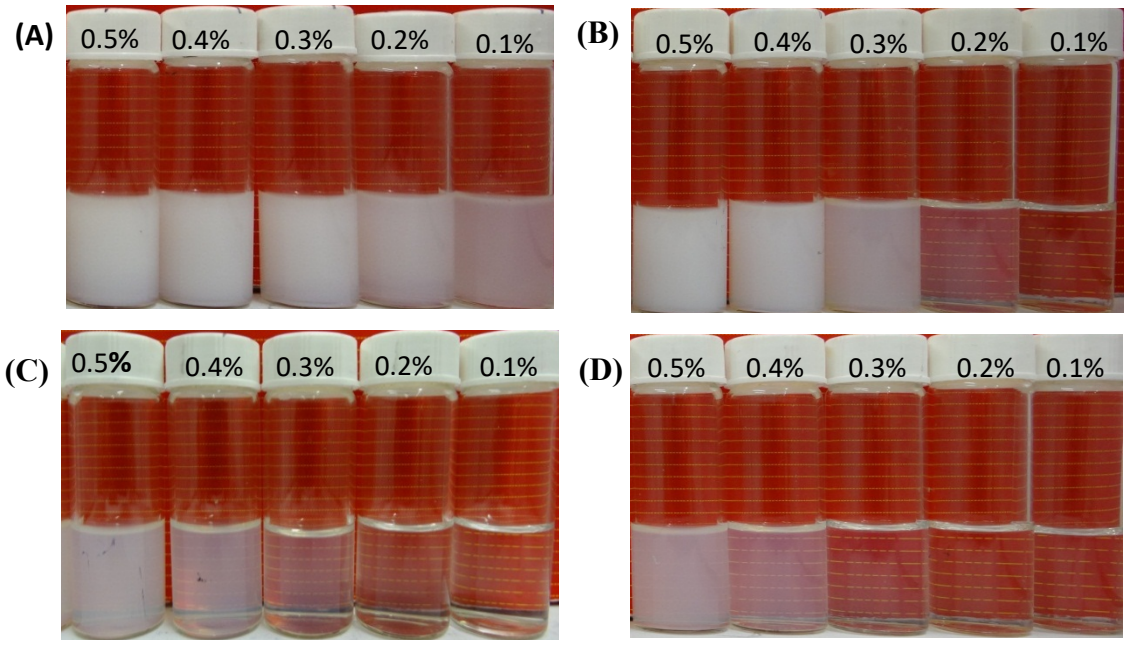

Figure 4.10 Photos of secondary emulsions (0.1-0.5% lemon oil) made from the dilution of 1% Tween 80-stabilised 10% lemon oil primary emulsion by different concentrations of Tween 80 solutions after storage at ambient temperature for 1 day. Dilution medium: (A) 0% Tween 80 (Milli-Q water), (B) 0.5% Tween 80, (C) 1% Tween 80 and (D) 2% Tween 80.

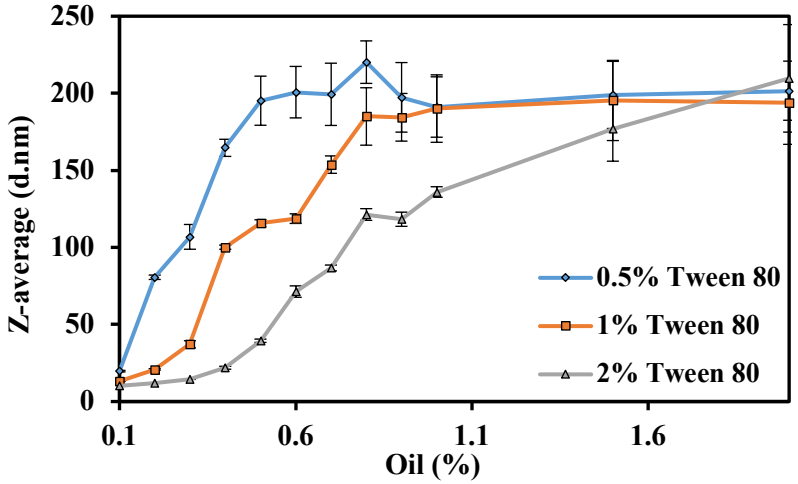

Figure 4.11 Particle size of secondary emulsions (0.1 - 2.0% oil) made from the dilution of 2% Tween 80-stabilised 10% lemon oil primary emulsion into Tween 80 micelle solutions at different surfactant concentrations (0.5, 1 and 2%) after storage at ambient temperature for 1 day. Data are presented as the mean and standard deviation of two independent measurements with duplicate (n=4) and error bars mean standard deviation.

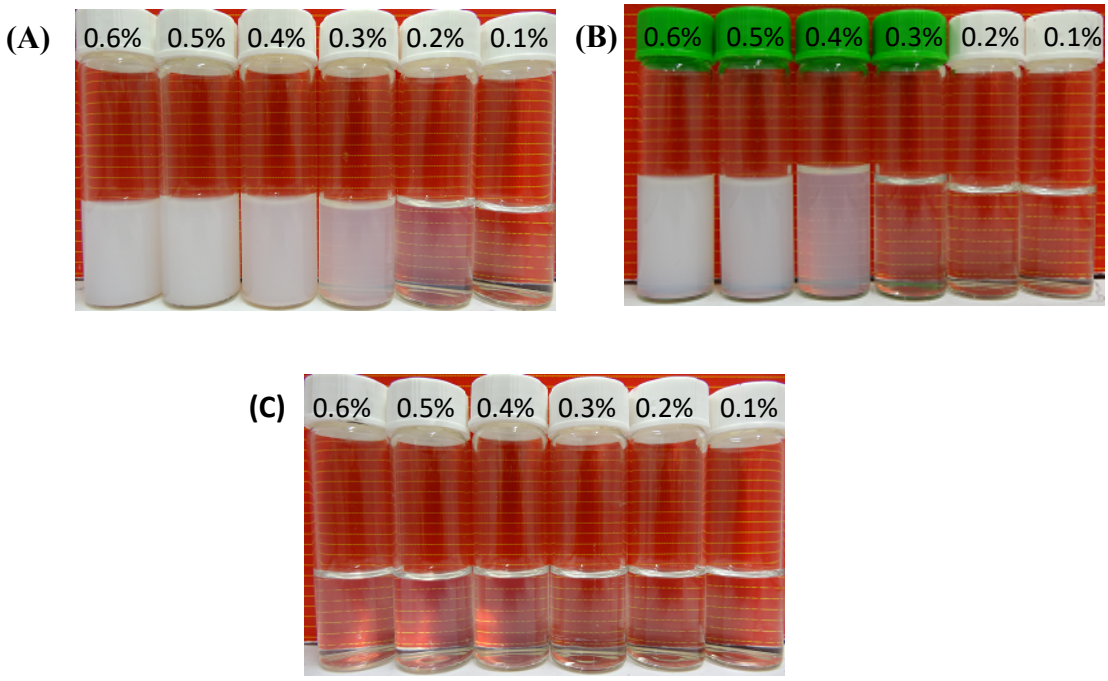

Figure 4.12 Photos of secondary emulsions (0.1-0.6% lemon oil) made from the dilution of 2% Tween 80-stabilised 10% lemon oil primary emulsion by 1% of different types of Tween solutions after storage at ambient temperature for 1 day. Dilution medium: (A) 0.5% Tween 80, (B) 1% Tween 80, (C) 2% Tween 80.

4.4.4 Influence of surfactant type on droplet solubilization

Four different types of surfactants (Tween 20, 40, 60 and 80) at 1% were employed to make 10% lemon O/W primary emulsions, which were then titrated by 1% Tween 20, 40, 60 or 80 solutions to fabricate a series of secondary emulsions. The particle size of primary emulsions is given in Table 4.2, which demonstrates that Tween 20, 40, 60 and 80 could all fabricate 10% lemon oil emulsion by high energy homogenisation method. The primary emulsions formed by all the surfactants had a similar Z-average particle size (approximate 230 nm in diameter) and PDI (about 0.40), which means Tween 20, 40, 60 and 80 had the similar emulsifying capacity.

Table 4.2 The particle size and PDI of primary emulsions in which 10% lemon oil was emulsified into 1% Tween 20, 40, 60 and 80 solutions. The measurement of particle size was conducted after the emulsion preparation. Data are presented as the mean and standard deviation of two independent measurements with duplicate (n=4).

Surfactant type	Z-average (d.nm)	PDI
Tween 20	231 ± 11	0.41 ± 0.03
Tween 40	227 ± 10	0.43 ± 0.04
Tween 60	222 ± 21	0.40 ± 0.05
Tween 80	226 ± 20	0.44 ± 0.04

The primary emulsions were then diluted by 1% Tween 20, 40, 60 or 80 solutions to determine the influence of surfactant type on the solubilisation degree of lemon oil in surfactant micelles. Figure 4.13 shows that regardless of the type of surfactants used to obtain primary emulsions, Tween 20 micelles as dilution medium could not accommodate lemon oil to make microemulsions (< 50 nm in diameter). However, the results show that when Tween 40 was used as the dilution medium, more lemon oil could be incorporated into micelles. Specifically speaking, when lemon oil concentration was 0.1%, the secondary emulsion was microemulsion. As such, it can

be concluded that the Cmax of Tween 40 solution was 0.1%. If primary emulsions (10% lemon oil stabilised by 1% Tween 20, 40, 60 and 80) were diluted by 1% Tween 60 solution or 1% Tween 80 solution, microemulsion was formed when lemon oil concentration was 0.1% and 0.2%, respectively. Absorbance and appearance data (Figures 4.14, 4.15, 4.16 and 4.17) were also in agreement with the data from particle size measurement.

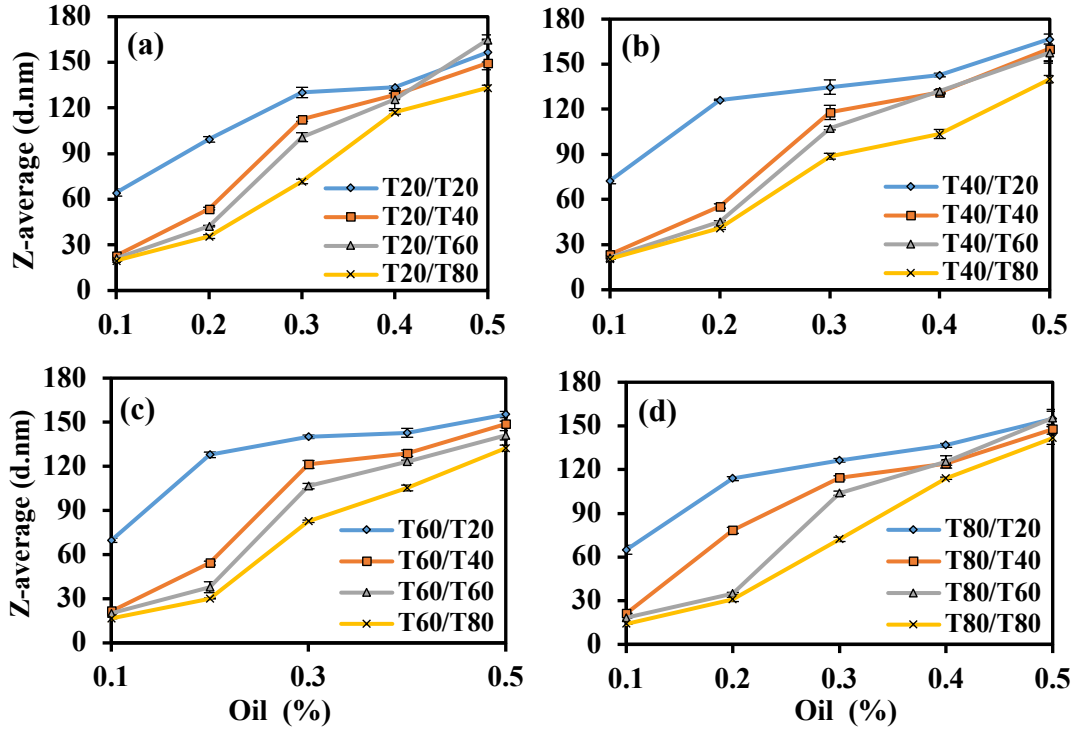

Figure 4.13 Particle size of secondary emulsions (0.1-0.5% oil) made from the dilution of 1% Tween (20, 40, 60 or 80)-stabilised 10% lemon oil primary emulsion by 1% Tween (20, 40, 60 or 80) solutions after storage at ambient temperature for one day. (a) 1% Tween 20 used to make primary emulsion. (b) 1% Tween 40 used to make primary emulsion. (c) 1% Tween 60 used to make primary emulsion. (d) 1% Tween 80 used to make primary emulsion. Data are presented as the mean and standard deviation of two independent measurements with duplicate (n=4) and error bars mean standard deviation.

The reason for the results observed could be due to a difference in the molecular characteristics of surfactant micelles. The chain length of the hydrocarbon tail of Tween 20 and 40 is 12 and 16, respectively, while that of Tween 60 and 80 is 18. The

longer hydrocarbon chain length means Tween 60 and 80 have a larger hydrophobic core, resulting in more lemon oil being incorporated. The results of this study was in agreement with those reported by Ziani and co-workers, who investigated the effect of surfactant type (Tween 20, 60 and 80) on droplet solubilisation (Ziani et al., 2012a). They also found 1% Tween 60 and 1% Tween 80 had the similar capacity to accommodate lemon oil. Nevertheless, more lemon oil could be incorporated compared to our study. In addition, a certain amount of lemon oil was able to transfer from initial emulsion into 1% Tween 20 micelle solution to fabricate microemulsions. This may be due to 4-fold lemon oil which was utilised in their study, whereas 1-fold lemon oil was used in this study. According to Rao and McClements (2012a), with increasing lemon oil fold, more lemon oil could be incorporated into micelles.

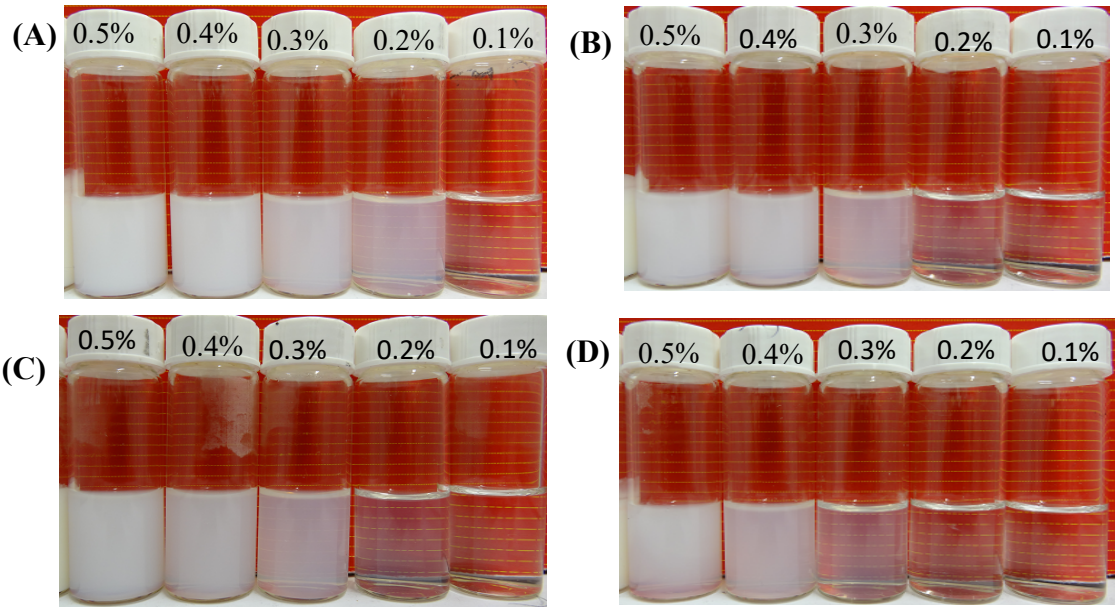

Figure 4.14 Photos of secondary emulsions (0.1-0.5% lemon oil) made from the dilution of 1% Tween 20-stabilised 10% lemon oil primary emulsion by 1% of different types of Tween solutions after storage at ambient temperature for 1 day. Dilution medium: (A) 1% Tween 20, (B) 1% Tween 40, (C) 1% Tween 60 and (D) 1% Tween 80.

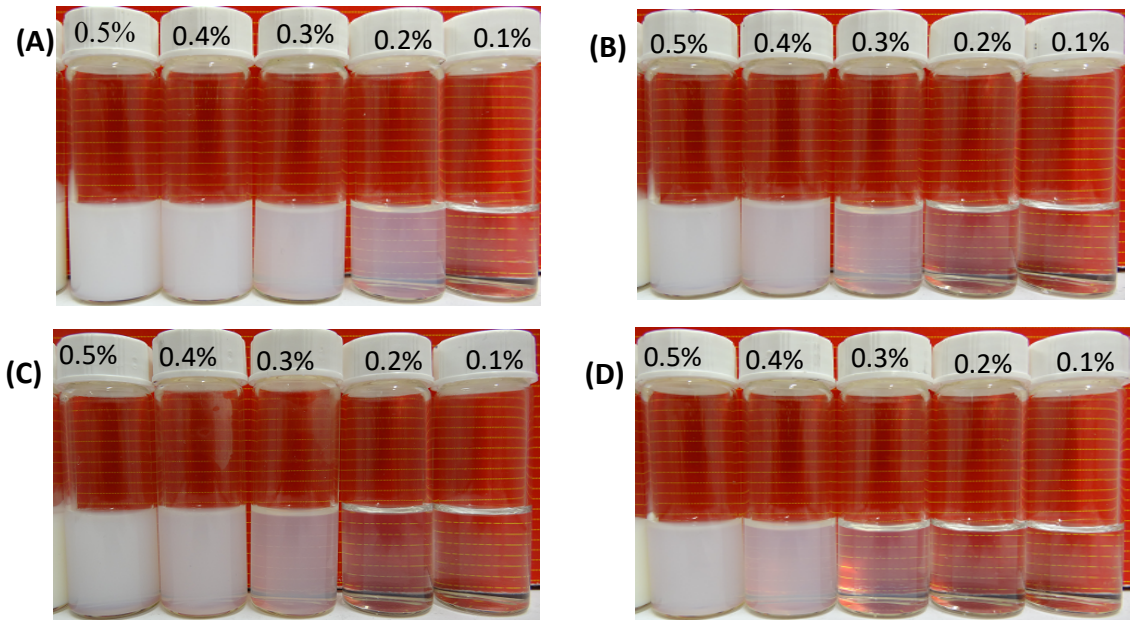

Figure 4.15 Photos of secondary emulsions (0.1-0.5% lemon oil) made from the dilution of 1% Tween 40-stabilised 10% lemon oil primary emulsion by 1% of different types of Tween solutions after storage at ambient temperature for 1 day. Dilution medium: (A) 1% Tween 20, (B) 1% Tween 40, (C) 1% Tween 60 and (D) 1% Tween 80.

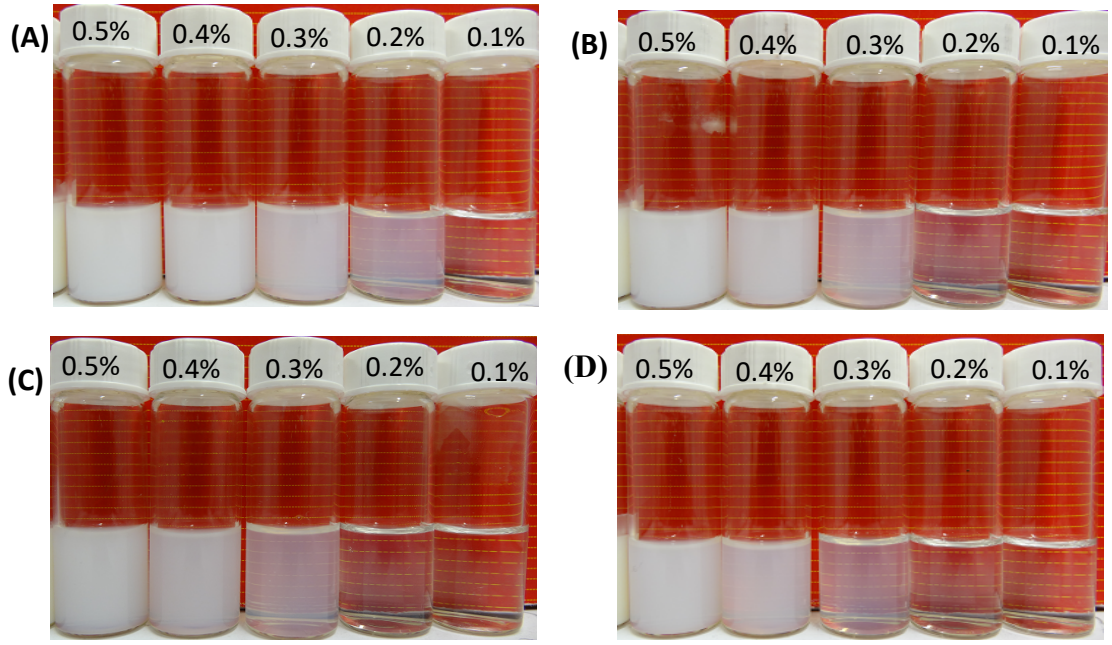

Figure 4.16 Photos of secondary emulsions (0.1-0.5% lemon oil) made from the dilution of 1% Tween 60-stabilised 10% lemon oil primary emulsion by 1% of different types of Tween solutions after storage at ambient temperature for 1 day. Dilution medium: (A) 1% Tween 20, (B) 1% Tween 40, (C) 1% Tween 60 and (D) 1% Tween 80.

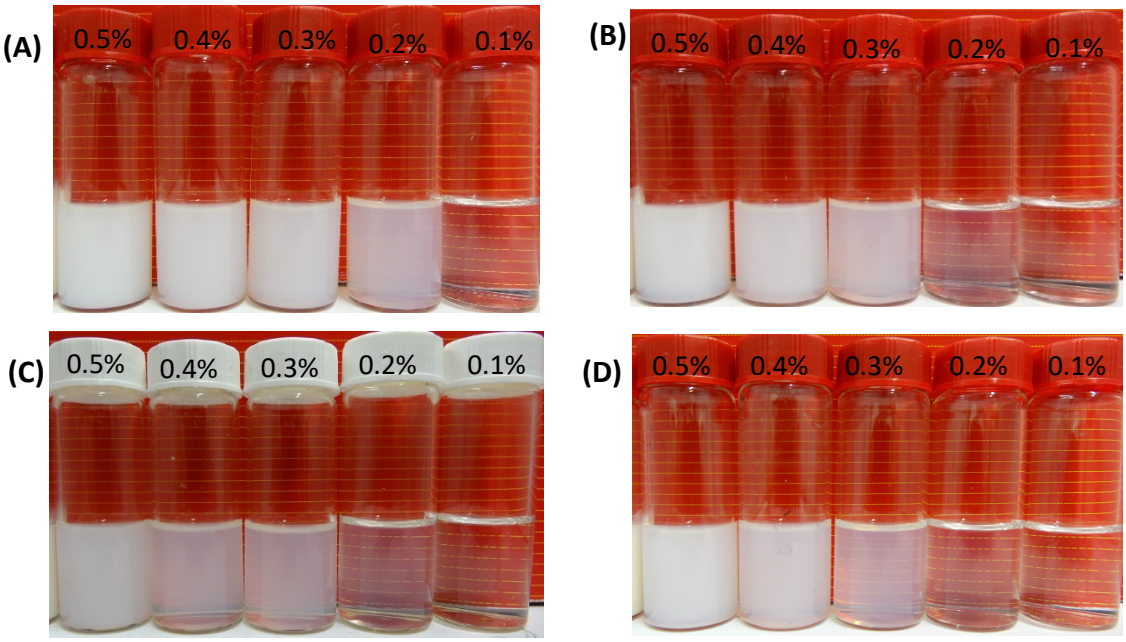

Figure 4.17 Photos of secondary emulsions (0.1-0.5% lemon oil) made from the dilution of 1% Tween 80-stabilised 10% lemon oil primary emulsion by 1% of different types of Tween solutions after storage at ambient temperature for 1 day. Dilution medium: (A) 1% Tween 20, (B) 1% Tween 40, (C) 1% Tween 60 and (D) 1% Tween 80.

4.5 Conclusions

This study focused on understanding the effects of type and concentration of oils and surfactants on the formation of microemulsion by emulsion dilution method. The principle of this method was due to the diffusion and transfer of oil phase from a stock emulsion into surfactant micelles. Triglycerides (peanut oil and coconut oil) which had a large molecular weight, water insolubility and high viscosity did not favour the formation of microemulsion by this method. On the other hand, IPM and lemon oil were able to produce microemulsions by emulsion dilution method because of their small molecular weight, non-triglyceride oil, and low viscosity. However, their ability to form microemulsions was dependent on the final oil concentration after dilution. In case of IPM, 0.1% IPM could be incorporated into the 1% Tween 80 solution to form a microemulsion. Lemon oil was the most efficient when fabricating microemulsions by emulsion dilution method. In addition, the type and concentration of surfactants

had an effect on the formation of microemulsion. The mean particle sizes of 10% lemon oil primary emulsions stabilised by 1% Tween 20, 40, 60 and 80 solutions were similar, at around 230 nm in diameter. However, if these four surfactant solutions were employed to dilute the primary emulsions, their ability to accommodate lemon oil was distinct. Tween 20 incorporated the least amount of lemon oil, while Tween 80 was able to incorporate the highest amount of lemon oil. In terms of surfactant concentration, 2% Tween 80 solution could incorporate the highest amount of lemon oil, in comparison to 0.5% and 1% Tween 80 solutions. When 2% Tween 80 solution was employed to dilute 1% Tween 80 stabilised-10% lemon oil emulsion, Cmax was 0.4%. Overall, this study provides some useful information about the formation of microemulsion via emulsion dilution method.

Chapter 5 Formation of microemulsions by water titration method: Effects of oil and surfactant type and concentration

5.1 Abstract

Water titration method is a common method being utilised to produce microemulsions. A ternary or pseudo ternary phase diagram is normally constructed using the water titration method. In this study, the water titration method was used to construct the ternary or pseudo ternary phase diagrams with different kinds of oils (Captex 100, Capmul PG-8, Capmul PG-12, Capmul PG-2L, lemon oil, Capmul MCM C8, Capmul 708G and Captex 355) and surfactants (Tween 80, Tween 20, Span 80 and Kolliphor EL). All these oils and surfactants could be used to make microemulsions by the water titration method, but their ability to form microemulsions were different. Among these oils, when Tween 80 was employed as the surfactant, Capmul 708G was most efficient in fabricating microemulsions, with the total one-phase microemulsion area (A_T) value as high as 65.1%.

As for surfactants, Tween 80, Tween 20 and Kolliphor, whose hydrophilic-lipophilic balance (HLB) values were not significantly distinct from each other, had similar emulsifying properties when constructing ternary phase diagrams with Capmul MCM C8 and Capmul 708G. Span 80 that has an HLB value of 4.3 was not as efficient because its mixture system (Span 80, water and Capmul 708G) only had an A_T value of 24.2%. Even when Span 80 was mixed with Tween 80 as a ratio of 1:1, 1:2 and 2:1, the A_T value was still much smaller than that of Campul 708G, water and Tween 80 mixture system. Furthermore, absolute ethanol and PG were employed as cosurfactant and cosolvent into Capmul MCM C8, Tween 80 and water system. They both had the ability to enlarge the area of microemulsions in the ternary phase diagrams. When 50% PG was added into Milli-Q water to construct the pseudo ternary diagram with Capmul

708G and Tween 80, A_T value was as high as 100%.

This study provides important information about the effects of type and concentration of surfactant and oil as well as cosurfactant and cosolvent on the formation of microemulsions fabricated via water titration method. Also, the measurements of samples for their conductivity, viscosity and dye staining are vindicated to be able to differentiate the type of microemulsions.

5.2 Introduction

In Chapter 4, emulsion dilution method was introduced to fabricate microemulsions. This method is based on a combined method of high energy and low energy emulsification. Apart from it, low energy emulsification methods to fabricate microemulsions also phase inversion temperature (PIT) method, water titration method, oil titration method and cosurfactant titration method.

Many researchers employed the water titration method to produce microemulsions (Feng et al., 2009b, Chen et al., 2014, Barradas et al., 2015, Guo et al., 2016, Cheng et al., 2017). In the water titration method, water is added continuously into the mixture of oil and surfactant, producing water droplets. When the concentration of water is over a critical amount, the coalescence rate of water droplets is higher than that of oil droplets, so phase inversion occurs. Small oil particles are formed at the phase inversion point, at which the interfacial tension is the lowest. Ternary or pseudo ternary phase diagrams are normally created to study the phase behaviours of each system during the process of the water titration method. In the phase diagram, a number of different systems can be formed, including W/O microemulsions, O/W microemulsions, bicontinuous microemulsions, coarse emulsions, liquid crystals, and three-phase regions (Acharya and Hartley, 2012, Lawrence and Rees, 2012). In a

bicontinuous microemulsion system, both water and oil are acted as the external phase and the quantity of water and oil is similar (Paul and Moulik, 1997).

In a study reported by Zheng et al. (2013a) to fabricate garlic oil encapsulated microemulsion, a mixture of 98% oleic acid and 2% garlic oil was introduced as the oil phase, Cremophor RH40 and ethanol or n-butanol were employed as surfactant and cosurfactant (the ratio of surfactant to cosurfactant (Km) was 1:1, 2:1 and 3:1). It was documented that both ethanol and n-butanol could be used to fabricate O/W microemulsion regardless of Km was 1:1, 2:1 or 3:1, but O/W microemulsion with n-butanol was more stable. Furthermore, when ethanol was used as cosurfactant and the Km value was 2:1, the area of O/W microemulsion region in the pseudo ternary phase diagram was the largest. Nevertheless, if n-butanol was used as cosurfactant, the O/W microemulsion region increased with increase in Km value from 1:1 to 3:1.

According to Garti and co-workers, 13% of the TPD was occupied by microemulsion area when the mixture system was composed by R (+)-limonene, water and Brij 96v. After introducing ethanol as the cosurfactant (ratio of R (+)-limonene to ethanol was 1:1), microemulsion area increased to 30.3%. If water mixed with PG at a ratio of 1:1 and the mixture was added as the aqueous phase, microemulsion area raised to 73.0%. On the other hand, Garti et al. (2001) replaced Brji 96v with Tween 20, 40, 60 and 80 and reported the microemulsion area in the TPD was 42.0%, 52.0%, 56.0% and 64.0%, respectively.

Macroscopic level and microscopic level approaches are introduced to characterize the mixture systems during the addition of water into oil and surfactant to determine the type of these systems. In the literature, these approaches included electrical conductivity (Zargar-Shoshtari et al., 2010, Klossek et al., 2014), viscosity (Garti et al., 2004, Shevachman et al., 2004), nuclear magnetic resonance (NMR) (Krauel et al.,

2005), small-angle neutron scattering (SANS) (Shukla et al., 2002, de Campo et al., 2004), small-angle X-ray scattering (SAXS) (Podlogar et al., 2004), electron microscopy (EM) (Gulikkrzywicki and Larsson, 1984, Boonme et al., 2006), differential scanning calorimetry (DSC) (Boonme et al., 2006), polarized light microscopy (Basheer et al., 2013) and etc.

The objective of this study was to investigate the influence of types and concentrations of oil and surfactant on the formation of microemulsion by the water titration method. The mixture systems were characterized by dye staining method, electrical conductivity, viscosity, visual observation, TEM and particle size determination. Results obtained from this study provide useful information in fabricating decent colloidal delivery systems which can be utilised for application in transparent foods or beverages.

5.3 Materials and Methods

5.3.1 Materials

In this chapter, Tween 80, Kolliphor EL and Span 80 were utilised as the surfactants. Lemon oil, Capmul MCM C8, Capmul 708G, Capmul PG-2L, Capmul PG-12, Capmul PG-8, Captex 100 and Captex 355 were used as the oil phase.

5.3.2 Analysis of mixture samples

TPDs were constructed using the method previously illustrated in Section 3.2.2 of Chapter 3. As Figure 3.4 illustrated, dilution line W91, W82, W73, W64, W55, W46, W37, W28 and W19 mean the ratios of oil to surfactant are 1:9, 2:8, 3:7, 4:6, 5:5, 6:4, 7:3, 8:2 and 9:1, respectively. Microemulsion type was further determined via the following techniques (e.g. dye staining and electrical conductivity), apart from particle size and PSD analysis.

5.3.3 Dye staining method

Microemulsion type was identified by dye staining method, in which two drops of water-soluble dye (Methylene Blue) and oil-soluble dye (Sudan Red) were added into 2 ml emulsion to evaluate the diffusion rate of these two dyes. If the external phase was blue, the microemulsion was O/W microemulsion, and if the external phase was red, the microemulsion was W/O microemulsion.

5.3.4 Electrical conductivity

Electrical conductivity meter (CyberScan CON 11, Eutech Instruments, Singapore) (Figure 5.1a) was employed to measure conductivity of the mixture at 20°C which is an indication of microemulsion type (O/W microemulsion or W/O microemulsion). The stainless-steel electrode of the conductivity meter was immersed into the microemulsion samples, which must be equilibrated until the reading of the conductivity meter was stable before measurement. Each sample was measured in duplicate.

5.3.5 Viscosity

Viscosity of samples was measured using an AR-550 rheometer (TA Instruments, Delaware, USA) (Figure 5.1b). Cone (40 mm diameter with an angle of 2°) and plate geometry was chosen. The temperature was maintained at 20 ± 0.5 °C throughout the measurement. Apparent viscosity was measured as a function of shear rate, which ranged from 1 s^{-1} to 200 s^{-1}). The viscosity value was recorded at the shear rate of 53 s^{-1}. Viscosity of each sample was measured in duplicate.

(a)  (b) 

Figure 5.1 Photos of (a) electrical conductivity meter (b) rheometer

5.3.6 Effect of some variables

5.3.6.1 Effect of oils

Different types of oils (Capmul MCM C8, lemon oil, Capmul 708G, Capmul PG-2L, Capmul PG-12, Capmul PG-8, Captex 100 and Captex 355) were used to construct ternary phase diagrams with the same surfactant, Tween 80, to determine the effect of oils on the fabrication of emulsions.

5.3.6.2 Effect of surfactants

Four different surfactants (Kolliphor EL, Tween 80, Tween 20 and Span 80) were employed to construct ternary phase diagrams with the same oil phase to determine the effect of surfactants on the formation of emulsions.

5.3.6.3 Effect of cosurfactant

Absolute ethanol was introduced into the mixture of Capmul MCM C8, Tween 80 and Milli-Q water as a cosurfactant. The mass ratios of Tween 80 and absolute ethanol (Km) were 1:1, 2:1 and 3:1. Tween 80 and absolute ethanol were mixed for 24 hours at ambient temperature. Then, the mixture was mixed with Capmul MCM C8 at weight

ratios of 1:9, 2:8, 3:7, 4:6, 5:5, 6:4, 7:3, 8:2 and 9:1. These mixtures were then diluted dropwise with Milli-Q water in 10% w/w increments, under moderate agitation using a vortex mixer. The four components together formed a pseudo ternary phase diagram. Apart from Capmul MCM C8, Capmul 708G and lemon oil mixture systems also included ethanol when Km was 1:1 as the cosurfactant.

5.3.6.4 Effect of cosolvent

Propylene glycol (PG) was utilized as a cosolvent to construct a pseudo ternary phase diagram. PG and Milli-Q water were mixed at ratios of 1:1, 1:3 and 3:1 for 24 hours at ambient temperature. Capmul MCM C8 was mixed with Tween 80 at weight ratios of 1:9, 2:8, 3:7, 4:6, 5:5, 6:4, 7:3, 8:2 and 9:1. These mixtures were then diluted dropwise with the mixture of PG and Milli-Q water in 10% w/w increments, under moderate agitation using a vortex mixer. The four components together formed a pseudo ternary phase diagram. Apart from Capmul MCM C8, Capmul 708G and lemon oil mixture systems also included PG when the ratio of Milli-Q water to PG was 1:1 as the cosolvent.

Moreover, the mixture system with Capmul MCM C8, Tween 80, Milli-Q water, propylene glycol and absolute ethanol was also constructed. The ratio of Tween 80 to absolute ethanol was 1:1 and that of Milli-Q water to PG was 1:1. A pseudo ternary phase diagram was formed to determine the total monophasic region (A_T value).

5.4 Results and discussions

5.4.1 Effect of oils on the construction of ternary phase diagrams

To ensure the repeatability, each formulation was prepared two times. Both phase diagrams were found to be the same. It was mentioned in the literature that A_T, which means total isotropic monophasic region (total one-phase microemulsion area), was

introduced to determine the solubilization ability of a mixture system (Garti et al., 1995, Shevachman et al., 2004).

Eight different types of oils were utilized to construct ternary phase diagrams with Tween 80 and Milli-Q water in order to study the effect of oil types on the formation of microemulsions. Appendix Figure 1 shows the appearance of samples from mixture systems containing Milli-Q water, Tween 80 and Capmul 708G. Appendix Figure 2 shows the appearance of samples from mixture systems containing Milli-Q water, Tween 80 and Capmul MCM C8. Figure 5.2 illustrates the results of ternary phase diagrams created. It can be stated from Figure 5.2 that Capmul 708G was the most efficient in terms of producing microemulsions (Figure 5.2g), which was followed by Capmul MCM C8 (Figure 5.2f). Apart from these two, A_T of other oils was as follows: Capmul PG-8 > Capmul PG-12 > Capmul PG-2L > lemon oil > Captex 100 > Captex 355. The last three oils almost had the same A_T values. Furthermore, no gels were formed when Capmul 708G or Capmul MCM C8 was employed as the oil phase. But a large amount of gels was produced when Capmul PG-2L, Capmul PG-12, lemon oil, Captex 355 or Captex 100 was utilized. As for Capmul PG-8, a few gels were formed during the dilution process and if the concentration of water was 60%, gels could be produced when the ratio of oil to Tween 80 was 3:7, 4:6, 5:5, 6:4 or 7:3. Interestingly, in the mixture system of Captex 355, Tween 80 and Milli-Q water, a large number of opaque single-phase liquids, which were coarse emulsions, were created as well. Liquid crystals formed in the systems constituting of Captex 355 or Capmul PG-12, Tween 80 and Milli-Q water.

Four oils used to construct ternary phase diagrams shown in Figure 5.2 (a), (b), (c) and (d) all belonged to propylene glycol (PG) esters. Capmul PG-2L is propylene glycol dilaurate, which contains 77% diester and 22% monoester and the concentration of lauric acid is 99.6%. Lauric acid is a medium-chain saturated fatty acid containing 12

carbons. Capmul PG-12 is propylene glycol monolaurate, more than 90% of which is monoester. Capmul PG-8 is propylene glycol monocaprylate, containing 97.6% of monoester and 100% of caprylic acid, which is an 8-carbon fatty acid. Captex 100 is propylene glycol dicaprate ester, which is comprised of 99.3% capric aid, a 10-carbon fatty acid, and 0.7% caprylic acid. All these four oils were not very efficient at forming microemulsions. For Captex 100 and Capmul PG-2L, microemulsion was only produced when water concentration was smaller than 10% and the ratio of oil to Tween 80 was less than 6:4. A_T of Capmul PG-12/Milli-Q water/Tween 80 system was a little higher than that of systems consisted of Capmul 100 or Capmul PG-2L. Clear regions also existed on the corner of water, when the ratio of Capmul PG-12 to Tween 80 was 1:9 and water concentration was 80% and above. Capmul PG-12 and Capmul PG-2L both contained lauric acid, but the former was mainly monoester and the latter mainly diester, which might be the reason that more microemulsions were formed when Capmul PG-12 was employed as the oil phase. In terms of Capmul PG-8 containing caprylic acid (C8:0), shorter fatty acid chains and its relatively lower viscosity might enable it to penetrate the interfacial film much easier, so it had the highest A_T value within all these four PG esters.

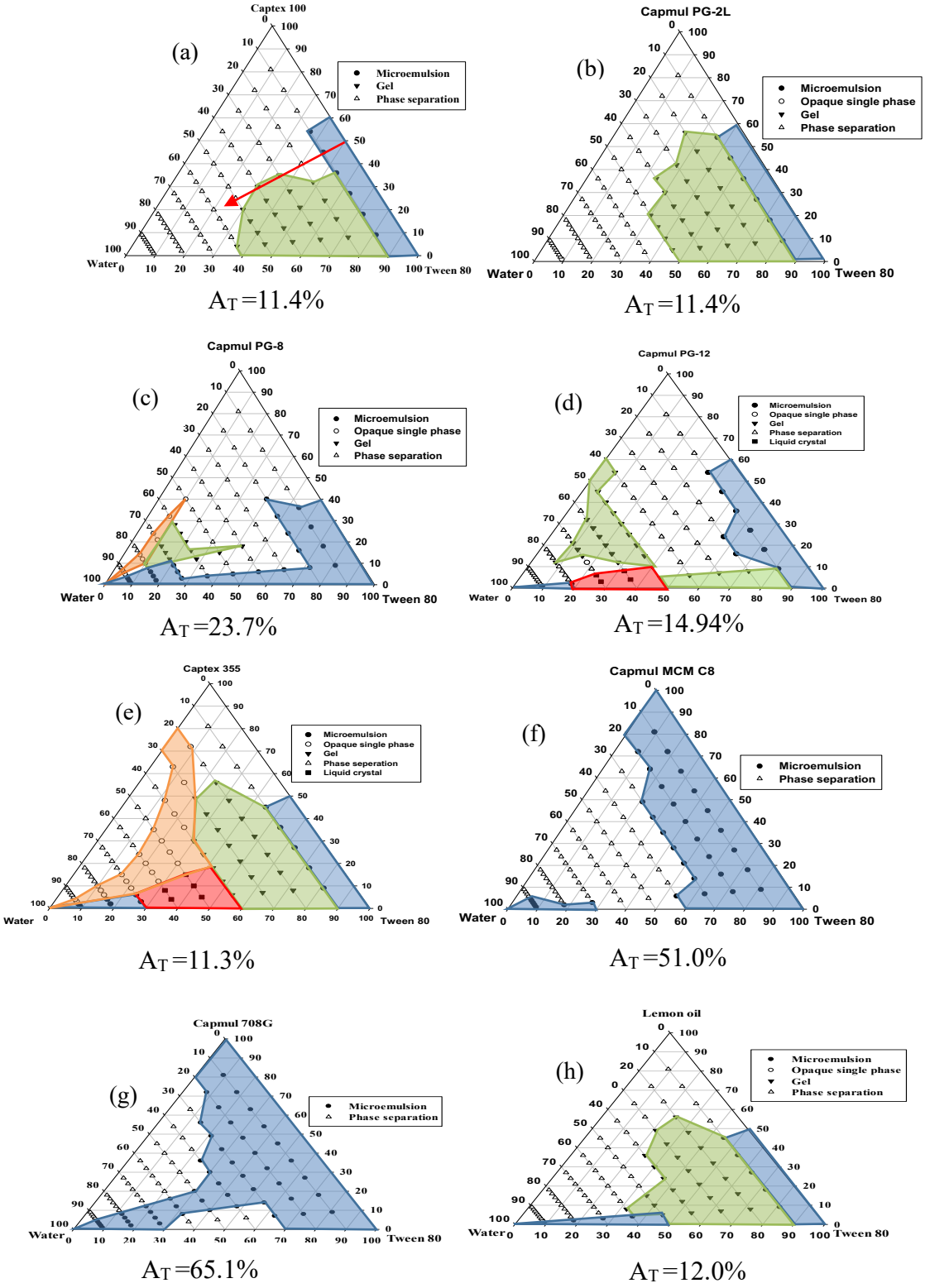

Figure 5.2 Ternary phase diagrams of mixture systems with water, Tween 80 and different types of oils; (a) Captex 100, (b) Capmul PG-2L, (c) Capmul PG-8, (d) Capmul PG-12, (e) Captex 355, (f) Capmul MCM C8, (g) Capmul 708G, and (h) lemon oil. Blue area means microemulsions, green area means gels, orange area represents opaque single-phase liquids and red area means liquid crystal. The arrow indicates the direction of adding water to the mixture of surfactant and oil.

On the other hand, Captex 355 is an MCT containing 57.2% caprylic acid, 42.1% capric acid and 0.7% lauric acid and Capmul 708G is glyceryl monocaprylate with 88.3% monoester. The main fatty acid of Capmul MCM C8 is also caprylic acid (97.3%) and it contains 58.2% monoester and 34.7% diester. As for the Captex 355 mixture system, its A_T value was only 11.3%. The microemulsions could be formed only when the concentration of water was not more than 10% and the ratio of Tween 80 to Captex 355 was not lower than 5:5, or when the concentration of water was not lower than 70% and the ratio of Tween 80 to Captex 355 was not smaller than 8:2. On the contrary, in case of Capmul MCM C8 and Capmul 708G, these oils could fabricate 51.0% and 65.1% microemulsion regions, respectively. When these two oils were introduced, microemulsions formed when water concentration was equal to or smaller than 20% regardless of the ratio of Tween 80 to oil. Moreover, in dilution lines W82, W73 and W64 of Capmul 708G system (Figure 5.2g), microemulsions were produced along the whole dilution line. Chemically, Capmul 708G is mostly made up of monoglyceride and Capmul MCM C8 is the combination of monoglyceride and diglyceride, rendering them amphiphilic functionalities. In other words, they both have emulsifying properties as well. This phenomenon was similar to what has been reported by Roohinejad et al. (2015), who stated almost 50% of the phase ternary diagram was covered by microemulsions. As for lemon oil, which is a mixture of mainly monoterpenes, only 12% of the ternary diagram was covered by monophasic regions (Figure 5.2h). The ternary phase diagram of lemon oil was similar to that of Captex 355 (Figure 5.2e), but only one formulation led to the formation of opaque single-phase liquid compared to a large region of opaque single-phase liquids in the Captex 355 ternary diagram.

5.4.2 Effect of cosurfactant and cosolvent on the construction of pseudo ternary phase diagrams

Capmul MCM C8 was chosen as the oil phase to study the effect of ethanol and PG,

as cosurfactant and cosolvent, respectively, on the formation of microemulsions. Figure 5.3 illustrates three pseudo ternary phase diagrams of the mixture systems of Capmul MCM C8, Milli-Q water, Tween 80 and ethanol, of which three different ratios of Tween 80 to ethanol (Km) were used, such as 1:1, 2:1 and 3:1. Without the addition of ethanol, the A_T value of Capmul MCM C8, Milli-Q water and Tween 80 was 51.0% as shown in Figure 5.2f. When 25% ethanol mixed with 75% Tween 80 (i.e. Km = 3:1) before their mixture mixed with oil and water, the A_T value was increased to 63.8% (Figure 5.3c). The A_T value was kept the same when Km was increased to 2:1. Even when Km was 1:1, the A_T value did not increase much which was only 65.2% (Figure 5.3a). Compared to the cosurfactant free mixture system (Figure 5.2f), the pseudo ternary phase diagrams of the mixture systems with ethanol could incorporate more water when the ratio of Tween 80 and ethanol to Capmul MCM C8 was not higher than 4:6. It is well documented in other studies that ethanol could increase the mobility of the hydrophobic tail of surfactant molecules and the flexibility of the interface between water and oil, thus decreasing the surface tension (Garti et al., 2001).

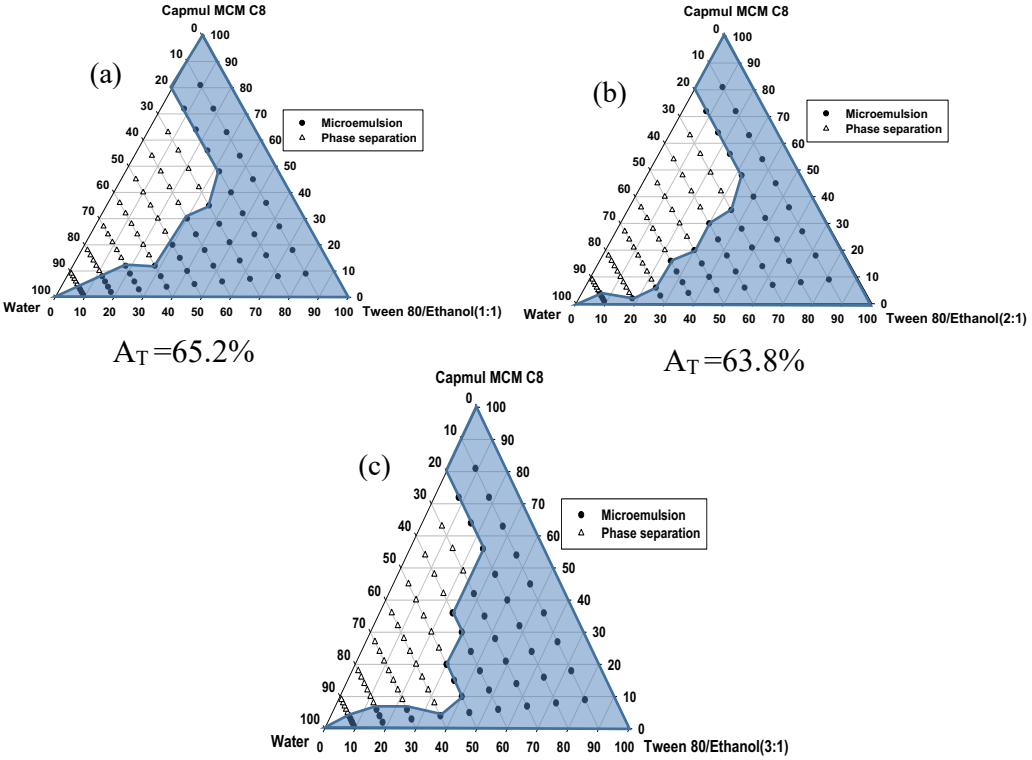

Figure 5.3 Pseudo ternary phase diagrams of mixture systems with Capmul MCM C8, water, Tween 80 and ethanol. (a) Km was 1:1, (b) Km was 2:1, and (c) Km was 3:1. Blue area means clear or microemulsions.

On the other hand, PG was introduced to Capmul MCM C8, Tween 80 and Milli-Q water to act as a cosolvent. Figure 5.4 shows the pseudo ternary phase diagrams of the related mixture systems, in which the ratios of water to PG was 3:1, 1:1 and 1:3. Compared to the cosolvent free system, when Milli-Q water was replaced by 25% PG, the A_T value had a substantial increase to 73.0%. It can be clearly seen from Figure 5.4a that more monophasic liquids were formed towards the corner of aqueous phase. When the ratio of Tween 80 to Capmul MCM C8 was 1:9 and 2:8, microemulsions were formed across the whole dilution line. If the percentage of PG in the aqueous phase increased to 50%, more monophasic liquids were created, covering 91.8% of the ternary graph (Figure 5.4b). Moreover, in dilution lines W91, W82 and W73, isotropic monophasic regions reached the aqueous phase corner. When the concentration of PG further increased to 75% in the aqueous phase, more isotropic

monophasic liquids were produced, covering 97.7% of the ternary phase diagram (Figure 5.4c). In dilution lines W91, W82, W73 and W64, isotropic monophasic regions reached the aqueous phase corner. Besides, when the concentration of aqueous phase was not more than 70%, microemulsions were formed regardless of the ratio of Capmul MCM C8 to Tween 80. It was noticeable that PG might be more efficient at forming isotropic monophasic liquids than ethanol when they were introduced separately into the mixture system of oil, water and surfactant as cosolvent or cosurfactant.

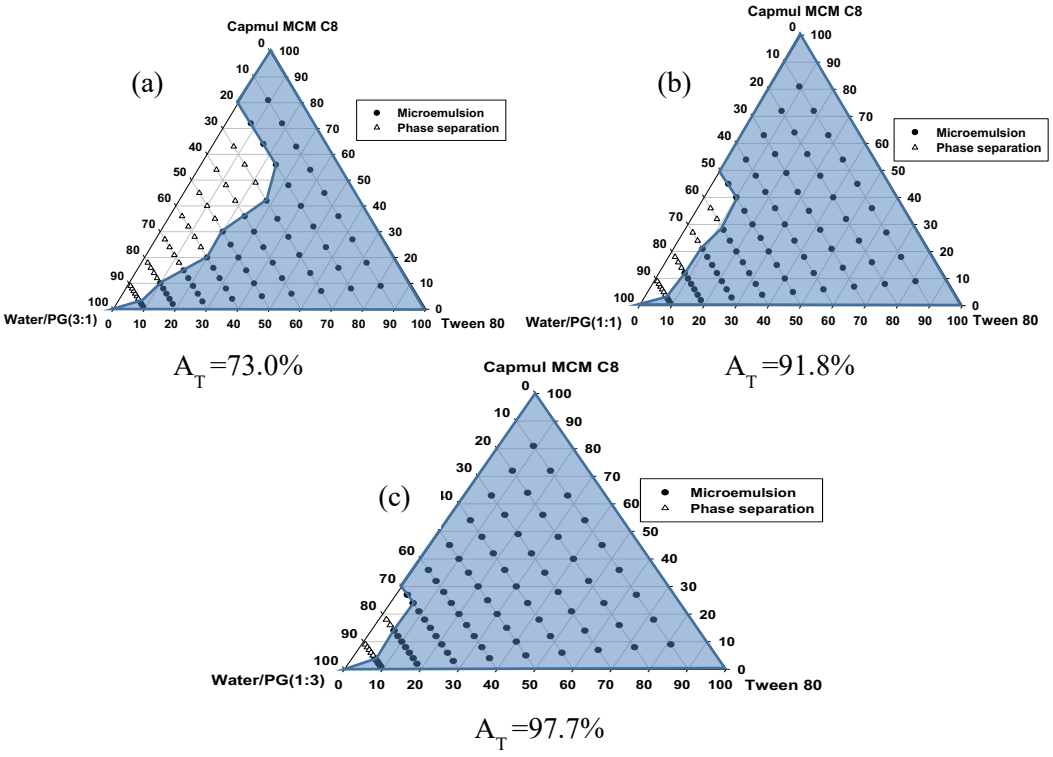

A_T=73.0%

A_T=91.8%

A_T=97.7%

Figure 5.4 Pseudo ternary phase diagrams of mixture systems with Capmul MCM C8, Tween 80, water and PG. The ratio of water to PG was (a) 3:1, (b) 1:1 and (c) 1:3. Blue area means clear or translucent single-phase liquids.

Study was also conducted in a five-component mixture system of Capmul MCM C8, Milli-Q water, Tween 80, PG and absolute ethanol, at which the ratios of Tween 80 to ethanol and water to PG were both 1:1. Figure 5.5 shows that 93.5% of the pseudo ternary phase diagram was covered by isotropic monophasic liquids, which was much larger than the system when only ethanol was used as the cosurfactant (Figure 5.3a).

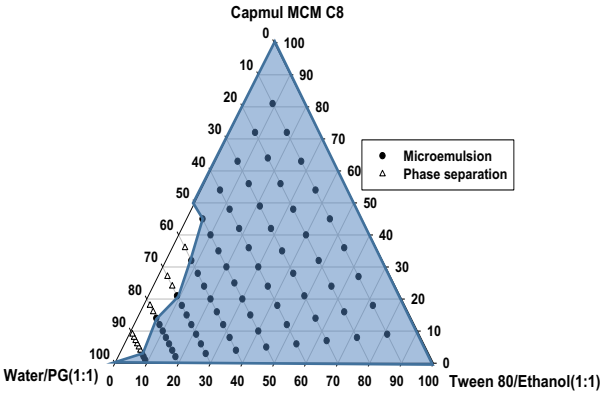

A_T=93.5%

Figure 5.5 Pseudo ternary phase diagram of Capmul MCM C8, Tween 80, ethanol, water and PG mixture system. The ratio of water to PG was 1:1 and that of Tween 80 to ethanol was 1:1. Blue area means microemulsions.

Capmul 708G and lemon oil were also utilised to study the effect of cosurfactant and/or cosolvent. Absolute ethanol mixed with Tween 80 at the ratio of 1:1, constructing the pseudo ternary phase diagram in Figure 5.6a, the A_T value of which was 75.5%, which was almost 10% more than the cosurfactant free system. However, if 50% PG was mixed with water to act as the aqueous phase to construct ternary phase diagram together with Capmul 708G and Tween 80, every single point in the graph shown in Figure 5.6b was isotropic monophasic liquids, i.e. microemulsions. The photos of samples from these mixture systems are shown in Appendix Figure 3.

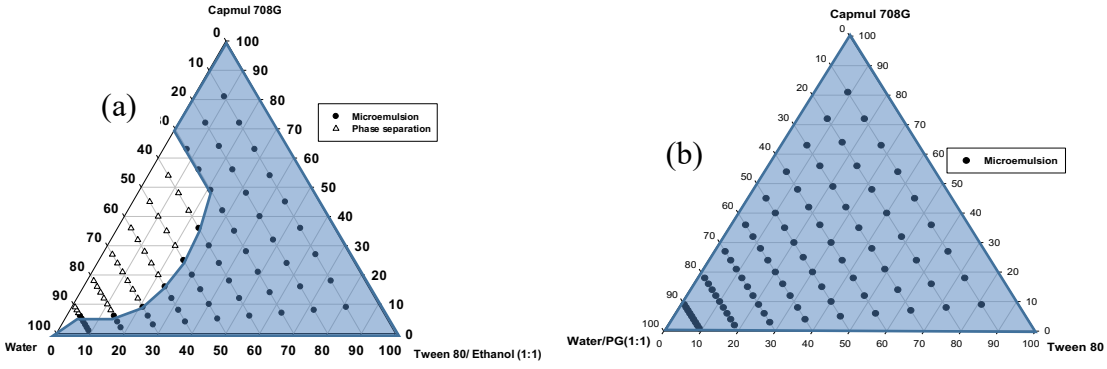

A_T=75.5% A_T=100%

Figure 5.6 Pseudo ternary phase diagrams. (a) Capmul 708G, Tween 80, water and ethanol mixture system in which the ratio of Tween 80 to ethanol was 1:1, and (b) Capmul 708G, Tween 80, water and PG mixture system in which the ratio of water to PG was 1:1. Blue area means microemulsions.

In terms of lemon oil, Tween 80 and Milli-Q water mixture system, the incorporation of 50% ethanol into Tween 80 caused the A_T value to increase from 12% to 24.6% (Figure 5.7a). Besides, no gels were detected in the ethanol-included system. When 50% PG was mixed with water to act as the aqueous phase, the A_T value was further increased to 34.7%, with more aqueous phase being incorporated into the monophasic liquids at higher oil concentration. At dilution line W91, microemulsions were formed across the whole dilution line. Nevertheless, a small amount of gels still existed at dilution lines W55, W46 and W37. In case of both PG and ethanol that were included in lemon oil/Tween 80/Milli-Q water mixture system, as shown in Figure 5.7c, 50.2% of the pseudo ternary phase diagram was covered by isotropic monophasic regions. In this case, clear single-phase liquids were formed when aqueous phase concentration was not higher than 10% regardless of the ratio of oil to surfactant. Like PG-incorporated system, monophasic liquids existed along the whole dilution line of W91. Moreover, at dilution lines W82 and W73, opaque single-phase liquids were created when the concentration of aqueous phase was equal to and more than 80%. This phenomenon was in good agreement with the results reported by Garti et al. (2001) that A_T value in R (+)-limonene/water/Brij 96v system was 13.0%, which was increased to 30.3% when 50% ethanol was mixed with R (+)-limonene. Besides, in addition to ethanol, if 50% PG was mixed with water, A_T value increased dramatically to 73.0%. They also stated that PG helped to increase the fluidity of the interface by being incorporated into the surfactant layer and to reduce the polarity of the water due to its solubility in water (Garti et al., 2001).

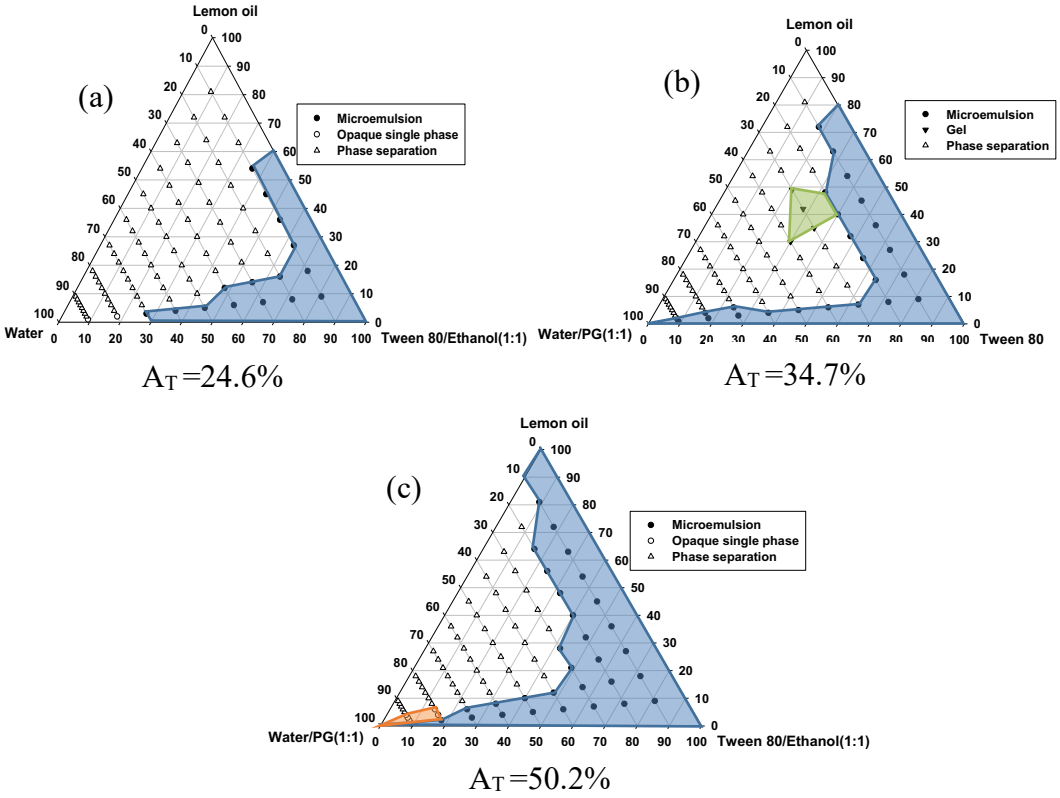

Figure 5.7 Pseudo ternary phase diagrams. (a) Lemon oil, Tween 80, water and ethanol mixture system with the 1:1 ratio of Tween 80 to ethanol, (b) Lemon oil, Tween 80, water and PG mixture system with the 1:1 ratio of water to PG, and (c) Lemon oil, Tween 80, water, ethanol and PG with the 1:1 ratios of water to PG and Tween 80 to ethanol. Blue area means microemulsions, green area means gels and orange area represents opaque single-phase liquids.

5.4.3 Effect of surfactants on the construction of ternary phase diagrams

Apart from Tween 80, Kolliphor EL and Tween 20 were also utilized as surfactants to construct ternary phase diagrams with water and Capmul MCM C8 or Capmul 708G. Figure 5.8 illustrates ternary phase diagrams created by a mixture system consisting of Kolliphor, water and Capmul MCM C8 or Capmul 708G. Figure 5.9 shows ternary phase diagrams created by mixing three components of Tween 20, water and Capmul MCM C8 or Capmul 708G. Compared to the ternary phase diagram formed with Tween 80, Milli-Q water and Capmul MCM C8, the A_T values of ternary phase diagrams created by Milli-Q water, Capmul MCM C8 and Kolliphor EL or Tween 20 did not have a significant change. Similarly, the A_T values of ternary phase diagrams

created by Milli-Q water, Capmul 708G and Kolliphor EL or Tween 20 were not significantly different from that of ternary phase diagram comprised of Milli-Q water, Capmul 708G and Tween 80.

Tween 20 and Tween 80 belong to polyoxyethylene-type non-ionic surfactants and their HLB values are 16.7 and 15.0, respectively. Kolliphor EL, which was previously known as Cremophor EL, is a registered trademark of BASF Co. (Ludwigshafen, Germany). It is a non-ionic emulsifier produced by the reaction of ethylene oxide and castor oil at their molar ratio of 35:1. The main component of Kolliphor EL is glyceryl polyethylene glycol ricinoleate, which is also known as GPGR. It has an HLB value of 12-14. Among these three types of surfactants, Tween 20 has the highest HLB value, meaning it is the most hydrophilic. But their HLB values do not have much difference, and HLB value is not the only factor which determines the ability of surfactant to form microemulsions.

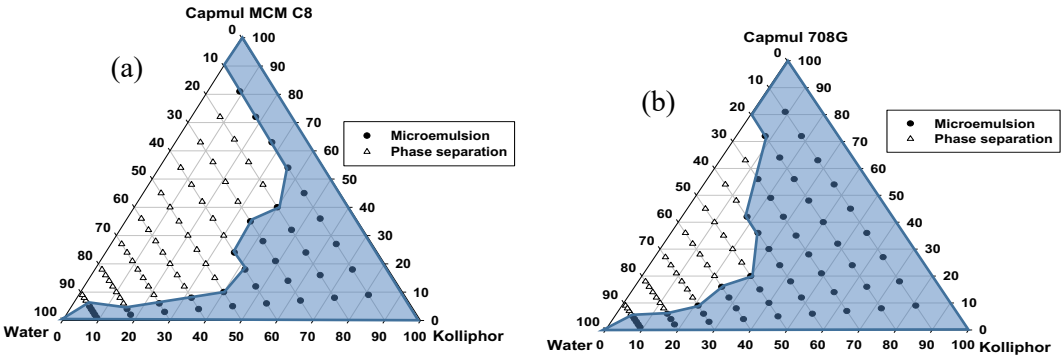

A_T =50.4% A_T =73.6%

Figure 5.8 Ternary phase diagrams of mixture systems with water, Kolliphor and two different types of oils; (a) Capmul MCM C8 and (b) Capmul 708G. Blue area means microemulsions.

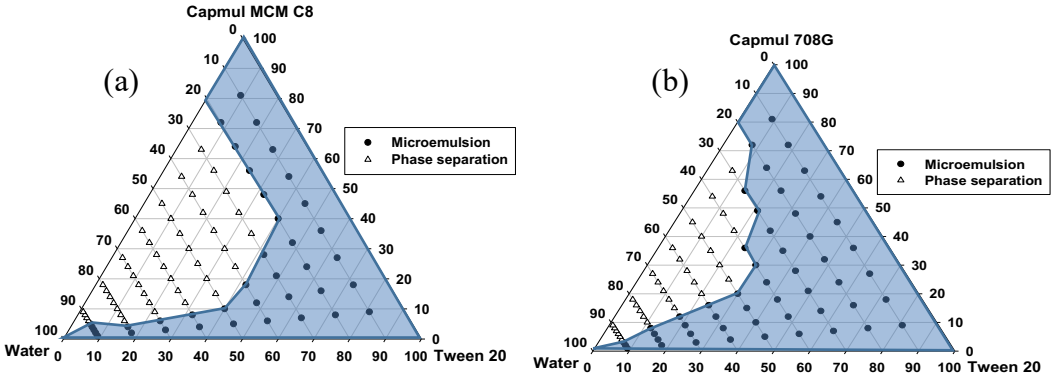

A_T=56.0%

A_T=69.1%

Figure 5.9 Ternary phase diagrams of mixture systems with water, Tween 20 and different types of oils; (a) Capmul MCM C8 and (b) Capmul 708G. Blue area means microemulsions.

On the other hand, Span 80 (sorbitan monooleate) which has an HLB value of 4.3 (Kassem et al., 2019) was employed and mixed with Tween 80 at different ratios of Tween 80 to Span 80 (1:1, 2:1 and 1:2) to construct the ternary phase diagrams with Capmul 708G and Milli-Q water as shown in Figure 5.10. HLB values for the mixtures of Tween 80 and Span 80 at ratios of 1:1, 1:2 and 2:1 were 9.65, 7.87 and 10.75, respectively. When Tween 80 was fully replaced by Span 80, only 24.2% of the ternary phase diagram was found to be covered by isotropic monophasic liquids (Figure 5.10a) unlike the A_T value of 65.1% was observed from the corresponding ternary system prepared with Tween 80 as shown in Figure 5.2g. Besides, monophasic liquids mainly existed near to the apex of Capmul 708G. It was also observed when the ratio of Span 80 to Capmul 708G was 9:1 and 8:2, phase separation occurred regardless of the concentration of water. In terms of Span 80 and Tween 80 which were mixed at the 1:1 ratio, A_T value increased to 42.1%. When the content of water was not higher than 20%, isotropic monophasic liquids existed regardless of the ratio of Capmul 708G to the surfactant mixture (Figure 5.10b). For the 2:1 ratio of Tween 80 to Span 80, only 36.1% of the ternary phase graph was occupied by microemulsions and gels existed along the dilution lines W91 and W82 (Figure 5.10c). On the other hand, if the ratio

of Tween 80 to Span 80 was 1:2, almost half of the ternary phase diagram was covered by monophasic regions (Figure 5.10d). Along the dilution line W28, isotropic monophasic regions existed when water content was above 80% and along the dilution line W19, isotropic monophasic regions existed when water content was above 70%. The results indicated that the addition of Span 80 did not improve the formation of monophasic regions compared to the ternary phase diagrams prepared using Tween 80 alone as a surfactant molecule.

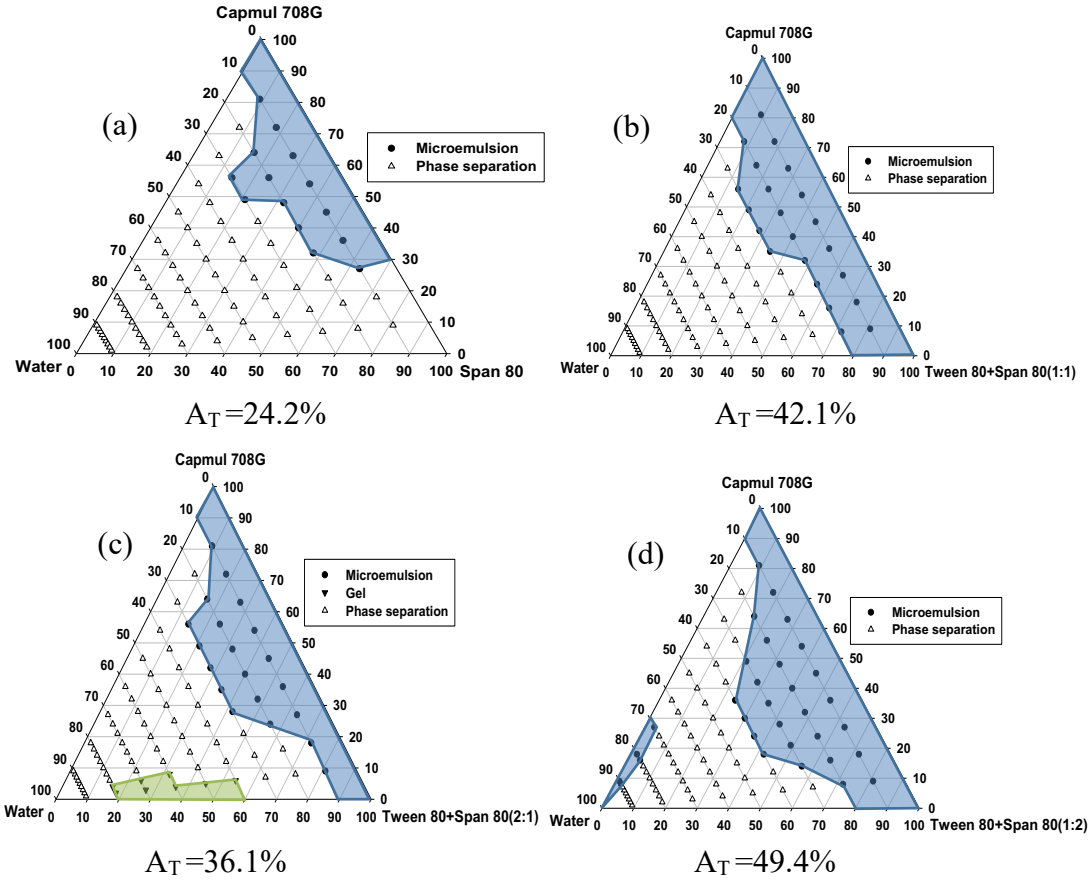

Figure 5.10 Ternary phase diagrams of mixture systems with water and Span 80 with or without Tween 80. (a) Without Tween 80 (i.e. only Span 80), (b) The ratio of Tween 80 to Span 80 was 1:1, (c) The ratio of Tween 80 to Span 80 was 2:1, and (d) The ratio of Tween 80 to Span 80 was 1:2. Blue area means microemulsions and green area means gels.

5.4.4 Electrical conductivity

The electrical conductivity of ternary mixtures was measured to determine the phase inversion and type of microemulsions (W/O, O/W or bicontinuous). At first, oil (Capmul MCM C8 or Capmul 708G) and Tween 80 were mixed at selected ratios, then Milli-Q water or 5 mM sodium chloride (NaCl) solution was added into the mixtures in increments of 5% w/w. Each sample was mixed for at least 5 minutes before it was undisturbed for 5 minutes to be equilibrated. Conductivity was then measured after equilibration using a conductivity meter. Tween 80 which was utilized as the surfactant may contain some impurities (e.g. ionic substances) which could affect and contribute to the conductivity of the ternary systems to some extent. Some studies added a small amount of electrolyte into the aqueous phase to better distinguish the change in conductivity without affecting the phase behaviour of the mixture system (Fanun, 2007, Deutch-Kolevzon et al., 2011). The ratio of Capmul MCM C8 to Tween 80 was 1:9 (w/w) (dilution line W91), and it was 3:7 and 4:6 (w/w) (dilution line W73 and W64) for Capmul 708G to Tween 80. Figures 5.11 and 5.12 illustrate the change in electrical conductivity with changing the concentration of aqueous phases. The conductivity values of Tween 80, Capmul MCM C8, Capmul 708G, Milli-Q water and 5 mM sodium chloride (NaCl) solution were 0.89, 0, 0, 3.24 and 542.33 μS/cm, respectively.

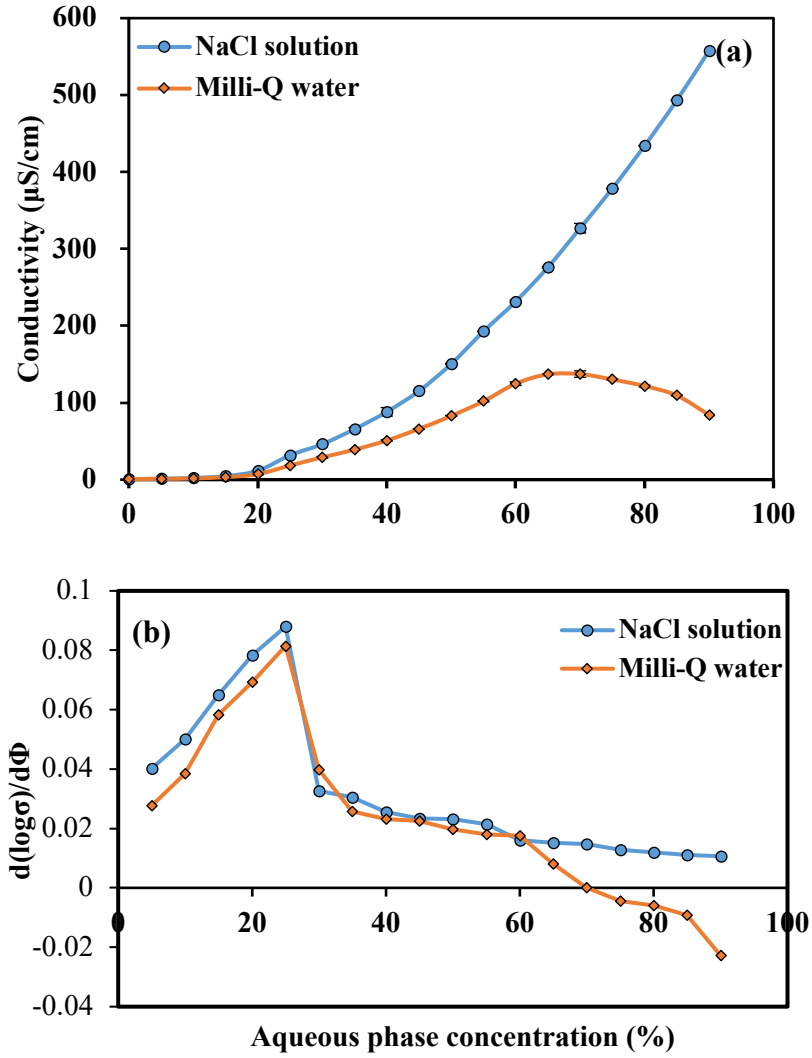

Figure 5.11 (a) Electrical conductivity change as a function of aqueous phase concentration in the mixture system of Capmul MCM C8, Tween 80 and Milli-Q water or 5 mM NaCl solution along the dilution line W91. Data points are presented as the mean and standard deviation of two independent measurements with duplicate (n=4) and error bars mean standard deviation. (b) d(logσ)/d(ϕ) as function of aqueous phase concentration of Capmul MCM C8, Tween 80 and Milli-Q water or 5 mM NaCl solution along the dilution line W91.

From Figure 5.11 (a), it can be concluded that the conductivity value was quite low when the concentration of aqueous phase was below 20%, at which the conductivity was 11.51 and 7.18 µS/cm when 5 mM NaCl solution and Milli-Q water were used, respectively. After that, when NaCl solution was utilized, the electrical conductivity value increased dramatically until the percentage of NaCl solution was 65%. After that, the conductivity increased more remarkedly than it did before. However, when Milli-

Q water was used, the conductivity value was increased from 25.00 to 124.70 μS/cm with the increase in Milli-Q water percentage from 30% to 60%. Then, it remained almost constant when the concentration of Milli-Q water was between 65% and 70%, after which point, it started to decrease slowly. Consequently, three different systems existed during this process, during which a W/O microemulsion was transited into a bicontinuous microemulsion and then it was transited into an O/W microemulsion. Specifically speaking, the two transitions happened when water concentration was 25-30% and 65-70%. In the beginning, aqueous phase concentration is quite low, and it is trapped in the micelles, so it does not contribute much to the conductivity. With the increase in aqueous phase concentration, W/O particles are slowly distorted, resulting in the formation of bicontinuous microemulsion (Garti et al., 2003). After that, aqueous solution became the external phase, which leads to the further increase in electrical conductivity value. Nevertheless, it should be noticeable that phase separation happened when water concentration was between 45% and 60%.

Figure 5.11 (b) was plotted to show the change in $d(\log\sigma)/d\Phi$ as a function of aqueous phase concentration (Φ), σ means conductivity value. It can be clearly seen from this figure that $d(\log\sigma)/d\Phi$ value had an abrupt change when Φ was 25%, which indicated a percolation transition happened at this point (Mehta and Kawaljit, 2002, Fanun, 2008). When Φ was lower than 25%, water or NaCl solution droplets were embedded in oil phase, which had zero conductivity, and they were isolated with each other. As a result, they did not interact with each other to create conductivity. After that, with the increase in aqueous phase concentration, some of these droplets started to contact each other, allowing counter ions to be transferred from one droplet to another (Fanun, 2008). Therefore, conductivity value started to increase dramatically after Φ reached 25%. So, 25% was considered as percolation threshold.

This finding is similar to the results shown in Figure 5.12 that illustrates the electrical conductivity change in the mixture system of Capmul 708G, Tween 80 and Milli-Q water or 5 mM NaCl solution as a function of aqueous phase concentration. When 5 mM NaCl solution was used as the aqueous phase for the dilution of the Capmul 708G and Tween 80 mixture, conductivity values increased continuously during the dilution process, indicating the transition process from a W/O microemulsion to a bicontinuous microemulsion and to an O/W microemulsion. On the other hand, when the aqueous phase did not contain NaCl solution and Milli-Q water was used as a dilution medium, conductivity kept quite low before the concentration of aqueous phase reached 20%.

After that, the conductivity increased to the highest value, which was approximately 100 μS/cm at 65% of water when the ratio of Capmul 708G to Tween 80 was 3:7 and at 60% of water when the ratio of Capmul 708G to Tween 80 was 4:6. At the end of dilution, when water concentration was larger than 70%, the conductivity value was reduced continuously after being remained constant between 65% and 70% for the samples along the dilution line W73 and between 60% and 70% along the dilution line W64. The reason that the conductivity value decreased was that it formed a relatively stable O/W microemulsion system and it created less electric current. With the increase in water concertation, the conductivity of the system was much closer to that of the water.

Figures (Appendix Figure 4 (a) and (b)) which illustrate the change in $d(\log\sigma)/d\Phi$ with the change in aqueous phase concentration were also created about the mixture system of Capmul 708G, Tween 80 and Milli-Q water or 5 mM NaCl solution along dilution line W73 and W64. The findings were the same as Figure 5.11 (b) that percolation threshold was 20%, which were in great agreement with the result from Figure 5.12.

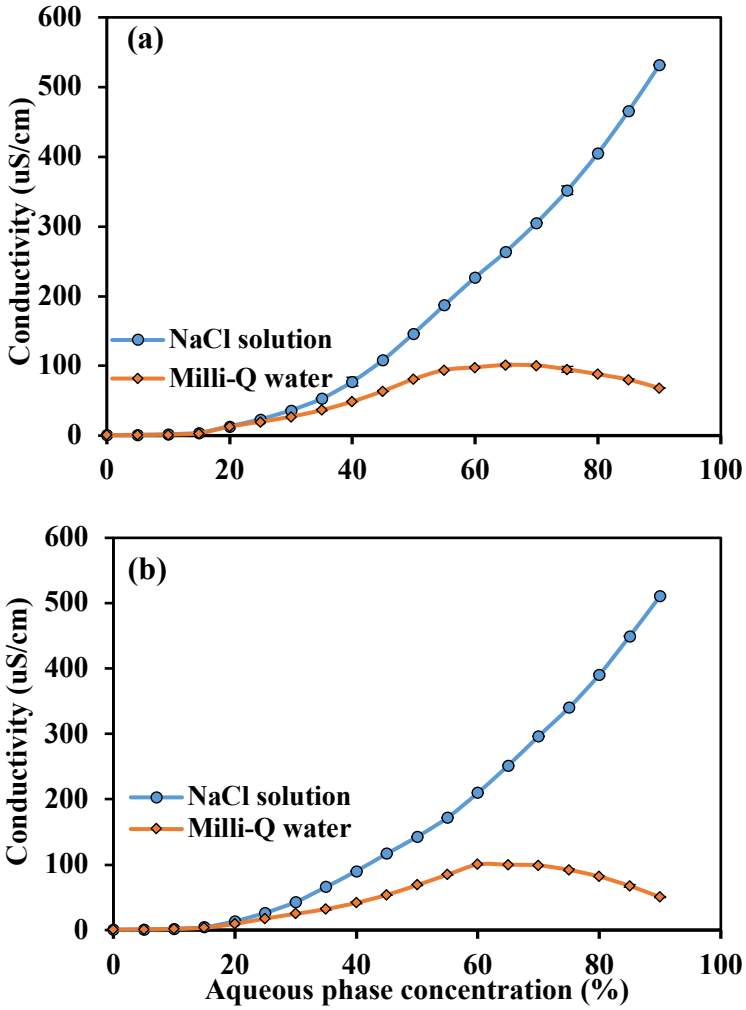

Figure 5.12 Electrical conductivity change as a function of aqueous phase concentration in the mixture system of Capmul 708G, Tween 80 and Milli-Q water or 5 mM NaCl solution. (a) The ratio of Capmul 708G to Tween 80 was 3:7, and (b) The ratio of Capmul 708G to Tween 80 was 4:6. Data points are presented as the mean and standard deviation of two independent measurements with duplicate (n=4) and error bars mean standard deviation.

The findings in this study are similar to what have been reported by Kalaitzaki et al. (2015) who also measured conductivity to determine the phase inversion and microemulsion type. The oil phase was R-(+)-limonene and absolute ethanol at a ratio of 1:1 and the surfactant was Tween 20 or Tween 40 or the mixture of Tween 20 and Tween 40 at a ratio of 1:2. Also, the aqueous phase they used to dilute samples was made up of Milli-Q water and PG at 2:1 ratio with or without 1.7 mM NaCl solution. They found that when NaCl solution was added, conductivity increased with

increasing aqueous solution along the dilution line W64. Based on conductivity values, it could be concluded when the concentration of aqueous phase was 20%, the system changed from a W/O microemulsion into a bicontinuous microemulsion, and when the concentration of aqueous phase was 70-80%, the bicontinuous microemulsion transited into an O/W microemulsion. Furthermore, at the absence of NaCl solution, conductivity values were very low along the dilution line, and it was increased from 0 to 60% aqueous concentration before it was reduced after 70% aqueous concentration. However, they also showed that phase transition occurred at 20% and 70-80% aqueous content, respectively (Kalaitzaki et al., 2015).

Cheng et al. (2017) also reported the similar results that when aqueous phase (containing 50% PG) content was between 20% and 40%, and between 60% and 70%, phase transitions occurred. In another study reported by Feng and co-workers, they found that in the water/vitamin E/ethyl butyrate/Cremophor EL/ethanol system along the dilution line W82 (ratio of vitamin E and ethyl butyrate to Cremophor EL and ethanol was 2:8), a W/O emulsion region existed when the concentration of water was less than 28%, which reached a plateau when water concentration was between 28% and 40%. After that, conductivity decreased sharply, which indicated a O/W emulsion region (Feng et al., 2009b).

On the other hand, Subongkot and Ngawhirunpat (2017) stated that there was not any specific conductivity value found by previous reports to categorize the type of a microemulsion. As such, based on previous researches, they had set a criterion to evaluate a microemulsion type, of which O/W microemulsion existed if the ratio of water was higher than that of oil and the conductivity value was more than 52.5 μS/cm. If the ratio of oil was higher than that of water, the product was W/O microemulsion. Moreover, when water concentration was equal to oil content or the ratio of water was higher than that of oil, the conductivity value was equal to or lower than 52.5 μS and

it was bicontinuous microemulsion (Subongkot and Ngawhirunpat, 2017).

5.4.5 Viscosity

It is well documented by studies that viscosity is a useful tool to determine the type of microemulsions in the ternary phase diagram (Garti et al., 2001, Feitosa et al., 2009, Zargar-Shoshtari et al., 2010). Therefore, viscosity was determined from selected formulations from the mixture systems of Capmul MCM C8, Tween 80 and water as well as Capmul 708G, Tween 80 and water. Samples whose shear stress increased proportionally with increasing shear rate ($R^2 > 0.99$) were considered as Newtonian liquids (Subramanian et al., 2005, Aboudzadeh et al., 2018). It can be concluded from Figure 5.13 and Appendix Figure 4 and 5 that samples, such as L110, L120, L130, L140, L170, L180, L190, L310, L320, L330, L390, L610, L620, L630, L910 and L920 from Capmul MCM C8, Tween 80 and Milli-Q mixture system as well as L110, L120, L130, L170, L180, L190, L310, L320, L330, L340, L350, L360, L370, L380, L390, L510, L520, L530, L540, L710, L720, L730, L910 and L920 from Capmul 708G, Tween 80 and Milli-Q mixture system were all Newtonian liquids because the viscosity of them was increased proportionally within the shear range studied. Besides, no yield stress was detected for these samples. Other researchers also found that microemulsions were Newtonian fluids (Shevachman et al., 2004, Guo et al., 2019a). On the other hand, it can be clearly seen from Figure 5.14 that viscosity value was the highest initially but decreased with increasing water concentration along the dilution line W73. At the beginning, viscosity decreased drastically until 20% water content, which continued to decrease between 30% and 70% while not as dramatic as it was previously. When water concentration was above 70%, viscosity again had a substantial reduction. In other words, phase transition occurred when water concentration was at 20% and 70%, which was consistent with the conductivity data shown in Figure 5.12. This result was similar to the finding reported by Fanun et al. (2001) that in the mixture system of sucrose monostearate, water, 1-butanol and MCT,

viscosity of microemulsions, when the ratio of 1-butanol to MCT to sucrose monostearate was 1:1:1.5, decreased from 40 to 15 cP with the increasing with concentration from 16% to 44%. Cheng et al. (2017) also came to the conclusion that viscosity value decreased along the dilution line W82 in Orange oil, Capmul MCM (orange oil : Capmul MCM = 1:2), Tween 20, Tween 60 (Tween 20 : Tween 60 = 6:4) and Water mixture system as well as in Orange oil, Capmul MCM (orange oil : Capmul MCM = 1:2), Tween 20, Labrasol (Tween 20 : Labrasol = 3:1) and water mixture system and dilution line W55 in the mixture system containing Capmul MCM, Labrasol and water. In addition, Todosijevic (Todosijevic et al., 2014) and co-researchers reported the same findings to the present study that viscosity value declined with the increasing aqueous phase concentration in microemulsions which were composed of IPM, sucrose laurate, isopropyl alcohol and water along the dilution line W19. When water concentration increased from 0 to 20%, viscosity value had a sharp reduction which then decreased slightly until water concentration was 70% (Todosijevic et al., 2014). However, other researchers reported different findings in terms of viscosity change with the increase in water concentration (Garti et al., 2003, Shevachman et al., 2004, Fanun, 2008, Deng et al., 2015, Guo et al., 2019a).

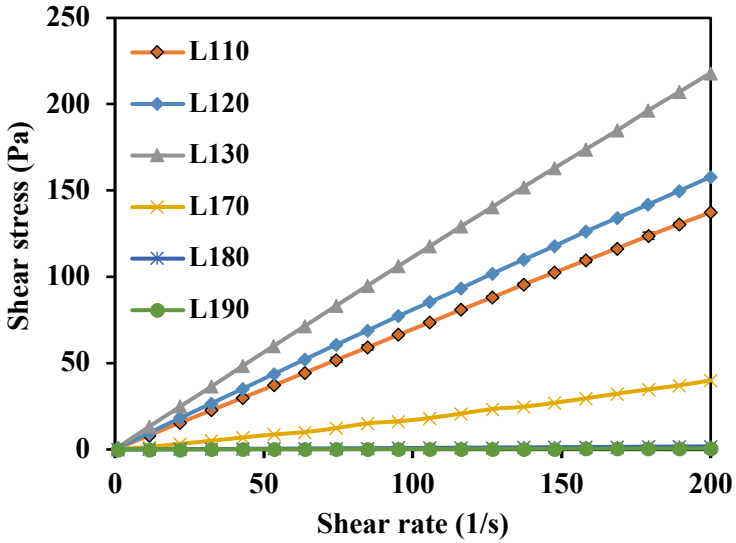

Figure 5.13 Shear stress as a function of shear rate of samples (L110, L120, 130, L170, L180 and L190) from Capmul 708G, Tween 80 and Milli-Q mixture system. L110, L120, L130, L140, L170, L180 and L190 denotes formulations along the dilution line W91 and their water contents are 10%, 20%, 30%, 40%, 70%, 80% and 90%, respectively.

In a study conducted by Fanun (2008) who measured the dynamic viscosity of water/sucrose laurate/EMDG/R (+)-limonene mixture system along the dilution line W64, it was stated that dynamic viscosity value increased with an increase in water content from 0 to 20%. When water concentration was higher than 20%, viscosity of the system was reduced slowly until the water content reached 70%, at which viscosity was increased again and reached a second peak at 75% water content. At the end, after water percentage was more than 80%, dynamic viscosity value had a sharp decrease, indicating the formation of an O/W microemulsion. The points at which phase transitions took place were similar to the results found in the present study.

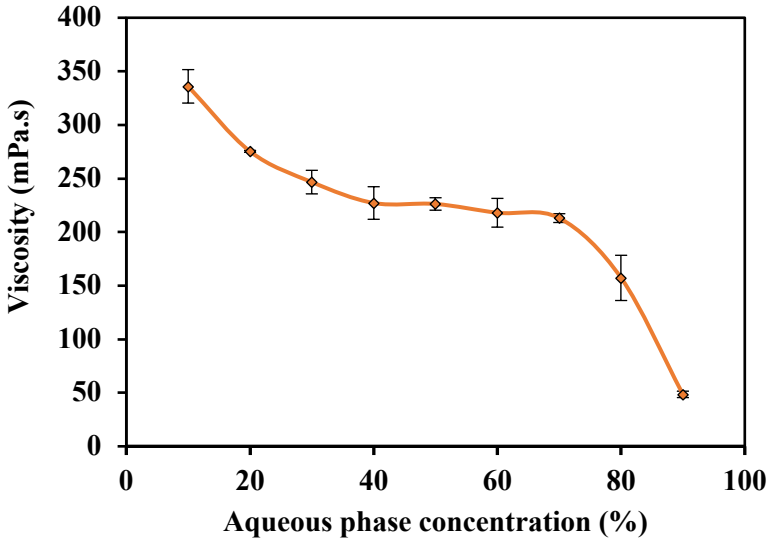

Figure 5.14 Viscosity as a function of aqueous phase concentration of mixture system of Capmul 708G, Tween 80 and Milli-Q along the dilution line W73. Data are presented as the mean and standard deviation of two independent measurements with duplicate (n=4) and error bars mean standard deviation.

In another study reported by Garti et al. (2003) who investigated the viscosity change of the mixture system, consisting of R(+)-limonene and ethanol (1:1) as oil phase, water and PG (1:1) as aqueous phase, and Tween 60 as emulsifier and the oil phase to emulsifier ratio of 4:6, viscosity was initially very low which was then increased gradually later when aqueous phase was added. However, the transition point from a W/O microemulsion to a bicontinuous microemulsion was not very obvious but was estimated to be when aqueous phase concentration was at 35%. After that, viscosity value had a substantial increase before it reached its highest value at 44% aqueous phase. It was decreased dramatically afterwards until the concentration of aqueous phase was 70%, indicating the transition of a bicontinuous microemulsion to an O/W microemulsion (Garti et al., 2003). The bell-shaped viscosity change was also reported by Guo et al. (2019a) and Deng et al. (2015).

Table 5.1 lists the viscosity values of selected microemulsion formulations from the mixture systems of Milli-Q water, Tween 80 and three different types of oils (Captex

355, Capmul MCM C8 and Capmul 708G). The results show that when water content was 10%, viscosity value increased with an increase in the ratio of surfactant to oil. Roohinejad et al. (2015) reported the same findings when they measured the viscosity of microemulsions containing Capmul MCM C8, Tween 80 and phosphate buffer (0.01 M, pH 6.8). For Capmul MCM C8 system, L150 and L160 samples were not microemulsion and for Capmul 708G system, L140, L150 and L160 samples had phase separation. As such, the viscosity of these formulations was not determined. However, viscosity alteration along the dilution line W91 was different from that along the dilution line W73. In dilution line W91, viscosity increased at the beginning, reaching its highest value at L140 for Capmul MCM C8 system and at L130 for Capmul 708G system. Moreover, from L170 to L190, there was a decline of viscosity value for both systems which was consistent with that in the dilution line W91.

Table 5.1 Viscosity, conductivity and microemulsion type of selected formulations from mixture systems of Milli-Q water, Tween 80 and Capmul MCM C8 or Capmul 708G. Data are presented as the mean and standard deviation of two independent measurements with duplicate (n=4).

Oil type	Sample name	% Oil	% Tween 80	% Water	Viscosity (mPa•s)	Conductivity (μS/cm)	Microemulsion type
Capmul MCM C8	L110	9	81	10	648 ± 67.4	4.04 ± 0.01	W/O
	L120	8	72	20	742 ± 73.4	11.2 ± 0.23	W/O
	L130	7	63	30	1213 ± 67.0	28.0 ± 0.14	Bicontinuous
	L140	6	54	40	2110 ± 105	55.9 ± 0.14	Bicontinuous
	L170	3	27	70	173 ± 2.20	137 ± 2.26	O/W
	L180	2	18	80	12.2 ± 0.70	122 ± 0.85	O/W
	L190	1	9	90	3.64 ± 0.02	84.2 ± 0.49	O/W
	L310	27	63	10	355 ± 25.0	3.26 ± 0.12	W/O
	L320	24	56	20	307 ± 0.42	10.9 ± 0.78	W/O
	L330	21	49	30	250 ± 9.12	30.0 ± 0.78	W/O
	L390	3	7	90	14.7 ± 0.47	81.6 ± 1.06	O/W
	L610	54	36	10	141 ± 6.72	2.68 ± 0.04	W/O
	L620	48	32	20	127 ± 0.42	8.56 ± 0.05	W/O
	L630	42	28	30	129 ± 5.30	17.6 ± 0.06	W/O
	L910	81	9	10	69.5 ± 7.20	1.78 ± 0.01	W/O
	L920	72	8	20	58.8 ± 1.50	4.73 ± 0.00	W/O
Capmul 708G	L110	9	81	10	711 ± 19.7	4.03 ± 0.04	W/O
	L120	8	72	20	837 ± 24.0	12.7 ± 0.28	W/O
	L130	7	63	30	1148 ± 31.1	29.6 ± 0.07	W/O
	L170	3	27	70	169 ± 8.40	98.4 ± 0.35	O/W
	L180	2	18	80	8.76 ± 0.07	94.0 ± 0.78	O/W
	L190	1	9	90	2.93 ± 0.11	63.7 ± 1.98	O/W
	L310	27	63	10	336 ± 15.6	3.10 ± 0.01	W/O
	L320	24	56	20	275 ± 0.92	12.8 ± 0.27	W/O
	L330	21	49	30	247 ± 11.0	27.2 ± 0.92	W/O
	L340	18	42	40	227 ± 15.2	51.0 ± 1.06	Bicontinuous
	L350	15	35	50	226 ± 5.80	83.2 ± 1.48	Bicontinuous
	L360	12	28	60	218 ± 13.4	98.1 ± 0.78	Bicontinuous
	L370	9	21	70	213 ± 4.10	101 ± 0.71	O/W
	L380	6	14	80	157 ± 21.1	88.0 ± 0.57	O/W
	L390	3	7	90	48.5 ± 2.99	68.2 ± 1.34	O/W
	L510	45	45	10	195 ± 9.19	3.11 ± 0.41	W/O

	L520	40	40	20	150 ± 0.14	11.0 ± 0.56	W/O
	L530	35	35	30	111 ± 8.63	25.8 ± 0.57	W/O
	L540	30	30	40	88.6 ± 5.21	41.6 ± 1.48	Bicontinuous
	L710	63	27	10	123 ± 1.77	2.95 ± 0.05	W/O
	L720	56	24	20	85.0 ± 3.16	8.65 ± 0.03	W/O
	L730	49	21	30	68.7 ± 0.88	16.0 ± 0.03	W/O
	L910	81	9	10	81.0 ± 2.66	3.18 ± 0.08	W/O
	L920	72	8	20	53.4 ± 3.65	6.14 ± 0.02	W/O

Apart from conductivity and viscosity determination, dye staining tests were also introduced to Capmul MCM C8 or Capmul 708G, Tween 80 and water mixture system to investigate the type of microemulsions. Methylene Blue and Sudan Red were utilized to evaluate the diffusion rate of these two dyes. When the diffusion rate of Methylene Blue was faster than that of Sudan Red, the sample tended to be an O/W microemulsion, and when Sudan Red was diffused faster than Methylene Blue, the sample tended to be a W/O microemulsion. Besides, if the diffusion rate of these two dyes were similar to each other, the sample might be a bicontinuous microemulsion.

Together the results of dye staining with conductivity and viscosity value, the type of microemulsions could be determined, which is illustrated in Table 5.1. Accordingly, ternary phase diagrams of these two mixture systems are rebuilt in Figure 5.15. Particle size and PDI of selected O/W formulations were determined from the mixture systems containing Capmul 708G, Tween 80 and water as well as Capmul MCM C8, Tween 80 and water to see whether they are within the range of microemulsions (Table 5.2). Particle diameter of these selected O/W microemulsions was all lower than 50 nm, matching with the size range of microemlsion. All clear single-phase samples from ternary phase diagrams in Figure 5.15 were stored at ambient temperature for one year, the samples remained still clear, indicating they were stable microemulsions. In terms of Capmul 708G, Water and Tween 80 mixtures system, in dilution line W82, W73 and W64, every point was a microemulsion. With the addition of water, the

macroscopic observed structure of the microemulsion did not have any changes. The aforementioned microemulsion was called U-type microemulsion by some researchers (Garti et al., 2003, Garti et al., 2006, Zhang et al., 2008a).

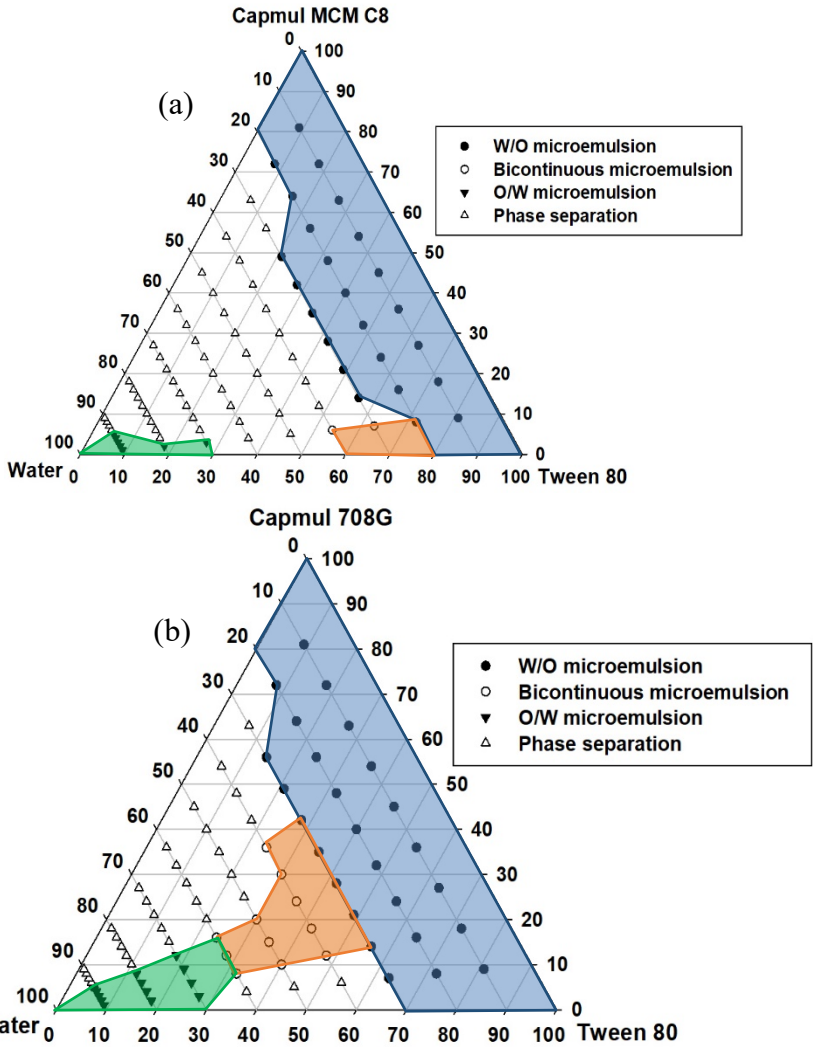

Figure 5.15 Ternary phase diagrams of mixture systems indicating the type of microemulsions, in which blue, orange and green areas represent W/O, bicontinuous and O/W microemulsion, respectively. (a) Tween 80, Capmul MCM C8 and Milli-Q water system, and (b) Tween 80, Capmul 708G and Milli-Q water system.

Table 5.2 Particle size and PDI of selected O/W microemulsions

Oil type	Sample name	% Oil	% Tween 80	% Water	Particle diameter (nm)	PDI
Capmul MCM C8	L170	3	27	70	13.3 ± 1.8	0.42 ± 0.03
	L180	2	18	80	13.2 ± 0.2	0.39 ± 0.01
	L190	1	9	90	13.1 ± 0.1	0.23 ± 0.01
	L390	3	7	90	25.8 ± 2.6	0.91 ± 0.13
Capmul 708G	L170	3	27	70	13.9 ± 0.7	0.52 ± 0.01
	L180	2	18	80	12.0 ± 0.2	0.38 ± 0.01
	L190	1	9	90	11.1 ± 0.1	0.21 ± 0.00
	L370	9	21	70	17.8 ± 0.7	0.56 ± 0.02
	L380	6	14	80	22.9 ± 1.4	0.49 ± 0.04
	L390	3	7	90	26.2 ± 2.4	0.67 ± 0.06

5.5 Conclusions

This study focused on understanding the effects of type and concentration of oils and surfactants on the formation of microemulsion by the water titration method. Also, cosurfactant and cosolvent were introduced to determine their effect on the formation of isotropic monophasic liquids. All the oils introduced were somewhat able to fabricate microemulsions with Tween 80 and water. Monoglyceride (Capmul 708G) and mono/diglyceride (Capmul MCM C8) which had self-emulsifying functionalities were efficient at forming microemulsions by the water titration method. Lemon oil, Captex 355 and PG esters did not favour the formation of microemulsions, but the A_T value of Capmul PG-8 mixture system was 23.7%. In addition, the type of surfactants also had an effect on the formation of microemulsions. When Capmul MCM C8 and Capmul 708G were mixed with Milli-Q water as well as one of the three surfactants (Tween 80, Tween 20 and Kolliphor), the A_T values were not significantly different with each other. However, when Span 80 was employed to replace Tween 80, the A_T value decreased substantially when Capmul 708G was utilised as the oil phase. On the

other hand, when absolute ethanol and PG were employed as cosurfactant and cosolvent, respectively, into Capmul MCM C8, water and Tween 80 mixture system, more microemulsions could be fabricated. Besides, if they were employed into lemon oil, Tween 80 and water system, the A_T value was increased and the regions of gels in the ternary diagram was reduced, which were disappeared when ethanol was in the system. Once a ternary phase diagram was constructed, conductivity, viscosity measurement and dye staining tests could be utilised to determine the type of microemulsions (O/W, W/O or bicontinous). Overall, this study provides some useful information about the formation of microemulsions via the water titration method and the characterization of microemulsions.

Chapter 6 Encapsulation of beta-carotene into microemulsions formed by emulsion dilution method

6.1 Abstract

Beta-carotene has been utilised by various studies to load into various types of delivery systems, which could then be further incorporated into functional foods. In this study, beta-carotene was encapsulated into 2% Tween 80-stabilised O/W microemulsions containing 0.1% or 0.4% lemon oil prepared by emulsion dilution method. Macroemulsion containing 1.5% lemon oil was also prepared under the same condition and used for comparison with the microemulsions. All emulsion samples were analysed for the determination of particle size, colour (expressed as CIE L*, a* and b*), total colour difference (ΔE*) and beta-carotene content and degradation during storage for 1 month under different environmental conditions (4, 25 and 37 °C; with and without exposure to oxygen and light). As part of the measurements, the effect of particle sizes on the stability of encapsulated beta-carotene against degradation was investigated as well. The encapsulation of beta-carotene into 0.1% and 0.4% lemon oil-in-water microemulsions increased the particle size of these two microemulsion significantly, but it was still within the size range of microemulsion and these two microemulsions were still observed to be visually transparent. However, the incorporation of beta-carotene did not significantly alter the particle size of 1.5% lemon oil-in-water macroemulsion. When 0.4% lemon oil microemulsion was kept away from oxygen and light, higher temperature accelerated the degradation of beta-carotene as expected. Also, the degradation rate of beta-carotene at a given temperature of 25 °C was the highest when it was subjected to both oxygen and light compared to the exposure only to either oxygen or light. The blank (control) samples with beta-carotene dissolved directly in n-hexane were also prepared at the same beta-carotene concentrations as the emulsion samples containing 0.1, 0.4 and 1.5% lemon

oil in order to compare the stability of beta-carotene with the microemulsion and macroemulsion delivery systems. The results showed that the stability of beta-carotene was significantly enhanced when it was encapsulated into the oil droplets of microemulsions and macroemulsion. This study provides information about the effects of different environmental conditions on the stability of beta-carotene-loaded microemulsion and macroemulsion during storage and indicates that microemulsion could be a good delivery system to encapsulate beta-carotene for application in clear foods or beverages although there are some other variables (e.g. surfactant concentration) that need to be considered as well.

6.2 Introduction

In the past few decades, functional foods have attracted increasing attention from consumers as well as researchers due to their beneficial effects on human health. However, the direct incorporation of lipophilic bioactive compounds into food products has some limitations because they are sensitive to degradation when exposed to oxygen, temperature and light during fabrication, transportation and storage of the food products. Consequently, a delivery system which can protect the bioactive compounds against physical and chemical conditions is required. Many different systems have been investigated as the delivery systems for the encapsulation of bioactive compounds, such as emulsion (Chee et al., 2007, Gu et al., 2018, Gomes et al., 2019), nanoemulsion (Hategekimana et al., 2015, Sotomayor-Gerding et al., 2016), microemulsion (Deutch-Kolevzon et al., 2011, Qian et al., 2012b, Roohinejad et al., 2014, Chen et al., 2015), multiple emulsion (Benichou et al., 2007, Pimentel-Gonzalez et al., 2009, Artiga-Artigas et al., 2019), solid lipid nanoparticle (Mandawgade and Patravale, 2008, Zhu et al., 2009, Zheng et al., 2013b), liposome/vesicle (Folmer et al., 2009) and etc.

Beta-carotene is a lipophilic bioactive compound, which is one of the most widespread carotenoids, that may be related to reduce the risk of some cancers and heart disease (Omenn et al., 1996, Miller and Snyder, 2012, Ruiz and Hernandez, 2016). It is not only sensitive to light, oxygen and high temperature but also has poor water solubility, thus, it needs to be encapsulated for its delivery into food products. Many researches have successfully fabricated delivery systems to encapsulate beta-carotene, such as liposomes (Tan et al., 2014, Zabodalova et al., 2014), solid lipid nanoparticles (Yi et al., 2014a), nanoemulsions (Yuan et al., 2008, Liang et al., 2013) and microemulsions (Yan and Wang, 2013, Roohinejad et al., 2015, Cheng et al., 2017). Of all the delivery systems, microemulsion is transparent, which renders its application in clear foods and beverages. Besides, it is thermodynamically stable, which gives the product a longer shelf life (Cheng et al., 2017).

In a study reported by Ariviani et al. (2015), beta-carotene (0.025% and 0.05% wt) enriched microemulsions were fabricated using virgin coconut oil (VCO) or palm oil as the lipid phase and a mixture of Span 80, Span 40 and Tween 80 as the surfactant via spontaneous emulsification (SE) method. It was reported that beta-carotene was more stable against degradation during storage at different temperatures (4 °C, 15 °C or ambient temperature) when palm oil was used over VCO. Cheng and co-workers encapsulated beta-carotene into different types of microemulsions via water titration method (Cheng et al., 2017). It was shown that the bicontinuous microemulsion system (12% orange oil and 24% Capmul MCM as oil phase, 18% Tween 20 and 6% Labrasol as surfactant, 20% PG as cosolvent and 20% water) had the maximum loading capacity of beta-carotene at 140.8 μg/ml (Cheng et al., 2017). In another study reported by Roohinejad et al. (2015) that produced beta-carotene encapsulated O/W microemulsions with Capmul MCM C8 and Tween 80 by the water titration method, the incorporation of beta-carotene into microemulsions did not significantly alter the phase behaviour, conductivity and viscosity of the empty microemulsions. In addition,

the beta-carotene loaded microemulsion samples were reported to remain stable after storage at room temperature for six months.

To the best of my knowledge, there have been no studies involving the use of emulsion dilution method to fabricate microemulsions encapsulating beta-carotene. Therefore, the objective of this study was to investigate the effect of incorporation of beta carotene on the formation and properties of microemulsions formed by emulsion dilution method. Besides, stability of microemulsions (e.g. colour, particle size, beta-carotene concentration) was investigated during storage for 1 month at different temperatures with or without oxygen and/or light. Food grade surfactant, Tween 80, was used to fabricate lemon oil-in-water microemulsions encapsulating beta-carotene. In Chapter 3, microemulsions containing lemon oil have been successfully fabricated using emulsion dilution method. Briefly speaking, a stock emulsion was prepared by mixing 10% lemon oil with 2% Tween 80 solution. The stock emulsion was then diluted with 2% Tween 80 solution which formed microemulsions when the lemon oil concentration after dilution was 0.6% or less. Therefore, in this chapter, microemulsions with 0.1% and 0.4% lemon oil were chosen as a model to encapsulate beta-carotene. Besides, a macroemulsion with 1.5% lemon oil was also prepared to determine the effect of the particle size of emulsion oil droplets on the stability of beta-carotene against degradation during storage.

6.3 Materials and methods

6.3.1 Materials

Lemon oil, Tween 80 and beta-carotene powder (≥ 93%, UV) were purchased from Sigma-Aldrich Co. (St Louis, MO, USA). Absolute ethanol (analytical grade), n-hexane (HPLC grade) and methanol (HPLC grade) were purchased from Fisher Scientific UK (Loughborough, UK).

6.3.2 Validation of spectrophotometric method for beta-carotene content

Validation of a UV-spectrophotometric method for the determination of beta-carotene content was initially studied based on the method illustrated in ICH harmonized tripartite guideline Q2 (R1) which includes the validation of analytical procedures. In this section, linearity, accuracy and precision were determined.

Linearity: 10 mg beta-carotene powder was dissolved into 100 ml n-hexane solution to make 100 μg/ml stock solution. The stock solution was then diluted by n-hexane to make a series of beta carotene concentrations in n-hexane solution (1, 2, 5, 10, 50, 75 and 100 μg/ml). After that, absorbance values of the beta-carotene solutions were measured by a UV-visible spectrophotometer (UV-1700, Shimadzu Corp., Japan) at the wavelength of 450 nm. A standard (calibration) curve was then created using the data obtained from which the value of slope, y-intercept and linearity were also obtained.

Precision and accuracy: Three different concentrations (10, 75 and 100 μg/ml) of beta-carotene standard solutions were chosen to measure their absorbance values in five different time points in one day to investigate the intra-day precision. 75 μg/ml beta-carotene in n-hexane solution was also chosen to measure the absorbance value over three different days (one time each day) to determine the inter-day precision. Accuracy (% recovery) and relative standard deviation (RSD) were therefore obtained using Equation 6.1 and 6.2 (Kayesh et al., 2013):

$$\text{Accuracy (\% recovery)} = \frac{\text{Measured concentration}}{\text{Theoretical concentration}} \times 100 \qquad [6.1]$$

$$\text{RSD (\%)} = \frac{\text{Standard deviation}}{\text{Mean}} \times 100\% \qquad [6.2]$$

6.3.3 Solubility of beta-carotene

In order to study the solubility of beta-carotene, an excess amount (4 mg) of beta-

carotene was added into 10 ml of different types of oils (Capmul MCM C8, Capmul 708G, Captex 355, Capmul PG-8, Capmul PG-12, Capmul PG-2L, Captex 100, lemon oil, fractionated coconut oil, IPM and peanut oil) and surfactants (Tween 20, Tween 40, Tween 60, Tween 80, Span 80 and Kolliphor), cosurfactant (absolute ethanol) and cosolvent (PG). Samples were flushed with nitrogen gas to avoid the degradation of beta-carotene before being placed in an 80 °C water bath for 5 minutes. The samples were then equilibrated under continuous shaking by a magnetic stirrer at 500 rpm overnight at ambient temperature (25 °C). After that, the samples were centrifuged at 15000 rpm for 15 minutes via a Sigma 6-16 KS centrifuge (Sigma Laborzentrifugen GmbH, Osterode am Harz, Germany) to remove any undissolved beta-carotene. The clear supernatant was taken and filtered through a 0.2 μm Minisart NY 25 hydrophilic polyamide syringe filter (Sartorius Stedim Biotech GmbH, Goettingen, Germany) before being further diluted by n-hexane. Absorbance of the obtained solutions was measured with n-hexane as a blank using the UV-visible spectrophotometer (UV-1700, Shimadzu Corp., Japan) at 450 nm at which beta-carotene has the maximum absorbance value. As such, the solubility of beta-carotene was able to be determined accordingly. Each experiment was conducted in duplicate.

6.3.4 Preparation of microemulsions encapsulating beta-carotene

As described in the above, an excess amount of beta-carotene powder was added into lemon oil in an amber glass bottle and the headspace of the bottle was flushed with nitrogen gas. The mixture was then placed in a water bath at 80 °C for 5 minutes and equilibrated under continuous shaking by a magnetic stirrer at 500 rpm overnight at ambient temperature. After that, the sample was centrifuged at 15000 rpm for 15 minutes using Sigma 6-16 KS centrifuge. The clear supernatant was collected and utilised to fabricate emulsions and microemulsions by emulsion dilution method as described in Section 3.2.1 in Chapter 3. Briefly, 10% lemon oil, which contained beta-carotene, was mixed with 1% Tween 80 solution using an Ultra-Turrax (VirTis

Company, NY, USA) at 11,000 rpm for 1 minute to form a coarse emulsion. The coarse emulsion was then homogenized using a two-stage high pressure valve homogenizer (APV 2000, SPX Corporation, NC, USA) at 500/50 bars by passing it through four times to produce a fine emulsion. The fine emulsion was diluted by 1% Tween 80 solution to fabricate microemulsions loaded with lemon oil concentrations of 0.1% and 0.4% and an emulsion with 1.5% lemon oil.

6.3.5 Analysis of beta-carotene content in emulsions

The method utilised by Yi et al. (2014b) was employed in this study to extract beta-carotene from the emulsions. A 0.5 ml emulsion sample was taken and added into a 10 ml glass tube. Then, 2.0 ml absolute ethanol and 3.0 ml n-hexane were added into the tube. The mixture was then mixed using a vortex mixer (VELP Scientifica, MB, Italy) for 10 seconds followed by standing for 2 minutes to separate the organic solvent and aqueous layers. The yellow-coloured supernatant (organic solvent layer) was then transferred into a 10 ml volumetric flask. The remaining sample was again mixed with 3.0 ml n-hexane using the vortex mixer before removing the supernatant into the volumetric flask. This process was repeated until the aqueous layer was clear. The volumetric flask containing the beta-carotene extract was made up to 10 ml by adding n-hexane. After mixing thoroughly by inverting the flask, the sample was measured for its absorbance at 450 nm using a UV-visible spectrophotometer against n-hexane as a blank. The amount of beta-carotene in the emulsion samples was consequently determined using a beta-carotene standard curve created with a series of known concentrations of beta-carotene in n-hexane. Each sample was analysed in duplicate.

6.3.6 Stability of encapsulated beta-carotene and emulsions during storage

Microemulsions and macroemulsion encapsulating beta-carotene which was incorporated into 0.1%, 0.4% and 1.5% oil phase were utilised to study the stability of encapsulated beta-carotene during storage at different conditions as shown in Table

6.1. In detail, beta-carotene-loaded microemulsion (0.1% lemon oil) and macroemulsion (1.5% lemon oil) were blanketed with nitrogen gas and stored at ambient temperature (25 °C) under dark condition. However, beta-carotene-loaded microemulsion containing 0.4% lemon oil was divided into four categories, three of which were blanketed with nitrogen gas before storage under dark condition at 4, 25 and 37 °C, respectively. The three samples were also stored at 25 °C, but one of them was stored under dark condition but subjected to oxygen, one of them was blanket by nitrogen gas but stored under light and the last one was subjected to both oxygen and light. When it comes to a sample stored under light, a light box with a fluorescent tube was utilised to provide consistent illumination and the sample was placed in a clear glass vial.

Table 6.1 List of three different emulsion samples with different concentrations of lemon oil loaded with beta-carotene used for analysis (particle size, colour) during storage for 1 month under different conditions.

Emulsion type	Lemon oil	Sample code	Storage conditions		
			Temperature	Oxygen	Light
Microemulsion	0.1%	0.1%25CNN	25 °C	No	No
Microemulsion	0.4%	0.4%4CNN	4 °C	No	No
		0.4%37CNN	37 °C	No	No
		0.4%25CNN	25 °C	No	No
		0.4%25CYY	25 °C	Yes	Yes
		0.4%25CNY	25 °C	No	Yes
		0.4%25CYN	25 °C	Yes	No
Macroemulsion	1.5%	1.5%25CNN	25 °C	No	No

In this part, some emulsion samples were specified with their sample codes, such as 0.4%4C, 0.4%25C and 0.4%37C, which represent beta-carotene-loaded, 0.4% lemon oil microemulsions stored at 4, 25 and 37 °C, respectively. In terms of the letter symbols (NN, YY, NY and YN) added to the sample codes, they represent respectively different storage conditions: NN: without oxygen and without light, YY: with oxygen and light, NY: without oxygen and with light, and YN: with oxygen and without light.

Particle size, colour and beta-carotene content were determined from the samples during storage for 1, 3, 7 days, 2 weeks, 3 weeks and 1 month. Particle size and PSD were measured using the method described in Section 3.2.3 in Chapter 3. Beta-carotene content was measured as described in the above. It should be mentioned that the content of beta-carotene encapsulated in 0.1% and 0.4% lemon oil microemulsions and 1.5% lemon oil macroemulsion measured after storage for 1 day was 15.39, 61.95 and 180.31 μg/ml, respectively. Blank samples containing 15, 62 and 180 μg/ml beta-carotene were prepared by dissolving beta-carotene into n-hexane solution, which were also subjected to the same storage conditions as the beta-carotene encapsulated emulsions. The colour change of the emulsions during storage was measured by a benchtop colour spectrophotometer (CM-5 Top-Port Spectrophotometer, Konica Minolta Inc., Osaka, Japan) (Figure 6.1) equipped with a Pulsed Xenon lamp as the light source. CIE L*, a*, b* colour space system was selected to be analysed in which L* represents lightness ranging from 0 (black) to 100 (white); a* represents redness-greenness with +a* (red) and -a* (green); b* represents yellowness-blueness with +b* (yellow)and -b* (blue). Each emulsion was measured in at least duplicate.

Figure 6.1 Picture of a benchtop colour spectrophotometer.

6.4 Results and discussions

6.4.1 Validation of spectrophotometric method for analysis of beta-carotene content

Beta-carotene was mixed with n-hexane at different concentrations (1, 2, 5, 10, 50, 75 and 100 µg/ml). After centrifugation, the supernatants were filtered and then measured for their absorbance at 450 nm using a UV-visible spectrophotometer to create a standard curve ($R^2 = 0.998$) as shown in Figure 6.2.

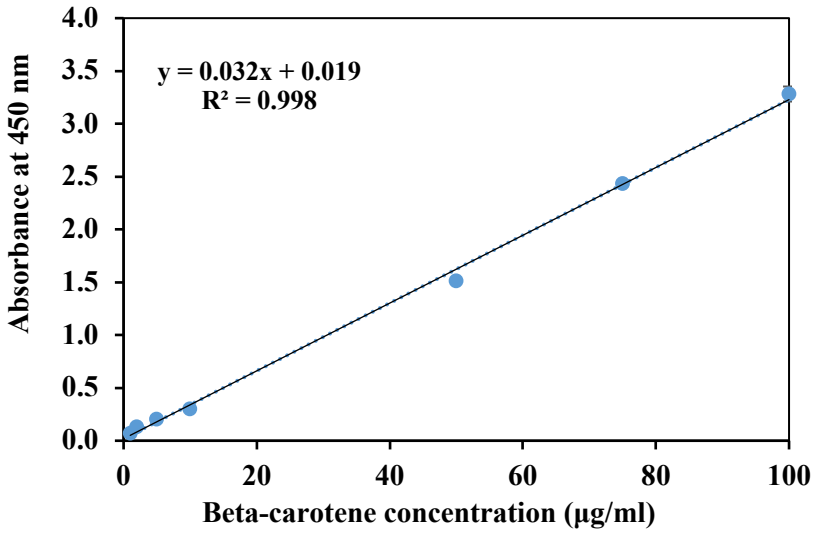

Figure 6.2 Beta-carotene standard curve generated from absorbance as a function of beta-carotene concentrations.

Beta-carotene solutions in n-hexane with the concentrations of 10, 75 and 100 μg/ml were selected to assess the intra-day precision and accuracy of the spectrophotometric method used in this study for the determination of beta-carotene content. Besides, 75 μg/ml was selected to determine the inter-day precision and accuracy of this method. Tables 6.2 and 6.3 illustrate the results of the intra-day and inter-day precision and accuracy, respectively. When beta-carotene concentration was 10 μg/ml, the recovery was a little poor being measured at 103.6% (Table 6.2). As for the 75 and 100 μg/ml beta-carotene solutions for the intra-day accuracy and the 75 μg/ml beta-carotene solutions for the inter-day accuracy, the recovery values ranged from 98.9% to 100.4%, indicating a high accuracy. In other words, the measured values were in good agreement with the true values. Apart from these, the results of RSD of all the three different concentrations of beta-carotene solutions in five different time points in the same day was less than 1% (Table 6.2). The RSD of 75 μg/ml beta-carotene solution in three consecutive days was also less than 1% (Table 6.3). Therefore, it can be concluded that the method used was also precise enough.

Table 6.2 Summary of intra-day precision and accuracy test. Data are presented as the mean and standard deviation of two independent measurements with duplicate (n = 4).

	Theoretical concentration (μg/ml)	Measured concentration (μg/ml)	Accuracy (% recovery)	Precision (% RSD)
Intra-day	10	10.364 ± 0.097	103.64	0.93
	75	75.280 ± 0.141	100.37	0.19
	100	101.484 ± 0.142	101.48	0.14

Table 6.3 Summary of inter-day precision and accuracy test. Data are presented as the mean and standard deviation of two independent measurements with duplicate (n = 4).

	Theoretical concentration (μg/ml)	Day	Measured concentration (μg/ml)	Accuracy (% recovery)	Precision (% RSD)
Inter-day	75	1	75.313 ± 0.026	100.42	0.03
		2	74.180 ± 0.143	98.91	0.19
		3	74.195 ± 0.030	98.93	0.04

6.4.2 Solubility of beta-carotene

On the basis of the standard curve shown in Figure 6.2, the solubility of beta-carotene in a certain material (oils, surfactants, cosurfactant and cosolvent) could be obtained as shown in Table 6.4. It can be concluded that among all the oils, lemon oil had the highest beta-carotene solubility (334.57 μg/ml), which was followed by Capmul 708G (159.04 μg/ml) and Capmul MCM C8 (148.33 μg/ml). In terms of triglyceride oil, the solubility of beta-carotene in peanut oil was significantly lower as 95.27 μg/ml than that in Captex 355 (125.45 μg/ml) and fractionated coconut oil (119.83 μg/ml). As shown in Table 3.2 in Chapter 3, peanut oil is a type of triglyceride oil esterified with a mixture of many different fatty acids whereas fractionated coconut oil is also triglyceride oil but contains mainly medium chain fatty acids (e.g. 57.6% caprylic acid and 42.4% capric acid). indicating the effect of fatty acid chain length on the solubility of beta-carotene. Captex 355 is also a triglyceride oil with medium chain fatty acids (57.2% caprylic acid, 42.1% capric acid and 0.7% lauric acid). The results obtained in this study were in consensus with the studies reported by Borel et al. (1996), who illustrated beta-carotene solubility decreased with an increase in the fatty acid chain length of triglycerides. The results in Table 6.4 also indicate that monoglyceride oil (Capmul 708G) had the highest beta-carotene solubility compared to diglyceride (Capmul MCM C8) and triglyceride oils (peanut, fractionated coconut oil, Captex 355). In case of PG esters, Captex 100 and Capmul PG-8 had the similar beta-carotene solubility, which was slightly higher than Capmul PG-12 and PG-2L. The reason

might be due to the fact that both Capmul PG-12 and PG-2L are comprised of lauric acid compared to Captex 100 and Capmul PG-8 with a shorter chain fatty acid, such as capric acid and caprylic acid, respectively. As to surfactants, cosurfactant and cosolvent, beta-carotene solubility in Tween 80 was the highest being 34.19 μg/ml. According to Roohinejad et al. (2015) who also studied the solubility of beta-carotene in Tween 20, 40 and 80, Tween 80 was shown to have the highest beta-carotene solubility, which was followed by Tween 20. The solubility of beta-carotene in ethanol and PG were relatively lower, especially in PG being 4.86 μg/ml.

Table 6.4 Solubility of beta-carotene in different types of oils and surfactants, ethanol and PG. Data are presented as the mean and standard deviation of two independent measurements with duplicate (n = 4). Data were divided into two groups, in which oils were in the same group and surfactants were in the same group including ethanol and PG. Data were analysed using one-way ANOVA with Tukey test. In each group, different superscripts represent a significant difference.

Material types		Solubility (μg/ml)
Oils	Lemon oil	334.57 ± 0.87^{a}
	Capmul 708G	159.04 ± 0.36^{b}
	Capmul MCM C8	148.33 ± 0.44^{c}
	IPM	134.51 ± 2.66^{d}
	Captex 355	125.45 ± 0.74^{e}
	Fractionated coconut oil	119.83 ± 0.84^{f}
	Capmul PG-8	116.43 ± 0.23^{fg}
	Captex 100	111.63 ± 1.37^{g}
	Capmul PG-12	105.11 ± 0.70^{h}
	Capmul PG-2L	102.95 ± 0.18^{h}
	Peanut oil	95.27 ± 0.40^{i}
Surfactants	Tween 80	34.19 ± 0.49^{a}
	Tween 20	30.20 ± 0.67^{b}
	Tween 60	28.20 ± 0.15^{c}
	Tween 40	26.11 ± 0.57^{d}
	Kolliphor	25.35 ± 0.14^{d}
	Span 80	19.67 ± 0.22^{e}
Cosurfactant	Ethanol	17.62 ± 0.14^{f}
Cosolvent	PG	4.86 ± 0.46^{g}

6.4.3 Particle size alteration during storage

The particle sizes of beta-carotene-loaded emulsions containing 0.1%, 0.4% and 1.5% lemon oil were measured after preparation which were 13.68, 79.06 and 177.89 nm in diameter, respectively. However, the particle sizes were reduced to 12.28, 30.61 and 167.49 nm, respectively, after 1-day storage at ambient temperature. As a result, 0.1% and 0.4% lemon oil emulsions were regarded as microemulsions (< 50 nm) while 1.5% lemon oil emulsion was classified as a macroemulsion (conventional emulsion) (> 100 nm). The decrease in the particle size of oil droplets during storage might be due to the formation of an equilibrium particle size with some lemon oil droplets being transferred into Tween 80 micelles, resulting the formation of smaller oil droplets. Table 6.5 shows the mean particle size and PDI of 0.1%, 0.4% and 1.5% lemon oil emulsions without or with beta-carotene after storage at ambient temperature for 1 day. It can be seen that the encapsulation of beta-carotene increased the particle size of microemulsions containing 0.1% and 0.4% lemon oil ($p < 0.05$). But their particle sizes were still within the range of microemulsion, which was also confirmed by visual observation with their optical appearance being transparent (Figure 6.7). On the other hand, the particle size of 1.5% lemon oil macroemulsion did not significantly change although that of beta-carotene-loaded emulsion was slightly smaller than that of blank emulsion. In terms of PDI, the incorporation of beta-carotene increased the PDI of 0.1% lemon oil microemulsion significantly ($p<0.05$) but decreased the PDI of 1.5% lemon oil macroemulsion significantly ($p>0.05$). PDI did not change after incorporation of beta-carotene into 0.4% lemon oil microemulsion.

Table 6.5 Particle size and PDI of blank and beta-carotene-loaded emulsions containing 0.1%, 0.4% and 1.5% lemon oil after storage for 1 day.

Lemon oil	Blank emulsion		Loaded emulsion	
	Particle size (d.nm)	PDI	Particle size (d.nm)	PDI
0.1%	10.18 ± 0.26	0.21 ± 0.01	12.28 ± 0.29	0.34 ± 0.02
0.4%	21.95 ± 0.94	0.67 ± 0.03	30.61 ± 1.25	0.67 ± 0.10
1.5%	176.93 ± 20.98	0.38 ± 0.03	167.49 ± 3.67	0.29 ± 0.01

In terms of beta-carotene encapsulated 0.1% and 0.4% lemon oil microemulsions, their particle size alteration during storage for 1 month at different storage conditions is shown in Figure 6.3. After being blanketed with nitrogen gas, beta-carotene loaded 0.1% lemon oil microemulsion was only stored at ambient temperature (25 °C) under dark condition. After 1 week, the particle size of this microemulsion did not significantly change but it was reduced from 12.3 nm at the first day to 10.7 nm after 1 month. However, for beta-carotene encapsulated 0.4% lemon oil microemulsion, it was stored at three different temperatures (4, 25 and 37 °C). At 4 and 37 °C, this microemulsions was stored under dark condition after flushing with nitrogen. At 25 °C, this microemulsion was subjected to four different storage conditions: with oxygen and light (YY), without oxygen and light (NN), with oxygen but without light (YN), and without oxygen but with light (NY). Figure 6.3 shows that the particle size of 0.4% lemon oil microemulsions decreased to some extent during storage regardless of the storage conditions. It clearly illustrates that the particle size of this microemulsion did not change too much when it was stored at 4 °C, which may indicate that beta-carotene was the most stable at this condition. On the contrary, when it was stored at 37 °C, its particle size was reduced significantly being changed from 30 nm at 1 day to 10.3 nm after 1 month. When it was stored at 25 °C under dark condition without oxygen (NN), the size was decreased to 15.2 nm after storage for 1 month. The difference in the extent of changes in the particle size of microemulsion oil droplets at different storage

temperatures was thus attributable to the fact that beta-carotene was unstable at higher temperature. On the other hand, when beta-carotene-loaded 0.4% lemon oil microemulsion was stored at 25 °C but subjected to oxygen and light (YY), its particle size dropped significantly to 9.8 nm only after 1 week, while remained constant afterwards. As mentioned before, beta-carotene is unstable when exposed to light and oxygen, so, the change in particle size was expectable during storage. However, when microemulsion was only subjected to one of the storage conditions (e.g. temperature, oxygen and light), the change in particle size of the microemulsion was not as pronounced as the microemulsions stored without both oxygen and light. Specifically speaking, when this microemulsion was stored in an environment with oxygen, its particle size was higher than that of microemulsion subjected to light until stored for 2 weeks. But after that, the microemulsion which was subjected to light had a constant particle size, whereas there was a significant particle size reduction from 11.8 to 9.8 nm when exposed to oxygen. The results indicate that both oxygen and light caused the degradation of beta-carotene, but it was not clear from Figure 6.3 which factor had a stronger influence on the instability of beta-carotene.

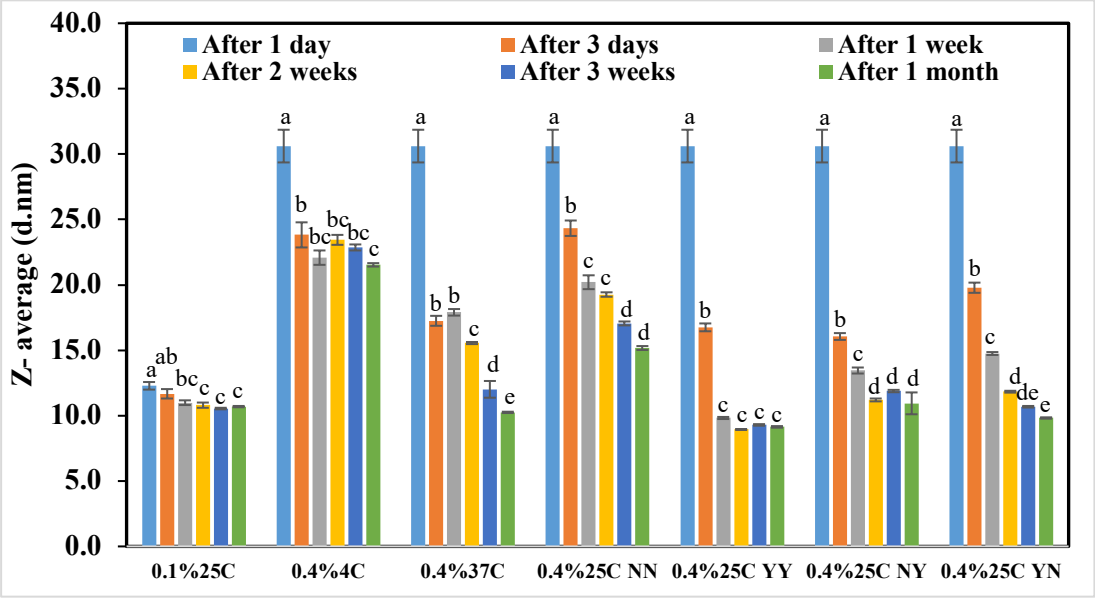

Figure 6.3 Particle size changes of beta-carotene loaded 0.1% and 0.4% lemon oil microemulsions during storage at different environmental conditions for 1 month. Data are presented as the mean and standard deviation of two independent measurements with duplicate (n = 4) and error bars mean standard deviation. Data were analysed using one-way ANOVA with Tukey test. Different numbers represent a significant difference ($P<0.05$).

As to beta-carotene-loaded macroemulsion containing 1.5% lemon oil, its particle size change is shown in Figure 6.4. The results indicate that during storage under dark condition without oxygen, its particle size was between 150 and 180 nm and seemed to have no significant change. Figure 6.6 shows that the PSD of these emulsions were similar with three peaks, one of which being located in the range of particle size greater than 1000 nm, regardless of storage duration. It should be noted that lemon oil has relatively high water solubility (Rao and McClements, 2012b), as described in Chapter 4, which can cause its oil droplets to undergo the Ostwald ripening process. This is believed to be the main reason why there existed a large population of large droplets in the PSD curves shown in Figure 6.5. Ostwald ripening is a process which involves the diffusion of oil molecules from small droplets to large droplets (Wooster et al., 2008) and it can accelerate the rate of phase separation indirectly as well as other demulsification process (Sjoblom, 1996, Friberg et al., 2004). In the current experiment, phase separation happened (photo not shown) so the measured particle

size might not be very accurate.

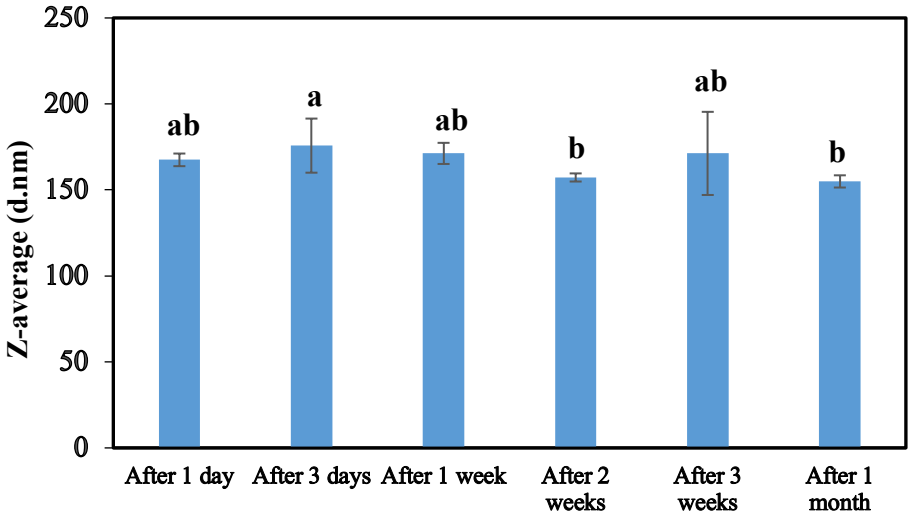

Figure 6.4 Particle size change of 1.5% lemon oil macroemulsion encapsulating beta-carotene during storage under dark condition without oxygen at 25 °C for 1 month. Data are presented as the mean and standard deviation of two independent measurements with duplicate (n = 4) and error bars mean standard deviation. Data were analysed using one-way ANOVA with Tukey test. Different numbers represent a significant difference.

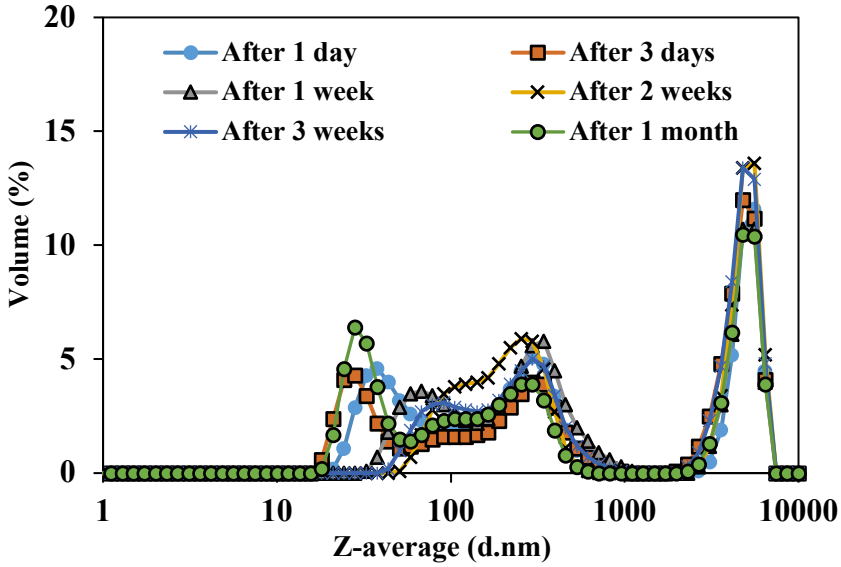

Figure 6.5 Particle size distribution of 1.5% lemon oil macroemulsion encapsulating beta-carotene during storage under dark without light at 25 °C for 1 month.

6.4.4 Colour alteration during storage

Beta-carotene belongs to the group of carotenoids found in plants (e.g. fruits and vegetables) as red, orange and yellow pigments (Henry et al., 2000). It is sensitive to degradation against light, oxygen and high temperature, resulting in a loss of its colour (Frederiksen et al., 2003, Gurak et al., 2014, Roa et al., 2017). Figure 6.6 illustrates the results of colour changes of emulsion samples which were measured using a colour spectrophotometer during storage for 1 month at different storage conditions. The colour measurement was expressed as CIE L*, a* and b* values. The emulsion samples analysed for their colour were beta-carotene incorporated 0.1% and 0.4% lemon oil microemulsions. For 1.5% lemon oil macroemulsion, it had phase separation during storage, making it difficult to measure its colour correctly, hence, L*, a* and b* values of 1.5% lemon oil macroemulsions were not included in Figure 6.6. Figure 6.7 shows the pictures of beta-carotene incorporated 0.1% and 0.4% lemon oil microemulsions and 1.5% lemon oil macroemulsions taken during storage at different conditions for 1 month. It should be mentioned that the content of beta-carotene encapsulated in 0.1% and 0.4% lemon oil microemulsions and 1.5% lemon oil macroemulsion measured after preparation storage for 1 day to be 15.39, 61.95 and 180.31 μg/ml, respectively.

It can be seen from Figure 6.6 that after preparation and after 1 day storage, the L* value of 0.1% microemulsion was higher than that of 0.4% microemulsion, indicating it is brighter in colour against lightness/darkness, while its a* and b* values were both positive, indicating redness and yellowness, respectively, but lower than those of 0.4% lemon oil microemulsions. This implies the colour saturation (intensity) of 0.1% lemon oil microemulsion sample was not strong as compared to that of 0.4% microemulsion. The reason for a* and b* values being smaller for the 0.1% lemon oil microemulsion was due to the concentration of beta-carotene encapsulated being lower in the 0.4% lemon oil microemulsion as mentioned above. The results obtained

could be also partly attributed to the particle size of 0.1% microemulsion which was much smaller than that of 0.4% microemulsion, as shown in Section 6.4.3 in this chapter. McClements (2002) reported the similar findings that L* value increased and a* and b* values decreased when the particle size of emulsion oil droplets decreased from 10 to 0.1 μm. Besides, the L* values of emulsion samples, especially 0.4% lemon oil microemulsion, appeared to be significantly increased during storage after 1 day compared to that after preparation (0 day). On the other hand, the a* value decreased but b* value increased significantly during the same time period. This means that the sample was less red but more yellow. A significant increase in the L* value for the 0.4% lemon oil microemulsion after 1 day storage might be partly attributable to the shrinkage of oil droplets due to the diffusion and transfer of lemon oil into Tween 80 micelles that could still take place after the emulsion preparation, resulting in a decrease in mean particle size of the emulsion oil droplets.

During storage, generally speaking, L* value increased, a* and b* values decreased from all the samples. However, it should also be mentioned that the a* and b* values of 0.4% lemon oil microemulsion remained stable when stored at 4 °C under dark without oxygen, indicating almost no degradation of beta-carotene at cold storage temperature. But when it was stored at higher temperatures of 25 and 37 °C, the colour intensity was significantly decreased, particularly the samples exposed to both oxygen and light during storage which caused the degradation of beta-carotene.

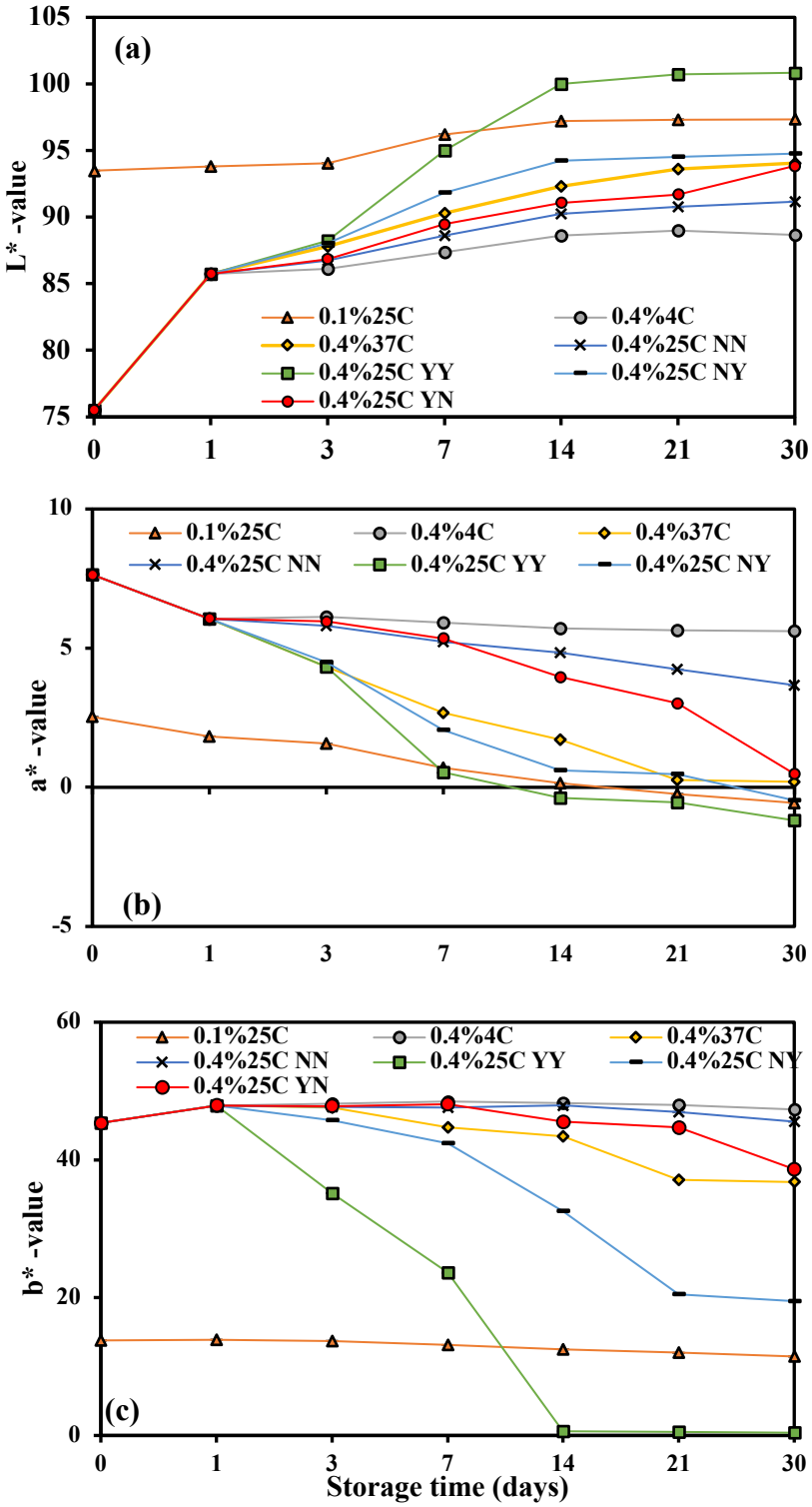

Figure 6.6 Change in colour of beta-carotene incorporated lemon oil microemulsions (0.1% and 0.4% lemon oil) during storage for 1 month under different conditions. (a) L* value (lightness), (b) a* value (redness) and (c) b* value (yellowness). Data are presented as the mean and standard deviation of two independent measurements with duplicate (n = 4) and error bars mean standard deviation.

As it was reported by other researchers, total colour difference (△E*) was employed to determine the total colour change between samples (Qian et al., 2012a). △E* can be calculated by Equation 6.3:

$$\triangle E^* = \sqrt{(L^* - L_0^*)^2 + (a^* - a_0^*)^2 + (b^* - b_0^*)^2} \qquad [6.3]$$

where L*, a* and b* represent the measured colour values of microemulsions at day 1, while L^*_0, a^*_0 and b^*_0 mean the measured colour values of the microemulsions during storage. The △E* values of 0.1% and 0.4% lemon oil microemulsions are shown in Figure 6.8. It can be seen clearly that the biggest total colour difference (change) occurred from the 0.4% lemon oil microemulsion (0.4%25C YY) that was stored at 25 °C but was subjected to oxygen and light. This was followed by the microemulsion samples which were 0.4%25C NY stored at 25 °C without oxygen and with light exposure and 0.4%37C stored at 37 °C without both oxygen and light. This suggests that light could be a more significant factor to cause beta-carotene degradation leading to its colour change compared to the effect of temperature between 25 and 37 °C on the total colour change. The results of ΔE* values seemed to be in agreement with the results obtained from particle size determination (Figure 6.3). Moreover, from the second week onwards, the△E* value of 0.4% lemon oil microemulsion (0.4%25C YY) remained relatively constant, which was because the a* and b* values did not change too much, at almost zero. This means the redness and yellowness of this microemulsion almost disappeared, which could be apparently confirmed by the results shown in Figure 6.6. This result was in accordance with visual observation shown in Figure 6.7, which showed that after storage for two weeks, 0.4% lemon oil microemulsion became clear.

Figure 6.7 Pictures of beta-carotene encapsulated lemon oil microemulsions (0.1% and 0.4% lemon oil) and macroemulsion (1.5% lemon oil) during storage at different storage conditions. (a) after preparation, (b) after 1 day, (c) after 3 days, (d) after 1 week, (e) after 2 weeks, (f) after 3 weeks, and (g) after 1 month.

While other storage conditions kept the same (without light and oxygen), the difference in temperature had an effect on the colour difference between 0.4% lemon oil microemulsions. To be specific, higher temperature resulted in the faster colour fading, meaning the rate of beta-carotene degradation was accelerated. This phenomenon was in good consensus with the findings reported by Qian et al. (2012b, 2012a), who studied the effect of storage temperature on the total colour difference of beta-carotene encapsulated orange oil-in-water nanoemulsions. They showed that colour fading increased with increasing temperature from 20 to 55 °C. When the lemon oil concentration of microemulsion was 0.1% and the microemulsion was stored at 25 °C without the influence of oxygen and light, the colour fading rate was also relatively very low. On the other hand, it was interesting that when 0.4% lemon oil microemulsion was stored at 25 °C without exposure to oxygen and light, its colour fading was the slowest. All the aforementioned results were in agreement with those obtained from the particle size determination. However, it can be seen clearly from Figure 6.8 that the colour fading rate of 0.4%25C NY was much faster than that of 0.4%25C YN as already mentioned above, which might mean that the influence of light on the degradation of beta-carotene was larger than oxygen did.

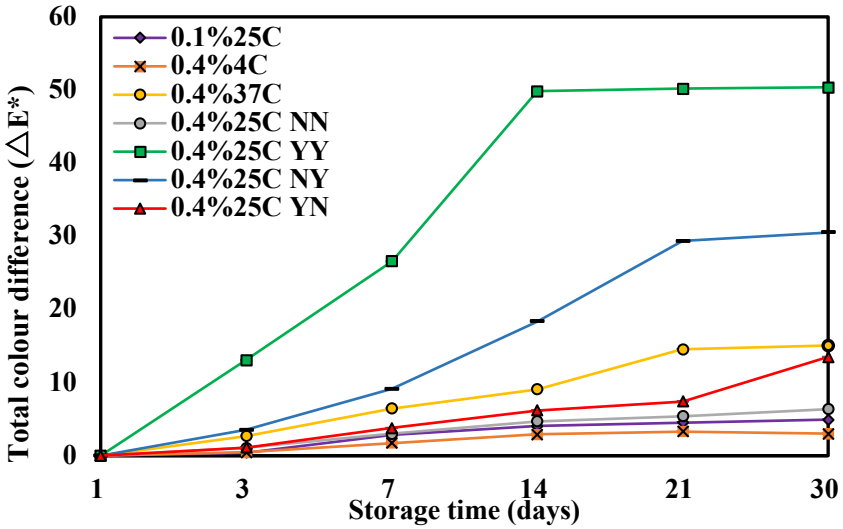

Figure 6.8 Total colour difference (△E*) of beta-carotene encapsulated lemon oil (0.1% and 0.4%) microemulsions measured during storage for 1 month at different environmental conditions. Data are presented as the mean and standard deviation of two independent measurements with duplicate (n = 4) and error bars mean standard deviation.

6.4.5 Changes in beta-carotene content in emulsions during storage

Microemulsions and macroemulsions were analysed for their content of beta-carotene during storage at different environmental conditions. A UV-visible spectrophotometer was employed to measure the absorbance values of the extracted beta-carotene in n-hexane to determine the contents of beta-carotene using the equation obtained in Section 6.4.1. Beta-carotene contents in 0.1% and 0.4% lemon oil microemulsions and 1.5% lemon oil macroemulsion after storage for one day were 15.39 ± 0.32, 61.95 ± 1.43 and 180.31 ± 3.49 μg/ml, respectively. Blank samples containing beta-carotene were prepared by dissolving in n-hexane and then stored under the same conditions as the related emulsion samples. The measured beta-carotene concentrations of the blank samples were 15.19 ± 0.08, 61.97 ± 0.14 and 181.33 ± 0.66 μg/ml, which were almost close to the beta-carotene content of micro- and macroemulsion samples. The stability of beta-carotene in emulsion and blank samples during storage was monitored by beta-carotene retention, which was calculated by (Ct/C0) x 100 (Ariviani et al., 2015, Chen and Zhong, 2015). In this equation, Ct means the content of beta-carotene during

storage for a certain time period (t) and C0 represents the content of beta-carotene at initial.

It can be seen clearly from Figure 6.9 (a) that beta-carotene retention was the highest when 0.4% lemon oil microemulsion was stored at 4 °C without the effect of oxygen and light. After storage for 1 month, 56% of beta-carotene was still retained in this microemulsion, which was significantly ($p < 0.05$) higher than that in the microemulsions stored at 25 and 37 °C without being exposed to oxygen and light. When it was stored at 37 °C, only 20% of beta carotene remained in the microemulsion after storage for one month. Furthermore, regardless of storage conditions, 0.4% microemulsion could efficiently protect beta-carotene from degradation compared to the blank sample containing beta-carotene dissolved in n-hexane. Even being stored at 4 °C, 79% beta-carotene was degraded after 1 month when it was not encapsulated in emulsions but dissolved in n-hexane solution.

Figure 6.9 (b) shows that when 0.4% lemon oil microemulsion was stored at 25 °C to study the influence of oxygen and light, the microemulsion which was not exposed to oxygen and light had the highest retention percentage of beta-carotene after 1-month storage. But if it was stored in contact with both oxygen and light, beta-carotene was completely degraded after 2 weeks. Moreover, only after 3 days, almost 30% of beta-carotene was degraded when it was stored under the environment of contacting oxygen and light. As to 0.4%25C NY and 0.4%25C YN samples, beta-carotene was degraded faster when it was subjected to oxygen instead of light, which is in good agreement with the findings of colour change described in Section 6.4.4. In details, after 1-month storage, 35% beta-carotene remained if this microemulsion was only subjected to oxygen, but this figure was substantially reduced to 15.9% when this microemulsion was subjected to light rather than oxygen. Same to what is shown Figure 6.9 (a), beta-carotene was degraded much faster in solvent solutions when not encapsulated. When

it was exposed to both oxygen and light, it was completely degraded even within 1 week.

0.1% lemon oil microemulsion and 1.5% lemon oil-loaded macroemulsion were also employed to study the retention rate of beta-carotene in these emulsions during storage at 25 °C without being exposed to oxygen and light. After storage for 1 month, 0.1% lemon oil microemulsion had significantly ($p < 0.05$) lower beta-carotene retention percentage than 1.5% lemon oil-loaded macroemulsion, but the beta-carotene retention percentage in these two emulsion delivery systems was both lower than that in 0.4% lemon oil-in-water microemulsion. 0.4% lemon oil-loaded microemulsion had a higher ratio of surfactant to oil, which might be the reason for its stronger protection of beta-carotene against degradation than 1.5% loaded conventional emulsion (Teo et al., 2016). In the present study, the ratio of surfactant to oil in 0.4% lemon oil microemulsion was 5, while that in 1.5% lemon oil macroemulsion was 1.3.

Compared to n-hexane, all these three types of emulsions could provide protection of beta-carotene against degradation during storage. When beta-carotene was encapsulated into 0.4% lemon oil-in-water microemulsions, which was then stored at 4 °C and at the environment without direct contact with oxygen and light, it had the lowest degradation rate.

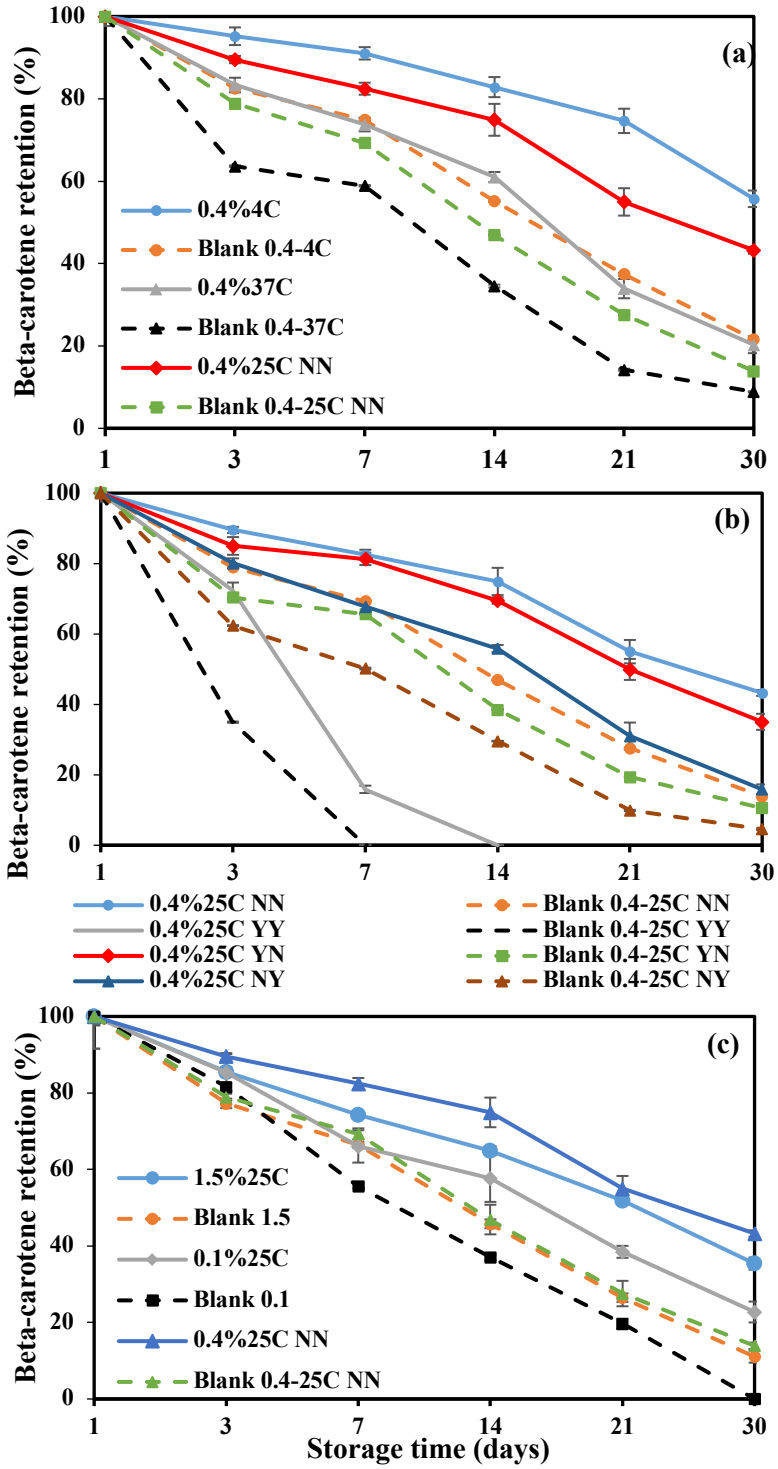

Figure 6.9 Stability of beta-carotene in 0.1% and 0.4% microemulsions and 1.5% macroemulsion (full line) and related blank samples (dotted line) during storage for 1 month at different environmental conditions. (a) 0.4% lemon oil microemulsion stored at different temperatures (4, 25 and 37°C) without oxygen and light, (b) 0.4% lemon oil microemulsions stored at 25°C with and without oxygen and/or light, and (c) 0.1%, 0.4% and 1.5% lemon oil emulsions stored at 25°C without oxygen and light. Data are presented as the mean and standard deviation of two independent measurements with duplicate (n = 4) and error bars mean standard deviation.

Ariviani et al. (2015) introduced 4 different storage conditions to study the stability of beta-carotene enriched VCO (virgin coconut oil)-in-water or palm oil-in-water microemulsions. In detail, these microemulsions were stored at 4 °C and 15 °C as well as at ambient temperature in a dark environment with and without heat treatment at 105 °C for 5 hours. The authors stated that beta-carotene in microemulsion which was subjected to heat treatment had lower degradation rate compared to the one without heat treatment. Beta-carotene tends to form crystal when its concentration is higher than its saturation point. So, in this study, heat treatment helped the crystallised beta-carotene to dissolve into the oil phase, which reduced the degradation rate of beta-carotene. Furthermore, degradation rates of beta-carotene in palm oil microemulsion stored at 4 °C and 15 °C were not significantly different from each other, while they were significantly lower than those stored at ambient temperature. After 12 weeks, the retention percentage of beta-carotene in VCO microemulsion at 4 °C was much higher than that stored at 15 °C.

In another study conducted by Chen and Zhong (2015) who fabricated beta-carotene loaded peppermint oil-in-water microemulsion which was emulsified by Tween 20 and lecithin using the PIT method, the stability of beta-carotene was dramatically increased after its encapsulation into the microemulsion system. When beta-carotene was dissolved into ethyl acetate solution as the control sample, it was degraded quickly up to 50% after 1 day and only 1.9% remained stable after 5-day storage. They also studied the effect of lecithin on the stability of Tween 20-stabilised peppermint oil-in-water microemulsion, noticing the addition of lecithin into the system substantially increased the retention rate of beta-carotene and the increase in lecithin concentration significantly improved the stability of beta-carotene. After stored for 15 days, 50% and 75% beta-carotene were still retained in the microemulsion with 1% and 3% lecithin, respectively. Besides, after storage for 65 days, there was 20% of beta-carotene still existing in the microemulsion with 3% lecithin, while the system without

lecithin only had less than 5% beta-carotene remained. Moreover, beta-carotene was completely degraded if the control solution was kept at 60 and 80 °C for 2 hours and 4 hours, respectively. However, after incubation at 60 °C for 16 hours, 35%, 55%, 60% and 64% beta-carotene were remained if beta-carotene was encapsulated into the microemulsions with 0%, 1%, 2% and 3% lecithin. Even kept at 80 °C, 61% of beta-carotene still existed in the microemulsion which had 3% lecithin.

According to the studies reported by Chen and Zhong (2015), beta-carotene degradation data during storage were fitted into a first order kinetic model (Equation 6.4):

$$\ln (Ct / C0) = - kt \qquad [6.4]$$

where k means the degradation rate constant and Ct and C0 mean the content of beta-carotene during storage for a certain time period (t) and at initial, respectively. Besides, half-life of beta-carotene ($t_{1/2}$) was accordingly obtained by Equation 6.5:

$$t_{1/2} = - \ln (0.5)\, k^{-1} \qquad [6.5]$$

Table 6.6 summarizes the degradation rate constant, half-life and coefficient of determination of beta-carotene degradation during storage when it was fitted into the first order kinetic equation. It can be concluded from the results shown in Table 6.6 that beta-carotene degradation was a typical first order kinetic since the coefficient of determination values ranged from 0.9507 to 1.0000. When 0.4% lemon oil-loaded microemulsion was kept at 25 °C and subjected to oxygen and light, half-life of beta-carotene was only 2.19 days, which was 19 times shorter than when it was stored at 4 °C and without the effect of oxygen and light.

Table 6.6 Degradation rate constant (k), half-life ($t_{1/2}$) and coefficient of determination (R^2) of beta-carotene degradation during storage in 0.1% and 0.4% lemon oil-loaded microemulsions and 1.5% lemon oil macroemulsion as well as their blank (control samples) when beta-carotene degradation was fitted into the first order kinetic equation. Data are presented as the mean and standard deviation of two independent measurements with duplicate (n = 4).

Sample	Condition	k (d^{-1})	R^2	$t_{1/2}$ (d)
0.1% microemulsion	25C NN	0.0471 ± 0.0045	0.9758 ± 0.0185	14.83 ± 1.42
1.5% macroemulsion	25C NN	0.0321 ± 0.0009	0.9848 ± 0.0021	21.60 ± 0.61
0.4% microemulsion	4C NN	0.0182 ± 0.0006	0.9507 ± 0.0237	38.01 ± 1.18
	37C NN	0.0522 ± 0.0020	0.9719 ± 0.0060	13.30 ± 0.51
	25C NN	0.0273 ± 0.0003	0.9749 ± 0.0116	25.41 ± 0.24
	25C YY	0.3171 ± 0.0111	0.9721 ± 0.0034	2.19 ± 0.08
	25C NY	0.0589 ± 0.0027	0.9698 ± 0.0094	11.79 ± 0.52
	25C YN	0.0334 ± 0.0008	0.9716 ± 0.0076	20.74 ± 0.49
Blank 0.1%	25C NN	0.0784 ± 0.0037	0.9920 ± 0.0020	8.85 ± 0.42
Blank 1.5%	25C NN	0.0509 ± 0.0004	0.9905 ± 0.0008	13.62 ± 0.11
Blank 0.4%	4C NN	0.0493 ± 0.0003	0.9925 ± 0.0007	14.06 ± 0.07
	37C NN	0.0802 ± 0.0005	0.9728 ± 0.0007	8.64 ± 0.06
	25C NN	0.0640 ± 0.0002	0.9928 ± 0.0005	10.83 ± 0.04
	25C YY	0.5257 ± 0.0019	1.0000 ± 0.0000	1.32 ± 0.00
	25C NY	0.1013 ± 0.0011	0.9834 ± 0.0008	6.84 ± 0.08
	25C YN	0.0739 ± 0.0008	0.9874 ± 0.0003	9.37 ± 0.10

6.5 Conclusions

This study focused on determining the effects of microemulsion encapsulation on the effect of environmental conditions (temperature, oxygen and light) to show the advantage of microemulsion which was fabricated by emulsion dilution method. 0.1% and 0.4% lemon oil-in-water microemulsion and 1.5% lemon oil-in-water macroemulsion were studied. The incorporation of beta-carotene had a significant effect on the particle size of 0.1% and 0.4% lemon oil microemulsions, but they still remained within a particle size range defined as microemulsion. During storage, temperature, oxygen and light all influenced the degradation rate of beta-carotene. Specifically speaking, when 0.4% lemon oil-loaded microemulsion was stored at different temperatures without contacting oxygen and light, lower temperature substantially reduced the degradation rate of beta-carotene. Moreover, if this microemulsion was kept at ambient temperature but was subjected to oxygen and light, it was degraded very fast. At this storage condition, the microemulsion lost its yellow-reddish colour, i.e., became colourless, after 2 weeks. Obviously, the highest percentage of beta-carotene was retained after 1 month if neither oxygen nor light was applied to this microemulsion. It is also found in this study that the degradation rate of beta-carotene was higher when it was exposed to light compared to the condition when it was only exposed to oxygen. Apart from these, both 0.1% lemon oil-loaded microemulsion and 1.5% lemon oil-loaded macroemulsion had higher degradation rate of beta-carotene than 0.4% oil-loaded microemulsion.

Overall, this study provides some useful information about the stability of beta-carotene in microemulsions and macroemulsions during storage at different environmental conditions and about which storage condition and delivery system might be the most efficient in the protection of bioactive compounds from degradation.

Chapter 7 Encapsulation of beta-carotene into microemulsions using water titration method

7.1 Abstract

Beta-carotene is the most widespread carotenoid which is also the most active precursor of vitamin A and may reduce the risk of heart disease and some cancers. However, beta-carotene is unstable to oxidative degradation, therefore, a certain type of system is required to encapsulate beta-carotene. In this study, water titration method was utilised to produce blank and beta-carotene encapsulated microemulsions along the dilution line W19 of a mixture system consisting of Capmul 708G, Tween 80, Milli-Q water and PG (the ratio of water to PG was 1:1). Viscosity and conductivity were determined from both blank and beta-carotene-loaded microemulsions. The results indicate that the encapsulation of beta-carotene did not significantly alter the properties of its corresponding blank microemulsions without containing beta-carotene, except for its particle size being significantly higher than that of blank microemulsions.

In this study, beta-carotene encapsulated O/W microemulsion (L990) containing 1% Tween 80, 9% Capmul 708G, 45% water and 45% PG as well as W/O microemulsion (L910) containing 9% Tween 80, 81% Capmul 708G, 5% water and 5% PG were fabricated to study the effect of microemulsions on the oxidative degradation rate of beta-carotene. These two systems were stored under different environmental conditions. Specifically speaking, 3 different temperatures (4, 25 and 37 °C) were used for storage. At 4 and 37 °C, the emulsion samples were stored under dark and without oxygen. On the other hand, at 25 °C, 4 different storage conditions were used; with oxygen and light (YY), without oxygen and light (NN), with oxygen and without light (YN) and without oxygen and with light (NY).

Both the analysis of total colour difference (△E*) and beta-carotene content showed the same results that when L910 and L990 microemulsions containing beta-carotene were stored at 4 °C under dark without oxygen, beta-carotene had the lowest degradation rate. Higher temperature accelerated the degradation rate of beta-carotene. When it was kept at 25 °C and exposed to oxygen and light (25C YY), the sample had the highest beta-carotene degradation which was found to be completely degraded when L910 microemulsion sample was kept at this condition for one month. In terms of the factor between oxygen and light, beta-carotene was degraded faster when it was subjected to light rather than oxygen in both L910 and L990 microemulsions. In addition, the stability of beta-carotene encapsulated in L910 or L990 microemulsion system was compared with the beta-carotene control sample (i.e. beta-carotene in n-hexane solution). The degradation rate of the former was much lower than that in n-hexane solution, meaning both L910 and L990 microemulsion systems could protect beta-carotene from degradation during storage. However, between these two microemulsions, the protection of beta-carotene against its degradation was stronger in L990 O/W microemulsion than in L910 W/O microemulsion. This may be due to the fact that beta-carotene was dispersed in the oil phase which was the internal phase of L910.

This study provides information about the effects of different environmental conditions on the stability of beta-carotene that was encapsulated in O/W and W/O microemulsions during storage which were fabricated by water titration method. The results indicate that microemulsion could be a good delivery system to encapsulate and protect beta-carotene against oxidative degradation.

7.2 Introduction

Microemulsion is defined as a thermodynamically stable emulsion system which can

be formed spontaneously without using a high mechanical shear force (e.g. high pressure homogenization, ultrasonication) (Flanagan and Singh, 2006). Nevertheless, a certain type of external energy, such as stirring and heating, is often applied when preparing microemulsions. Water titration method which involves the titration of a surfactant and oil mixture with an aqueous phase under continuous stirring has been used to fabricate microemulsions (Garti et al., 2003, Feng et al., 2009a, Fanun, 2010, Yi et al., 2012). Microemulsion is a clear system in its optical properties which has a potential for its utilisation in making foods or beverages without altering their original clear appearance and matrix. Moreover, microemulsions are can be utilised as a delivery system by encapsulating labile bioactive substances.

Microemulsions have been investigated for applications in pharmaceutical (Garti et al., 2006, Aboudzadeh et al., 2018), cosmetics (Garti et al., 2004, Valenta and Schultz, 2004, Volpe et al., 2018) and food (Amar et al., 2004, Flanagan and Singh, 2006, Feng et al., 2009b), to incorporate and deliver water insoluble and/or oil insoluble active compounds. Based on Flanagan and Singh (2006), extremely small particle size results in large surface area of oil particles in O/W microemulsion, which leads to the rapid absorption of incorporated compounds. As such, microemulsion has been shown to increase the bioavailability of enveloped active compounds (He et al., 2010, Hu et al., 2012, Xiao et al., 2013). In addition, microemulsion system is able to control the release of incorporated active compounds (Feng et al., 2009b, Aboudzadeh et al., 2018).

Many different types of bioactive compounds have been encapsulated into microemulsion systems via the water titration method, such as curcumin (Hu et al., 2012, Lin et al., 2012, Xiao et al., 2013), beta-carotene (Chen and Zhong, 2015, Roohinejad et al., 2015, Cheng et al., 2017), lycopene (Spernath et al., 2002, Garti et al., 2004), lutein (Amar et al., 2004), CoQ10 (Deutch-Kolevzon et al., 2011, Chen et

al., 2015) and vitamin E (Feng et al., 2009b). It is well documented that microemulsions could also enhance the solubility of bioactive compounds (Garti et al., 2004, Deutch-Kolevzon et al., 2011, Chen et al., 2017, Cheng et al., 2017) and protect them from degradation (Szymula, 2004, Chen and Zhong, 2015, Chen et al., 2017).

In a study conducted by Chen et al. (2017), alpha-linolenic (ALA) encapsulated microemulsion containing castor oil ethoxylates 35 (EL-35), ethanol, isoamyl acetate and water was prepared by using the water titration method. The solubility of ALA in microemulsion was much higher than that in pure oil phase. Also, the solubility of ALA was increased with increasing surfactant concentration and the degradation of ALA in microemulsion was much lower than that in pure oil phase (26.3% versus 50% after storage for 10 days). However, when vitamin C was added into the water phase of the microemulsion, only 12.7% of ALA was lost during 10-day storage at 20 °C.

In another study, beta-carotene encapsulated microemulsion which was comprised of pentanol, SDS and water was fabricated by Szymula (2004) by the water titration method, finding beta-carotene was more easily to be oxidized in O/W microemulsion than in pentanol, W/O microemulsion and bicontinuous microemulsion. The reason for this phenomenon might be caused by the fact that the concentration of oxygen, which was one of the reasons for oxidation, in the organic phase was much higher than in the water phase.

It was shown in Chapter 5 that when the pseudo ternary phase diagram was constructed by Tween 80, Capmul 708G, PG and water (ratio of PG to water was 1:1), A_T was 100%, meaning every formulation in the pseudo ternary phase diagram formed a certain type of microemulsion (e.g. W/O, O/W and bicontinuous microemulsion) via the water titration method. In Chapter 6, emulsion dilution method was utilised to fabricate beta-carotene encapsulated lemon O/W microemulsions (0.1% and 0.4%

lemon oil) and macroemulsions (1.5% lemon oil). These micro- and macroemulsions were stored under different environment conditions (e.g. temperature, oxygen and light) to study their effects on the stability of beta-carotene. It was concluded that temperature, oxygen and light all accelerated the degradation of beta-carotene. When stored at 4 °C under dark condition without oxygen, 0.4% lemon oil microemulsion provided the strongest protection to beta-carotene against degradation. In this study (Chapter 7), two microemulsion systems (L910 W/O microemulsion and L990 O/W microemulsion), which were composed of Tween 80, Capmul 708G, PG and water and produced by water titration method, were chosen from the results of Chapter 5 for encapsulation of beta-carotene to investigate its effect on the physicochemical properties of microemulsions. The microemulsions encapsulating beta-carotene prepared were then analysed during storage for 1 month at different temperatures (4, 25 and 37 °C) with and without oxygen and light to study their effects on the stability of beta-carotene.

7.3 Materials and methods

7.3.1 Materials

Capmul 708G, Tween 80, PG and beta-carotene powder (≥ 93%, UV) were purchased from Sigma-Aldrich Co. (St Louis, MO, USA). Absolute ethanol (analytical grade), n-hexane (HPLC grade), methanol (HPLC grade), acetonitrile (HPLC grade) and dichloromethane (HPLC grade) were purchased from Fisher Scientific Ltd. (Loughborough, UK).

7.3.2 Validation of HPLC method for beta-carotene content

HPLC measurement was conducted using a Shimadzu Nexera liquid chromatography system (Figure 7.1) equipped with system controller SCL-10A VP, autosampler SIL-10AF, solvent delivery unit LC-10AT VP, column oven CTO-10AS VP and photodiode

array detector SPD-M10A VP (Shimadzu Corp., Japan). Beta-carotene was separated via a reverse phase C18-column (Synergi 4 µm Fusion-RP 80 Å, 250 x 4.6 mm, Phenomenex, Torrance, CA, USA). The mobile phase was comprised of 70% methanol, 20% acetonitrile and 10% dichloromethane with a flow rate of 1.0 ml/min at 25 °C. A 10 µl of samples were injected automatically by the equipment to determine the beta-carotene content. Retention time and area under curve (AUC) were obtained.

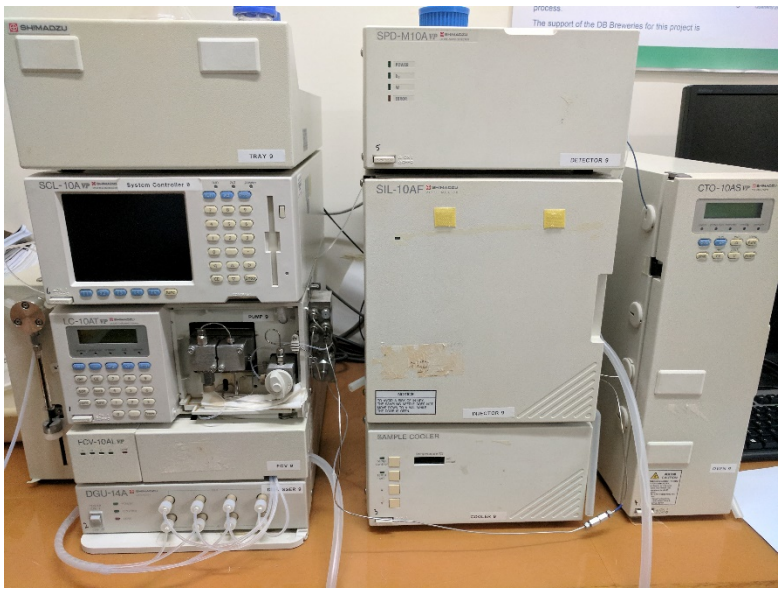

Figure 7.1 Picture of high-performance liquid chromatography system

HPLC to study the content of beta-carotene was validated based on the method illustrated in ICH harmonized tripartite guideline Q2 (R1) which includes the validation of analytical procedures. In this section, linearity, accuracy, precision and robustness were determined. The determination of linearity, accuracy and precision was similar to what was mentioned in Section 6.3.2. in Chapter 6. Briefly, beta-carotene powder was dissolved into 100 ml n-hexane solution to make 100 µg/ml stock solution, which was then diluted by n-hexane to make beta-carotene-in-hexane solutions with the concentrations of 1, 2, 5, 10, 50 and 75 µg/ml. These solutions were measured by HPLC to obtain the values of AUC, which were plotted as a function of beta-carotene concentration to create the standard curve for beta-carotene. Three

different concentrations (2, 50 and 75 μg/ml) of standard solutions were then chosen to measure AUC in three different time points in one day to determine the intra-day precision. 75 μg/ml beta-carotene in n-hexane solution was also chosen to measure the AUC in three different days (one time each day) to determine the inter-day precision. Accuracy and relative standard deviation (RSD) were therefore able to be obtained. Different flow rates (0.8, 0.9, 1.0, 1,1 and 1.1 ml/min) of the mobile phase were chosen to study the robustness of HPLC method. The retention time of beta-carotene and AUC values were documented.

7.3.3 Solubility of beta-carotene

Solubility of beta-carotene in Capmul 708G, PG and Tween 80 were determined by HPLC method to compare with that measured by the spectrophotometric method. The method was described in Section 6.3.3 in Chapter 6. Simply speaking, 4 mg of beta-carotene was added into 10 ml Capmul 708G, Tween 80 and PG. Samples were flushed with nitrogen gas before being placed in an 80 °C water bath for 5 minutes. The samples were then equilibrated under continuous shaking by a magnetic stirrer at 500 rpm overnight at 25 °C. After that, the samples were centrifuged at 15000 rpm for 15 minutes via a Sigma 6-16 KS centrifuge (Sigma Laborzentrifugen GmbH, Osterode am Harz, Germany) to remove any undissolved beta-carotene. The clear supernatant was taken and filtered through a 0.2 μm Minisart NY 25 hydrophilic polyamide syringe filter (Sartorius Stedim Biotech GmbH, Goettingen, Germany) before being further diluted by n-hexane. The obtained solutions were placed in Shimadzu Nexera liquid chromatography system to determine beta-carotene content.

7.3.4 Fabrication of beta-carotene encapsulated microemulsions

In Section 5.4.2 in Chapter 5, it showed that if 50% PG was mixed with water to act as the aqueous phase to construct ternary phase diagram together with Capmul 708G and Tween 80, every single point in the TPD was a microemulsion. Of all the mixture

systems in TPD, mixtures in dilution line W19 have the lowest ratio of surfactant to oil (1:9). Therefore, microemulsions in dilution line W19 were chosen to encapsulate beta-carotene.

Microemulsions were manufactured using the water titration method with Tween 80, Capmul 708G, PG and Milli-Q water as described in Section 3.2.2 in Chapter 3. Briefly, PG and Milli-Q water were mixed at a ratio of 1:1 (w/w) to form an aqueous phase. In the meantime, a Tween 80 and Capmul 708G mixture at a ratio of 1:9 (w/w) was also prepared by stirring gently which was then diluted with the aqueous phase in dropwise under moderate agitation using a vortex mixer to prepare microemulsions designated as L910, L920, L930, L940, L950, L960, L970, L980 and L990. These The composition of these samples is listed in Appendix (Table 1). These samples were further kept at 25 °C for 24 hours for equilibrium. After that, an excess amount of beta-carotene powder (5mg) was added into these microemulsions (10 ml). The mixtures were flushed with nitrogen gas before being placed in an 80 °C water bath for 5 minutes. then equilibrated under continuous shaking by a magnetic stirrer at 500 rpm overnight at 25 °C. After that, the samples were centrifuged at 15000 rpm for 15 minutes using Sigma 6-16 KS centrifuge. The clear supernatant was filtered through a 0.2 μm Minisart NY 25 hydrophilic polyamide syringe filter to fabricate the so-called beta-carotene loaded microemulsions. Microemulsions without beta-carotene were also manufactured as the blank microemulsions.

7.3.5 Determination of microemulsion types

Microemulsion types of blank and loaded microemulsions were determined by conductivity and viscosity measurement by using the same methods as described in Section 5.3.4 and 5.3.5 in Chapter 5. Besides, particle size and PDI of blank and beta-carotene loaded microemulsions were measured by using the same methods as described in Section 3.2.3 in Chapter 3.

7.3.6 Determination of beta-carotene content in microemulsions

Beta-carotene was extracted from all the loaded microemulsions using the method described in Section 6.3.5 in Chapter 6. The extracted sample was analysed for the content of beta-carotene by using the UV-visible spectrophotometer (UV-1700, Shimadzu Corp., Japan) as described in Section 6.3.5 and Chapter 6 as well as high performance liquid chromatography (HPLC) at the wavelength of 450 nm.

7.3.7 Stability of beta-carotene encapsulated microemulsions

Beta-carotene loaded L910 and L990 microemulsions were selected to study the stability of beta-carotene during storage at different conditions. The conditions chosen were the same as those used in Chapter 6. Specifically, both L910 and L990 loaded microemulsions were stored at 3 different temperatures (4, 25 and 37 °C). At 4 and 37 °C, they were kept away from oxygen and light. On the other hand, at 25 °C, they were stored at 4 different environments as designated as follows: with oxygen and light (YY), without oxygen and light (NN), with oxygen and without light (YN), and without oxygen and with light (NY).

After beta-carotene loaded microemulsions were prepared, they were stored at the conditions mentioned above for 1 month. During storage for 3 days, 1 week, 2 weeks, 3 weeks and 1 month, colour and beta-carotene content of L910 (W/O) and L990 (O/W) beta-carotene loaded microemulsions were determined using the methods as described in Section 6.3.6 and 6.3.5 in Chapter 6. Each emulsion sample was measured in at least duplicate.

7.4 Results and discussions

7.4.1 HPLC Validation

Beta-carotene standard solutions which were prepared by adding into n-hexane at

concentrations of 1, 2, 5, 10, 50, 75 and 100 µg/ml were analysed by HPLC. As such retention time of beta-carotene and AUC were able to be obtained. Figure 7.2 shows the chromatogram of 100 µg/ml beta-carotene in n-hexane solution which illustrates that the retention time of beta-carotene was approximately 22.8 minutes. Apart from this, AUC of beta-carotene from this standard sample was 11220586 mAU. Figure 7.3 shows the standard curve created by plotting AUC values of the beta-carotene standard solutions vs their concentrations. It can be concluded from the standard curve that when beta-carotene concentration was between 1 to 100 µg/ml, AUC values formed a linear equation, y = 109103x – 137854, which had a high correlation coefficient value (R^2) of 0.9964.

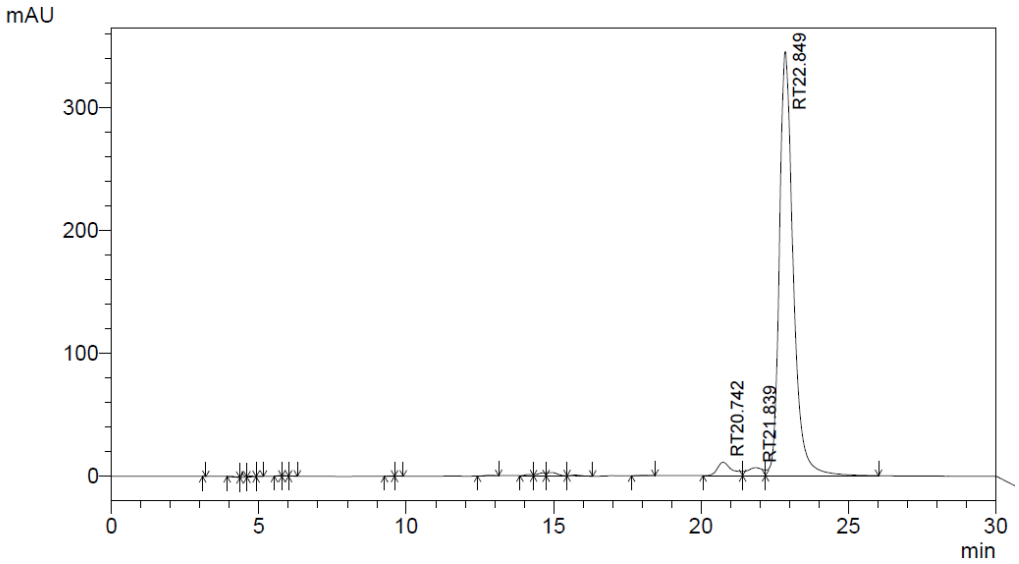

Figure 7.2 HPLC chromatogram of 100 µg/ml beta-carotene in n-hexane solution.

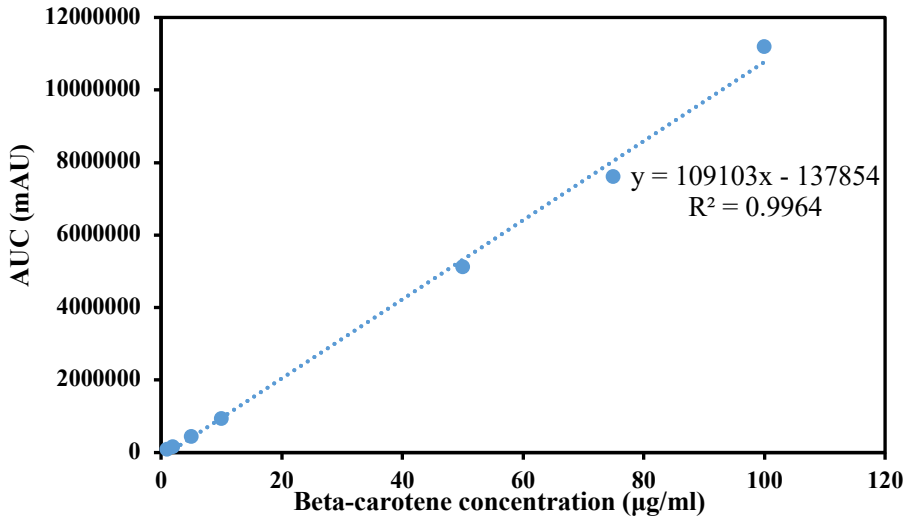

Figure 7.3 Standard curve generated from AUC as a function of beta-carotene concentration by using HPLC.

Beta-carotene in n-hexane solutions with the concentrations of 2, 50 and 75 µg/ml were selected to study the accuracy and intra-day precision of this method. Besides, 75 µg/ml was selected to study the accuracy and inter-day precision of this method. Tables 7.1 and 7.2 summarize the results of the intra-day and inter-day precision and accuracy tests, respectively. It can be seen clearly from Table 7.1 that when beta-carotene concentration was 2 µg/ml, the method had the poorest accuracy which was 129.41%. When beta-carotene was 50 and 75 µg/ml, the recovery was around 93.5% in both cases. In terms of inter-day test, the accuracy for the determination of 75 µg/ml beta-carotene in n-hexane solution was approximately 95%. In terms of RSD, both inter-day and inter-day precision tests were more than 1% but less 3% in all cases, except for the case of beta-carotene concentration with 50 µg/ml which had the RSD value of 3.58%. This indicates the method used to determine the content of beta-carotene was reasonably precise, but its accuracy was not very high.

Table 7.1 Summary of intra-day precision and accuracy tests. Data are presented as the mean and standard deviation measured in triplicate (n = 3).

	Theoretical concentration (μg/ml)	Measured concentration (μg/ml)	Accuracy (% recovery)	Precision (% RSD)
Intra-day precision	2	2.69 ± 0.07	129.41	2.50
	50	46.67 ± 1.67	93.33	3.58
	75	70.40 ± 1.03	93.86	1.47

In addition to the inter- and intra-day precision and accuracy for the method to determine the beta-carotene concentration spectrophotometrically, 30 and 60 μg/ml beta-carotene in n-hexane solutions were used to determine the accuracy (% recovery) and precision (% RSD) of the HPLC method as well. The measured beta-carotene concentration values in these two solutions were 26.28 ± 0.37 and 55.06 ± 0.35 μg/ml, respectively. This resulted in the recovery of 87.60% and 91.77%, respectively, and the RSD values of 1.40% and 0.64%, respectively. Therefore, it could be concluded that the HPLC method was relatively precise, but it was not as precise as the UV-visible spectrophotometry method used in Chapter 6.

Table 7.2 Summary of inter-day precision and accuracy tests. Data are presented as the mean and standard deviation measured in triplicate (n = 3).

	Theoretical concentration (μg/ml)	Day	Measured concentration (μg/ml)	Accuracy (% recovery)	Precision (% RSD)
Inter-day precision	75	1	71.03 ± 1.32	94.70	1.86
		2	71.98 ± 1.91	95.98	2.65
		3	70.64 ± 1.68	94.19	2.38

7.4.2 Beta-carotene content in selected microemulsions

The solubility of beta-carotene in Tween 80, PG and Capmul 708G was measured by HPLC method, which was 38.24 ± 1.78, 5.01 ± 0.89 and 165.22 ± 14.77 μg/ml,

respectively. In Section 6.4.2 of Chapter 6, it was mentioned the solubility of beta-carotene in Tween 80, PG and Capmul 708G was 34.19 ± 0.49, 4.86 ± 0.46 and 159.04 ± 0.36 μg/ml. The solubility data obtained by HPLC method were not significantly different ($P > 0.05$) from those measured by UV-visible spectrophotometer.

Both HPLC and UV-visible spectrophotometry methods were employed to determine the concentration of beta-carotene in samples designated as L910, L920, L930, L940, L950, L960, L970, L980 and L990. The results are shown in Table 7.3, which states that the concentrations measured by HPLC were not significantly ($p > 0.05$) different from those determined by UV-visible spectrophotometer. Also, the concentrations of beta-carotene in all samples (L910 to L990) were decreased with an increase in aqueous phase concentration (Figure 7.4). This finding was same to the results of researches conduct by Roohinejad et al. (2015) and Guo et al. (2019a). L910 had the highest concentration of oil and lowest concentration of aqueous phase, therefore, it contained the highest amount of beta-carotene. As the aqueous phase concentration increased from 10% to 20%, beta-carotene concentration had a steep decrease. When the aqueous phase concentration was between 20% to 60%, beta-carotene concentration did not reduce as dramatically as it was between 20% to 20%. After that, beta-carotene concentration reduced moderately.

Table 7.3 Contents of beta-carotene in selected microemulsion samples measured by HPLC and UV-visible spectrophotometer. Data are presented as the mean and standard deviation of two independent measurements with duplicate (n=4).

Sample No.	Beta-carotene concentration (μg/ml)	
	HPLC	UV-visible spectrophotometer
L910	193.34 ± 1.38	200.08 ± 0.85
L920	123.40 ± 0.85	123.52 ± 1.13
L930	97.66 ± 0.02	98.83 ± 1.18
L940	62.20 ± 0.10	59.96 ± 2.31
L950	38.27 ± 0.35	41.17 ± 0.91
L960	37.38 ± 0.75	38.32 ± 0.29
L970	36.05 ± 0.22	36.56 ± 0.37
L980	32.48 ± 0.17	33.28 ± 0.29
L990	30.47 ±0.09	31.33 ± 0.78

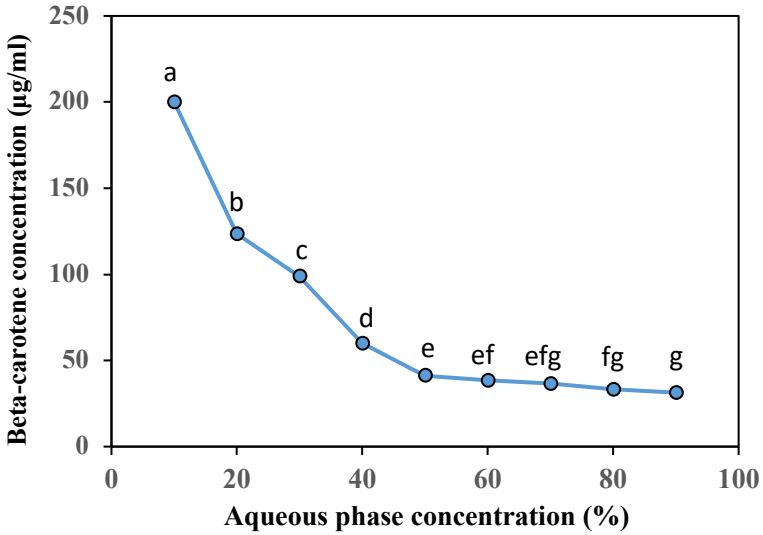

Figure 7.4 Beta-carotene concentration obtained by UV-visible spectrophotometer of samples along the dilution line W19 (L910, L920, L930, L940, L950, L960, L970, L980 and L990). Data are presented as the mean and standard deviation of two independent measurements with duplicate (n=4) and error bars mean standard deviation.

7.4.3 Characterization of blank microemulsions and beta-carotene microemulsions

Dilution line W19 was chosen to study the effect of beta-carotene on the properties of microemulsions fabricated with Capmul 708G, Tween 80, Milli-Q water and PG. All these samples (blank and loaded) were shown to be Newtonian properties as shown in Appendix (Figure 7). Figure 7.5 illustrates the change in viscosity along the dilution line W19 of blank microemulsions and beta-carotene loaded microemulsions. With an increase in aqueous phase concentration, viscosity of both blank and loaded microemulsions decreased continuously. When aqueous phase concentration was 10%, the viscosity of blank and loaded microemulsion was 78.43 and 87.6 mPa.s, respectively. On the other hand, when the concentration of aqueous phase became 90%, the viscosity of blank and loaded microemulsion was 9.24 and 9.59 mPa.s, respectively. The results indicated that the encapsulation of beta-carotene did not significantly alter the viscosity of the blank microemulsions. In the beginning, viscosity had a dramatic reduction until aqueous phase content reached 20%, which continued to decrease afterwards while not as dramatic as it was previously. Therefore, when aqueous phase concentration was 20%, W/O microemulsion transformed into bicontinuous microemulsion. But when bicontinuous microemulsion turned into O/W microemulsion was not quite clear from viscosity data. According to Guo et al. (2019a), the incorporation of 150 ppm beta-carotene only slightly increased the viscosity of empty microemulsions along the dilution line W64 in the mixture system which was comprised of Tween 60, water, glycerol, IPM and ethanol (the ratio of water to glycerol was 1:1 and that of IPM to ethanol was 1:3). However, while the incorporated beta-carotene increased to 300 ppm, viscosity of the loaded microemulsions was significantly higher than that of the empty microemulsions when the aqueous concentration was 35 to 50%.

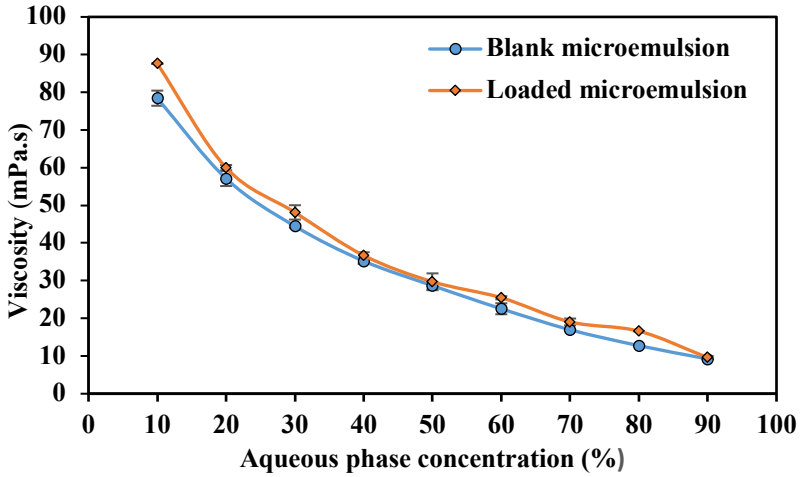

Figure 7.5 Change in viscosity as a function of aqueous phase concentration of Capmul 708G, Tween 80, water and PG mixture system with/without beta-carotene along the dilution line W19. Data are presented as the mean and standard deviation of two independent measurements with duplicate (n=4) and error bars mean standard deviation.

The change in electrical conductivity of the mixture system of Capmul 708G, Tween 80, water and PG with or without beta-carotene along dilution W19 is illustrated in Figure 7.6 (a). The conductivity values of both blank and loaded microemulsions were very low, with the highest value lower than 5 μS/cm, which was much lower than the mixture system with only water as the dilution medium as shown in Section 5.4.4 in Chapter 5. The reason for this might be due to the lower conductivity of PG (0.51 μS/cm) compared to Milli-Q water (3.24 μS/cm). In terms of the blank microemulsion, the conductivity value increased in a small degree when the aqueous phase concentration was less than 20%, after which point the conductivity value increased dramatically. The conductivity value kept almost constant when the percentage of aqueous phase was between 55% and 65%. After that, conductivity started to decrease substantially. The incorporation of beta-carotene did not substantially change the conductivity of the blank microemulsions, which was in good agreement with results reported by Guo et al. (2019a) and Deutch-Kolevzon et al. (2011). The reason for this finding might be due to the fact that beta-carotene was solubilised deep in the oil phase (Deutch-Kolevzon et al., 2011).

It can also be concluded from Figure 7.6 (b) that percolation threshold happened when aqueous phase concentration was 25% which meant at this point, aqueous phase droplets started to interact with each other (Fanun, 2008). As a result, W/O microemulsion transited to bicontinuous microemulsion when aqueous phase concentration was 25% and bicontinuous microemulsion transited to O/W microemulsion when aqueous phase concentration was 55% to 65%.

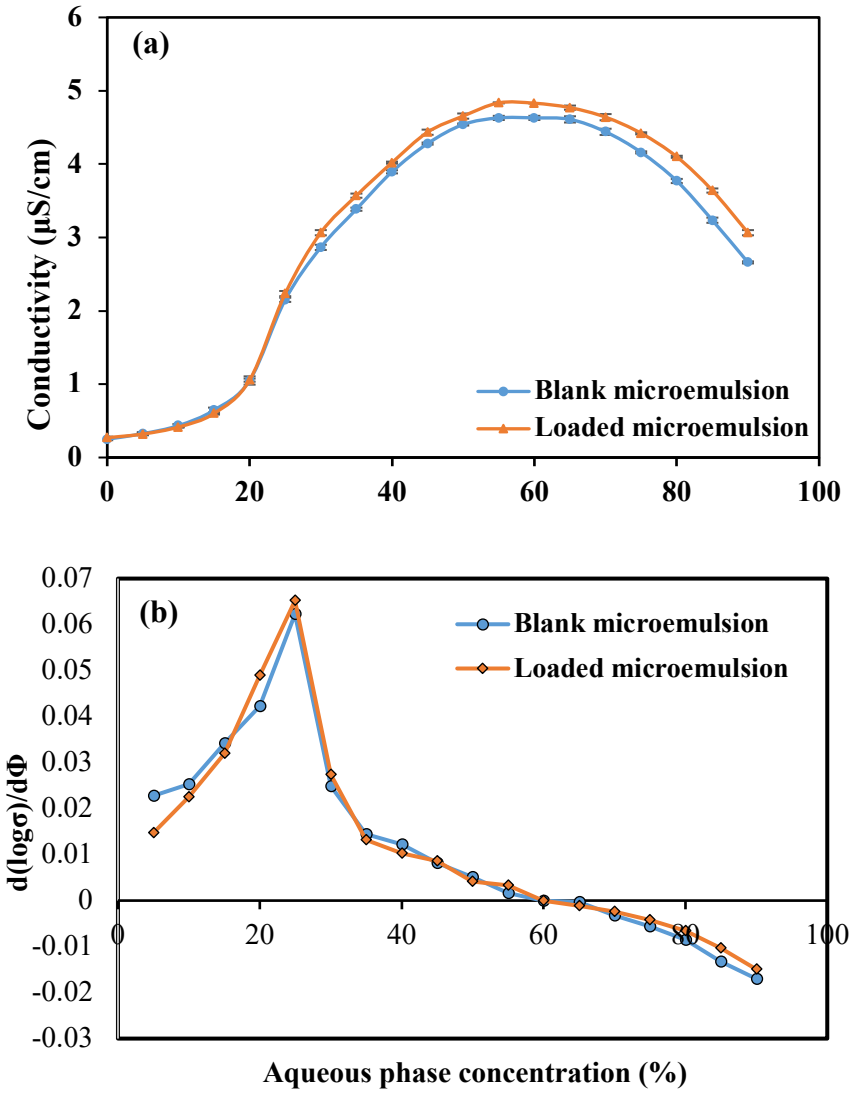

Figure 7.6 Change in conductivity and d(logσ)/d(ϕ) as a function of aqueous phase concentration of Capmul 708G, Tween 80, water and PG mixture system with/without beta-carotene along the dilution line W19. (a) Conductivity alteration (b) d(logσ)/d(ϕ) alteration. Data are presented as the mean and standard deviation of two independent measurements with duplicate (n=4) and error bars mean standard deviation.

Considering the data of conductivity and viscosity, it can be concluded that L910 and L920 were W/O microemulsions, L930, L940, L950 and L960 were bicontinuous microemulsions, while L970, L980 and L990 were O/W microemulsions. Particle size of microemulsions was determined by Zetasizer and the results are shown in Table 7.4, which illustrated that the incorporation of beta-carotene significantly ($p < 0.05$) increased the particle size of blank microemulsions. Roohinejad and co-workers also studied the effect of encapsulation of beta-carotene on the particle size of selected microemulsions from the mixture system, which was composed of Tween 80, Capmul MCM and phosphate buffer (0.01 M, pH 6.8). Their findings showed that after the incorporation of beta-carotene, particle size of some formulations was significantly increased, which that of some other formulations did not have a significant change (Roohinejad et al., 2015).

Table 7.4 Particle size and PDI of blank and loaded microemulsions (L910, L920, L970, L980 and L990). Data are presented as the mean and standard deviation of two independent measurements with duplicate (n=4).

Sample Name		L910	L920	L970	L980	L990
% Capmul 708G		81	72	27	18	9
% Tween 80		9	8	3	2	1
% Water		5	10	35	40	45
% PG		5	10	35	40	45
Blank microemulsion	Particle diameter (nm)	27.1 ± 2.4	26.1 ± 0.4	11.5 ± 0.3	11.3 ± 0.2	12.8 ± 0.3
	PDI	0.28 ± 0.04	0.64 ± 0.03	0.22 ± 0.03	0.23 ±0.03	0.34 ± 0.01
Loaded microemulsion	Particle diameter (nm)	55.9 ± 8.1	33.1 ± 1.3	17.4 ± 0.4	19.8 ±0.2	22.0 ± 0.5
	PDI	0.25 ± 0.02	0.30 ± 0.04	0.29 ± 0.04	0.19 ± 0.07	0.40 ± 0.05

7.4.4 Colour change during storage of L910 and L990 beta-carotene encapsulated Capmul 708G microemulsions

Colour changes in L910 and L990 beta-carotene incorporated Capmul 708G microemulsions were measured using a colour spectrophotometer during storage at different conditions for 1 month. The results are shown in Figures 7.7 and 7.8. In case of L910 W/O microemulsion sample as shown Figure 7.7, L* value was increased during storage while a* and b* values were decreased gradually, regardless of the storage conditions. When stored at 4 °C in the absence of light and oxygen, the L* value (lightness) of L910 loaded microemulsion (L910 4C) was increased slightly from 88.7 to 90.8 during storage for 1 month. On the contrary, when it was kept at 25 °C but subjected to oxygen and light (L910 25C YY), the lightness L* value had the largest augment among all samples after storage for 1 month compared to its initial L* value before storage. While stored at the ambient temperature without oxygen but exposed to light (L910 25C NY), lightness had the second largest increase after storage for 1 month, which was followed by the storage condition when the sample (L910 37C) was kept at 37 °C without exposure to oxygen and light. Between L910 25C NN and L910 25C YN samples, the former had slightly less increase in lightness during storage time.

As to a* value representing redness (if +ve) or greenness (if -ve), L910 loaded microemulsion was in the range of redness with its a* value of +10.8 initially, but it became less reddish during storage because of its decrease over time during storage (Figure 7.7b). Of all the environmental conditions, a* value had the smallest extent of reduction if L910 loaded microemulsion was stored at 4 °C without oxygen and light. While kept at a higher temperature of 25 °C without oxygen and light (L910 25C NN), redness had the second smallest rate of reduction; when oxygen was introduced (L910 25C YN) during storage, a* value decreased more dramatically. When the sample was kept at a higher temperature 37 °C under dark condition without oxygen (L910 37C),

a* value decreased from +10.8 to +1.5 after storage for 1 month. Moreover, if L910 loaded microemulsion was kept at 25 °C under light without oxygen (L910 25C NY), it had the second largest decrease in a* value. While exposed to both light and oxygen (L910 25C YY), the a* value had the most significant further change after storage for 1 month with its red hue changed to green as compared to the storage condition when it was only exposed to light without oxygen (L910 25C NY).

The change in b* value representing yellowness (if +ve) or blueness (if -ve) of all these samples had the same trend as that in a* value. In all cases regardless of storage conditions, the b* value of L910 loaded microemulsion measured initially before storage was +138 being its b* scale much larger compared to the a* scale (+10.8). This indicated the colour hue of beta-carotene-loaded microemulsion was a lot more yellowish than reddish. This was in agreement with the visual observation of the samples (Figure 7.9). When L910 loaded microemulsion was stored at 4 °C without oxygen and light (L910 4C), b* value was relatively very stable being decreased by 58%. However, if the storage condition was changed to 25 °C with exposure to oxygen and light (L910 25C YY), the b* value decreased from +138 to only +1 as shown in Table 7.5c, indicating a loss of yellowness in colour. Between the different storage conditions, the degree of yellowness reduction (b* value) in L910 beta-carotene encapsulated microemulsions was as follows: L910 4C < L910 25C NN < L910 37C < L910 25C YN < L910 25C NY <L910 25C YY. In terms of a* value, the degree of redness change was as follows: L910 4C < L910 25C NN < L910 37C < L910 25C YN < L910 25C NY <L910 25C YY which was the same order as the samples for their b* value changes. In terms of lightness L* value, it was also the same trend with L910 4C < L910 25C NN < L910 37C < L910 25C YN < L910 25C NY <L910 25C YY. These results suggest that storage condition would be more or less affecting the stability of encapsulated beta-carotene against degradation during storage for 1 month.

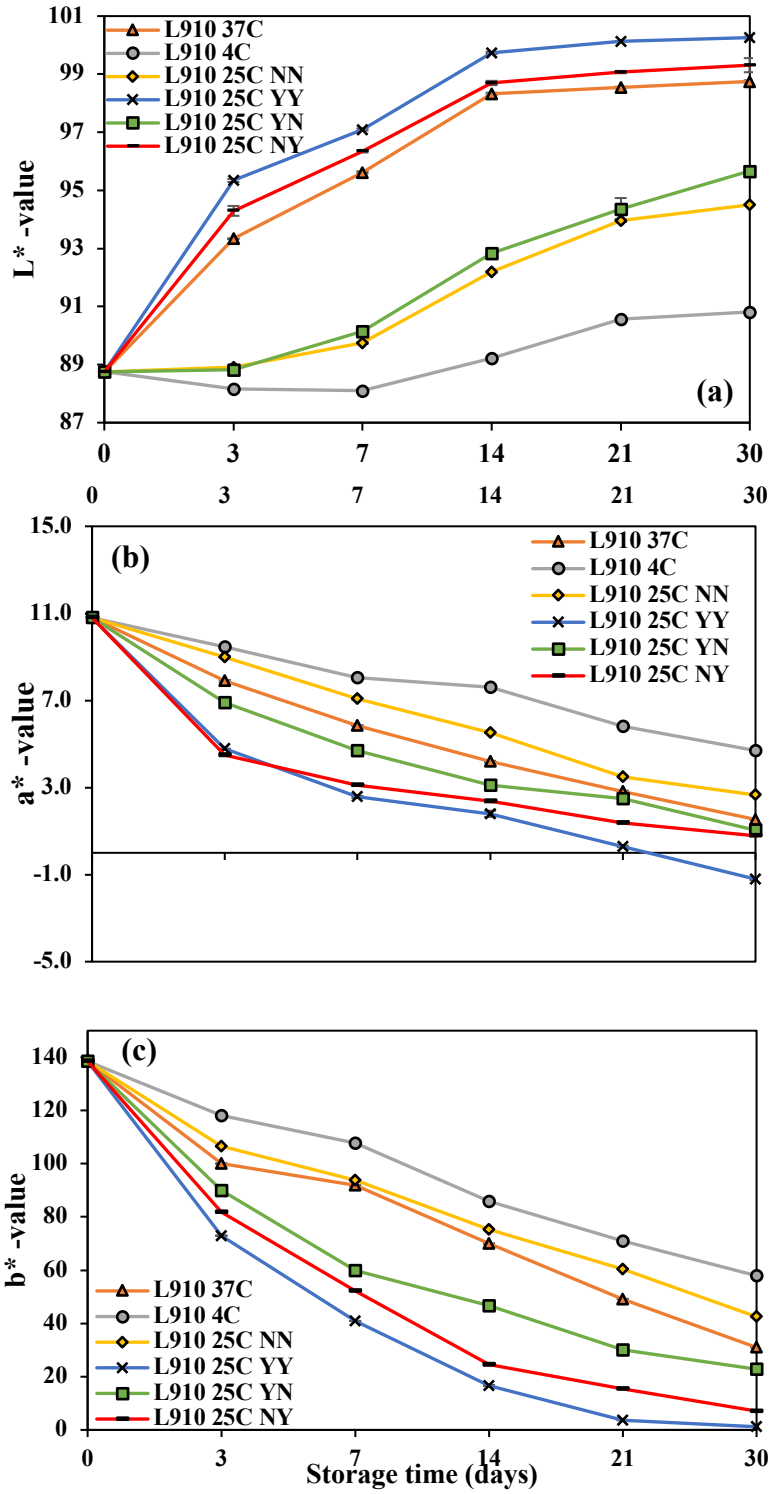

Figure 7.7 Change in colour of beta-carotene incorporated Capmul 708G microemulsion (L910 W/O microemulsion) during storage for 1 month under different conditions. (a) L* value (lightness), (b) a* value (redness if +ve or greenness if -ve), and (c) b* value (yellowness if +ve or blueness if -ve). Data are presented as the mean and standard deviation of two independent measurements with duplicate (n = 4) and error bars mean standard deviation.

A total colour difference (ΔE*) was also calculated to determine the total colour change during storage which is shown in Figure 7.10a. It can be seen clearly that total colour changes increasingly augmented during storage of L910 loaded microemulsion at all conditions with the same order as described in the above for L*, a* and b* scales which was L910 4C < L910 25C NN < L910 37C < L910 25C YN < L910 25C NY <L910 25C YY. This means that the biggest total colour difference occurred among those 6 different storage conditions when L910 loaded microemulsion was stored at 25C with exposure to oxygen and light. If the sample was flushed with nitrogen gas during preparation (i.e. without oxygen), the total colour change after 1 month became smaller. When the sample was kept at 4 °C and was not exposed to oxygen and light, ΔE* was the smallest with its ΔE* value being 80.81 after 1 month. With an increase in storage temperature, the total colour difference was increased as well. For example, when L910 loaded microemulsion was stored 25 and 37 °C for 1 month under dark without oxygen, the ΔE* value for L910 25C NN and L910 37C was increased to 96.5 and 108.37, respectively.

As for the colour measurement of L990 beta-carotene incorporated O/W microemulsion as shown in Figure 7.8, the results of L*, a* and b* values after preparation and before storage were 97.9, +4.2 and +25.9, respectively. This indicated that its colour was yellow with some red rue, like that of L910 W/O microemulsion. Figure 7.8 shows that L* value increased and a* and b* value decreased with increasing storage time. On the other hand, b* value of L990 loaded microemulsion was +25.9 after preparation, which was much lower than that of L910 loaded microemulsion (b*=+138). This phenomenon might be due to the fact that L990 was an O/W microemulsion while L910 was a W/O microemulsion. The external phase of L910 was oil where beta-carotene was added and dissolved, so the sample has more beta-carotene than L990. As mentioned in Section 7.4.2, the concentration of beta-carotene encapsulated in L910 and L990 was 200.08 ± 0.85 and 31.33 ± 0.80 μg/ml.

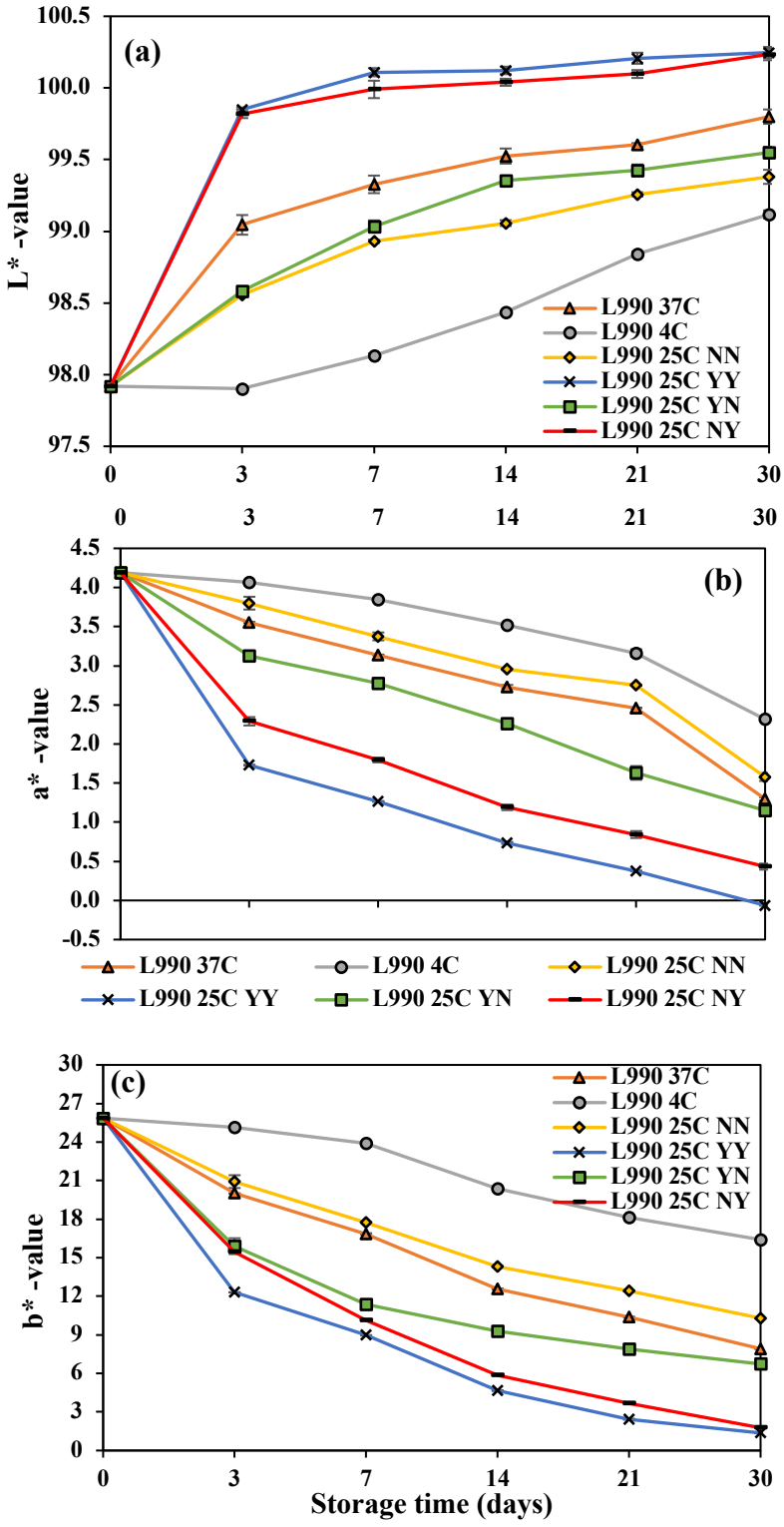

Figure 7.8 Change in colour of beta-carotene incorporated Capmul 708G microemulsion (L990) during storage for 1 month under different conditions. (a) L*value (lightness), (b) a* value (redness if +ve or greenness if -ve) and (c) b* value (yellowness if +ve or blueness if -ve). Data are presented as the mean and standard deviation of two independent measurements with duplicate (n = 4) and error bars mean standard deviation.

Figure 7.10 (b) illustrates total colour difference alteration during storage for 1 month of L990 loaded microemulsion. Change in the ΔE* value of L990 loaded microemulsion was similar to that of L910 loaded microemulsion. When it was kept at 4 °C and not exposed to light and oxygen, the ΔE* value was the lowest, meaning it provided the strongest protection to beta-carotene against degradation during storage. However, if the sample was stored at ambient temperature (25 °C) and exposed to oxygen and light, the ΔE* value was the largest. The extent of total colour changes among L990 microemulsion samples exposed to different storage conditions used in this study was in the order of L910 4C < L910 25C NN < L910 37C < L910 25C YN < L910 25C NY <L910 25C YY as shown in Figure 7.10 (b) which was the same for the L910 microemulsion samples.

Total colour difference changes of L910 and L990 beta-carotene encapsulated microemulsions were in great agreement with the results shown in Section 6.4.4 in Chapter 6. Therefore, it can be concluded that temperature, oxygen and light all had an influence on the degradation of beta-carotene. When the microemulsion sample was kept 4 °C and without contacting oxygen and light, it had the lowest ΔE* value but when the storage temperature was increased to 25 °C and exposed to oxygen and light, the ΔE* value has a substantial increase during the storage period, reaching the highest value among all the samples.

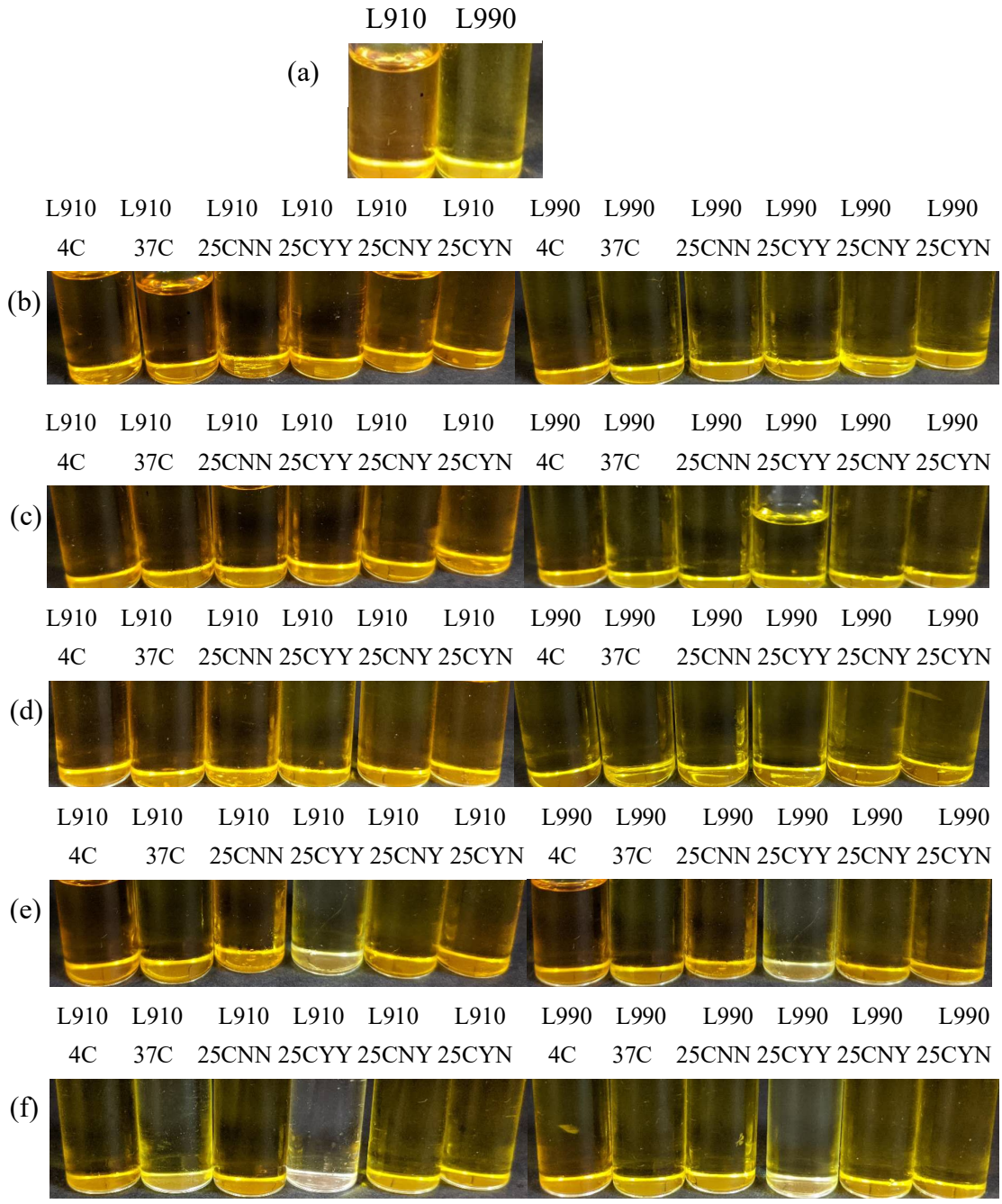

Figure 7.9 Pictures of beta-carotene encapsulated microemulsions (L910 and L990) during storage at different storage conditions. (a) after preparation, (b) after 3 days, (c) after 1 week, (d) after 2 weeks, (e) after 3 weeks, and (f) after 1 month.

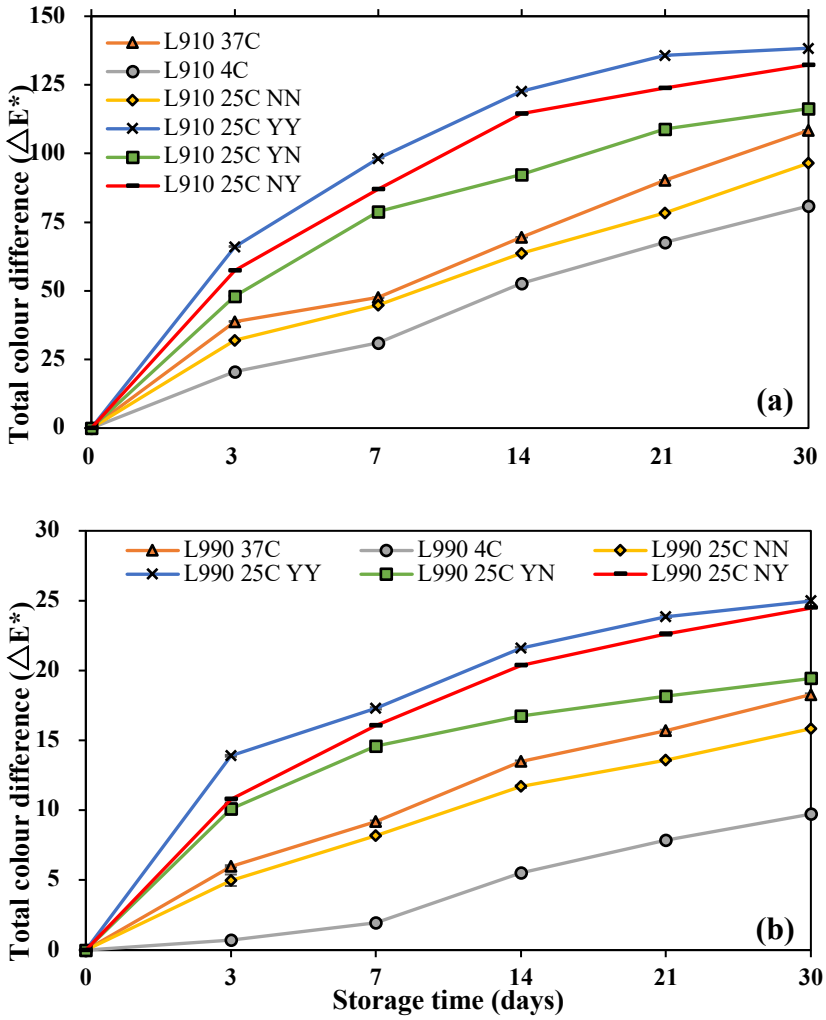

Figure 7.10 Total colour difference (∆E*) of L910 and L990 beta-carotene encapsulated Capmul 708G microemulsions during storage for 1 month at different environmental conditions. (a) L910 W/O microemulsion and (b) L990 O/W microemulsion. Data are presented as the mean and standard deviation of two independent measurements with duplicate (n = 4) and error bars mean standard deviation.

7.4.5 Stability of beta-carotene in L910 and L990 microemulsions during storage

Beta-carotene was extracted from L910 and L990 microemulsion samples which was then measured by UV-visible spectrophotometer to determine its concentration. Beta-carotene contents in L910 (W/O) and L990 (O/W) beta-carotene loaded microemulsions after preparation were 200.08 ± 0.85 and 31.33 ± 0.80 μg/ml, respectively. Blank samples, which were stored at the same conditions with L910 and

L990 loaded microemulsions, with 199 and 30 μg/ml of beta-carotene were prepared by dissolving beta-carotene into n-hexane solutions. The respective measured beta-carotene concentrations of these blank samples were 200.16 ± 0.20 and 31.21 ± 0.51 μg/ml. The stability of beta-carotene in microemulsions and related blank samples during storage was monitored by beta-carotene retention, which was calculated by (Ct/C0) x 100. In this equation, Ct means the content of beta-carotene during storage for a certain time period (t) and C0 represents the content of beta-carotene at initial stage.

Figure 7.11a shows that beta-carotene retention was the highest when L910 loaded microemulsion was stored at ambient temperature (25 °C) without exposed to oxygen and light (L910 25C NN). After storage for 1 month, 28% of beta-carotene was still retained in this microemulsion, which was significantly ($p < 0.05$) higher than that in the microemulsions stored at 25 °C but exposed to oxygen or light. When it was subjected to both oxygen and light at 25 °C (L910 25CYY), none beta-carotene remained in the microemulsion after 1-month storage and 2.9% beta-carotene was still in the microemulsion after three-week storage. It was shown in Figure 7.9 that L910 loaded microemulsion lost its yellow colour after 1-month storage at this storage condition. On the other hand, when it was stored at 4 °C without oxygen and light after 1 month, the microemulsion appeared to contain 38% of beta carotene (Figure 7.11b). When stored at higher temperature (37 °C) without oxygen and light, degradation of beta-carotene was faster than when stored at lower temperatures as expected. The results of beta-carotene content were in great agreement with the results from colour determination in Section 7.4.4 in this chapter. Moreover, L910 microemulsion provided protection to beta-carotene against oxidative degradation of samples under all experimental conditions examined. Because when beta-carotene was dissolved in n-hexane solution, its beta-carotene retention was very low after storage for 1 month at every experimental condition as shown in Figure 7.11. For blank samples, when n-

hexane solution containing 200.16 μg/ml beta-carotene was stored at 4 °C without oxygen and light, the retention percentage of beta-carotene was 27.3%, which was the highest among all the blank samples. Furthermore, when it was kept at 25 °C and exposed to both light and oxygen, beta-carotene was degraded almost completely after 3 weeks. According to Ariviani et al. (2015), degradation rate of beta-carotene in palm oil microemulsions containing Span 80, Span 40 and Tween 80 at a ratio of 10:5:85 which were stored at 4ºC did not have a significantly difference with those stored at 15ºC, but it was significantly smaller than those stored at 27 ºC.

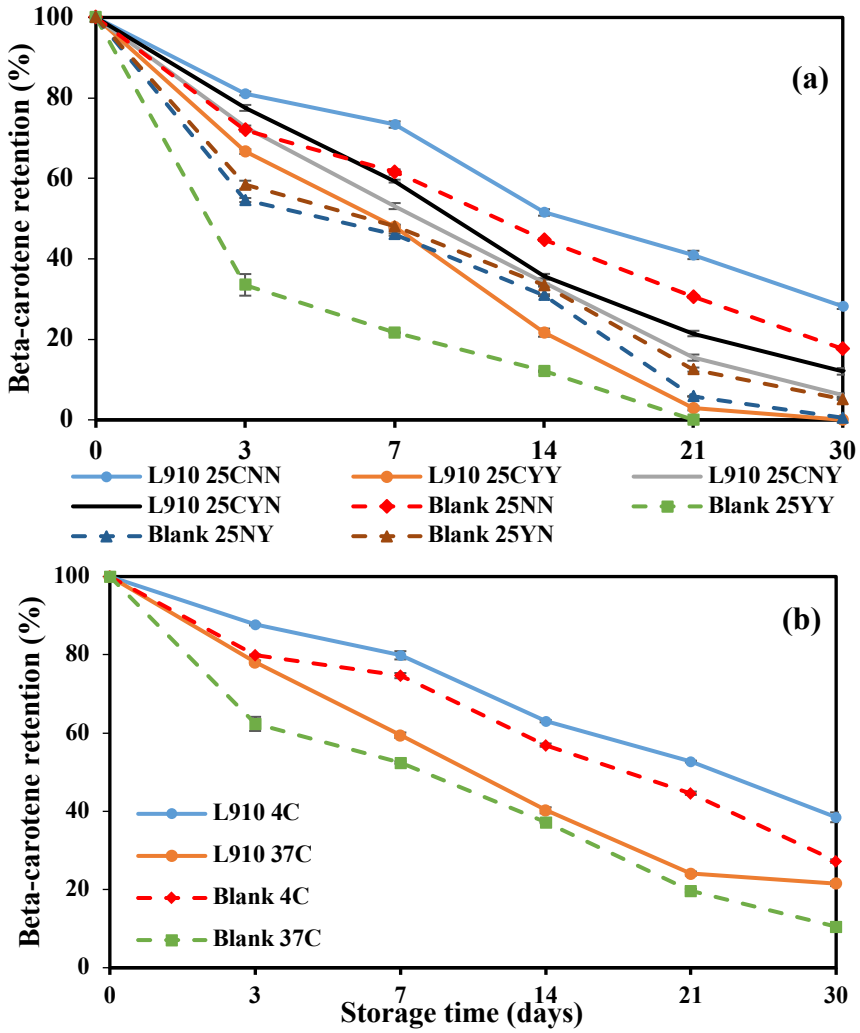

Figure 7.11 Stability of beta-carotene in L910 W/O microemulsions (full line) and related blank solutions (dotted line) during storage for 1 month at different environmental conditions. (a) at 25 °C and (b) at 4 and 37 °C. Data are presented as the mean and standard deviation of two independent measurements with duplicate (n = 4) and error bars mean standard deviation.

Figure 7.12 shows the retention of beta-carotene during storage for L990 loaded O/W microemulsion samples. The results were similar to the findings of L910 loaded W/O microemulsions. Specifically speaking, after storage for 1 month at 4 °C, the microemulsion which was not exposed to oxygen and light had the highest retention percentage of beta-carotene, which was 64.4%. The second highest retention percentage of beta-carotene was 45.6% when it was kept at 25 °C without oxygen and light. However, when the sample was placed in contact with oxygen and light, more than 70% beta-carotene was degraded only after 3 weeks and only 10% left after 1 month. Similar to the L910 W/O microemulsion system, L990 O/W microemulsion could also decrease the degradation rate of beta-carotene compared to the blank sample (beta-carotene dissolved in n-hexane solution). Apart from that, it should be mentioned that beta-carotene was degraded faster when it was subjected to light instead of oxygen in both L910 and L990 microemulsions, which was also in good agreement with the results of colour measurement shown in Section 7.4.4 in this chapter.

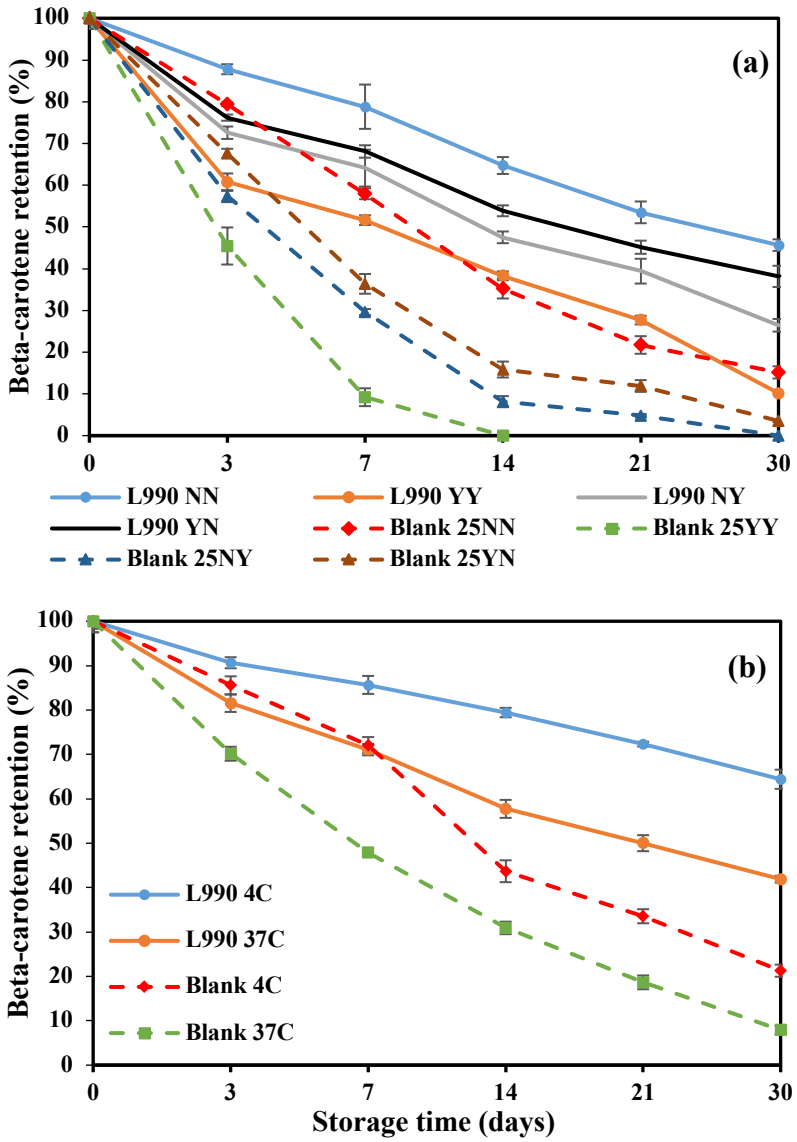

Figure 7.12 Stability of beta-carotene in L990 O/W microemulsions (full line) and related blank solution (dotted line) during storage for 1 month at different environmental conditions. (a) at 25 °C and (b) at 4 and 37 °C. Data are presented as the mean and standard deviation of two independent measurements with duplicate (n = 4) and error bars mean standard deviation.

Figure 7.13 shows that when beta-carotene was encapsulated by L990 O/W microemulsion system, it had significantly higher ($p < 0.05$) retention percentage after storage for 1 month compared to that incorporated by L910 W/O microemulsion system, regardless of storage conditions. L910 was a W/O microemulsion and oil was acted as the external phase, so it directly contacted with the environment. However, in L990 O/W microemulsion, oil droplets, which contained beta-carotene, dispersed in

the internal phase. In this case, beta-carotene was protected by external phase as well as the interface (Rozman and Gasperlin, 2007). Therefore, even though O/W microemulsion could incorporate more beta-carotene, it was not as efficient as O/W microemulsion in protecting the incorporated beta-carotene.

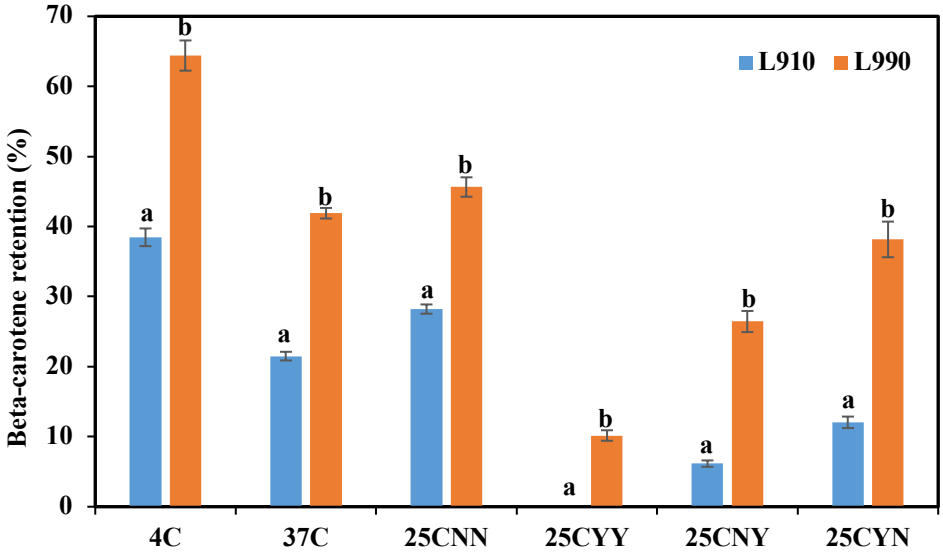

Figure 7.13 Retention of beta-carotene in L910 (W/O) and L990 (O/W) loaded microemulsions after storage for 1 month. Data are presented as the mean and standard deviation of two independent measurements with duplicate (n = 4) and error bars mean standard deviation. Data were analysed using one-way ANOVA with Tukey test. Different numbers represent a significant difference.

As described in Section 6.4.5 in Chapter 6, beta-carotene concertation alteration with the change in time was fitted into the first order kinetic equation (Equation 6.4 and 6.5) to obtain the degradation rate constant, half-life and coefficient of determination of beta-carotene degradation during storage (Table 7.5). It can be concluded that beta-carotene degradation was a typical first order kinetic since the coefficient of determination values (R^2) ranged from 0.8704 to 0.9989. When L990 beta-carotene loaded O/W microemulsion was stored at 4 °C without light and oxygen (4C NN), half-life of beta-carotene was the longest, which was 50.78 days. On the other hand, when it was stored at 25 °C and exposed to light and oxygen (25C YY), 50% of beta-

carotene was degraded after 11.14 days. As to L990 beta-carotene encapsulated O/W microemulsion, half of beta-carotene was degraded after 4.34 days if it was stored at 25 °C and subjected to both oxygen and light (25C YY), which was almost 4 times shorter than when it was kept at 4 °C without oxygen and light. Moreover, it can be also clearly seen that half-life of beta-carotene in L990, which was an O/W microemulsion, was longer than that in L910 which was a W/O microemulsion. This was in good agreement with the results shown in Figure 7.12.

Rozman and Gasperlin (2007) encapsulated Vitamin E and Vitamin C into both W/O microemulsion and O/W microemulsion system. The W/O microemulsion contained 10% water, 60% IPM, 15% Tween 40 and 15% Imwitor 308, while the O/W microemulsion was comprised of 45% water, 25% IPM, 15% Tween 40 and 15% Imwitor 308. They found both microemulsion could protect Vitamin E from UV light and oxygen degradation and O/W microemulsion had better protection ability than O/W microemulsion. Nevertheless, W/O microemulsion was found to protect Vitamin C, which was soluble in water, significantly better than O/W microemulsion (Rozman and Gasperlin, 2007).

Gallarate and co-workers fabricated an O/W microemulsion using 3.07% soy lecithin, 7.77% capryl glucoside, 1.85% ethanol, 6.63% IPP, 2.63% hexylene glycol, 0.5% alpha-tocopherol and 78% water. After 3 hours of irradiation by a UAB lamp, only 12% alpha-tocopherol degraded, compared to 88% if alpha-tocopherol was only dissolved in ethanol. In this O/W microemulsion, alpha-tocopherol was dispersed in the internal phase since it was soluble in oil, so it was protected by the interface (Gallarate et al., 2004).

Table 7.5 Degradation rate constant (k), half-life ($t_{1/2}$) and coefficient of determination (R^2) of beta-carotene degradation during storage in L910 (W/O) and L990 (O/W) beta-carotene loaded microemulsions as well as their blank controls when beta-carotene degradation was fitted into the first order kinetic equation. Data are presented as the mean and standard deviation of two independent measurements with duplicate (n = 4).

Sample	Storage condition	k (d^{-1})	R^2	$t_{1/2}$ (d)
L910 W/O microemulsion	4C NN	0.0310 ± 0.0009	0.9966 ± 0.0007	22.37 ± 0.66
	37C NN	0.0535 ± 0.0007	0.9564 ± 0.0101	12.96 ± 0.17
	25C NN	0.0411 ± 0.0002	0.9732 ± 0.0008	16.86 ± 0.09
	25C YY	0.1601 ± 0.0084	0.9362 ± 0.0052	4.34 ± 0.23
	25C NY	0.0910 ± 0.0015	0.9910 ± 0.0013	7.62 ± 0.12
	25C YN	0.0706 ± 0.0022	0.9989 ± 0.0007	9.83 ± 0.31
L990 O/W microemulsion	4C NN	0.0137 ± 0.0005	0.9716 ± 0.0287	50.78 ± 1.92
	37C NN	0.0436 ± 0.0052	0.9321 ± 0.0256	16.07 ± 2.15
	25C NN	0.0261 ± 0.0015	0.9763 ± 0.0091	26.64 ± 1.54
	25C YY	0.0622 ± 0.0015	0.8778 ± 0.0421	11.14 ± 0.26
	25C NY	0.0409 ± 0.0008	0.9672 ± 0.0079	16.97 ± 0.33
	25C YN	0.0302 ± 0.0013	0.9415 ± 0.0405	22.95 ± 0.97
L910 Blank	4C NN	0.0406 ± 0.0005	0.9853 ± 0.0008	17.06 ± 0.20
	37C NN	0.0710 ± 0.0006	0.9850 ± 0.0027	9.76 ± 0.08
	25C NN	0.0545 ± 0.0007	0.9906 ± 0.0032	12.72 ± 0.17
	25C YY	0.1377 ± 0.0033	0.8704 ± 0.0260	5.04 ± 0.12
	25C NY	0.1196 ± 0.0001	0.9072 ± 0.0017	5.80 ± 0.01
	25C YN	0.0945 ± 0.0009	0.9778 ± 0.0021	7.33 ± 0.07
L990 Blank	4C NN	0.0523 ± 0.0023	0.9934 ± 0.0020	13.28 ± 0.60
	37C NN	0.0808 ± 0.0044	0.9894 ± 0.0031	8.59 ± 0.46
	25C NN	0.0646 ± 0.0044	0.9867 ± 0.0049	10.76 ± 0.73
	25C YY	0.3476 ± 0.0418	0.9841 ± 0.0170	2.02 ± 0.24
	25C NY	0.1495 ± 0.0018	0.9726 ± 0.0210	4.64 ± 0.06
	25C YN	0.1068 ± 0.0035	0.9801 ± 0.0039	6.49 ± 0.21

Tween 80, ethanol, ethyl butyrate and water were introduced by Yan and Wang (2013) to fabricate a O/W microemulsion by the water titration method and beta-carotene was mixed with the oil phase, ethyl butyrate, to manufacture beta-carotene incorporated microemulsion. The authors found that degradation rate of beta-carotene in the O/W microemulsion was much lower than that in ethyl butyrate when the samples were

stored under light or high temperature. Besides, their experimental results illustrated that sunlight had a stronger effect on the degradation of beta-carotene than fluorescent lamp.

7.4.6 Comparison of beta-carotene stability in microemulsions fabricated by emulsion dilution method and water titration method

Figure 7.14 summarizes half-life of beta-carotene in L910 and L990 microemulsion samples which were fabricated by water titration method as well as in 0.1% and 0.4% lemon oil-in-water microemulsions which were fabricated by emulsion dilution method during storage under different storage conditions. It indicates that the longest half-life existed when L990 O/W microemulsion was stored at 4 °C and was away from oxygen and light. On the other hand, the shortest half-life appeared when 0.4% lemon oil-in-water encapsulated microemulsion was stored at 25 °C and exposed to both light and oxygen, which matches with the visual appearance of samples as shown in Figure 6.8 in Chapter 6 that this microemulsion did not contain yellow colour after 2 weeks. Half-life of beta-carotene in L990 O/W microemulsion was the longest compared to that in L910 W/O microemulsion and 0.4% microemulsion at all storage conditions.

The content of beta-carotene in L910, L990, 0.4% and 0.1% microemulsions was 200.6, 31.9, 62.0 and 15.4 μg/ml, respectively. Therefore, L910 could encapsulate the highest amount of beta-carotene, and it did not have a strong protection capability of beta-carotene against degradation. However, if beta-carotene was encapsulated in L990, it had the longest half-life. In other words, L990 might be the most efficient delivery system among all the microemulsions investigated in the present study.

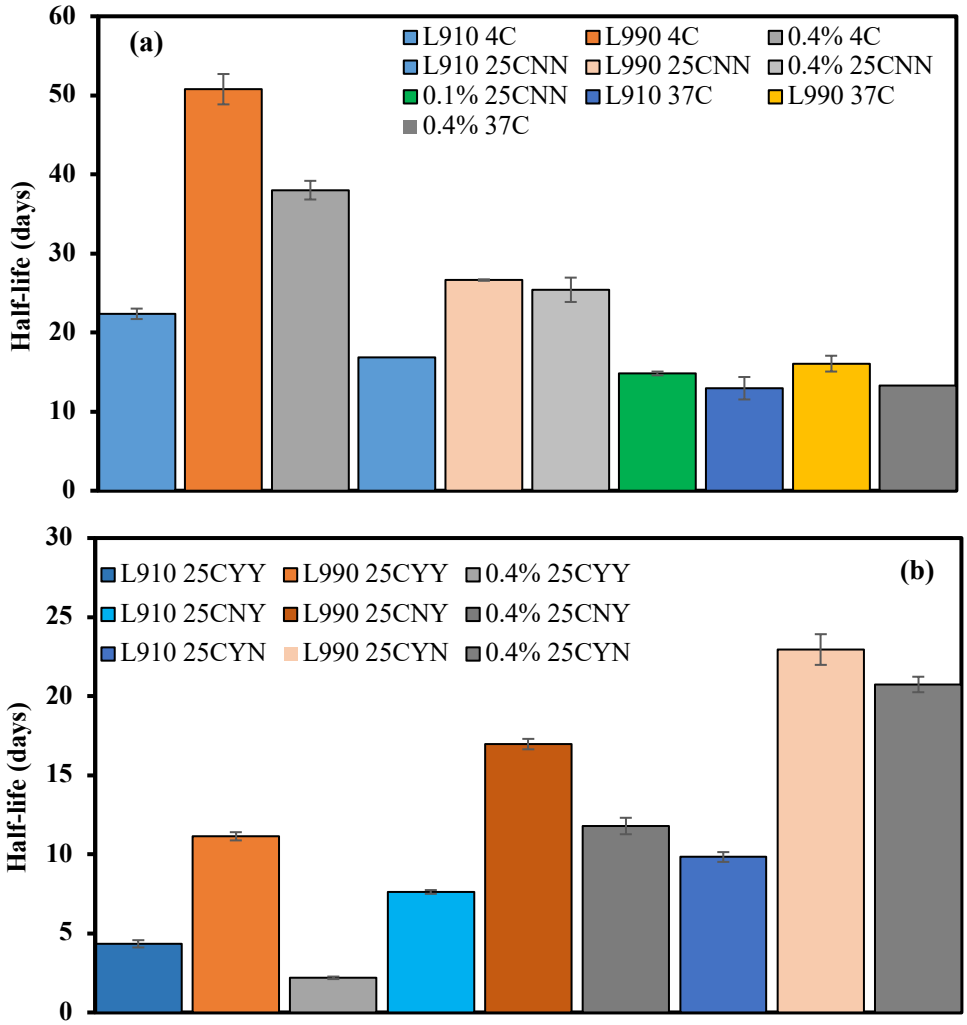

Figure 7.14 Half-life of beta-carotene in L910 W/O loaded microemulsion, L990 O/W microemulsion, 0.1% and 0.4% lemon oil-in-water loaded microemulsions stored at different environmental conditions. (a) storage at different temperatures (4, 25 and 37 °C) and (b) storage at 25 °C with exposure to oxygen and/or light.

7.5 Conclusions

This study focused on determining the effect of microemulsion encapsulation on the effect of environmental to show the advantage of microemulsion which was prepared by the water titration method. The ratio of PG to Milli-Q water was 1:1, and that of Tween 80 to Capmul 708G was 1:9. As a consequence, microemulsions L910 to L990 were prepared. The encapsulation of beta-carotene into these microemulsions did not significantly influence their conductivity and viscosity, but significantly increased

their particle size. Viscosity of these microemulsions decreased with an increase in the concentration of aqueous phase. Together with conductivity determination and dye staining test, it could be concluded L910 and L920 were W/O microemulsions, and L970, L980 and L990 were O/W microemulsions.

L910 and L990 were selected to study the effect of microemulsions on the stability of beta-carotene during storage under different environmental conditions. During storage, temperature, oxygen and light all influenced the degradation rate of beta-carotene. The degradation rate of beta-carotene increased with increasing temperature if other conditions were kept the same. On the other hand, when stored at ambient temperature (25 °C) and exposed to both oxygen and light, the degradation rate of beta-carotene was the fastest. L910 loaded O/W microemulsion lost its yellow-red colour after storage for 1 month under this condition. It was found in this study that the degradation rate of beta-carotene was higher when it was exposed to light compared to when exposed to oxygen. However, both L910 and L990 microemulsion systems could decrease the degradation rate of beta-carotene compared to beta-carotene in n-hexane solutions. Besides, when beta-carotene was encapsulated in L990 O/W microemulsions, its half-life was much longer than when it was loaded in L910 W/O microemulsion.

Overall, this study provides some useful information about the stability of beta-carotene in both W/O and O/W microemulsions during storage at different environmental conditions and about which storage condition and delivery system might be the most efficient in the protection of bioactive compounds.

Chapter 8 Overall Conclusions and Recommendations

In this research work, microemulsions containing small droplets were successfully fabricated by two different methods such as emulsion dilution method and water titration method. The results showed that when emulsion dilution method was used, microemulsions could not be fabricated with triglyceride oils (such as peanut oil and fractionated coconut oil) but could be produced by non-triglyceride oils (e.g. IPM and lemon oil). When a conventional emulsion prepared by emulsifying 10% oil phase into 1% Tween 80 emulsifier solution by high pressure homogenization was further diluted by 1% Tween 80 micelle solution, microemulsions could be fabricated only when the conventional emulsion was diluted to contain IPM less than 0.1% or lemon oil less than 0.2%. In terms of the effect of type of small molecule surfactants, compared to Tween 20, 40 and 60, Tween 80 had the strongest emulsifying properties when they were employed to dilute the conventional emulsion. Besides, different concentrations (0.5%, 1% and 2%) of Tween 80 micelle solutions were utilised to dilute the conventional emulsions, which showed that 2% Tween 80 solution could incorporate a larger amount of lemon oil.

The microemulsions with 0.1% and 0.4% lemon oil and macroemulsion with 1.5% lemon oil were then selected as a delivery system to encapsulate beta-carotene. Particle size of 0.1% and 0.4% lemon oil-in-water microemulsions were increased after the incorporation of beta-carotene while that of 1.5% lemon oil-in-water macroemulsion did not significantly change. The particle size of 0.1% and 0.4% lemon oil-in-water microemulsions was still within the size range of microemulsion and these two loaded microemulsions were also still clear in their visual appearance. These three different types of emulsions were then stored at different environmental conditions. For example, 0.1% and 1.5% lemon oi-in-water emulsions were stored at 25 °C without exposing to oxygen and light. Besides, 0.4% lemon oil-in-water microemulsions were exposed to three different temperatures (4, 25 and 37 °C). When the storage

temperature of 25 °C was applied to this microemulsion, the conditions of oxygen and light were controlled. When this sample was stored contacting with oxygen and light, the degradation rate of beta-carotene was the highest. On the other hand, when no oxygen and light were introduced during the storage of 0.4% lemon oil-in-water microemulsion, beta-carotene had the highest retention rate, but it was not as high as when the sample was stored at 4 °C and away from oxygen and light. Nevertheless, both 0.1% and 0.4% lemon oil microemulsions and 1.5% lemon oil macroemulsion could protect beta-carotene against oxidative degradation compared to the blank sample (i.e. beta-carotene in n-hexane solution).

While water titration method was employed to fabricate microemulsions, ternary or pseudo ternary phase diagrams were constructed to investigate the formation of microemulsion from a mixture system consisting of three or four components at different ratios. Every oil used in the study could somewhat fabricate microemulsions with surfactant, but the ternary phase diagrams created showed that Capmul 708G (glyceryl monocaprylate) was the most efficient in producing microemulsions, which was followed by Capmul MCM C8 (glyceryl mono-dicaprylate). Chemically, Capmul 708G is a monoglyceride, making it easily to penetrate the interfacial films. In terms of PG esters (Captex 100, Capmul PG-8, Capmul PG-12, Capmul PG-2L), Capmul PG-8 was the most efficient in terms of forming microemulsions. In addition, the incorporation of PG and/or absolute ethanol could assist in the formation of microemulsions. When a mixture system was comprised of Capmul 708G, Tween 80, water and PG (the ratio of water to PG was 1:1), every formulation in the ternary phase diagram led to the formation of microemulsions. As to surfactants, Span 80 with its HLB value of 4.3 was the least efficient in terms of fabricating microemulsions compared to Tween 20, Tween 80 and Kolliphor.

Encapsulation of beta-carotene was investigated using the mixture system made up of

Capmul 708G, Tween 80, water and PG (water : PG = 1:1) in which the ratio of Capmul 708G to Tween 80 was 9:1. The incorporation of beta-carotene did not significantly alter the conductivity and viscosity of the blank microemulsions, but it significantly enhanced the particle size of the blank microemulsions. L910 (W/O microemulsion) and L990 (O/W microemulsion) were then chosen to study the stability of beta-carotene in these two microemulsions under different storage conditions. The results showed that the degradation rate of beta-carotene increased as increasing storage temperature. When stored at 25 °C, retention of beta-carotene was the highest if the beta-carotene loaded microemulsion was not exposed to oxygen and light. However, it was found that beta-carotene was more susceptible to light than oxygen. Both L910 and L990 microemulsion samples could significantly reduce the degradation of beta-carotene during storage under all the investigated conditions compared to its control sample (beta-carotene in n-hexane solution). L990 O/W microemulsion system was shown to have a better protection against degradation than L910 W/O microemulsion system when encapsulating beta-carotene.

In summary, this research project has successfully fabricated beta-carotene encapsulated microemulsions by two different low energy emulsification methods: water titration method and emulsion dilution method. Water titration method is more effective in forming microemulsions than emulsion dilution method and it is much easier to conduct this method since it does not need a high pressure homogenizer. The microemulsions produced by both methods could substantially reduce the rate of beta-carotene degradation during storage under different environmental conditions. Beta-carotene loaded in L990 microemulsion had a half-life of almost 51 days if the sample was stored at 4 °C and away from oxygen and light. As a consequence, the next step of this study will be to incorporate the fabricated beta-carotene loaded microemulsions into liquid foods or beverages. Bioavailability of beta-carotene in these microemulsions will be studied *in vitro* and *in vivo* to find out the amount of beta-

carotene that can be absorbed by human body. In addition, i*n vitro* and *in vivo* investigation to determine the toxicity of the present fabricated beta-carotene loaded microemulsions is required to ensure the safety of these microemulsions.

References

Aboudzadeh, M. A., E. Mehravar, M. Fernandez, L. Lezama, and R. Tomovska. 2018. Low-energy encapsulation of alpha-tocopherol using fully food grade oil-in-water microemulsions. Acs Omega 3(9):10999-11008.

Acevedo-Fani, A., L. Salvia-Trujillo, M. A. Rojas-Grau, and O. Martin-Belloso. 2015. Edible films from essential-oil-loaded nanoemulsions: Physicochemical characterization and antimicrobial properties. Food Hydrocolloids 47:168-177.

Acharya, D. P. and P. G. Hartley. 2012. Progress in microemulsion characterization. Current Opinion in Colloid & Interface Science 17(5):274-280.

Al-Malah, K. I., H. Mousa, and E. B. Hani. 2011. Effect of electrolytes on formulation and stability of water/di-ethyl oxalate/tween microemulsions. Journal of Dispersion Science and Technology 32(5):749-754.

Alany, R. G., T. Rades, S. Agatonovic-Kustrin, N. M. Davies, and I. G. Tucker. 2000. Effects of alcohols and diols on the phase behaviour of quaternary systems. International Journal of Pharmaceutics 196(2):141-145.

Alarcon de la Lastra, C. and I. Villegas. 2005. Resveratrol as an anti-inflammatory and anti-aging agent: mechanisms and clinical implications. Molecular Nutrition and Food Research 49(5):405-430.

Alexander, K. S., A. T. Riga, and P. J. Haines. 2019. Thermoanalytical instrumentation and applications. in Ewing's analytical instrumentation handbook. Fourth edition ed. N. Grinberg, S. Rodriguez, and G. W. Ewing, ed. CRC Press, Taylor & Francis Group.

Amar, I., A. Aserin, and N. Garti. 2004. Microstructure transitions derived from solubilization of lutein and lutein esters in food microemulsions. Colloids and Surfaces B-Biointerfaces 33(3-4):143-150.

Anoopinder, K., T. Purva, S. Shikha, and S. Bharti. 2016. Green tea extract in microemulsion: Stability, dermal sensitization and efficacy against uv induced damages. International Journal of Pharmacy and Pharmaceutical Sciences 8(13).

Anton, N., P. Gayet, J.-P. Benoit, and P. Saulnier. 2007. Nano-emulsions and nanocapsules by the PIT method: An investigation on the role of the temperature cycling on the emulsion phase inversion. International Journal of Pharmaceutics 344(1-2):44-52.

Anton, N. and T. F. Vandamme. 2011. Nano-emulsions and Micro-emulsions: Clarifications of the Critical Differences. Pharmaceutical Research 28(5):978-985.

Arab, L. and S. Steck. 2000. Lycopene and cardiovascular disease. American Journal of Clinical Nutrition 71(6):1691S-1695S.

Araujo, E. A., F. D. S. Curbelo, A. I. C. Garnica, R. P. F. Sousa, E. A. Araujo, G. S. Braga, and J. C. O. Freitas. 2018. Rheological properties of brine/vegetable oil/polyethoxylated nonionic surfactants based microemulsion. Holos 34(2):16-25.

Ariviani, S., S. Anggrahini, S. Naruki, and S. Raharjo. 2015. Characterization and chemical stability evaluation of beta-carotene microemulsions prepared by spontaneous emulsification method using VCO and palm oil as oil phase. International Food Research Journal 22(6):2432-2439.

Artiga-Artigas, M., A. Molet-Rodriguez, L. Salvia-Trujillo, and O. Martin-Belloso. 2019. Formation of double (w-1/o/w-2) emulsions as carriers of hydrophilic and lipophilic active compounds. Food and Bioprocess Technology 12(3):422-435.

Badiu, D. and R. Luque. 2010. Vitamin ddeficiency and its health consequences. in Vitamin D : Biochemistry, Nutrition and Roles. W. J. Stackhouse, ed. Nova Science Publishers, Inc, Hauppauge, N.Y.

Barradas, T. N., V. E. Bucco de Campos, J. P. Senna, C. d. S. Cerqueira Coutinho, B. S. Tebaldi, K. G. de Holanda e Silva, and C. R. Elias Mansur. 2015. Development and characterization of promising o/w nanoemulsions containing sweet fennel essential oil and non-ionic sufactants. Colloids and Surfaces a-Physicochemical and Engineering Aspects 480:214-221.

Basheer, H. S., M. I. Noordin, and M. M. Ghareeb. 2013. Characterization of microemulsions prepared using isopropyl palmitate with various surfactants and cosurfactants. Tropical Journal of Pharmaceutical Research 12(3):305-310.

Basu, A. and V. Imrhan. 2007. Tomatoes versus lycopene in oxidative stress and carcinogenesis: conclusions from clinical trials. European Journal of Clinical Nutrition 61(3):295-303.

Bayrak, O., E. Uz, R. Bayrak, F. Turgut, A. F. Atmaca, S. Sahin, M. E. Yildirim, A. Kaya, E. Cimentepe, and A. Akcay. 2008. Curcumin protects against ischemia/reperfusion injury in rat kidneys. World Journal of Urology 26(3):285-291.

Belkoura, L., C. Stubenrauch, and R. Strey. 2004. Freeze fracture direct imaging: A new freeze fracture method for specimen preparation in cryo-transmission electron microscopy. Langmuir 20(11):4391-4399.

Belluzzi, A. 2002. n-3 Fatty acids for the treatment of inflammatory bowel diseases. Proceedings of the Nutrition Society 61(3):391-395.

Benichou, A., A. Aserin, and N. Garti. 2007. W/O/W double emulsions stabilized with WPI-polysaccharide complexes. Colloids and Surfaces a-Physicochemical and Engineering Aspects 294(1-3):20-32.

Bergenstahl, B. and K. Fontell. 1983. Phase-equilibria in the system soybean lecithin water. Progress in Colloid and Polymer Science 68:48-52.

Bergonzi, M. C., R. Hamdouch, F. Mazzacuva, B. Isacchi, and A. R. Bilia. 2014. Optimization, characterization and in vitro evaluation of curcumin microemulsions. Lwt-Food Science and Technology 59(1):148-155.

Bhushani, J. A., P. Karthik, and C. Anandharamakrishnan. 2016. Nanoemulsion based delivery system for improved bioaccessibility and Caco-2 cell monolayer permeability of green tea catechins. Food Hydrocolloids 56:372-382.

Bilia, A. R., B. Isacchi, C. Righeschi, C. Guccione, C. Maria, and M. Bergonzi. 2014. Flavonoids loaded in nanocarriers: An opportunity to increase oral bioavailability and bioefficacy. Vol. 05.

Boon, C. S., D. J. McClements, J. Weiss, and E. A. Decker. 2010. Factors Influencing the Chemical Stability of Carotenoids in Foods. Critical Reviews in Food Science and Nutrition 50(6):515-532.

Boonme, P., K. Krauel, A. Graf, T. Rades, and V. B. Junyaprasert. 2006. Characterization of

microemulsion structures in the pseudoternary phase diagram of isopropyl palmitate/water/Brij 97 : 1-butanol. Aaps Pharmscitech 7(2).
Borel, P., P. Grolier, M. Armand, A. Partier, H. Lafont, D. Lairon, and V. AzaisBraesco. 1996. Carotenoids in biological emulsions: Solubility, surface-to-core distribution, and release from lipid droplets. Journal of Lipid Research 37(2):250-261.
Burauer, S., L. Belkoura, C. Stubenrauch, and R. Strey. 2003. Bicontinuous microemulsions revisited: a new approach to freeze fracture electron microscopy (FFEM). Colloids and Surfaces a-Physicochemical and Engineering Aspects 228(1-3):159-170.
Burri, B. J. 1997. Beta-carotene and human health: A review of current research. Nutrition Research 17(3):547-580.
Calder, P. C. 2004. n-3 fatty acids and cardiovascular disease: evidence explained and mechanisms explored. Clinical Science 107(1):1-11.
Calder, P. C. 2008a. Polyunsaturated fatty acids, inflammatory processes and inflammatory bowel diseases. Molecular Nutrition & Food Research 52(8):885-897.
Calder, P. C. 2008b. PUFA, inflammatory processes and rheumatoid arthritis. Proceedings of the Nutrition Society 67(4):409-418.
Calder, P. C. 2013. Food enrichment with omega-3 fatty acids. Woodhead Publishing Limited, UK.
Calligaris, S., L. Manzocco, F. Valoppi, P. Comuzzo, and M. C. Nicoli. 2019. Microemulsions as delivery systems of lemon oil and beta-carotene into beverages: stability test under different light conditions. Journal of the science of food and agriculture.
Calligaris, S., F. Valoppi, L. Barba, L. Pizzale, M. Anese, L. Conte, and M. C. Nicoli. 2017. Development of transparent curcumin loaded microemulsions by phase inversion temperature (pit) method: Effect of lipid type and physical state on curcumin stability. Food Biophysics 12(1):45-51.
Chai, J. L., N. Liu, T. T. Bai, H. M. Zhang, N. N. Liu, and D. Wang. 2014. Compositions and physicochemical properties of tween type surfactants-based microemulsions. Journal of Dispersion Science and Technology 35(3):441-447.
Chan, M. M.-Y., H.-I. Huang, M. R. Fenton, and D. Fong. 1998. In vivo inhibition of nitric oxide synthase gene expression by curcumin, a cancer preventive natural product with anti-inflammatory properties. Biochemical Pharmacology 55(12):1955-1962.
Chantrapornchai, W., F. Clydesdale, and D. J. McClements. 1998. Influence of droplet size and concentration on the color of oil-in-water emulsions. Journal of Agricultural and Food Chemistry 46(8):2914-2920.
Chatzidaki, M. D., E. Mitsou, A. Yaghmur, A. Xenakis, and V. Papadimitriou. 2015. Formulation and characterization of food-grade microemulsions as carriers of natural phenolic antioxidants. Colloids and Surfaces a-Physicochemical and Engineering Aspects 483:130-136.
Chauhan, L., P. Thakur, and S. Sharma. 2019. Microemulsions: New vista in novel drug delivery system. Innovations in Pharmaceuticals and Pharmacotherapy 7(2):37-44.
Chee, C. P., D. Djordjevic, H. Faraji, E. A. Decker, R. Hollender, D. J. McClements, D. G. Peterson, R. F. Roberts, and J. N. Coupland. 2007. Sensory properties of vanilla and strawberry flavored Ice cream supplemented with omega-3 fatty acids. Milchwissenschaft-Milk Science

International 62(1):66-69.
Chen, B., M. Hou, B. Zhang, T. Liu, Y. Guo, L. Dang, and Z. Wang. 2017. Enhancement of the solubility and antioxidant capacity of alpha-linolenic acid using an oil in water microemulsion. Food & Function 8(8):2792-2802.
Chen, C. C. and G. Wagner. 2004. Vitamin E nanoparticle for beverage applications. Chemical Engineering Research & Design 82(A11):1432-1437.
Chen, H. Q., Y. G. Guan, and Q. Zhong. 2015. Microemulsions based on a sunflower lecithin-tween 20 blend have high capacity for dissolving peppermint oil and stabilizing coenzyme q(10). Journal of Agricultural and Food Chemistry 63(3):983-989.
Chen, H. Q. and Q. X. Zhong. 2015. Thermal and UV stability of beta-carotene dissolved in peppermint oil microemulsified by sunflower lecithin and Tween 20 blend. Food Chemistry 174:630-636.
Chen, S., J. K. Xuma, Y. B. Zhang, X. B. Yang, L. L. Chen, and Y. F. Wang. 2014. Construction of a microemulsion system and the antibacterial performance of peppermint essential oil. Vol. 30.
Chen, X. W., Y. J. Chen, J. M. Wang, J. Guo, S. W. Yin, and X. Q. Yang. 2016. Phytosterol structured algae oil nanoemulsions and powders: improving antioxidant and flavor properties. Food & Function 7(9):3694-3702.
Chen, Y., T. X. Shou, Q. Y. Zhang, and D. Li. 2013. Bioavailability of diacylglycerol microemulsion. Journal of Food Biochemistry 37(2):144-150.
Cheng, P., D. Svirskis, S. J. Lee, I. Oey, H.-S. Kwak, G. Chen, C. Bunt, and J. Wen. 2017. Design of microemulsion system suitable for the oral delivery of poorly aqueous soluble beta carotene. Pharmaceutical development and technology:1-17.
Cho, H. T., L. Salvia-Trujillo, J. Kim, Y. Park, H. Xiao, and D. McClements. 2014. Droplet size and composition of nutraceutical nanoemulsions influences bioavailability of long chain fatty acids and Coenzyme Q10. Food Chemistry 156:117-122.
Chouhan, P. and T. R. Saini. 2016. D-optimal design and development of microemulsion based transungual drug delivery formulation of ciclopirox olamine for treatment of onychomycosis. Indian Journal of Pharmaceutical Sciences 78(4):498-511.
Combs, G. F. 2012. The Vitamins. Vol. 4th ed. Academic Press, London.
Cui, S. X., S. F. Nie, L. Li, C. G. Wang, W. S. Pan, and J. P. Sun. 2009. Preparation and Evaluation of Self-Microemulsifying Drug Delivery System Containing Vinpocetine. Drug Development and Industrial Pharmacy 35(5):603-611.
Damodaran, S. 2007. Amino acids, peptides and proteins. Pages 219-323 in Fennema's Food Chemistry, Fourth Edition. K. L. Parkin, S. Damodaran, and O. R. Fennema, ed. CRC Press, Bosa Roca, United States.
Dar, A. H., N. Rashid, I. Majid, S. Hussain, and M. A. Dar. 2019. Nanotechnology interventions in aquaculture and seafood preservation. Critical reviews in food science and nutrition:1-10.
de Campo, L., A. Yaghmur, N. Garti, M. E. Leser, B. Folmer, and O. Glatter. 2004. Five-component food-grade microemulsions: structural characterization by SANS. Journal of Colloid and Interface Science 274(1):251-267.

Delmas, D., V. Aires, E. Limagne, P. Dutartre, F. Mazue, F. Ghiringhelli, and N. Latruffe. 2011. Transport, stability, and biological activity of resveratrol. Pages 48-59 in Resveratrol and Health. Vol. 1215. O. Vang and D. K. Das, ed.

Deng, L. L., F. Que, H. W. Wei, G. W. Xu, X. W. Dong, and H. Zhang. 2015. Solubilization of tea seed oil in a food-grade water-dilutable microemulsion. Plos One 10(5).

Deng, L. L., M. Taxipalati, F. Que, and H. Zhang. 2016. Physical characterization and antioxidant activity of thymol solubilized Tween 80 micelles. Scientific Reports 6.

Deutch-Kolevzon, R., A. Aserin, and N. Garti. 2011. Synergistic cosolubilization of omega-3 fatty acid esters and CoQ(10) in dilutable microemulsions. Chemistry and Physics of Lipids 164(7):654-663.

Dolai, S., W. Shi, C. Corbo, C. Sun, S. Averick, D. Obeysekera, M. Farid, A. Alonso, P. Banerjee, and K. Raja. 2011. "Clicked" sugar–curcumin conjugate: Modulator of amyloid-β and tau peptide aggregation at ultralow concentrations. ACS Chemical Neuroscience 2(12):694-699.

Dong, X., Q. Zhu, Y. Q. Dai, J. F. He, H. Y. Pan, J. Chen, and Z. P. Zheng. 2016. Encapsulation artocarpanone and ascorbic acid in O/W microemulsions: Preparation, characterization, and antibrowning effects in apple juice. Food Chemistry 192:1033-1040.

Edris, A. E. and C. F. R. Malone. 2012. Preferential solubilization behaviours and stability of some phenolic-bearing essential oils formulated in different microemulsion systems. International Journal of Cosmetic Science 34(5):441-450.

European Food Safety, A. 2009. Danacol and blood cholesterol Scientific substantiation of a health claim related to a low fat fermented milk product (Danacol) enriched with plant sterols/stanols and lowering/reducing blood cholesterol and reduced risk of (coronary) heart disease pursuant to Article 14 of Regulation (EC) No 1924/2006. EFSA Journal 7(7):1177-Article 1177.

Ezrahi, S., E. Wachtel, A. Aserin, and N. Garti. 1997. Structural polymorphism in a four-component nonionic microemulsion. Journal of Colloid and Interface Science 191(2):277-290.

Fanun, M. 2007. Conductivity, viscosity, NMR and diclofenac solubilization capacity studies of mixed nonionic surfactants microemulsions. Journal of Molecular Liquids 135(1-3):5-13.

Fanun, M. 2008. A study of the properties of mixed nonionic surfactants microemulsions by NMR, SAXS, viscosity and conductivity. Journal of Molecular Liquids 142(1-3):103-110.

Fanun, M. 2009. Microemulsions formation on water/nonionic surfactant/peppermint oil mixtures. Journal of Dispersion Science and Technology 30(3):399-405.

Fanun, M. 2010. Properties of microemulsions with mixed nonionic surfactants and citrus oil. Colloids and Surfaces a-Physicochemical and Engineering Aspects 369(1-3):246-252.

Fanun, M., E. Wachtel, B. Antalek, A. Aserin, and N. Garti. 2001. A study of the microstructure of four-component sucrose ester microemulsions by SAXS and NMR. Colloids and Surfaces a-Physicochemical and Engineering Aspects 180(1-2):173-186.

Fasolin, L. H., R. C. Santana, and R. L. Cunha. 2012. Microemulsions and liquid crystalline formulated with triacylglycerols: Effect of ethanol and oil unsaturation. Colloids and Surfaces a-Physicochemical and Engineering Aspects 415:31-40.

Feitosa, E., V. R. O. Cavalcante, and L. Q. Amaral. 2009. Phase behavior of the orange

essential oil/sodium bis(2-ethylhexyl)sulfosuccinate/water system. Colloids and Surfaces a-Physicochemical and Engineering Aspects 348(1-3):82-86.
Feng, F. Q., H. Zhang, S. Sha, Z. H. Lu, Y. Shen, and X. D. Zheng. 2009a. Characterization and antimicrobial evaluation of dilution-stable microemulsions against stenotrophomonas maltrophilia. Journal of Dispersion Science and Technology 30(4):503-509.
Feng, J. L., Z. W. Wang, J. Zhang, Z. N. Wang, and F. Liu. 2009b. Study on food-grade vitamin E microemulsions based on nonionic emulsifiers. Colloids and Surfaces a-Physicochemical and Engineering Aspects 339(1-3):1-6.
Fernandez, P., V. Andre, J. Rieger, and A. Kuhnle. 2004. Nano-emulsion formation by emulsion phase inversion. Colloids and Surfaces a-Physicochemical and Engineering Aspects 251(1-3):53-58.
Filip, V., M. Plockova, J. Smidrkal, Z. Spickova, K. Melzoch, and S. Schmidt. 2003. Resveratrol and its antioxidant and antimicrobial effectiveness. Food Chemistry 83(4):585-593.
Flanagan, J., K. Kortegaard, D. N. Pinder, T. Rades, and H. Singh. 2006. Solubilisation of soybean oil in microemulsions using various surfactants. Food Hydrocolloids 20(2-3):253-260.
Flanagan, J. and H. Singh. 2006. Microemulsions: A potential delivery system for bioactives in food. Critical Reviews in Food Science and Nutrition 46(3):221-237.
Folmer, B. M., D. Barron, E. Hughes, L. Miguet, B. Sanchez, O. Heudi, M. Rouvet, L. Sagalowicz, P. Callier, M. Michel, and G. Williamson. 2009. Monocomponent hexa- and dodecaethylene glycol succinyl-tocopherol esters: Self-assembly structures, cellular uptake and sensitivity to enzyme hydrolysis. Biochemical Pharmacology 78(12):1464-1474.
Frederiksen, C. S., V. K. Haugaard, L. Poll, and E. M. Becker. 2003. Light-induced quality changes in plain yoghurt packed in polylactate and polystyrene. European Food Research and Technology 217(1):61-69.
Freiberger, N., C. Moitzi, L. de Campo, and O. Glatter. 2007. An attempt to detect bicontinuity from SANS data. Journal of Colloid and Interface Science 312(1):59-67.
Friberg, S. E., K. Larsson, and J. Sjoblom. 2004. Food emulsions. 4th ed. Marcel Dekker, NY, USA.
Fu, X. W., B. Huang, and F. Q. Feng. 2008. Shelf life of fresh noodles as affected by the food grade monolaurin microemulsion system. Journal of Food Process Engineering 31(5):619-627.
Fu, X. W., M. Z. Zhang, B. Huang, J. Liu, H. J. Hu, and F. Q. Feng. 2009. Enhancement of antimicrobial activities by the food-grade monolaurin microemulsion system. Journal of Food Process Engineering 32(1):104-111.
Gallarate, M., M. E. Carlotti, M. Trotta, and E. Ugazio. 2004. Disperse systems as topical formulations containing alpha-tocopherol. Journal of Drug Delivery Science and Technology 14(6):471-477.
Galooyak, S. S. and B. Dabir. 2015. Three-factor response surface optimization of nano-emulsion formation using a microfluidizer. Journal of Food Science and Technology-Mysore 52(5):2558-2571.
Garti, N., I. Amar, A. Yaghmur, A. Spernath, and A. Aserin. 2003. Interfacial modification and

structural transitions induced by guest molecules solubilized in U-type nonionic microemulsions. Journal of Dispersion Science and Technology 24(3-4):397-410.
Garti, N., A. Aserin, S. Ezrahi, and E. Wachtel. 1995. Water solubilization and chain length compatibility in nonionic microemulsions. Journal of Colloid and Interface Science 169(2):428-436.
Garti, N., M. Avrahami, and A. Aserin. 2006. Improved solubilization of Celecoxib in U-type nonionic microemulsions and their structural transitions with progressive aqueous dilution. Journal of Colloid and Interface Science 299(1):352-365.
Garti, N., M. Shevachman, and A. Shani. 2004. Solubilization of lycopene in jojoba oil microemulsion. Journal of the American Oil Chemists Society 81(9):873-877.
Garti, N., A. Yaghmur, M. E. Leser, V. Clement, and H. J. Watzke. 2001. Improved oil solubilization in oil/water food grade microemulsions in the presence of polyols and ethanol. Journal of Agricultural and Food Chemistry 49(5):2552-2562.
Glatter, O., D. Orthaber, A. Stradner, G. Scherf, M. Fanun, N. Garti, V. Clement, and M. E. Leser. 2001. Sugar-ester nonionic microemulsion: Structural characterization. Journal of Colloid and Interface Science 241(1):215-225.
Gomes, A., G. D. Furtado, and R. L. Cunha. 2019. Bioaccessibility of lipophilic compounds vehiculated in emulsions: Choice of lipids and emulsifiers. Journal of Agricultural and Food Chemistry 67(1):13-18.
Graca, M., J. H. H. Bongaerts, J. R. Stokes, and S. Granick. 2007. Friction and adsorption of aqueous polyoxyethylene (Tween) surfactants at hydrophobic surfaces. Journal of Colloid and Interface Science 315(2):662-670.
Gradzielski, M. 1998. Effect of the cosurfactant structure on the bending elasticity in nonionic oil-in-water microemulsions. Langmuir 14(21):6037-6044.
Griffin, W. C. 1946. Classification of surface-active agents by "HLB". Journal Of The Society Of Cosmetic Chemists 1:311–326.
Grynberg, A. 2005. Hypertension prevention: from nutrients to (fortified) foods to dietary patterns. Focus on fatty acids. Journal of Human Hypertension 19:S25-S33.
Gu, L. P., C. Pan, Y. J. Su, R. J. Zhang, H. Xiao, D. J. McClements, and Y. J. Yang. 2018. In vitro bioavailability, cellular antioxidant activity, and cytotoxicity of beta-carotene-loaded emulsions stabilized by catechin-egg white protein conjugates. Journal of Agricultural and Food Chemistry 66(7):1649-1657.
Gulik-Krzywicki, T. 1997. Freeze-fracture transmission electron microscopy. Current Opinion in Colloid & Interface Science 2(2):137-144.
Gulikkrzywicki, T. and K. Larsson. 1984. An electron-microscopy study of the l2-phase (microemulsion) in a ternary-system - triglyceride monoglyceride water. Chemistry and Physics of Lipids 35(2):127-132.
Gulotta, A., A. H. Saberi, M. C. Nicoli, and D. J. McClements. 2014. Nanoemulsion-based delivery systems for polyunsaturated (omega-3) oils: Formation using a spontaneous emulsification method. Journal of Agricultural and Food Chemistry 62(7):1720-1725.
Guo, J., L. Zhang, Y. Wang, T. Liu, and X. Gu. 2019a. Microstructural transitions in beta-carotene loaded nonionic microemulsions upon aqueous phase dilution. Colloids and Surfaces

a-Physicochemical and Engineering Aspects 567:288-296.
Guo, R. X., X. Fu, J. Chen, L. Zhou, and G. Chen. 2016. Preparation and characterization of microemulsions of myricetin for improving its antiproliferative and antioxidative activities and oral bioavailability. Journal of Agricultural and Food Chemistry 64(32):6286-6294.
Guo, Y. L., X. Y. Mao, J. Zhang, P. Sun, H. Y. Wang, Y. Zhang, Y. J. Ma, S. Xu, R. J. Lv, and X. P. Liu. 2019b. Oral delivery of lycopene-loaded microemulsion for brain-targeting: preparation, characterization, pharmacokinetic evaluation and tissue distribution. Drug Delivery 26(1):1191-1205.
Gurak, P. D., A. Z. Mercadante, M. L. Gonzalez-Miret, F. J. Heredia, and A. J. Melendez-Marinez. 2014. Changes in antioxidant capacity and colour associated with the formation of beta-carotene epoxides and oxidative cleavage derivatives. Food Chemistry 147:160-169.
Guttoff, M., A. H. Saberi, and D. J. McClements. 2015. Formation of vitamin D nanoemulsion-based delivery systems by spontaneous emulsification: Factors affecting particle size and stability. Food Chemistry 171:117-122.
Hamed, S. F., Z. Sadek, and A. Edris. 2012. Antioxidant and Antimicrobial Activities of Clove Bud Essential Oil and Eugenol Nanoparticles in Alcohol-Free Microemulsion. Journal of Oleo Science 61(11):641-648.
Hanh, N. D., A. Mitrevej, K. Sathirakul, P. Peungvicha, and N. Sinchaipanid. 2015. Development of phyllanthin-loaded self-microemulsifying drug delivery system for oral bioavailability enhancement. Drug Development and Industrial Pharmacy 41(2):207-217.
Hao, J. C., H. Q. Wang, S. Shi, R. H. Lu, T. T. Wang, G. Z. Li, and H. Y. Sun. 1997. Phase behaviour and microstructures of microemulsions .1. Science in China Series B-Chemistry 40(3):225-235.
Hasenhuettl, G. L. and R. W. Hartel. 2008. Food emulsifiers and their applications. Springer, New York, USA.
Hategekimana, J., M. V. M. Chamba, C. F. Shoemaker, H. Majeed, and F. Zhong. 2015. Vitamin E nanoemulsions by emulsion phase inversion: Effect of environmental stress and long-term storage on stability and degradation in different carrier oil types. Colloids and Surfaces a-Physicochemical and Engineering Aspects 483:70-80.
He, C.-X., Z.-G. He, and J.-Q. Gao. 2010. Microemulsions as drug delivery systems to improve the solubility and the bioavailability of poorly water-soluble drugs. Expert Opinion on Drug Delivery 7(4):445-460.
Henry, L. K., N. L. Puspitasari-Nienaber, M. Jaren-Galan, R. B. van Breemen, G. L. Catignani, and S. J. Schwartz. 2000. Effects of ozone and oxygen on the degradation of carotenoids in an aqueous model system. Journal of Agricultural and Food Chemistry 48(10):5008-5013.
Higdon, J. V. and B. Frei. 2003. Tea catechins and polyphenols: Health effects, metabolism, and antioxidant functions. Critical Reviews in Food Science and Nutrition 43(1):89-143.
Ho, M. J., S. H. Im, H. T. Jeong, H. T. Kim, J. E. Lee, D. H. Won, S. W. Jang, and M. J. Kang. 2019. Preparation and in vivo pharmacokinetic evaluation of stable microemulsion system of cholecalciferol. Journal of Dispersion Science and Technology.
Horrocks, L. A. and Y. K. Yeo. 1999. Health benefits of docosahexaenoic acid (DHA). Pharmacological Research 40(3):211-225.

Hu, J., X. Zhang, Z. Wang, and J. Mei. 2011. Vitamin E : Nutrition, Side Effects, And Supplements. in Vitamin E : Nutrition, Side Effects, and Supplements. A. E. Lindberg, ed. Nova Science Publishers, Inc, New York.

Hu, L., Y. Jia, F. Niu, Z. Jia, Y. Xun, and K. Jiao. 2012. Preparation and enhancement of oral bioavailability of curcumin using microemulsions vehicle. Journal of Agricultural and Food Chemistry 60(29):7137-7141.

Hu, S. Y., J. X. Chen, Y. T. Zhu, Y. L. Wei, T. T. Di, and H. Y. Shen. 2019. Preparation of Stable Microemulsions with Different Droplet Size. American Journal of Nanosciences 5(4):76-82.

Huang, Q. R., H. L. Yu, and Q. M. Ru. 2010. Bioavailability and Delivery of Nutraceuticals Using Nanotechnology. Journal of Food Science 75(1):R50-R57.

Jesse, F. and I. Gregory. 2017. Vitamins. Pages 545-625 in Fennema's Food Chemistry. 5 ed. S. Damodaran and K. L. Parkin, ed. Taylor & Francis Group, London, UNITED KINGDOM.

Johnson, K. A. and D. O. Shah. 1985. Effect of oil chain-length and electrolytes on water solubilization in alcohol-free pharmaceutical microemulsions. Journal of Colloid and Interface Science 107(1):269-271.

Jones, L. 1990. Individual oils: Cotton, Peanut, Corn, Safflower. Pages 299-373 in Edible Fats and Oils Processing: Basic Principles and Modern Practices : World Conference Proceedings. D. R. Erickson, ed. American Oil Chemists' Society.

Joy, D. C. 2019. Scanning electron microscopy: Theory, history and development of the field emission scanning electron microscope. Pages 1-6 in Biological Field Emission Scanning Electron Microscopy. R. A. Fleck and B. M. Humbel, ed. John Wiley & Sons Ltd.

Juškaitė, V., K. Ramanauskienė, and V. Briedis. 2015. Design and formulation of optimized microemulsions for dermal delivery of resveratrol. Evidence-Based Complementary and Alternative Medicine 2015:540916.

Juškaitė, V., K. Ramanauskienė, and V. Briedis. 2017. Testing of resveratrol microemulsion photostability and protective effect against UV induced oxidative stress. Acta Pharm 67(2):247-256.

Kalaitzaki, A., A. Xenakis, and V. Papadimitriou. 2015. Highly water dilutable microemulsions: a structural study. Colloid and Polymer Science 293(4):1111-1119.

Karthik, P. and C. Anandharamakrishnan. 2016. Fabrication of a nutrient delivery system of docosahexaenoic acid nanoemulsions via high energy techniques. Rsc Advances 6(5):3501-3513.

Kassem, M. G. A., A.-M. M. Ahmed, H. H. Abdel-Rahman, and A. H. E. Moustafa. 2019. Use of Span 80 and Tween 80 for blending gasoline and alcohol in spark ignition engines. Energy Reports 5:221-230.

Kayesh, R., M. Z. Sultan, A. Rahman, M. G. Uddin, F. Aktar, and M. A. Rashid. 2013. Development and validation of a rp-hplc method for the quantification of omeprazole in pharmaceutical dosage form. Journal of Scientific Research 5:335-342.

Khar, A., A. M. Ali, B. V. V. Pardhasaradhi, Z. Begum, and R. Anjum. 1999. Antitumor activity of curcumin is mediated through the induction of apoptosis in AK-5 tumor cells. FEBS Letters 445(1):165-168.

Kim, K. T., J. Y. Lee, J. H. Park, H. J. Cho, I. S. Yoon, and D. D. Kim. 2017. Capmul

MCM/Solutol HS15-based microemulsion for enhanced oral bioavailability of rebamipide. Journal of Nanoscience and Nanotechnology 17(4):2340-2344.
Kitts, D. D. 1994. Bioactive substances in food - identification and potential uses. Canadian Journal of Physiology and Pharmacology 72(4):423-434.
Klaffenbach, P. and D. Kronenfeld. 1997. Analysis of impurities of isopropyl myristate by gas-liquid chromatography. Journal of Chromatography A 767(1-2):330-334.
Klossek, M. L., J. Marcus, D. Touraud, and W. Kunz. 2014. Highly water dilutable green microemulsions. Colloids and Surfaces a-Physicochemical and Engineering Aspects 442:105-110.
Kohling, R., J. Woenckhaus, N. L. Kylachko, and R. Winter. 2002. Small-angle neutron scattering study of the effect of pressure on AOT-n-octane-water mesophases and the effect of alpha-chymotrypsin incorporation. Langmuir 18(22):8626-8632.
Komaiko, J. S. and D. J. McClements. 2016. Formation of food-grade nanoemulsions using low-energy preparation methods: A review of available methods. Comprehensive Reviews in Food Science and Food Safety 15(2):331-352.
Krauel, K., N. M. Davies, S. Hook, and T. Rades. 2005. Using different structure types of microemulsions for the preparation of poly(alkylcyanoacrylate) nanoparticles by interfacial polymerization. Journal of Controlled Release 106(1-2):76-87.
Kris-Etherton, P. M., K. D. Hecker, A. Bonanome, S. M. Coval, A. E. Binkoski, K. F. Hilpert, A. E. Griel, and T. D. Etherton. 2002. Bioactive compounds in foods: Their role in the prevention of cardiovascular disease and cancer. American Journal of Medicine 113(Supplement 9B):71S-88S.
Lane, K. E., W. L. Li, C. Smith, and E. Derbyshire. 2014. The bioavailability of an omega-3-rich algal oil is improved by nanoemulsion technology using yogurt as a food vehicle. International Journal of Food Science and Technology 49(5):1264-1271.
Lawrence, M. J. and G. D. Rees. 2012. Microemulsion-based media as novel drug delivery systems. Advanced Drug Delivery Reviews 64:175-193.
Lawrence, M. J. and W. Warisnoicharoen. 2006. Recent advances in microemulsions as drug delivery vehilcles. Pages 125-172 in Nanoparticulates as Drug Carriers. V. P. Torchilin, ed. Imperial College Press.
Lee, K. L. 2011. Applications and use of microemulsions. arXiv e-prints.
Lee, S. J. and D. J. McClements. 2010. Fabrication of protein-stabilized nanoemulsions using a combined homogenization and amphiphilic solvent dissolution/evaporation approach. Food Hydrocolloids 24(6-7):560-569.
Li, J., I.-C. Hwang, X. Chen, and H. J. Park. 2016. Effects of chitosan coating on curcumin loaded nano-emulsion: Study on stability and in vitro digestibility. Food Hydrocolloids 60:138-147.
Liang, R., C. F. Shoemaker, X. Q. Yang, F. Zhong, and Q. R. Huang. 2013. Stability and Bioaccessibility of beta-Carotene in Nanoemulsions Stabilized by Modified Starches. Journal of Agricultural and Food Chemistry 61(6):1249-1257.
Liang, W. P. 2001. The scientific and technical fundamental of emulsions. Science Press, Beijing, China.

Lidich, N., A. Aserin, and N. Garti. 2016. Structural characteristics of oil-poor dilutable fish oil omega-3 microemulsions for ophthalmic applications. Journal of Colloid and Interface Science 463:83-92.
Lim, T. K. 2012. Edible medicinal and non-medicinal plants: Volume 1, fruits. Springer Netherlands.
Lin, C. C., H. Y. Lin, M. H. Chi, C. M. Shen, H. W. Chen, W. J. Yang, and M. H. Lee. 2014. Preparation of curcumin microemulsions with food-grade soybean oil/lecithin and their cytotoxicity on the HepG2 cell line. Food Chemistry 154:282-290.
Lin, H. Y., J. L. Thomas, H. W. Chen, C. M. Shen, W. J. Yang, and M. H. Lee. 2012. In vitro suppression of oral squamous cell carcinoma growth by ultrasound-mediated delivery of curcumin microemulsions. International Journal of Nanomedicine 7:941-951.
Lin, Y. H., M. J. Tsai, Y. P. Fang, Y. S. Fu, Y. B. Huang, and P. C. Wu. 2018. Microemulsion formulation design and evaluation for hydrophobic compound: Catechin topical application. Colloids and Surfaces B-Biointerfaces 161:121-128.
Liu, F. and Z. W. Wang. 2010. Formulation of alpha-linolenic acid microemulsion free of co-surfactant. Chinese Chemical Letters 21(1):105-108.
Ma, Q. M., P. M. Davidson, and Q. X. Zhong. 2016. Antimicrobial properties of microemulsions formulated with essential oils, soybean oil, and Tween 80. International Journal of Food Microbiology 226:20-25.
Maiani, G., M. J. Periago Caston, G. Catasta, E. Toti, I. Goni Cambrodon, A. Bysted, F. Granado-Lorencio, B. Olmedilla-Alonso, P. Knuthsen, M. Valoti, V. Boehm, E. Mayer-Miebach, D. Behsnilian, and U. Schlemmer. 2009. Carotenoids: Actual knowledge on food sources, intakes, stability and bioavailability and their protective role in humans. Molecular Nutrition & Food Research 53:S194-S218.
Malcolmson, C., C. Satra, S. Kantaria, A. Sidhu, and M. J. Lawrence. 1998. Effect of oil on the level of solubilization of testosterone propionate into nonionic oil-in-water microemulsions. Journal of Pharmaceutical Sciences 87(1):109-116.
Mandawgade, S. D. and V. B. Patravale. 2008. Development of SLNs from natural lipids: Application to topical delivery of tretinoin. International Journal of Pharmaceutics 363(1):132-138.
Maruotti, N. and F. P. Cantatore. 2013. Vitamin d in the immune system and the role of its deficiency in rheumatic diseases. in Vitamin D : Daily Requirements, Dietary Sources and Symptoms of Deficiency. H. Smits and C. Meer, ed. Nova Science Publishers, Inc, Hauppauge, NY.
McClements, D. J. 2002. Theoretical prediction of emulsion color. Advances in Colloid and Interface Science 97(1-3):63-89.
McClements, D. J. 2005. Food emulsions: Principles, practices, and techniques. CRC Press, Boca Raton, USA.
McClements, D. J. 2007. Critical review of techniques and methodologies for characterization of emulsion stability. Critical Reviews in Food Science and Nutrition 47(7):611-649.
McClements, D. J. 2011. Edible nanoemulsions: fabrication, properties, and functional performance. Soft Matter 7(6):2297-2316.

McClements, D. J. 2012. Nanoemulsions versus microemulsions: terminology, differences, and similarities. Soft Matter 8(6):1719-1729.
McClements, D. J., E. A. Decker, and J. Weiss. 2007. Emulsion-based delivery systems for lipophilioc bioactive components. Journal of Food Science 72(8):R109-R124.
McClements, D. J. and J. Rao. 2011. Food-Grade Nanoemulsions: Formulation, Fabrication, Properties, Performance, Biological Fate, and Potential Toxicity. Critical Reviews in Food Science and Nutrition 51(4):285-330.
Mehta, S. K. and Kawaljit. 2002. Phase diagram and physical properties of a waterless sodium bis(2-ethylhexylsulfosuccinate)ethylbenzene-ethyleneglycol microemulsion: An insight into percolation. Physical Review E 65(2).
Mihindukulasuriya, S. D. F. and L. T. Lim. 2014. Nanotechnology development in food packaging: A review. Trends in Food Science & Technology 40(2):149-167.
Miller, P. E. and D. C. Snyder. 2012. Phytochemicals and cancer risk: A review of the epidemiological evidence. Nutrition in Clinical Practice 27(5):599-612.
Misharina, T. A., M. B. Terenina, N. I. Krikunova, and I. B. Medvedeva. 2010. Autooxidation of a mixture of lemon essential oils, methyl linolenoate, and methyl oleinate. Applied Biochemistry and Microbiology 46(5):551-556.
Mittal, K. L. and P. Kumar. 1999. Handbook of microemulsion science and technology. New York : Marcel Dekker, 1999.
Momin, J. K., C. Jayakumar, and J. B. Prajapati. 2013. Potential of nanotechnology in functional foods. Emirates Journal of Food and Agriculture 25(1):10-19.
Moreno, M. A., M. P. Ballesteros, and P. Frutos. 2003. Lecithin-based oil-in-water microemulsions for parenteral use: Pseudoternary phase diagrams, characterization and toxicity studies. Journal of Pharmaceutical Sciences 92(7):1428-1437.
Moulik, S. P. and B. K. Paul. 1998. Structure, dynamics and transport properties of microemulsions. Advances in Colloid and Interface Science 78(2):99-195.
Nakajima, M., Z. Wang, O. Chaudhry, H. J. Park, and L. R. Juneja. 2015. Nano-science-engineering-technology applications to food and nutrition. Journal of Nutritional Science and Vitaminology 61:S180-S182.
Namitha, K. K. and P. S. Negi. 2010. Chemistry and biotechnology of carotenoids. Critical Reviews in Food Science and Nutrition 50(8):728-760.
Narayan, B., K. Miyashita, and M. Hosakawa. 2006. Physiological effects of eicosapentaenoic acid (EPA) and docosahexaenoic acid (DHA) - A review. Food Reviews International 22(3):291-307.
Naves, M. M. V. and F. S. Moreno. 1998. Beta-carotene and cancer chemoprevention: From epidemiological associations to cellular mechanisms of action. Nutrition Research 18(10):1807-1824.
Nazari, M., M. A. Mehrnia, H. Jooyandeh, and H. Barzegar. 2019. Preparation and characterization of water in sesame oil microemulsion by spontaneous method. Journal of Food Process Engineering 42(4).
Omenn, G. S., G. E. Goodman, M. D. Thornquist, J. Balmes, M. R. Cullen, A. Glass, J. P. Keogh, F. L. Meyskens, B. Valanis, J. H. Williams, S. Barnhart, and S. Hammar. 1996. Effects

of a combination of beta carotene and vitamin A on lung cancer and cardiovascular disease. New England Journal of Medicine 334(18):1150-1155.
Onwulata, C. I. 2013. Microencapsulation and functional bioactive foods. Journal of Food Processing and Preservation 37(5):510-532.
Ou, J. Y., M. F. Wang, J. Zheng, and S. Y. Ou. 2019. Positive and negative effects of polyphenol incorporation in baked foods. Food Chemistry 284:90-99.
Ozturk, A. A. and U. M. Guven. 2019. Cefaclor monohydrate loaded microemulsion formulation for topical application: Characterization with new developed UPLC method and stability study. Journal of Research in Pharmacy 23(3):426-440.
Pandolfe, W. D. 1981. Effect of dispersed and continuous phase viscosity on droplet size of emulsions generated by homogenization. Journal of Dispersion Science and Technology 2(4):459-474.
Patel, K. R., V. A. Brown, D. J. L. Jones, R. G. Britton, D. Hemingway, A. S. Miller, K. P. West, T. D. Booth, M. Perloff, J. A. Crowell, D. E. Brenner, W. P. Steward, A. J. Gescher, and K. Brown. 2010. Clinical pharmacology of resveratrol and its metabolites in colorectal cancer patients. Cancer Research 70(19):7392-7399.
Patel, M. B., S. Mandal, and K. S. Rajesh. 2012. Formulation and kinetic modeling of curcumin loaded intranasal mucoadhesive microemulsion. Vol. 4.
Patel, M. R., R. B. Patel, J. R. Parikh, A. B. Solanki, and B. G. Patel. 2011. Investigating effect of microemulsion components: In vitro permeation of ketoconazole. Pharmaceutical Development and Technology 16(3):250-258.
Patel, N., U. Schmid, and M. J. Lawrence. 2006. Phospholipid-based microemulsions suitable for use in foods. Journal of Agricultural and Food Chemistry 54(20):7817-7824.
Paul, B. K. and S. P. Moulik. 1997. Microemulsions: An overview. Journal of Dispersion Science and Technology 18(4):301-367.
Pimentel-Gonzalez, D. J., R. G. Campos-Montiel, C. Lobato-Calleros, R. Pedroza-Islas, and E. J. Vernon-Carter. 2009. Encapsulation of Lactobacillus rhamnosus in double emulsions formulated with sweet whey as emulsifier and survival in simulated gastrointestinal conditions. Food Research International 42(2):292-297.
Pinheiro, A. C., M. A. Coimbra, and A. A. Vicente. 2016. In vitro behaviour of curcumin nanoemulsions stabilized by biopolymer emulsifiers - Effect of interfacial composition. Food Hydrocolloids 52:460-467.
Podlogar, F., M. Gagperlin, M. Tomsic, A. Jamnik, and M. B. Rogac. 2004. Structural characterisation of water-Tween 40((R))/Imwitor 308((R))-isopropyl myristate microemulsions using different experimental methods. International Journal of Pharmaceutics 276(1-2):115-128.
Polizelli, M. A., A. L. dos Santos, and E. Feitosa. 2008. The effect of sodium chloride on the formation of W/O microemulsions in soy bean oil/surfactant/water systems and the solubilization of small hydrophilic molecules. Colloids and Surfaces a-Physicochemical and Engineering Aspects 315(1-3):130-135.
Prajapati, H., D. Patel, N. Patel, D. Dalrymple, and A. Serajuddin. 2011. Effect of difference in fatty acid chain lengths of medium- chain lipids on lipid/surfactant/water phase diagrams

and drug solubility. Vol. 2.
Qian, C., E. A. Decker, H. Xiao, and D. J. McClements. 2012a. Inhibition of beta-carotene degradation in oil-in-water nanoemulsions: Influence of oil-soluble and water-soluble antioxidants. Food Chemistry 135(3):1036-1043.
Qian, C., E. A. Decker, H. Xiao, and D. J. McClements. 2012b. Physical and chemical stability of beta-carotene-enriched nanoemulsions: Influence of pH, ionic strength, temperature, and emulsifier type. Food Chemistry 132(3):1221-1229.
Qu, D., J. J. He, C. Y. Liu, J. Zhou, and Y. Chen. 2014. Triterpene-loaded microemulsion using Coix lacryma-jobi seed extract as oil phase for enhanced antitumor efficacy: preparation and in vivo evaluation. International Journal of Nanomedicine 9:109-119.
Qu, G. J., J. H. Chen, and X. L. Guo. 2018. The beneficial and deleterious role of dietary polyphenols on chronic degenerative diseases by regulating gene expression. Bioscience Trends 12(6):526-536.
Radko, Y., S. B. Pedersen, and L. Christensen. 2016. Anti-inflammatory activity of resveratrol metabolites. Planta Medica 82.
Rao, A. V. R. and S. Agarwal. 2000. Role of antioxidant lycopene in cancer and heart disease. Journal of the American College of Nutrition 19(5):563-569.
Rao, J. J., E. A. Decker, H. Xiao, and D. J. McClements. 2013. Nutraceutical nanoemulsions: influence of carrier oil composition (digestible versus indigestible oil) on -carotene bioavailability. Journal of the Science of Food and Agriculture 93(13):3175-3183.
Rao, J. J. and D. J. McClements. 2011. Formation of flavor oil microemulsions, nanoemulsions and emulsions: Influence of composition and preparation method. Journal of Agricultural and Food Chemistry 59(9):5026-5035.
Rao, J. J. and D. J. McClements. 2012a. Food-grade microemulsions and nanoemulsions: Role of oil phase composition on formation and stability. Food Hydrocolloids 29(2):326-334.
Rao, J. J. and D. J. McClements. 2012b. Impact of lemon oil composition on formation and stability of model food and beverage emulsions. Food Chemistry 134(2):749-757.
Rao, J. J. and D. J. McClements. 2012c. Lemon oil solubilization in mixed surfactant solutions: Rationalizing microemulsion & nanoemulsion formation. Food Hydrocolloids 26(1):268-276.
Rao, J. J. and D. J. McClements. 2013. Optimization of lipid nanoparticle formation for beverage applications: Influence of oil type, cosolvents, and cosurfactants on nanoemulsion properties. Journal of Food Engineering 118(2):198-204.
Regev, O., S. Ezrahi, A. Aserin, N. Garti, E. Wachtel, E. W. Kaler, A. Khan, and Y. Talmon. 1996. A study of the microstructure of a four-component nonionic microemulsion by cryo-TEM, NMR, SAXS, and SANS. Langmuir 12(3):668-674.
Ribeiro, H. S., Schuchmann, H.P., Engel, R., Walz, E., Briviba, K. 2009. Encapsulation Technologies for Active Food Ingredients and Food Peocessing. Springer Science, New York.
Roa, D. F., M. P. Buera, M. P. Tolaba, and P. R. Santagapita. 2017. Encapsulation and Stabilization of beta-Carotene in Amaranth Matrices Obtained by Dry and Wet Assisted Ball Milling. Food and Bioprocess Technology 10(3):512-521.
Rohatgi-Mukherjee, K. K. 1986. Introducing Photochemistry. Pages 1-9 in Fundamentals of Photochemistry: Revised Edition. New Age International Ltd., Delhi, India.

Roohinejad, S., D. Middendorf, D. J. Burritt, U. Bindrich, D. W. Everett, and I. Oey. 2014. Capacity of natural p-carotene loaded microemulsion to protect Caco-2 cells from oxidative damage caused by exposure to H2O2. Food Research International 66:469-477.

Roohinejad, S., I. Oey, J. Wen, S. J. Lee, D. W. Everett, and D. J. Burritt. 2015. Formulation of oil-in-water β-carotene microemulsions: Effect of oil type and fatty acid chain length. Food Chemistry 174(0):270-278.

Rozman, B. and M. Gasperlin. 2007. Stability of vitamins C and E in topical microemulsions for combined antioxidant therapy. Drug Delivery 14(4):235-245.

Ruiz, R. B. and P. S. Hernandez. 2016. Cancer chemoprevention by dietary phytochemicals: Epidemiological evidence. Maturitas 94:13-19.

Rukmini, A., S. Raharjo, P. Hastuti, and S. Supriyadi. 2012. Formulation and stability of water-in-virgin coconut oil microemulsion using ternary food grade nonionic surfactants. International Food Research Journal 19(1):259-264.

Ruth, H. S., D. Attwood, G. Ktistis, and C. J. Taylor. 1995. Phase studies and particle-size analysis of oil-in-water phospholipid microemulsions. International Journal of Pharmaceutics 116(2):253-261.

Saberi, A. H., Y. Fang, and D. J. McClements. 2014. Stabilization of vitamin E-enriched mini-emulsions: Influence of organic and aqueous phase compositions. Colloids and Surfaces a-Physicochemical and Engineering Aspects 449:65-73.

Sagalowicz, L. and M. E. Leser. 2010. Delivery systems for liquid food products. Current Opinion in Colloid & Interface Science 15(1-2):61-72.

Sajilata, M. G., R. S. Singhal, and M. Y. Kamat. 2008. The carotenoid pigment zeaxanthin - A review. Comprehensive Reviews in Food Science and Food Safety 7(1):29-49.

Salimi, A., E. Motaharitabar, M. Goudarzi, A. Rezaie, and H. Kalantari. 2014. Toxicity evaluation of microemulsion (nano size) of sour cherry kernel extract for the oral bioavailability enhancement. Jundishapur J Nat Pharm Prod 9(1):16-23.

Schroffenegger, M. and E. Reimhult. 2019. Thermoresponsive core-shell nanoparticles and their potential applications. Pages 145-170 in Comprehensive Nanoscience and Nanotechnology (Second Edition). D. L. Andrews, R. H. Lipson, and T. Nann, ed. Academic Press, Oxford.

Schwarz, S., U. C. Obermueller-Jevic, E. Hellmis, W. Koch, G. Jacobi, and H.-K. Biesalski. 2008. Lycopene inhibits disease progression in patients with benign prostate hyperplasia. Journal of Nutrition 138(1):49-53.

Sevcikova, P., V. Kasparkova, I. Hauerlandova, P. Humpolicek, Z. Kucekova, and L. Bunkova. 2014. Formulation, antibacterial activity, and cytotoxicity of 1-monoacylglycerol microemulsions. European Journal of Lipid Science and Technology 116(4):448-457.

Shaaban, H. A., Z. Sadek, A. E. Edris, and A. Saad-Hussein. 2015. Analysis and antibacterial activity of nigella sativa essential oil formulated in microemulsion system. Journal of Oleo Science 64(2):223-232.

Shevachman, M., A. Shani, and N. Garti. 2004. Formation and investigation of microemulsions based on Jojoba oil and nonionic surfactants. Journal of the American Oil Chemists Society 81(12):1143-1152.

Shi, J. and M. Le Maguer. 2000. Lycopene in tomatoes: Chemical and physical properties affected by food processing. Critical Reviews in Food Science and Nutrition 40(1):1-42.
Shim, J. S., J. Lee, H.-J. Park, S.-J. Park, and H. J. Kwon. 2004. A new curcumin derivative, hbc, interferes with the cell cycle progression of colon cancer cells via antagonization of the ca2+/calmodulin function. Chemistry & Biology 11(10):1455-1463.
Shinoda, K., M. Araki, A. Sadaghiani, A. Khan, and B. Lindman. 1991. Lecithin-based microemulsions - phase-behavior and microstructure. Journal of Physical Chemistry 95(2):989-993.
Shukla, A., M. Janich, K. Jahn, A. Krause, M. A. Kiselev, and R. H. H. Neubert. 2002. Investigation of pharmaceutical oil/water microemulsions by small-angle scattering. Pharmaceutical Research 19(6):881-886.
Simopoulos, A. P. 1991. Omega-3-fatty-acids in health and disease and in growth and development. American Journal of Clinical Nutrition 54(3):438-463.
Singh, H. 2016. Nanotechnology applications in functional foods; opportunities and challenges. Preventive Nutrition and Food Science 21(1):1-8.
Singh, P. S. 2017. Small-Angle Scattering Techniques (SAXS/SANS). Pages 95-111 in Membrane Characterization. N. Hilal, A. F. Ismail, T. Matsuura, and D. Oatley-Radcliffe, ed. Elsevier.
Sjoblom, J. 1996. Emulsions and emulsion stability: Surfactant science series. No. 61. Marcel Dekker, NY, USA.
Solans, C., P. Izquierdo, J. Nolla, N. Azemar, and M. J. Garcia-Celma. 2005. Nano-emulsions. Current Opinion in Colloid & Interface Science 10(3-4):102-110.
Solans, C. and I. Sole. 2012. Nano-emulsions: Formation by low-energy methods. Current Opinion in Colloid & Interface Science 17(5):246-254.
Sole, I., C. M. Pey, A. Maestro, C. Gonzalez, M. Porras, C. Solans, and J. M. Gutierrez. 2010. Nano-emulsions prepared by the phase inversion composition method: Preparation variables and scale up. Journal of Colloid and Interface Science 344(2):417-423.
Sotomayor-Gerding, D., B. D. Oomah, F. Acevedo, E. Morales, M. Bustamante, C. Shene, and M. Rubilar. 2016. High carotenoid bioaccessibility through linseed oil nanoemulsions with enhanced physical and oxidative stability. Food Chemistry 199:463-470.
Souza, V. B., L. S. Spinelli, G. Gonzalez, and C. R. E. Mansur. 2009. Determination of the phase inversion temperature of orange oil/water emulsions by rheology and microcalorimetry. Analytical Letters 42(17):2864-2878.
Sozen, E., T. Demirel, and N. K. Ozer. 2019. Vitamin E: Regulatory role in the cardiovascular system. Iubmb Life 71(4):507-515.
Spernath, A., A. Yaghmur, A. Aserin, R. E. Hoffman, and N. Garti. 2002. Food-grade microemulsions based on nonionic emulsifiers: Media to enhance lycopene solubilization. Journal of Agricultural and Food Chemistry 50(23):6917-6922.
Spernath, A., A. Yaghmur, A. Aserin, R. E. Hoffman, and N. Garti. 2003. Self-diffusion nuclear magnetic resonance, microstructure transitions, and solubilization capacity of phytosterols and cholesterol in Winsor IV food-grade microemulsions. Journal of Agricultural and Food Chemistry 51(8):2359-2364.

Springer, M. and S. Moco. 2019. Resveratrol and Its Human Metabolites-Effects on Metabolic Health and Obesity. Nutrients 11(1).
Stringham, J. M. and B. R. Hammond. 2005. Dietary lutein and zeaxanthin: Possible effects on visual function. Nutrition Reviews 63(2):59-64.
Subongkot, T. and T. Ngawhirunpat. 2017. Development of a novel microemulsion for oral absorption enhancement of all-trans retinoic acid. International Journal of Nanomedicine 12:5585-5599.
Subramanian, N., S. K. Ghosal, A. Acharya, and S. P. Moulik. 2005. Formulation and physicochemical characterization of microemulsion system using isopropyl myristate, medium-chain glyceride, polysorbate 80 and water. Chemical & Pharmaceutical Bulletin 53(12):1530-1535.
Swaroopa, A., C. Aparna, and S. Prathima. 2014. Formulation, evaluation and characterization of periodontal microemulsion gel. International Journal of Pharmaceutical Sciences and Drug Research 6(1).
Syed, H. K. and K. K. Peh. 2014. Identification of phases of various oil, surfactant/co-surfactants and water system by ternary phase diagram. Acta Poloniae Pharmaceutica 71(2):301-309.
Syed, H. K. and K. K. Peh. 2018. Antibacterial activity of curcumin and solubility-enhanced curcumin in microemulsion: A comparative study. Latin American Journal of Pharmacy 37(7):1468-1477.
Sylvester, P. W., M. R. Akl, and N. M. Ayoub. 2011. Tocotrienol supplementation and health. in Vitamin E: nutrition, side effects, and supplements. A. E. Lindberg, ed. Nova Science Publishers.
Szkudelska, K. and T. Szkudelski. 2010. Resveratrol, obesity and diabetes. European Journal of Pharmacology 635(1-3):1-8.
Szymula, M. 2004. Atmospheric oxidation of beta-carotene in aqueous, pentanol, SDS microemulsion systems in the presence and absence of vitamin C. Journal of Dispersion Science and Technology 25(2):129-137.
Tadros, T., R. Izquierdo, J. Esquena, and C. Solans. 2004. Formation and stability of nano-emulsions. Advances in Colloid and Interface Science 108:303-318.
Talegaonkar, S., A. Azeem, F. Ahmad, R. Khar, S. Pathan, and Z. Iqbal. 2008. Microemulsions: A novel approach to enhanced drug delivery. Recent patents on drug delivery & formulation 2:238-257.
Tan, C., J. Xue, X. W. Lou, S. Abbas, Y. Guan, B. Feng, X. M. Zhang, and S. Q. Xia. 2014. Liposomes as delivery systems for carotenoids: comparative studies of loading ability, storage stability and in vitro release. Food & Function 5(6):1232-1240.
Tang, H. W., S. Xiang, X. Z. Li, J. Zhou, and C. T. Kuang. 2019. Preparation and in vitro performance evaluation of resveratrol for oral self-microemulsion. Plos One 14(4).
Tarafdar, J. C. and R. Raliya. 2012. The Nanotechnology. Scientific Publishers.
Teo, A., S. J. Lee, K. K. T. Goh, and F. M. Wolber. 2016. Kinetic stability and cellular uptake of lutein in WPI-stabilised nanoemulsions and emulsions prepared by emulsification and solvent evaporation method. Food Chemistry.

Thakkar, H., A. Patel, and N. Chauhan. 2014. Formulation and optimization of mucoadhesive microemulsion containing mirtazapine for intranasal delivery. Chronicles of Young Scientists 5(1):25-32.
Todosijevic, M. N., N. D. Cekic, M. M. Savic, M. Gasperlin, D. V. Randelovic, and S. D. Savic. 2014. Sucrose ester-based biocompatible microemulsions as vehicles for aceclofenac as a model drug: formulation approach using D-optimal mixture design. Colloid and Polymer Science 292(12):3061-3076.
Trotta, M., R. Cavalli, E. Ugazio, and M. R. Gasco. 1996. Phase behaviour of microemulsion systems containing lecithin and lysolecithin as surfactants. International Journal of Pharmaceutics 143(1):67-73.
Vaidya, S. and A. K. Ganguli. 2019. Microemulsion methods for synthesis of nanostructured materials. Pages 1-12 in Comprehensive Nanoscience and Nanotechnology (Second Edition). D. L. Andrews, R. H. Lipson, and T. Nann, ed. Academic Press, Oxford.
Valenta, C. and K. Schultz. 2004. Influence of carrageenan on the rheology and skin permeation of microemulsion formulations. Journal of Controlled Release 95(2):257-265.
Valoppi, F., R. Frisina, and S. Calligaris. 2017. Fabrication of transparent lemon oil loaded microemulsions by phase inversion temperature (pit) method: Effect of oil phase composition and stability after dilution. Food Biophysics 12(2):244-249.
Vang, O. 2013. What is new for resveratrol? Is a new set of recommendations necessary? Annals of the New York Academy of Sciences 1290(1):1-11.
Velikov, K. P. and E. Pelan. 2008. Colloidal delivery systems for micronutrients and nutraceuticals. Soft Matter 4(10):1964-1980.
Vinson, P. K., J. G. Sheehan, W. G. Miller, L. E. Scriven, and H. T. Davis. 1991. Viewing microemulsions with freeze-fracture transmission electron-microscopy. Journal of Physical Chemistry 95(6):2546-2550.
Volpe, V., D. S. Nascimento, M. Insausti, and M. Grünhut. 2018. Octyl p-methoxycinnamate loaded microemulsion based on Ocimum basilicum essential oil. Characterization and analytical studies for potential cosmetic applications. Colloids and Surfaces A: Physicochemical and Engineering Aspects 546:285-292.
Walker, R., E. A. Decker, and D. J. McClements. 2015. Development of food-grade nanoemulsions and emulsions for delivery of omega-3 fatty acids: opportunities and obstacles in the food industry. Food & Function 6(1):42-55.
Walle, T., F. Hsieh, M. H. DeLegge, J. E. Oatis, and U. K. Walle. 2004. High absorption but very low bioavailability of oral resveratrol in humans. Drug Metabolism and Disposition 32(12):1377-1382.
Wang, Q., H. Montgomery, N. Ahmed, and C. Smith. 2010. Spectroscopy. Pages 257-289 in Biomedical Science Practice: Experimental and Professional Skills. H. Glencross, N. Ahmed, C. Smith, and Q. Wang, ed. OUP Oxford, New York, United States.
Wang, X., Y. Jiang, Y. Wang, M. Huang, C. Ho, and Q. Huang. 2008. Enhancing anti-inflammation activity of curcumin through O/W nanoemulsions. Food Chemistry 108(2):419-424.
Wang, Y. F., R. P. Zhao, L. Yu, Y. B. Zhang, Y. He, and J. Yao. 2014. Evaluation of cinnamon

essential oil microemulsion and its vapor phase for controlling postharvest gray mold of pears (Pyrus pyrifolia). Journal of the Science of Food and Agriculture 94(5):1000-1004.
Warisnoicharoen, W., A. B. Lansley, and M. J. Lawrence. 2000. Nonionic oil-in-water microemulsions: the effect of oil type on phase behaviour. International Journal of Pharmaceutics 198(1):7-27.
Weiss, J., J. N. Coupland, D. Brathwaite, and D. J. McClements. 1997. Influence of molecular structure of hydrocarbon emulsion droplets on their solubilization in nonionic surfactant micelles. Colloids and Surfaces a-Physicochemical and Engineering Aspects 121(1):53-60.
Weiss, J. and D. J. McClements. 2000. Mass transport phenomena in oil-in-water emulsions containing surfactant micelles: Solubilization. Langmuir 16(14):5879-5883.
Weiss, J., D. J. McClements, and P. Takhistov. 2007. Functional materials in food nanotechnology. Food Australia 59(6):274-275.
Whitehurst, R. J. 2004. Emulsifiers in food technology. Blackwell Publishing Ltd, Lowa, USA.
Winsor, P. A. 1948. Hydrotropy, solubilisation and related emulsification processes .1. to .4. Transactions of the Faraday Society 44(6):376-398.
Wooster, T. J., M. Golding, and P. Sanguansri. 2008. Impact of Oil Type on Nanoemulsion Formation and Ostwald Ripening Stability. Langmuir 24(22):12758-12765.
Xiao, Y., X. Chen, L. Yang, X. Zhu, L. Zou, F. Meng, and Q. Ping. 2013. Preparation and oral bioavailability study of curcuminoid-loaded microemulsion. Journal of Agricultural and Food Chemistry 61(15):3654-3660.
Xu, J., Q.-J. Fan, Z.-Q. Yin, X.-T. Li, Y.-H. Du, R.-Y. Jia, K.-Y. Wang, C. Lv, G. Ye, Y. Geng, G. Su, L. Zhao, T.-X. Hu, F. Shi, L. Zhang, C.-L. Wu, C. Tao, Y.-X. Zhang, and D.-X. Shi. 2010. The preparation of neem oil microemulsion (Azadirachta indica) and the comparison of acaricidal time between neem oil microemulsion and other formulations in vitro. Veterinary Parasitology 169(3-4):399-403.
Xu, S. X., Y. C. Li, X. Liu, L. J. Mao, H. Zhang, and X. D. Zheng. 2012. In vitro and in vivo antifungal activity of a water-dilutable cassia oil microemulsion against Geotrichum citri-aurantii. Journal of the Science of Food and Agriculture 92(13):2668-2671.
Yadav, V., P. Jadhav, K. Kanase, A. Bodhe, and S. Dombe. 2018. Preparation and evaluation of microemulsion containing antihypertensive drug. International Journal of Applied Pharmaceutics 10:138.
Yan, X. and Z. Wang. 2013. Preparation and evaluation of β-carotene containing microemulsion. Tenside Surfactants Detergents 50(2):113-117.
Yang, F. F., J. Zhou, C. Y. Liu, X. Hu, R. L. Pan, Q. Chang, X. M. Liu, and Y. H. Liao. 2017a. Cytochromes p450 inhibitory excipient-based self-microemulsions for the improved bioavailability of protopanaxatriol and protopanaxadiol: Preparation and evaluation. Planta Medica 83(5):453-460.
Yang, J., W. Jiang, B. S. Guan, X. H. Qiu, and Y. J. Lu. 2014. Preparation of d-limonene oil-in-water nanoemulsion from an optimum formulation. Journal of Oleo Science 63(11):1133-1140.
Yang, J. H., H. H. Xu, S. S. Wu, B. W. Ju, D. D. Zhu, Y. Yan, M. Wang, and J. P. Hu. 2017b. Preparation and evaluation of microemulsion-based transdermal delivery of Cistanche

tubulosa phenylethanoid glycosides. Molecular Medicine Reports 15(3):1109-1116.
Yang, Y., C. Marshall-Breton, M. E. Leser, A. A. Sher, and D. J. McClements. 2012. Fabrication of ultrafine edible emulsions: Comparison of high-energy and low-energy homogenization methods. Food Hydrocolloids 29(2):398-406.
Yi, C. X., H. Zhong, S. S. Tong, X. Cao, C. K. Firempong, H. F. Liu, M. Fu, Y. Yang, Y. S. Feng, H. Y. Zhang, X. M. Xu, and J. N. Yu. 2012. Enhanced oral bioavailability of a sterol-loaded microemulsion formulation of Flammulina velutipes, a potential antitumor drug. International Journal of Nanomedicine 7:5067-5078.
Yi, J., T. I. Lam, W. Yokoyama, L. W. Cheng, and F. Zhong. 2014a. Cellular uptake of beta-carotene from protein stabilized solid lipid nanoparticles prepared by homogenization-evaporation method. Journal of Agricultural and Food Chemistry 62(5):1096-1104.
Yi, J., Y. Li, F. Zhong, and W. Yokoyama. 2014b. The physicochemical stability and in vitro bioaccessibility of beta-carotene in oil-in-water sodium caseinate emulsions. Food Hydrocolloids 35:19-27.
Yu, H. and Q. Huang. 2013. Bioavailability and delivery of nutraceuticals and functional foods using nanotechnology. Bio-nanotechnology: a revolution in food, biomedical and health sciences.
Yu, Y. l., Z. f. He, and H. j. Li. 2016. Research and applications of nano-packaging films in meat preservation. Food and Fermentation Industries (No. 10):282-286.
Yuan, Y., Y. Gao, J. Zhao, and L. Mao. 2008. Characterization and stability evaluation of β-carotene nanoemulsions prepared by high pressure homogenization under various emulsifying conditions. Food Research International 41(1):61-68.
Zabodalova, L., T. Ishchenko, N. Skvortcova, D. Baranenko, and V. Chernjavskij. 2014. Liposomal beta-carotene as a functional additive in dairy products. Agronomy Research 12:825-834.
Zargar-Shoshtari, S., J. Wen, and R. G. Alany. 2010. Formulation and physicochemical characterization of imwitor 308 based self microemulsifying drug delivery systems. Chemical & Pharmaceutical Bulletin 58(10):1332-1338.
Zhang, H., Z. Lu, S. Wang, Y. Shen, F. Feng, and X. Zheng. 2008a. Development and antifungal evaluation of a food-grade U-type microemulsion. Journal of Applied Microbiology 105(4):993-1001.
Zhang, H., Z. Lu, L. Zhang, Y. Bao, X. Zhan, F. Feng, and X. Zheng. 2008b. Antifungal activity of a food-grade dilution-stable microemulsion against Aspergillus niger. Letters in Applied Microbiology 47(5):445-450.
Zhang, H., Y. Shen, P. F. Weng, G. Q. Zhao, F. Q. Feng, and X. D. Zheng. 2009. Antimicrobial activity of a food-grade fully dilutable microemulsion against Escherichia coli and Staphylococcus aureus. International Journal of Food Microbiology 135(3):211-215.
Zhang, W. N. and Q. X. Zhong. 2010. Microemulsions as nanoreactors to produce whey protein nanoparticles with enhanced heat stability by thermal pretreatment. Food Chemistry 119(4):1318-1325.
Zheng, H. M., H. Bin Li, D. W. Wang, and D. Liu. 2013a. Preparation methods for monodispersed garlic oil microspheres in water using the microemulsion technique and their

potential as antimicrobials. Journal of Food Science 78(8):N1301-N1306.
Zheng, K., A. Zou, X. Yang, F. Liu, Q. Xia, R. Ye, and B. Mu. 2013b. The effect of polymer–surfactant emulsifying agent on the formation and stability of α-lipoic acid loaded nanostructured lipid carriers (NLC). Food Hydrocolloids 32(1):72-78.
Zhou, G.-Z., S.-N. Zhang, L. Zhang, G.-C. Sun, and X.-B. Chen. 2014. A synthetic curcumin derivative hydrazinobenzoylcurcumin induces autophagy in A549 lung cancer cells. Pharmaceutical Biology 52(1):111-116.
Zhu, R. R., L. L. Qin, M. Wang, S. M. Wu, S. L. Wang, R. Zhang, Z. X. Liu, X. Y. Sun, and S. D. Yao. 2009. Preparation, characterization, and anti-tumor property of podophyllotoxin-loaded solid lipid nanoparticles. Nanotechnology 20(5).
Ziani, K., Y. Fang, and D. J. McClements. 2012a. Encapsulation of functional lipophilic components in surfactant-based colloidal delivery systems: Vitamin E, vitamin D, and lemon oil. Food Chemistry 134(2):1106-1112.
Ziani, K., Y. Fang, and D. J. McClements. 2012b. Fabrication and stability of colloidal delivery systems for flavor oils: Effect of composition and storage conditions. Food Research International 46(1):209-216.

Appendices

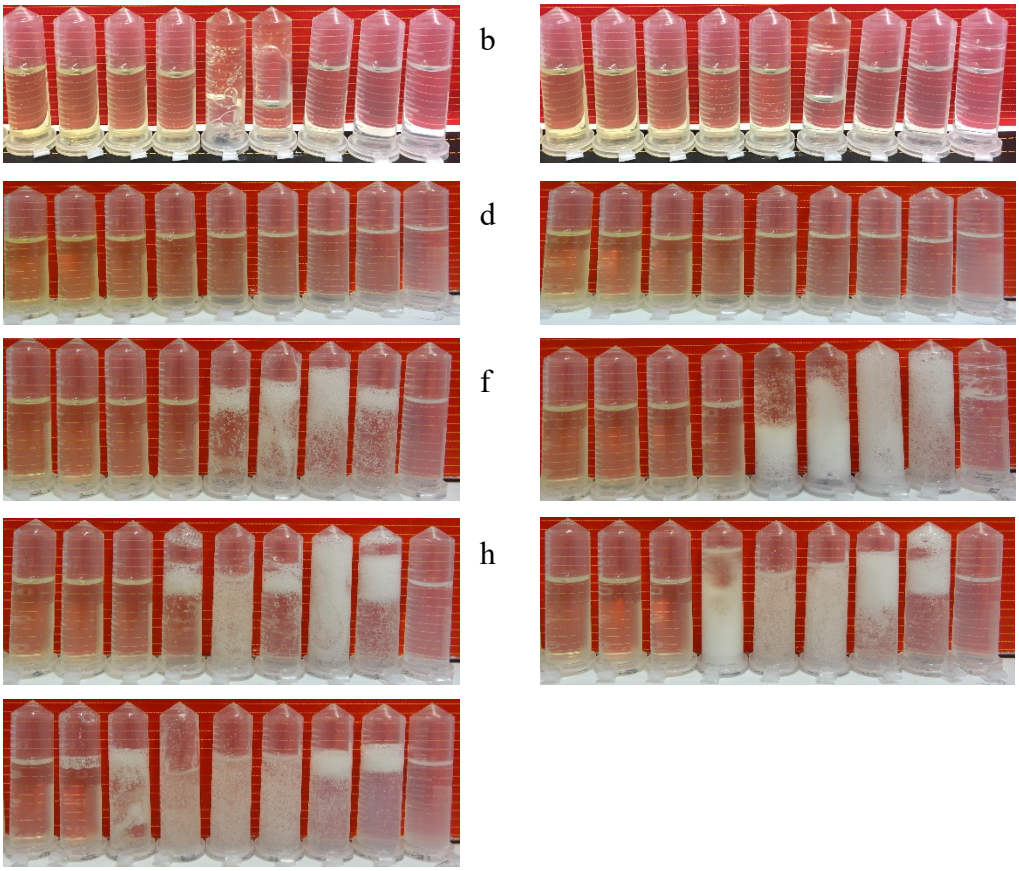

Figure 1 Photos of samples, which were composed of Capmul 708G, Tween 80 and Milli-Q water, fabricated by water titration method. (a) L110 to L190 (b) L210 to L290 (c) L310 to L390 (d) L410 to L490 (e) L510 to L590 (f) L610 to L690 (g) L710 to L790 (h) L810 to L890 (i) L910 to L990.

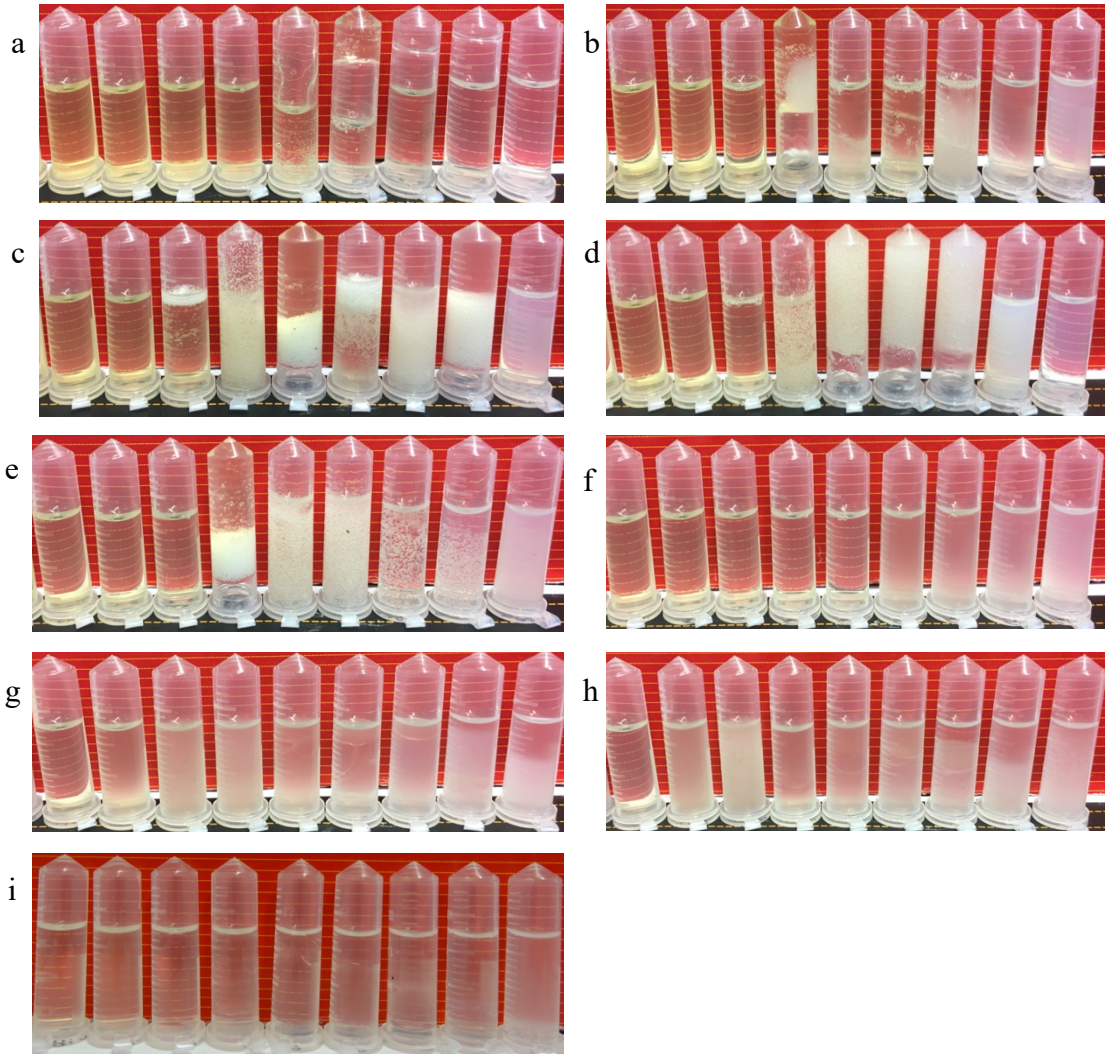

Figure 2 Photos of samples, which were composed of Capmul MCM C8, Tween 80 and Milli-Q water, fabricated by water titration method. (a) L110 to L190 (b) L210 to L290 (c) L310 to L390 (d) L410 to L490 (e) L510 to L590 (f) L610 to L690 (g) L710 to L790 (h) L810 to L890 (i) L910 to L990.

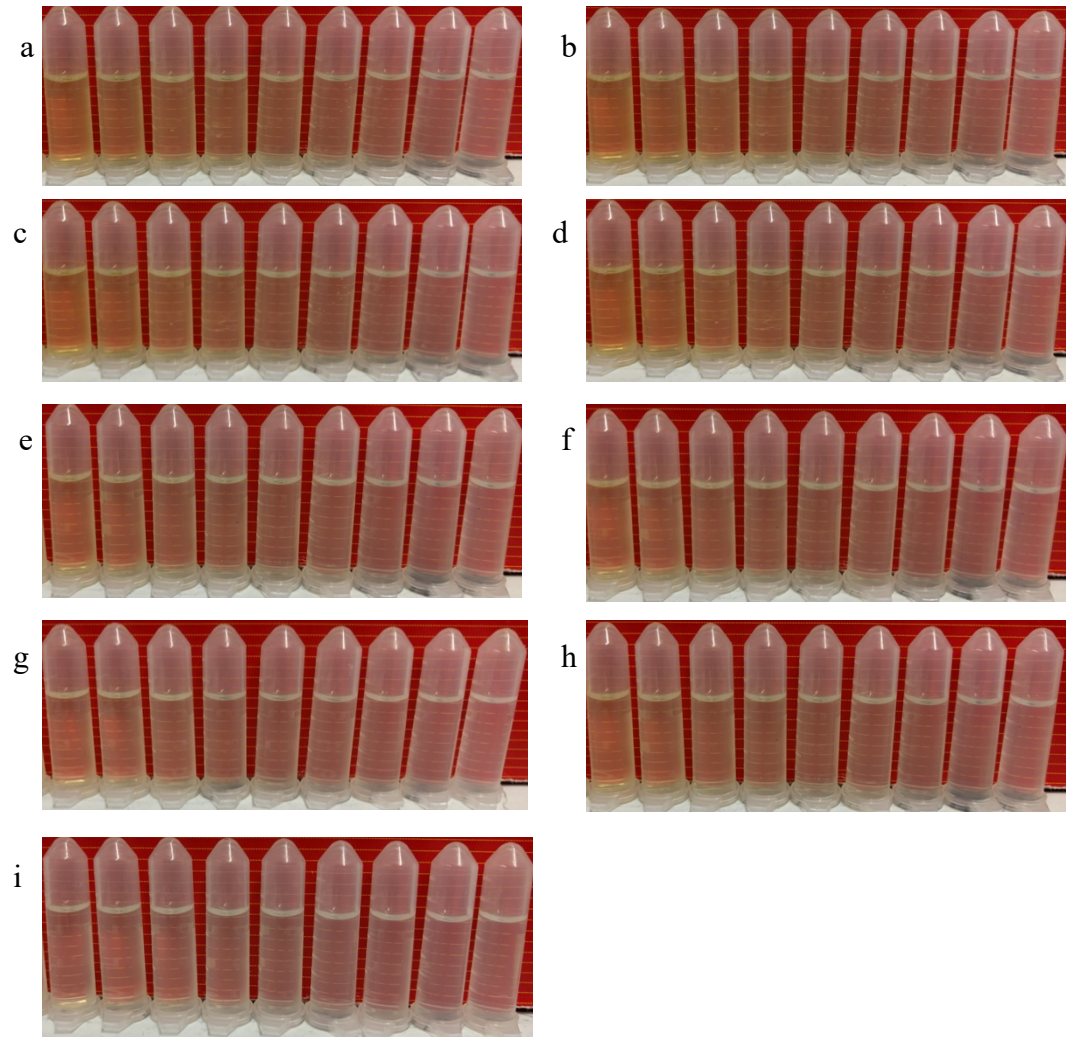

Figure 3 Photos of samples, which were composed of Capmul 708G, Tween 80, PG and Milli-Q water (ratio of PG to water was 1:1), fabricated by water titration method. (a) L110 to L190 (b) L210 to L290 (c) L310 to L390 (d) L410 to L490 (e) L510 to L590 (f) L610 to L690 (g) L710 to L790 (h) L810 to L890 (i) L910 to L990.

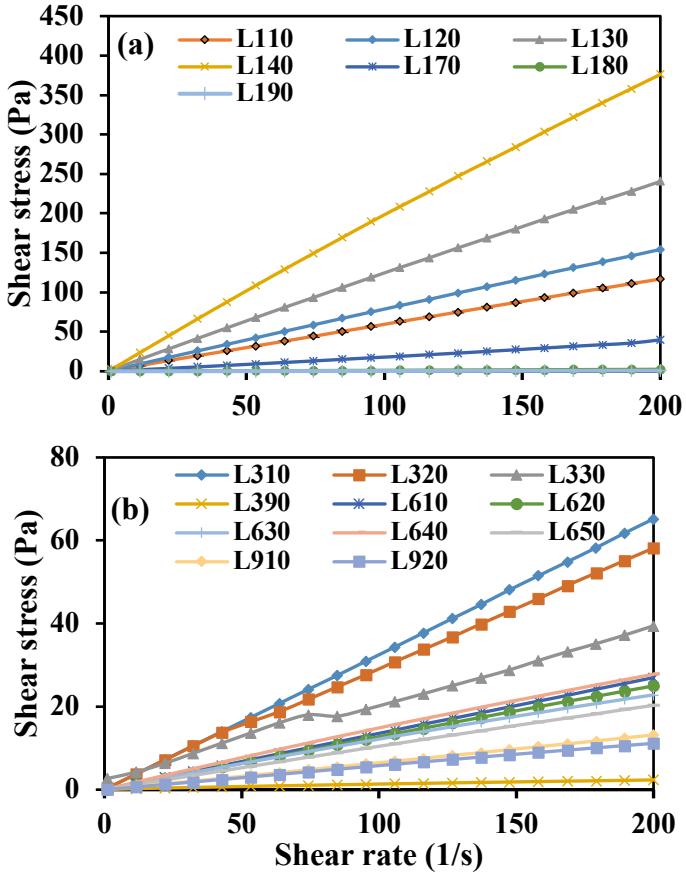

Figure 4 Shear stress as a function of shear rate of samples from Capmul MCM C8, Tween 80 and Milli-Q mixture system. (a) L110, L120, L130, L140, L180, L180 and L190. (b) L310, L320, L330, L390, L610, L620, L630, L640, L650, L910 and L920.

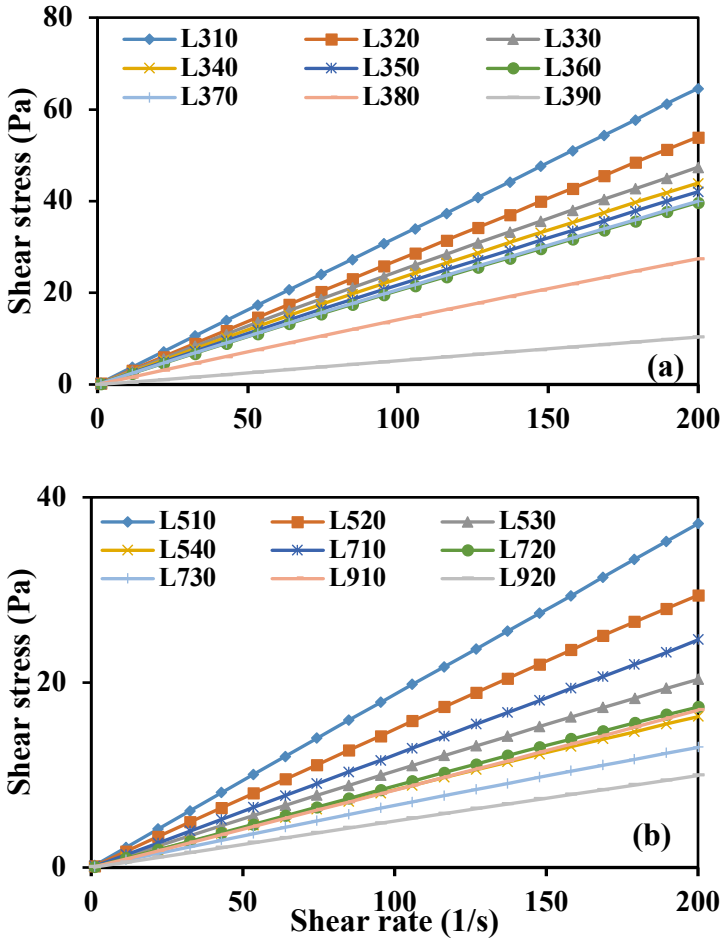

Figure 5 Shear stress as a function of shear rate of samples from Capmul 708G, Tween 80 and Milli-Q mixture system. (a) L310, L320, L330, L340, L350, L360, L370, L380 and L390. (b) L510, L520, 530, L540, L710, L720, L730, L910 and L920.

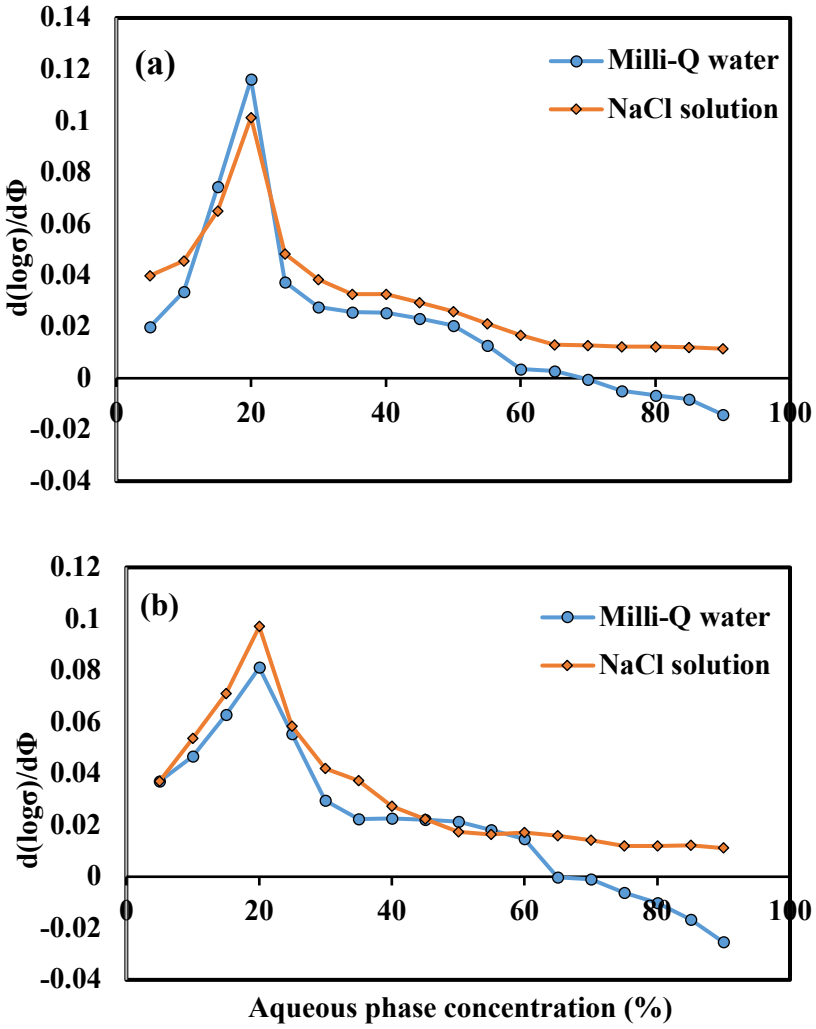

Figure 6. d(log σ)/d(ϕ) as function of aqueous phase concentration of Capmul 708G, Tween 80 and Milli-Q water or 5 mM NaCl solution along the dilution line W91.

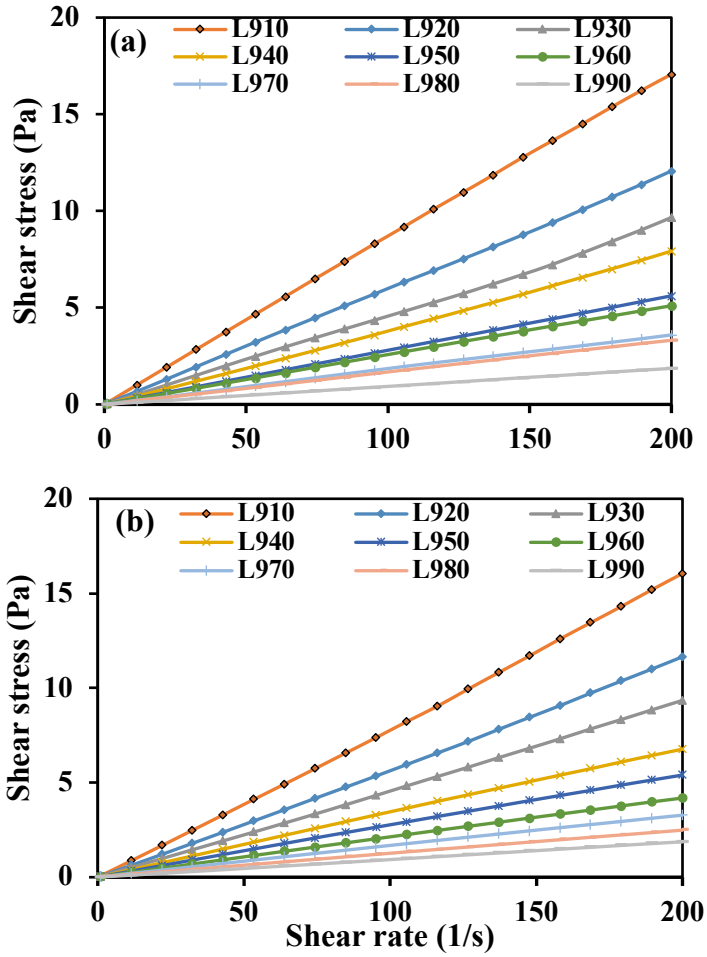

Figure 7. Shear stress as a function of shear rate of samples (L910, L920, L930, L940, L950, L960, L970, L980 and L990) from Capmul 708G, Tween 80, PG and Milli-Q mixture system. The ratio of PG to Milli-Q water was 1:1. (a) Blank microemulsions (b) Beta-carotene loaded microemulsions.

Table 1 Compositions of some samples in the ternary phase diagram

Sample code	% Oil	% Surfactant (with or without cosurfactant)	% Water (with or without cosolvent)
L110	9	81	10
L120	8	72	20
L130	7	63	30
L140	6	54	40
L150	5	45	50
L160	4	36	60
L170	3	27	70
L180	2	18	80
L190	1	9	90
L310	27	63	10
L320	24	56	20
L330	21	49	30
L340	18	42	40
L350	15	35	50
L360	12	28	60
L370	9	21	70
L380	6	14	80
L390	3	7	90
L510	45	45	10
L520	40	40	20
L530	35	35	30
L540	30	30	40
L550	25	25	50
L560	20	20	60
L570	15	15	70
L580	10	10	80
L590	5	5	90
L610	54	36	10
L620	48	32	20
L630	42	28	30
L640	36	24	40
L650	30	20	50
L660	24	16	60
L670	18	12	70
L680	12	8	80
L690	6	4	90

L710	63	27	10
L720	56	24	20
L730	49	21	30
L740	42	18	40
L750	35	15	50
L760	28	12	60
L770	21	9	70
L780	14	6	80
L790	7	3	90
L910	81	9	10
L920	72	8	20
L930	63	7	30
L940	54	6	40
L950	45	5	50
L960	36	4	60
L970	27	3	70
L980	18	2	80
L990	9	1	90